9TH INTERNATIONAL CONFERENCE

ON

SIMULATION AND MODELLING

IN THE

FOOD AND BIO-INDUSTRY

2016

FOODSIM'2016

EDITED BY

Jan F.M. Van Impe

APRIL 3-7, 2016

GHENT, BELGIUM

A Publication of EUROSIS-ETI

Printed in Ghent, Belgium

9th International Conference on
Simulation and Modelling
in the
Food and Bio-Industry

GHENT, BELGIUM

APRIL 3-7, 2016

Organised by

ETI
The European Technology Institute

In Cooperation with

12th International Trends in Brewing Symposium

Katholieke Universiteit Leuven
Technology Campus Ghent

Sponsored by

EUROSIS
The European Simulation Society

Ghent University

University of Skövde

Hosted by

Katholieke Universiteit Leuven
Technology Campus
Ghent, Belgium

EXECUTIVE EDITOR

PHILIPPE GERIL
(BELGIUM)

EDITORS

General Conference Chair

Jan F.M. Van Impe, Katholieke Universiteit Leuven, Ghent, Belgium

International Programme Committee

Simulation in Food Engineering and Processing
Lionel Boillereaux (ONIRIS, Nantes, France)
Cedric Brandam (INPT-ENSIACET, Toulouse, France)
Jean-Yves Monteau (ONIRIS, Nantes, France)
Gianpaolo Ruocco (University of Basilicata, Potenza, Italy)
Olivier Vitrac (INRA-UMR FARE, Reims, France)

Simulation in Food Sciences and Biotechnology
Francis Butler (UCD, Dublin, Ireland)
Enda Cummins (UCD, Dublin, Ireland)

Methods and Tools Applied to Food and Bio-Industries
Paolo Masi (University of Naples Federico II, Portici, Italy)
Pierre-Sylvain Mirade (INRA-Theix, St Genes Champanelle, France)
Leon Rothkrantz (Delft University of Technology, Delft, The Netherlands)

Methods and tools applied to Food Quality and Safety Evaluation
Manuel Rui Alves (IPV, Viana Castelo, Portugal)
Joana Amaral (ESTiG-IPB, Bragança, Portugal)
Ursula Gonzales Barron (University College Dublin, Food Science and Veterinary Medicine, Ireland)
Vasco Cadavez (ESA-IPB, Bragança, Portugal)
Luis Dias (ESA-IPB, Bragança, Portugal)
Isabel Ferreira (ESA-IPB, Bragança, Portugal)
Isabel Mafra (REQUIMTE, Porto, Portugal)
Pedro João Soares Rodrigues (ESTiG-IPB, Bragança, Portugal)
Isabel M. Vicariao (University of Sevilla, Spain)

Methods and tools applied to Beverages Production and Safety
Jan F.M. Van Impe, Katholieke Universiteit Leuven, Ghent, Belgium

Simulation in Functional Foods
Maria Baka, (KU Leuven, Technology Campus Ghent, Ghent, Belgium)
Lourdes Amigo Garrido (CSIC, Madrid, Spain)

Simulation in Food Production Management, Economics and Traceability
Martin Cloutier (UQAM, Montreal, Canada)

Sustainable Food Production
Björn Johansson (Chalmers University of Technology, Sweden)

Innovation in Traditional Food Products
Elsa Ramalhosa (ESA-IPB, Bragança, Portugal)

EUROSIS-ETI Publications are ISI-Thomson, IET, SCOPUS and Elsevier Engineering Village referenced
Legal Repository: Koninklijke Bibliotheek van België, Keizerslaan 4, 1000 Brussels, Belgium
CIP 12.620 D/2011/12.620/1

Selected papers of this conference are published in scientific journals.

For permission to publish a complete paper write EUROSIS, c/o Philippe Geril, ETI Executive Director, Greenbridge Science Park, Ghent University Ostend Campus, Wetenschapspark 1, Plassendale 1, B-8400 Ostend, Belgium.

EUROSIS is a Division of ETI Bvba, The European Technology Institute, Torhoutsesteenweg 162, Box 4, B-8400 Ostend, Belgium

Printed and bound in Belgium by Reproduct NV, Ghent, Belgium
Cover Design by Grafisch Bedrijf Lammaing, Ostend, Belgium
Cover pictures are reproduced under Wikimedia Commons

EUROSIS-ETI Publication
ISBN: 978-90-77381-92-2
EAN: 978-90-77381-92-2

PREFACE

Dear Colleagues,

Welcome in Ghent on KU Leuven's local Technology Campus, to attend the FOODSIM'2016 conference!

Apart from being organized in one of the most friendly cities worldwide, this 9th edition of the FOODSIM conference offers an attractive scientific programme to all colleagues interested in mathematical modeling, simulation, and model based design and optimization of food products and processes. Next to a variety of Technical Sessions devoted to intelligent Monitoring and Modeling in Food Technology, Food Engineering and Food Production, a dedicated session presents Quantitative Tools for Sustainable Food and Energy in the Food Chain while recent advances in multi-scale Predictive Food Microbiology also receive special attention. Other programme highlights include state-of-the-art Tutorials and a Software Fair with direct interaction with the developers.

The presentation of recent EU initiatives including an Erasmus Mundus MSc program, an Erasmus+ Training programme and a COST Action illustrates the importance of Quantitative Food Science in both teaching as well as training of early stage researchers.

For the first time since its origin in 2000 in France, FOODSIM is running in parallel with another food related event, Trends in Brewing. The organizers of both events expect significant synergies. First of all, participants can easily attend lectures or even full sessions from the parallel event. Secondly, software developers are given the chance to demonstrate their tools to a new Trends in Brewing audience while FOODSIM participants will be interested in visiting the attractive TiB Technical Exhibition. Thirdly, FOODSIM has its own Keynote Lecture focusing on the human factor in the study of complex systems applied to food science, while the Keynote Lectures Session "Diversity of Beer Styles" shared with Trends in Brewing offers the chance to broaden interests. Last but not least, both events share the Social Programme, with specialty beer tasting as one of the daily highlights and the visit to a Belgian brewery to conclude the conference in style.

The FOODSIM programme has all ingredients needed to provide you with a rewarding experience at the interface of science and "savoir vivre". The organizers look forward to lively discussions and hope to provide you with a forum for networking and intensified collaboration.

Jan F.M. VAN IMPE &
KU Leuven/BioTeC+ Research Division

CONTENTS

Preface ..... **VII**
Scientific Programme **1**
Author Listing **177**

KEYNOTE

Complex Systems in Food Science: Human Factor Issues
Evelyne Lutton, Alberto Tonda, Nadia Boukhelifa and Nathalie Perrot **5**

TUTORIAL PAPERS

Predictive Modelling under Dynamic Conditions in Food Processing Environments
Vasilis P. Valdramidis, Kirk Dolan, Dries Telen and Jan F.M. Van Impe **11**

Parameter Estimations in Predictive Microbiology: How to build Statistically Sound Secondary Models
Simen Akkermans, Filip Logist and Jan F.M. Van Impe **14**

RECENT EU-INITIATIVES IN FOOD MODELLING AND SIMULATION

FoodMC: A European COST Action on Food Modelling
Alberto Tonda **23**

Q-Safe Erasmus Training Programme – Teaching and Student Learning Experiences
Enda Cummins, Jeanne-Marie Membré, Jan Van Impe, Kostas Koutsoumanis, Serafim Bakalis, Aludena Hospido, Ismael Martínez Lede and Vasilis Valdramidis **26**

Q-SAFE QUANTITATIVE TOOLS FOR SUSTAINABLE FOOD & ENERGY IN THE FOOD CHAIN

Effect of Ultrasound on Recovery Kinetics of *Alicyclobacillus Acidoterrestris* Spores
Myrsini N. Kakagianni, Konstantinos P. Koutsoumanis and Vasilis P. Valdramidis **33**

CONTENTS

Artificial Neural Networks as a Tool to predict the Migration of Silver from Antimicrobial Nano-Coated LPDE Films
Joseph C. Hannon, Enda Cummins, Joseph P. Kerry, Malco Cruz-Romero, Shafrina Azlin-Hasim and Michael Morris **38**

Second Order Monte Carlo Simulation to Characterise the Health Impact of Different Infant Feeding Strategies
Géraldine Boué, Sandrine Guillou, Jeanne-Marie Membré, Jean-Philippe Antignac, Bruno Le Bizec and Enda Cummins **44**

Modelling the Mycelium Formation Ability of Penicillium Expansum as a Function of Propolis pH ad NaCi
Arianne Muscat, Ioannis Mourtzinos, Maria Gougouli, Vasilis Valdramidis and Konstantinos P. Koutsoumanis **49**

Modelling of a Nutrient Feedback Mechanism during Human Digestion of Carbohydrates
Tom Moxon, Philippe Nimmegeers, Dries Telen, Jan Van Impe and Serafim Bakalis **53**

MODELLING IN FOOD ENGINEERING AND FOOD TECHNOLOGY

Modeling the Drying of a Food Processing Plant
Logan Lecoq, Onrawee Laguerre, Evelyne Derens, Hong-Minh Hoang and Denis Flick **61**

Prediction of Material Behaviour and Flows in Industrial Food Processing
Benoit Debbaut **66**

Model Based Prevention of Powder Build-Up in Spray Driers, including Visualization
Kevin N. van Koerten, Martijn B. Fox , Han Straatsma, Maykel Verschueren and Coen Akkerman **71**

SPATIOTEMPORAL PREDICTIVE MODELLING IN FOODS

Individual Based Modeling of Microbial Colony Dynamics on Food Surfaces in a Parallel Simulator
Ignace Tack, Fabrice Harrouet, Gireg Desmeulles, Filip Logist and Jan F.M. Van Impe **77**

Towards an individual-based Simulator of the Yeast *Saccharomyces Cerevisiae* for the Food Science with predictive Capabilities
Xavier Portell and Marta Ginovart **83**

Modelling Spatiotemporal Dynamics in a Food Matrix initiated by Injected Starter Cultures
Thorsten Stefan 88

3D Individual Based Model for Bacteria Growth and Spatial Interactions: Application to the Case of *Listeria Monocytogenes* and *Carnobacterium Piscicola*
Fabrice Harrouet, Gireg Desmeulles, Pascal Redou and Laurent Gaubert 92

FOOD PRODUCT AND PROCESS MONITORING

Role of Differential Plating Methods in the Detection of Sublethal Injury Induced to *Listeria Monocytogenes* by Natural Plant Extracts
Davy Verheyen, Maria Baka, Estefanía Noriega and Jan F.M. Van Impe.....99

Application of Near-Infrared Transmission (NIT) Spectroscopy for Determination of Fat and Protein in Quinoa (Chenopodium Quinoa Willd) Grains
Christian Encina-Zelada, José A. Teixeira, Jorge Pereda, Luz Gómez-Pando, Martha Ibañez, Vasco Cadavez and Ursula Gonzales-Barron.....104

Explorative MS-Fingerprinting to assess Novel Applications of Non-Thermal Plasma in Food Research
Jeroen Vandamme and Jim Van Durme 109

PREDICTIVE FOOD MICROBIOLOGY

Development of Vacuum-Packed Meat-Based Model Systems for the Evaluation of the Food Intrinsic Complexity on *Listeria Monocytogenes* Growth at Refrigeration and Abuse Temperatures
Maria Baka, Estefanía Noriega, Kristof Van Langendonck and Jan F.M. Van Impe.....117

The Role of Food Intrinsic Factors on the Inactivation Efficacy of Cold Atmospheric Plasma
Cindy Smet, Estefania Noriega, Ioannis Matsoukas, Frederik Rosier, James Walsh, Vasilis Valdramidis and Jan Van Impe 122

Predictive modelling of the Growth of Listeria as influenced by the Antimicrobial Activity of Lactococcus Lactis in Liquid and Solid State
Parika Ale, Simy Paul, Jorge Gutierrez and Eirini Velliou 127

CONTENTS

Development of Fish-Based Model Systems for Kinetic Studies of Foodborne Pathogens
Davy Verheyen, Maria Baka, Torstein Skåra, Stijn Vercruyssen, Nicolas Cornette and Jan F.M. Van Impe **130**

MODELLING IN FOOD PRODUCTION

Coupling Fluid Flow, Heat Transfer and Food Product Transformation in a Tubular Heat Exchanger, including the Influence of Curved Sections
Artemio Plana-Fattori, Emilie Auger, Christophe Doursat and Denis Flick..... **135**

Classifying Beef Carcasses according to Meat Quality using Animal/Carcass Characteristics and pH/Temperature Decline Descriptors Early *Post Mortem*
Cristina Xavier, Ursula Gonzales-Barron, Vasco Cadavez and Alexandra Müller **143**

Optimization of a Thermal Process with Reciprocal Agitation by computational modelling
Dagbjørn Skipnes, Ferruh Erdogdu, Mustafa Tutar, Sigurd Øines, Igor Barreno and Trond Løvdal..... **149**

Reduction of 3 Monochloropropane 1, 2-Diol (3-MCPD) Esters during Palm Oil Refining
Chin Ping Tan and Musfirah Zulkurnain..... **152**

Sustainable Production Logistics-Location Problem for Reusable Transport Packages in Multi-food Production Network with Production Cycle
Di Zhang **155**

SOFTWARE TOOLS

FoodRisk-Labs Open Source Software Tools Supporting Food Safety Decision Making
Matthias Filter, Christian Thöns, Carolina Plaza Rodriguez, Miguel de Alba Aparicio, Alexander Falenski, Annemarie Käsbohrer, Bernd Appel and Armin A. Weiser **163**

Microhibro: An On-Line Tool for Quantitative Microbial Risk Assessment in Foods
Fernando Perez-Rodriguez, Antonio Valero, Elena Carrasco, Denisse Posada-Izquierdo, Rosa Maria Garcia-Gimeno and Gonzalo Zurera..**165**

CONTENTS

LATE PAPER

Erasmus Mundus Joint Master Degree in Food Science, Technology and Business
Monika Polanska, Jan Van Impe and Guido Aerts.....**171**

SCIENTIFIC PROGRAMME

KEYNOTE

COMPLEX SYSTEMS IN FOOD SCIENCE: HUMAN FACTOR ISSUES

Evelyne Lutton[1], Alberto Tonda[1], Nadia Boukhelifa[2], Nathalie Perrot[1],
[1]UMR 782 GMPA, Université Paris-Saclay, INRA, 78850 Thiverval-Grignon, France
[2]Télécom ParisTech & CNRS LTCI, 46 rue Barrault, 75634 Paris Cedex 13
{evelyne.lutton,alberto.tonda,nathalie.perrot}@grignon.inra.fr, nadia.boukhelifa@telecom-paristech.fr

KEYWORDS
Complex Systems, Food Science, Human Factors

ABSTRACT

Building in-silico decision making systems is essential in the food domain, albeit highly difficult. This task strongly relies on multidisciplinary research and in particular on advanced techniques from artificial intelligence. The success of such systems depends on how well they cope with the complex properties of food processes, such as the large variety of interacting components including those related to human expertise; and their dynamic, non-linear, multi-scale, uncertain and non-equilibrium behaviors. Robust stochastic optimization techniques, evolutionary computation and in particular Interactive Evolutionary Computation (IEC) seem to be a fruitful framework for developing food science models. A Human-Centered approach to Interactive Evolutionary Computation is discussed in this paper as a possible pertinent way to cope with challenges related to human factors in this context.

FOOD SCIENCE AND COMPLEX SYSTEMS

Food is a major factor for health and public well-being. It is one of the most important sectors of industry and deals with chemicals, agriculture, animal feed, food processing, trade, retail and consumer sectors. Providing an adequate food supply to a growing world population is one of the grand challenges our global society has to address. Enterprises need to continuously provide safe, tasty, healthy, affordable, and sustainable food in sufficient volumes. This requires adapting to a range of factors, such as the increase in human population and health requirements, and the reduction in crops and livestock due to environmental factors and changes in the socio-political scene (van Mil et al. (2014)). Besides, there is a need for an integrated vision looking at these factors from multiple scales and perspectives:

- from emotion and pleasure generated when eating food to nano-structures of a food emulsion or food microbial ecosystems,
- from regional organization to nutritional and sociological impact,
- from health considerations to inter-crop culture and microbial complexities, within the human body and in relation to food microbial ecosystems.

In these conditions, creativity, pragmatism and optimization methods are crucial to reach breakthrough innovations and sustainable solutions. We foresee a huge opportunity for research in mathematical programming, integrative models and decision-support tools (Perrot et al. (2016)) to address the aforementioned challenges. Any proposed mathematical programming framework, however, has to deal with the following characteristic features of food systems:

- The uncertainty and variability (in process, data and available knowledge) that severely influences the dynamics and emergence of various properties,
- The heterogeneity of the data, from big volumes at the genomic scale to scarce samples at a more macroscopic level (i.e. process scales). For instance an ecosystem of 9 microorganisms can be characterized using 40,000 genes, and its dynamics with 10 aromatic compounds,
- The complexity of qualitative and quantitative information, for instance for social and environmental evaluation, at various scales in space and time,
- The variety of perspectives, types of models, research goals and data produced by conceptually disjoint scientific disciplines, ranging from physics and physiology to sociology and ethics.

Moreover, there is a need to find an appropriate description level, able to express the complexity of an ecosystem with minimum uncertainty. Building models is essential, but highly difficult; efficient modeling necessitates a rigorous iterative process combining computationally intensive methods, formal reasoning and expertise from different fields.

THE HUMAN FACTOR

The specifics of food domain bring to focus another major player, what can be called the human factor. Although not very evident, most of the computing approaches rely on human capabilities, for example, to

organize a model and generalize it. They also rely on domain experts and an appropriate methodology to handle their expertise. In fact, at every stage, human expertise and decision making are highly important for improving the understanding of food systems, and as such, they should be integrated in the computation.

There is a long tradition in artificial intelligence (AI) of involving humans in the computational loop. Expert systems, for instance, have been specifically designed for mimicking the decision-making ability of a human expert. Learning, classification, natural language processing, search and optimization are many facets of this domain, all aimed at answering fundamental questions like: How does the human mind work, and can non-humans have minds? (Kohavi and Provost (1998), Tonda et al. (2013)).

Real-world applications of AI are definitely complex, but not only. The questions asked are themselves complex. In particular, when dealing with optimization, the evaluation of a complex system state relies on multiple criteria that may be numerous, uncertain, noisy and subjective. The possible answers are dealing more with tradeoff and equilibrium stages than with the classical notion of optimum. Several, and often many, objectives have to be considered simultaneously.

The vast subject of sustainability, for instance, clearly needs multi-objective optimization tools. The United Nations have adopted the following definition on March 20, 1987: a sustainable development is a development that meets the needs of the present without compromising the ability of future generations to meet their own needs. This statement has the major advantage to emphasize management policies where economy is not the unique concern. However, it definitely requires an evaluation of a series of criteria, and an optima that represent compromises between various incompatible aims, like financial profit and nature preservation.

Evaluating sustainability in practice is extremely difficult, subjective and scale dependent. Current techniques, such as Life Cycle Analysis (LCA), consist of creating an inventory of flows from and to nature for a given system. This inventory is supposed to take into consideration every input and every output of the system. Then, some impact factors are computed according to international standards (ISO 14000 for environmental management) and available databases of typical values. Various global environmental impact factors are then computed via weightings, in which it is recognized that a high degree of subjectivity is at play. These quantities are then used for decision making.

Various critiques can be made to these types of approaches: a LCA strongly depends on available data, and databases may become obsolete as new material and manufacturing methods constantly appear. Additionally, even if LCA is a powerful tool for analyzing measurable aspects of quantifiable systems, some effects (human, social, psychological) cannot be reduced to numbers and inserted into existing models. Once again, efficient and versatile computer optimizations are desirable for improving the accuracy of existing approaches, but at the same time, it seems clear that in this context, decision making cannot be delegated to machines.

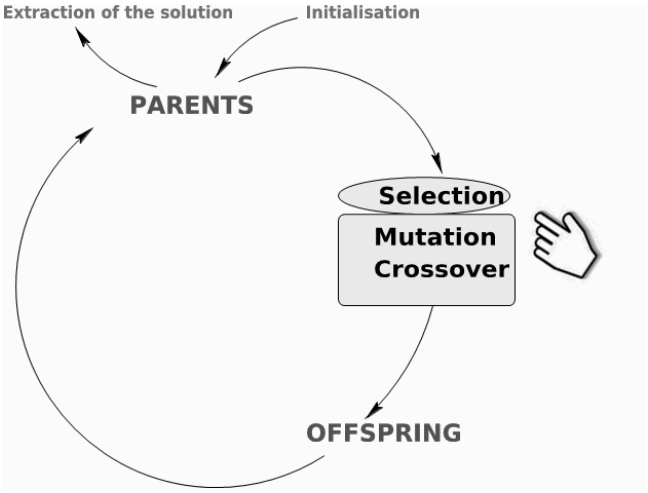

Figure 1: The evolutionary loop. User interactions can occur at any stage including selection/evaluation of individuals and the genetic operators.

THE HUMANIZED COMPUTATION PERSPECTIVE

The idea of a humanized computational intelligence consists of directly embedding the capability of a human in a computational system, instead of using a representative model as more classical AI approaches. In other terms, it aims at dealing with complex problems by combining human capabilities with autonomous computations, leveraging the strengths of both sides (Takagi (1998)).

Interactive Evolution

One of the most advanced techniques in this direction are interactive evolutionary computation (IEC) approaches, based on evolutionary algorithms. Evolutionary Algorithms (EAs) are stochastic optimization heuristics that copy, in a very abstract manner, the principles of natural evolution that let a population of individuals be adapted to its environment (Goldberg (1989)). An EA considers populations of potential solutions exactly like a natural population of individuals that live, fight, and reproduce, but the natural environment pressure is replaced by an optimization pressure. Reproduction (see Fig. 1) consists of generating new solutions via variation schemes (the genetic operators), that, by analogy with nature, are called mutation if they involve one individual, or crossover if they involve two

parent solutions. A fitness function, computed for each individual, is used to drive the selection process, and is thus optimized by the EA. More specifically, Interactive Evolutionary Computation (IEC) is focused on the optimization of subjective quantities captured via a user interface.
Whereas current IEC research has focused on improving the robustness of the underlying algorithms, much work is still needed to tackle human-factors in systems where adaptation between users and systems is likely to occur (Mackay (2000)). Applications of IEC range from artistic to scientific projects (Takagi (1998), Lutton (2006), Tonda et al. (2013)). For scientific and engineering applications, IEC is interesting when the exact form of a more generalized fitness function is not known or is difficult to compute, say for producing a visual pattern that would interest a particular user. Here, the human visual system, together with the emotional and psychological responses of the user in question are far superior than any pattern detection or learning algorithm.

The Visible & Hidden Roles of Humans in IEC

The role of humans in IEC can be characterized by the evolutionary component at which they operate (Fig. 1), namely: initialization, evolution, selection, genetic operators, constraints, local optimization, genome structure variation and parameters tuning, which may or may not be desirable from a usability perspective especially for non-technical users.
The general approach when humans are involved, especially for parameter tuning, is mostly by trial-and-error and reducing the number of parameters. Such tasks are often visible, in that they are facilitated by a user interface. However, there exists a hidden role of humans in IEC that has often been neglected. Algorithm and system designers play a central role in deciding the details of the fitness function to be optimized and in setting the default values of system parameters (contributing to the "black box" effect of IEC systems). Such tasks are influenced by the previous experience of the designers and end-user task requirements. Besides this hidden role in the design stage, there is a major impact of the human in the loop on the IEC itself. This problem is known as the "user bottleneck" (Poli and Cagnoni (1997)), i.e. a human fatigue due to the fact that the user and machine do not live and react at the same speed. Various solutions have been considered in order to avoid systematic and repetitive or tedious interactions, such as: (i) reducing the size of the population and the number of generations; (ii) choosing specific models to constrain the exploration in a-priori interesting areas of the search space; and (iii) performing an automatic learning (based on a limited number of characteristic quantities) in order to assist the user and only present interesting individuals of the population, with respect to previous votes or feedback from the user. These solutions require considerable computational effort.

Example: Guided Search for Agronomy

EvoGraphDice (Boukhelifa et al. (2013)), was designed to aid the exploration of multidimensional datasets where 2D projections of combined dimensions are of interest to agronomists. Starting from dimensions whose values are automatically calculated by a Principal Component Analysis (PCA), an IEC progressively builds non-trivial viewpoints in the form of linear and non-linear dimension combinations, to help users discover new interesting views and relationships in their data. The criteria for evolving new dimensions is not known a-priori and is partially specified by the user via an interactive interface. Pertinence of views is modelled using a fitness function that plays the role of a predictor: (i) users select views with meaningful or interesting visual patterns and provide a satisfaction score; (ii) the system calibrates the fitness function optimized by the evolutionary algorithm to incorporate user's input, and then calculates new views. A learning algorithm was implemented to provide pertinent projections to the user based on their past interactions. The evaluation of EvoGraphDice (Boukhelifa et al. (2015a;b)), followed a mixed approach where, on the one hand we observed the utility and effectiveness of the system for the end-user (user-centered approach); and on the other hand we analysed the computational behaviour of the system (algorithm-centered approach). Based on these evaluations, it appears that the interactive evolutionary algorithm, with the help of user feedback, was able to converge quickly to an interesting view when a clear task was specified (Boukhelifa et al. (2015a)). In the other direction, the IEC allowed users to laterally explore different possibilities (Landrin-Schweitzer et al. (2006)),better formulate their research questions and build new hypotheses for further investigation (Boukhelifa et al. (2015b)).

CONCLUSION: RESEARCH OPPORTUNITIES FOR IEC IN FOOD SCIENCE

Decision making in food science requires methods able to efficiently cope with experts knowledge. IEC represents an attractive framework for embedding expertise and human factors in computational systems. However, user-driven optimization processes rely on systems that adapt their behavior based on user feedback, while users themselves adapt their goals and strategies based on the solutions proposed by the system. This two way communication and adaptation presents prospects to conduct future research. We discuss these below as research opportunities aiming to facilitate and support the different roles humans play in IEC, i.e. in the design, interaction and evaluation of IEC systems.

- *Human-Centered Design:* during the design, development and evaluation of many of our tools (see Tonda et al. (2013)), we worked with domain experts at different levels. For EvoGraphDice, for instance, we largely benefited from having a domain expert as part of the design and evaluation team. However, this was carried out in an informal way. Involving end-users in the design team is a long-time tradition in the field of Human-Computer interactions (HCI) as part of the user-centered design methodology. Participatory design, for instance, could be conducted with IEC end-users to incorporate their expertise in food domain at the design level of the algorithm.
- *Interaction and Visualization:* often the solutions proposed by the IEC are puzzling to the end-user. This is because the inner workings of the evolutionary algorithm and user exploration strategies that led to the solution are often not available to the user. This black box effect is challenging to address as there is a fine balance to find between the richness of a transparent interface and the simplicity of a more obscure one. Finding the tipping point requires an understanding of evolving user expertise in manipulating the system, and the task requirements. Whereas user-centered design can help elicit these requirements and tailor tools to user needs over time, visualization techniques can make the provenance of views and the system status more accessible: there exists rich and varied interaction techniques to facilitate user feedback in parallel to developing robust user models that try to learn from the provided input.
- *Multifaceted Evaluation:* the evaluation of an IEC system remains a difficult task as the system adapts to user preferences but also the user interprets and adapts to system feedback. Getting a clear understanding of the subtle mechanisms of this co-adaptation (Mackay (2000)) is challenging and requires to consider evaluation criteria other than speed of algorithm convergence and the usability of the interface. In the context of data exploration, desirable features can be characterized by lateral thinking, surprising findings, and the way users learn how to operate the interactive system and construct their own way to use it. Our observation is that the tunable balance between randomness and user-guided search provided by IEC seems to be very efficient for this purpose.

REFERENCES

Boukhelifa N.; Bezerianos A.; Cancino W.; and Lutton E., 2015a. *Evolutionary Visual Exploration: Evaluation of an IEC Framework for Guided Visual Search. Evolutionary computation.*

Boukhelifa N.; Bezerianos A.; and Lutton E., 2015b. *A Mixed Approach for the Evaluation of a Guided Exploratory Visualization System.* In *EuroVis Workshop on Reproducibility, Verification and Validation in Visualization (EuroRV^3).*

Boukhelifa N.; Cancino W.; Bezerianos A.; and Lutton E., 2013. *Evolutionary Visual Exploration: Evaluation With Expert Users.* In *EuroVis 2013, 15th annual Visualization Symposium.* June 17-21, Leipzig, Germany.

Goldberg D.A., 1989. *Genetic Algorithms in Search, Optimization, and Machine Learning.* Addison-Wesley Publishing Company, inc., Reading, MA.

Kohavi R. and Provost F., 1998. *Glossary of terms. Machine Learning*, 30, no. 2-3, 271–274.

Landrin-Schweitzer Y.; Collet P.; and Lutton E., 2006. *Introducing Lateral Thinking in Search Engines. GPEM, Genetic Programming an Evolvable Hardware Journal, W Banzhaf et al Eds*, 1, no. 7, 9–31.

Lutton E., 2006. *Evolution of Fractal Shapes for Artists and Designers. IJAIT, International Journal of Artificial Intelligence Tools*, 15, no. 4, 651–672. Special Issue on AI in Music and Art.

Mackay W.E., 2000. *Responding to cognitive overload: Co-adaptation between users and technology. Intellectica*, 30, no. 1, 177–193.

Perrot N.; Vries H.D.; Lutton E.; van Mil H.G.; Donner M.; Tonda A.; Martin S.; Alvarez I.; Bourgine P.; van der Linden E.; and Axelos M.A., 2016. *Some remarks on computational approaches towards sustainable complex agri-food systems. Trends in Food Science and Technology*, 48, 88 – 101.

Poli R. and Cagnoni S., 1997. *Genetic Programming with User-Driven Selection : Experiments on the Evolution of Algorithms for Image Enhancement.* In *2nd Annual Conf. on Genetic Programming.*

Takagi H., 1998. *Interactive Evolutionary Computation: System Optimisation Based on Human Subjective Evaluation.* In *IEEE Int. Conf. on Intelligent Engineering Systems (INES'98).* Vienna, Austria.

Tonda A.; Spritzer A.; and Lutton E., 2013. *Balancing User Interaction and Control in Bayesian Network Structure Learning.* In *11th Biannual International Conference on Artificial Evolution (EA-2013), Bordeaux, France.* 21-23 October.

van Mil H.; Foegeding E.; Windhab E.; Perrot N.; and van der Linden E., 2014. *A complex system approach to address world challenges in food and agriculture. Trends in Food Science and Technology*, 40, no. 1, 20–32.

TUTORIAL PAPERS

PREDICTIVE MODELLING UNDER DYNAMIC CONDITIONS IN FOOD PROCESSING ENVIRONMENTS

Vasilis P. Valdramidis[1]
[2]Department of Food Studies and Environmental Health
Faculty of Health Sciences
University of Malta
MSD2080, Msida
Malta
E-mail: vasilis.valdramidis@um.edu.mt

Kirk Dolan[2]
[2]Department of Food Science & Human Nutrition
Department of Biosystems & Agricultural Engineering 135
Trout Food Science Building Michigan State University East
Lansing, MI 48824
USA
E-mail: dolank@anr.msu.edu

Dries Telen, Jan F.M. Van Impe[3]
[3]KU Leuven - Department of Chemical Engineering
BioTeC - Chemical and Biochemical Process Technology and Control
Gebroeders De Smetstraat 1, B-9000 Gent
Belgium
E-mail: dries.telen@cit.kuleuven.be jan.vanimpe@cit.kuleuven.be

KEYWORDS
Parameter estimation, microbial dynamics, temperature, inverse problems.

ABSTRACT

Commercial thermal and non-thermal processes for food are dynamic, where temperature, water activity, and other variables can change with time. An efficient process design requires knowing the parameters of microbial mathematical models describing the underlying dynamic processes. However, most research to obtain these parameters is performed under simulated constant conditions. The objective of this session is to address some of the recent developments to model predictive microbial dynamics of food processes describing examples on how to perform inverse (parameter estimation) problems for a number of different primary-secondary models. Therefore, appropriate experimental designs, such as optimal experimental design, parameter identification under dynamic conditions, and properly statistical indices to discriminate among models are discussed.

DYNAMIC ENVIRONMENTS

The majority of most food technologies are dynamic in nature. The main changing processing factor is temperature and its impact to biological/chemical reponses in most cases is significant and can result in induced microbial/chemical stress responses hence making some processes less effective. Some examples, include the classical pasteurization and sterilation treatments which include nonisothermal heating-up phases and temperature fluctuations during the process. Others include adiabatic heating during the application of High Hydrostatic Temperautre (e.g., Valdramidis et al., 2009) and high-pressure carbon dioxide processing (Garcia-Gonzalez et al., 2009) as well as the increase of the temperature during the application of Pulsed Electric Field (PEF) processing inside PEF chambers (Jaeger et al. , 2010). Nevertheless, the chemical, microbial, and enzymatic responses as they change during these processing conditions are usually studied assuming that operations are applied at static conditions.

In this approach, the kinetic parameters of a model describing the evolution of the concentration of a component (e.g., chemical, microbial) over time are estimated for at least three different static environmental conditions. These estimates are correlated with the tested conditions in order to identify the kinetic parameters of interest. Hereafter, a validation step is applied usually under dynamic conditions. If predicted and measured results are close to each other, this closeness can confirm the assumption that parameters derived from static conditions are nearly equal to parameters during dynamic conditions.

Despite the easiness of the implementation of this modeling methodology, also known as two-step modeling methodology, its drawbacks will be discussed in this session and it will be highlighted that even if the results are excellent following the use of isothermal inactivation parameters, one does not know the actual values of nonisothermal estimates. Concluding, the importance to apply parameter identification techniques under dynamic conditions representative of a realistic (processing) environment will be introduced.

OPTIMAL EXPERIMENTAL DESIGN

Both the selection of an appropriate model structure and the identification of accurate model parameters are data-driven processes. Therefore, the quality of the experimental data is critical for appreciating the efficiency and accuracy of these procedures. Experimental data should be informative enough and this could improve the model building and parameter estimation. A novel methodology for the collection of more informative data via dynamic input profiles (e.g., temperature) is based on the concepts of Optimal Experiment Design for Parameter Estimation (OED/PE). In OED the (time-varying) process inputs are designed such that the resulting process outputs have maximum information

content, and this within the validity region of the proposed process operation.

This methodology has been applied on traditional thermal processes (sterilization or mild heating) for microbial and chemical inactivation kinetics (Balsa-Canto et al., 2007; Cunha et al., 1997; Versyck et al., 1999) as well as on microbial growth studies (e.g., Van Derlinden et al., 2008, 2010, 2013).

Most applications of OED in food science focus on D-optimal design, which aims at maximizing the determinant of an information matrix. It has been proven that optimal experimental design can significantly reduce the number of experiments and increase the accuracy of parameters by indicating the best times to collect data. Presuming model validity, the mathematical technique of optimal experiment design for parameter estimation (OED/ PE) can be designed to estimate accurate and precise parameters. When applying dynamic experiments, this approach also guarantees parameter estimates which are valid under varying, more realistic conditions

Thereofore, this session will also focus on the importance of experimental data collection for the modelling of bioprocesses. The various steps towards accurate bioprocess models will be revised. The concepts of OED will be outlined while optimal dynamic experiment design for parameter estimation of the Ratkowsky square root model will be presented as case study. In addition, novel developments as the integration of multiple objectives will be discussed. In particular criteria which aim at a better conditioning of the system, i.e., the modified E-criterion or anti-correlation criteria, and criteria which aim at the global maximization of the information content will be discussed. Furthermore, a more recent trend of integrating the final goal of the model in the optimal experiment design procedure will be highlighted (Houska et al., 2015).

INVERSE PROBLEM IN REALISTIC ENVIRONMENTS

Previous studies have shown that non-isothermal microbial inactivation parameters can be estimated accurately and precisely with a minimum of experiments collected under realistic processing conditions, even without the application of OED, and by applying either ordinary least squares nonlinear regression or a sequential procedure. This session will also focus on presenting tools that can be applied to rate-dependent parameters in food safety computations. Methods such as OLS and sequential estimation will be demonstrated and presented as alternatives to numerous isothermal experiments and multiple-step linear regression, which typically have too few degrees of freedom to attain desirable small standard error for microbial models.

The key points of this session will be to demonstrate that non-static microbial kinetic model parameters could be accurately and precisely estimated using one-step nonlinear regression following an ordinary least squares and a sequential approach (Dolan et al., 2013); and to demonstrate the use of appropriate statistical indices on choosing the best performing out of different differential models (Dolan and Mishra, 2013).

Even after the parameters have been accurately estimated there will remain a level of uncertainty. In order to deliver accurate predictions the uncertainty on the model predictions have to be accounted for. The accurate propagation of uncertainty of a stochastic nature can be performed by employing smart sampling based techniques as the unscented transformation (Julier, 1996).

CONCLUSIONS

This tutorial will focus on the advances in predictive microbial dynamics of food processes for estimating accurate and precise modeling parameters that can reliably be used to predict realistic processing conditions. The problem statement for dynamic modeling approaches will be showcased and appropriate experimental designs, such as optimal experimental design, parameter identification under dynamic conditions, and proper statistical indices to discriminate among models will be discussed.

ACKNOWLEDGEMENTS

This research was funded with the support of the Erasmus+ programme of the European Union (Project No. 2014-1-MT01-KA200-000327), the KU Leuven research council: PFV/10/002 (OPTEC), Dries Telen holds a postdoctoral grant 2015/134, the Flemish Fund for Scientific Research: FWO KAN2013 1.5.189.13, FWO-G.0930.13 and the Belgian Science Policy Office: IAP VII/19 (DYSCO).

REFERENCES

Julier, S., Uhlmann, J. 1996. “A general method for approximating nonlinear transformations of probability distributions”. *Departement of Chemical Engineering Science, University of Oxford*.

Houska, B., Telen, D., Logist, F., Diehl, M., Van Impe, J., 2015. “An economic objective for optimal experiment design of nonlinear dynamic processes”. *Automatica* No. 51, 98–103.

Dolan, K.D., Valdramidis, V.P., Mishra, D.K. 2013. “Parameter estimation for dynamic microbial inactivation: which model, which precision? ” *Food Control* No. 29:(2): 401-408.

Dolan, K.D., Mishra, D.K. 2013. “Parameter estimation in food science”. *Annual Reviews in Food Science & Technology* No. 4: 401-422.

Valdramidis, V.P., Graham, W.D., Beattie, A., Linton, M., McKay, A., Fearon, A.M., Patterson, M.F. 2009. “Defining the stability interfaces of apple juice: Implications on the optimization and design of high hydrostatic pressure treatment”. *Innovative Food Science and Emerging Technologies* No.10, 396_404.

Garcia-Gonzalez, L., Geeraerd, A.H., Elst, K., Van Ginneken, L., Van Impe, J.F., Devlieghere, F., 2009. “Inactivation of naturally occurring microorganisms in liquid whole egg using high pressure carbon dioxide processing as an alternative to heat pasteurization”. *The Journal of Supercritical Fluids* No. 51, 74_82.

Jaeger, H., Meneses, N., Moritz, J., Knorr, D., 2010. “Model for the differentiation of temperature and electric field effects during thermal assisted PEF processing”. *Journal of Food Engineering* No. 100, 109-118.

Balsa-Canto, E., Rodriguez-Fernandez, M., Banga, J.R., 2007. “Optimal design of dynamic experiments for improved estimation of kinetic parameters of thermal degradation”. *Journal of Food Engineering* No. 82, 178-188.

Cunha, L.M., Oliveira, F.A.R., Brandao, T.R.S., Oliveira, J.C., 1997. “Optimal experimental design for estimating the kinetic parameters of the Bigelow model”. *Journal of Food Engineering* No. 33, 111_128.

Versyck, K.J., Bernaerts, K., Geeraerd, A.H., Van Impe, J.F., 1999. “Introducing optimal experimental design in predictive

modeling: a motivating example". *International Journal of Food Microbiology* No. 51, 39-51.
Van Derlinden, E., Mertens, L., Van Impe, J.F. (2015). "The impact of experiment design on the parameter estimation of cardinal parameter models in predictive microbiology". *Food Control* No. 29(2), 300-308.
Van Derlinden, E., Bernaerts, K., Van Impe, J.F. (2010). "Simultaneous versus sequential optimal experiment design for the identification of multi-parameter microbial growth kinetics as a function of temperature". *Journal of Theoritical Biology* No. 264(2), 347-355.
Van Derlinden, E., Bernaerts, K., Van Impe, J.F. (2008). "Accurate estimation of cardinal growth temperatures of Escherichia coli from optimal dynamic experiments". *International Journal of Food Microbiology* No. 128(1), 89-100.

AUTHOR BIOGRAPHIES

VASILIS VALDRAMIDIS is a member of the Faculty of Health Sciences at the University of Malta. He is leading the research group on the Food Sciences and Environmental Health Research (FSEH) at the Unviersity of Malta http://www.um.edu.mt/healthsciences/research/fseh He is the coordinator of the education programme Erasmus + : Cooperation for innovation and the exchange of good practices. Strategic Partnerships. Quantitative Tools for Sustainable Food and Energy in the food chain, Q-SAFE https://www.um.edu.mt/healthsciences/projects/q-safe 2014-2017. He is member of the International Committee on Food Microbiology and Hygiene of the IUMS and member of the International Committee of Predictive Modelling in Food since 2011.

KIRK DOLAN is an associate professor at Michigan State Univeristy and has joint appointments in Department of Food Science & Human Nutrition (lead), and Department of Biosystems & Agricultural Engineering. His research is on modeling thermal processing of foods (canning, drying, aseptic, etc.), and on inverse problems and parameter estimation http://www.fshn.msu.edu/directory/kirk_dolan. His research group is a leading user of MATLAB with COMSOL for parameter estimation, and has demonstrated new statistical analysis methods for food researchers. He is the chairman and organizer of the triennial Inverse Problems Symposia at Michigan State University http://www.inverseproblems2016.org/. He is a member of Institute for Thermal Processing Specialists, and regularly interacts with food companies. His extension work includes organizing and co-teaching the FDA-mandated Better Process Control School for certification, co-teaching an annual HACCP course to industry, and assisting Michigan food entrepreneurs with FDA product registration.

DRIES TELEN Dr. Telen obtained the MSc degree in Mathematical Engineering from KU Leuven in 2010 and his PhD degree in Chemical Engineering at the same university. Currently he is a post-doctoral researcher at KU Leuven. He guides a team of 4 PhD. students. This research focusses on optimal experiment design for nonlinear dynamic systems (integrated in NMPC), robust dynamic optimization, multiobjective optimization.

JAN VAN IMPE is a full professor at the chemical engineering department of KU Leuven. He obtained his MSc from the University of Gent in 1988, and his PhD from the KU Leuven in 1993. Immediately thereafter he founded the BioTeC (Chemical and Biochemical Process Technology and Control) research group [www.cit.kuleuven.be/biotec]. In the period 2005-2011 he has served as Departmental Head. He has been visiting professor at the UA (University Antwerpen) [2006-2015]. He is a founding partner of the KU Leuven Center-of-Excellence OPTEC (Optimization in Engineering) in 2005, and at present he is coordinating OPTEC's continuation (Phase II: 2010-2017 www.kuleuven.be/optec). In 2008 he started the Flemish Cluster for Predictive Modeling in Foods [www.cpmf2.be], to facilitate the transfer of the broad expertise in the area of predictive microbiology to industry/government. From 2009-2014 on, he held the essenscia-chair, funded by the Belgian Chemical and Life Sciences Industry platform [www.scores4chem.be].

PARAMETER ESTIMATIONS IN PREDICTIVE MICROBIOLOGY: HOW TO BUILD STATISTICALLY SOUND SECONDARY MODELS

Simen Akkermans, Filip Logist, Jan F.M. Van Impe*
KU Leuven, Department of Chemical Engineering,
BioTeC - Chemical and Biochemical Process Technology and Control,
OPTEC - Optimization in Engineering Center-of-Excellence,
CPMF2 - Flemish Cluster Predictive Microbiology in Foods,
Gebroeders De Smetstraat 1, B-9000 Gent, Belgium
*E-mail address: Jan.VanImpe@cit.kuleuven.be

KEYWORDS

Parameter estimation, secondary model, variance stabilizing transformation.

ABSTRACT

When building models to describe the effect of environmental conditions on the microbial growth rate, parameter estimations can be performed either with a *one-step method*, i.e., directly on the cell density measurements, or in a *two-step method*, i.e., via the estimated growth rates. The *two-step method* is often preferred due to its simplicity. The current research demonstrates that the *two-step method* is, however, only valid if the correct data transformation is applied and a strict experimental protocol is followed for all experiments. Moreover, the *one-step method* leads to a better approximation of the confidence intervals on the estimated parameters. Therefore, the *one-step method* is preferred and the *two-step method* should be avoided.

INTRODUCTION

In predictive microbiology, the effect of environmental conditions on the growth rate of microorganisms is generally modeled in two steps (i.e., via the so-called two-step method). In the first step, the microbial specific growth rate (hereafter referred to as growth rate) is determined at several values of the studied conditions by fitting a primary model to the measured growth curves. In the second step, the relationship between the experimental conditions and the growth rate is modeled by fitting a secondary model to the growth rates determined in the first step (Whiting and Buchanan, 1993). At the end of the previous century, the use of experiments with environmental conditions that change as a function of time was introduced into predictive microbiology as a means of obtaining more information from growth experiments (Versyck et al., 1999). A consequence of using these dynamic conditions is that the two-step parameter estimation methods could no longer be applied. Instead, the primary models, which describe the microbial growth as a function of time, were combined with the secondary models, which describe the effect of environmental conditions on microbial growth, and the combined models were identified by minimizing the error on the predicted growth. In this way, the parameter estimation is performed in a single step on the cell density data (leading to the so-called one-step method). Such parameter estimation techniques can also be applied when a set of static experiments is available. A choice should thus be made between the one-step and two-step method.

A first point of comparison between the one-step and two-step modeling methods is the compatibility of their objective functions with the application of predictive microbiology. In the one-step method the error on the predicted growth of a population is minimized whereas in the two-step method the error on the predicted growth rate is minimized. The goal of predictive microbiology is to minimize or prevent the growth of microorganisms in food products for a certain period of time. This goal is more closely linked with the objective function of the one-step method than that of the two-step method. Moreover, the models used in predictive microbiology are overall largely empirical. This means that the models, and the assumptions they represent, are an oversimplification of the true behavior of microorganisms and can thus never be expected to completely agree with the reality. It should be stressed that this is an entirely different matter than model(parameter) uncertainty. As a consequence, it is worth considering how there should be dealt with the discrepancies that exist between a model for the growth rate and the real microbial response, since this is also determined by the objective function. Comparing the objective functions of the modeling methods considered here, the objective function of the one-step method is preferred for modeling the effect of environmental conditions on the growth rate in predictive microbiology.

Ratkowsky et al. (1991) was probably the first publication in predictive microbiology to draw attention to one of the main difficulties when working with the two-step method. They pointed out that the variance of bacterial growth responses such as the growth rate or lag time are dependent on the magnitude of the mean, i.e., that they are heteroscedastic. However, when a least squares regression is used to fit a model to data, this data should be homoscedastic, i.e., independent of its value. When heteroscedastic data is used in an unweighted least squares regression, too much confidence is placed in data with a high variance compared to data with a low variance. Such errors in the application of least squares regression techniques can lead to consistent deviations between the model and the microbial system, which in their turn lead to poor predictions and too much confidence being placed in these predictions. A possible solution to this problem is making a variance stabilizing transformation of the data before commencing the fitting procedure. Several authors proposed the use of either a square root transformation (Augustin and Carlier, 2000; Coroller, 2005; Zwietering, 1994) or logarithmic transformation (Alber and Schaffner, 1992; Masana, 2000; te Giffel and Zwietering, 1999) to obtain homoscedastic data. No consensus has been reached on the required transformation since (i) the uncertainty

distribution of measurements depends on the experimental methods, (ii) experimental studies of the variance were based on very limited data sets and (iii) simulation studies are highly dependent on their assumptions (Schaffner, 1998). If a transformation of the growth rates is made, the objective of minimizing the error on the transformed growth rate should be compared with the objective of minimizing the error on the microbial growth. This question of heteroscedasticity of the growth rates is of no importance to the one-step modeling method, since the model is fitted to the data of the population density and not to the estimates of the growth rate.

The one-step and two-step modeling methods also differ in the calculation of the confidence intervals of the model parameters. Since these confidence intervals are essential for modelers to know how much trust can be placed in the estimated parameters (and consequently in the model predictions), it is worth considering the effect of the chosen modeling method on the calculation of the confidence intervals. Even though the importance of determining the confidence intervals is generally accepted, this matter has not been discussed in previous publications in the field of predictive microbiology.

To select a modeling method that is compatible with the estimation of parameters for secondary models in predictive microbiology, this research studies the variance of the growth rate and the calculation of confidence intervals in the one-step and two-step modeling method.

MATERIALS AND METHODS

Primary model

Since only the exponential phase of growth is studied in this research, the following simple primary model is applied:

$$\frac{dN(t)}{dt} = \mu_{max} \cdot N(t) \tag{1}$$

with $N(t)$ $[CFU/mL]$ the cell density as a function of time and $\mu_{max}[h^{-1}]$ the specific growth rate. The logarithmic form of this equation is often preferred:

$$\frac{dn(t)}{dt} = \mu_{max} \tag{2}$$

where $n(t)$ $[\ln(CFU/mL)]$ is the natural logarithm of the cell density.

Monte Carlo simulations

Random values are taken from various probability distributions during the simulations in this research by using the function *random* from the Statistical Toolbox of Matlab version 7.14 (The MathWorks Inc.).

Parameter estimations

The objective function of the parameter estimations considered in this research is the minimization of the sum of squared errors (SSE) for $M_\#$ measurements of the output variable X, i.e., the cell density or the growth rate :

$$SSE = \sum_{i=1}^{M_\#} \left(X_{m,i} - X_{p,i}(p)\right)^2 \tag{3}$$

with $X_{m,i}$ the measured value and $X_{p,i}(p)$ the predicted value for a set of parameters p. The $(100-\alpha)\%$ confidence interval of every parameter p_i is calculated based on the Student's t-distribution:

$$\left[p_i \pm t_{\left(100-\frac{\alpha}{2}\right),M_\#-P_\#} \cdot \sqrt{\sigma_{p_i}^2}\right] \tag{4}$$

where $P_\#$ is the number of parameters and consequently $M_\# - P_\#$ is the number of degrees of freedom. $\sigma_{p_i}^2$ is the variance on the model parameter p_i and is found on the main diagonal of the variance covariance matrix V, which is approximated as the inverse of the Fisher Information Matrix F (Walter and Pronzato, 1997):

$$\sigma_{p,i}^2 = V(i,i) \tag{5}$$

$$V = F^{-1} \tag{6}$$

$$F = \frac{1}{MSE} \cdot J^T \cdot J \tag{7}$$

$$MSE = \frac{SSE}{M_\# - P_\#} \tag{8}$$

with J the Jacobian matrix and MSE the mean sum of squared errors. The optimal set of parameters are calculated using the *lsqnonlin* routine of the Optimization Toolbox of Matlab version 7.14.

Experimental protocol assumed in the simulations

The variability on the measurements is of course dependent on the experimental protocol. The simulations are performed assuming a widely adopted protocol with viable plate counting. For this protocol, dilutions of a sample are made and the cells in this diluted sample are grown on a Petri plate containing solid medium. The concentration of cells in the sample is calculated after counting the number of colonies that originate from the individual cells. In this protocol, a relatively high cell density is needed (e.g., more than 1,000 CFU/mL). For the simulations in this research, 50 µL is transferred from a 10-fold dilution to a plate to obtain between 40 and 400 colonies.

RESULTS AND DISCUSSION

Two options present themselves to study the variance of the microbial specific growth rate. The first being an experimental study and the second a simulation study. In case of an experimental study of the variance of the growth rate, both the experimental measurement error and the microbial variability would be included. The problem with an experimental determination of the variance of the specific growth rate (or in fact any variance) is that a large amount of data is needed to obtain an accurate estimate of the variance. Even though it is a common practice to

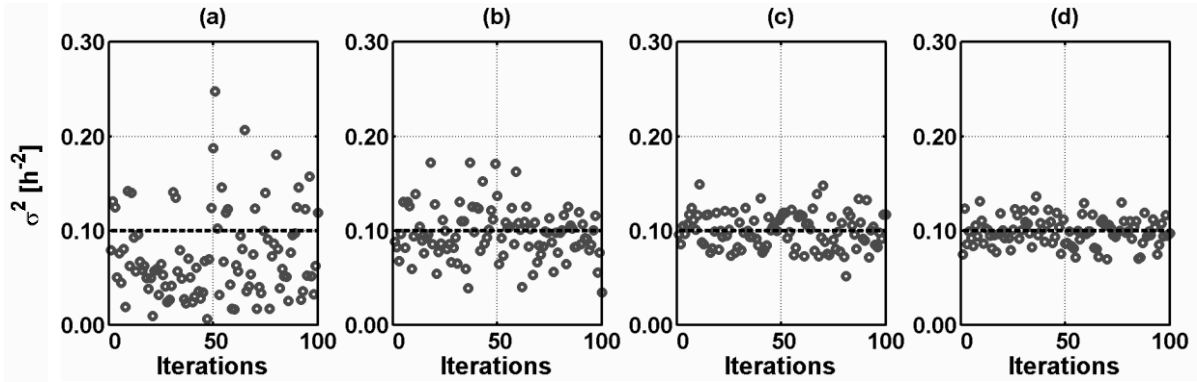

Fig. 1: 100 Simulations of calculated variances based on (a) 5, (b) 20, (c) 50 and (d) 100 samples generated with a normal distribution and variance of $0.1\ h^{-2}$.

determine a variance, standard deviation or standard error on as little as three data points, many more are needed to obtain an accurate estimate of the population variance. This point can be proven by means of a simple simulation study.

Say that for a certain experiment the growth rate is normally distributed with a variance of $0.10\ h^{-2}$, than a number of growth rates can be randomly sampled from this distribution. The variance of the growth rate is calculated with the general formula for the sample variance. This calculation is represented by Eq. (8), with the number of parameters equal to one and the predicted value equal to the mean. This same calculation is performed 100 times for situations with 5, 20, 50 and 100 samples. The calculated values of the variance of the growth rate are plotted in Fig. 1. These simulation results illustrate that a large number of samples is needed to obtain an accurate estimate of the variance, i.e., with a high certainty of being close to the true population variance. This could also be concluded by calculating the confidence bounds of the variance for different sample sizes (for further information, see, e.g., Neter et al., 1990). For this reason, it is in practice infeasible to obtain information on the homo- or heteroscedasticity of the growth rate measurements based on an experimental method. Consequently, this study of the variance of the growth rate is performed by means of simulations.

In a first step, the variance of the growth rate that is characteristic to the variability of the individual cells in a population is studied. Continuing on these results, the effect of the experimental uncertainty of the cell density measurements on the calculated growth rates is determined. Then, the effect of the experimental protocol on the variance of the growth rate is examined. Finally, the calculation of confidence intervals is discussed.

Variance due to the variability between individual cells

It is well known that individual cells have varying division times under the exact same environmental conditions. The combination of the cell division times of all the individual cells results in the growth rate of a population and therefore also in the variability on the growth rate that is due to the behavior of individual cells. The variance of the growth rate that originates from this variability between individual cells is discussed in this section based on simulations of the growth of a population as a group of individually considered cells. For the first simulation, the growth of a population is simulated starting from a single cell.

Examples of studies of single cell behavior are found, e.g., in Metris et al. (2005), Pin and Baranyi (2006) and Koutsoumanis and Lianou (2013). In these publications, the probability distributions of the division times of several generations are reported. The results indicated that the mean and variance of these distributions are approximately constant after the lag phase. Since only the growth rate is considered in this research, and not the lag phase duration, the parameters of the probability distributions are assumed to be constant. The probability distribution is assumed to be lognormal, since the division time can never have a negative value. It is important to stress that the conclusions of the following simulation study would remain unchanged if, e.g., a Weibull or gamma probability distribution is used. Based on the results of Pin and Baranyi (2006) for *Escherichia coli* K12 at $32°C$, the mean and variance of the division time are set equal to $0.50\ h$ and $0.04\ h^2$, respectively. This probability distribution is used to simulate 500 growth curves, starting from a single cell. The simulations are performed in time steps of $0.1\ min$. Each time a cell reaches the division age, the mother cell is replaced by two daughter cells and they are each assigned a random division time according to the previously described probability distribution. The resulting growth curves are shown in Fig. 2. Fig. 2 (a) illustrates that a large variation in cell densities can occur, due to the variability of the individual cells. However, when looking at the logarithm of the cell densities in Fig. 2 (b), it seems that the main divergence between the growth curves of the different simulations is confined to the first 2-ln increase of the cell density. After this point, the logarithmic cell densities increase more or less parallel to one another. This can easily be explained by the law of large numbers or mathematically by this simple formula to calculate the variance of the mean σ_m^2 of a number of uncorrelated samples $S_\#$, each of which has a known variance σ^2:

$$\sigma_m^2 = \frac{\sigma^2}{S_\#} \tag{9}$$

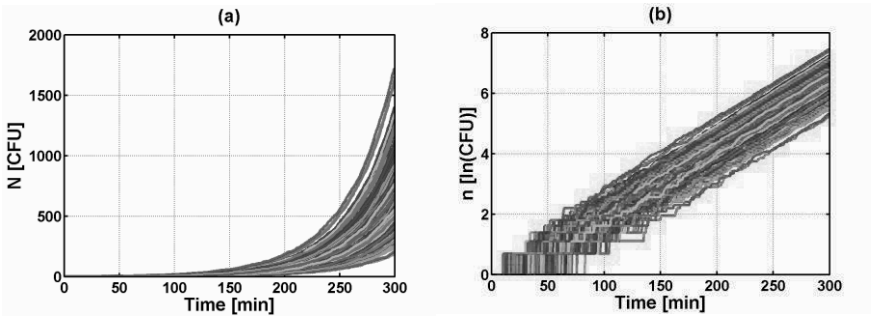

Fig. 2: Growth of a population during 5 h, starting from a single cell expressed in (a) cell density and (b) logarithm of the cell density.

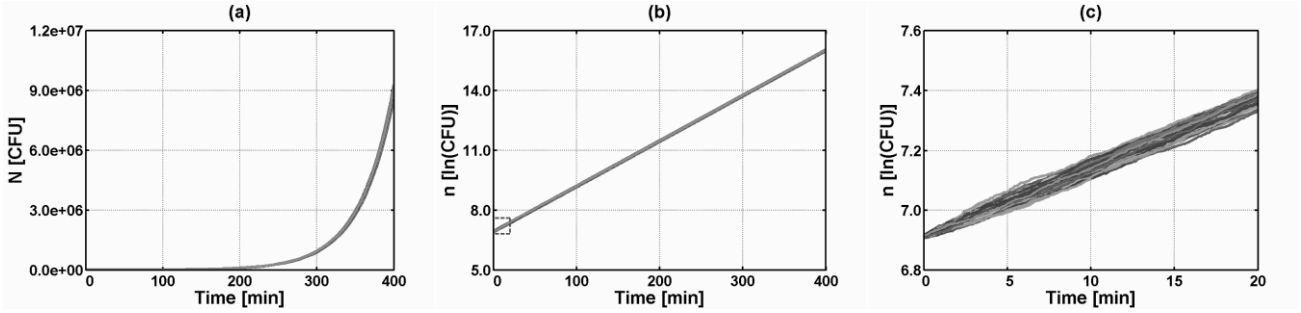

Fig. 3: 500 Monte Carlo simulations of the growth of a population starting from the point it reaches 1,000 cells. The population size is presented both in (a) untransformed and (b) logarithmically transformed units. A detailed view of the divergence between the simulations is represented in (c).

Applied to the current case study, this means that the probability distribution of the growth rate of a population becomes narrower with an increasing number of cells. Since growth experiments in liquid media are traditionally performed with concentrations between 10^3 and $10^9\ CFU/mL$ and in volumes of at least several milliliters, it is worth wondering if this variability is still relevant if such a high number of cells is considered.

To investigate this question, 500 Monte Carlo simulations of the growth of a population are performed starting from a single cell to about $9 \cdot 10^6$ cells. All these simulations are plotted in Fig. 3, starting from the point where they reach 1,000 cells. In this way, the figure illustrates the possible differences in the growth of a population starting from 1,000 cells. Where the growth of cultures starting from 1 cell (Fig. 2) showed clearly that many different scenarios are possible, there is almost no distinction visible in the growth curves starting from 1,000 cells (Fig. 3 (a) and (b)). Only when looking very closely at the first minutes after 1,000 cells are reached in Fig. 3 (c), the slight differences between the simulations are clear.

When studying the growth rate of a population considering the variability in single cell behavior, it is worth making a distinction between the *instantaneous* specific growth rate and the *time-independent* specific growth rate. In this distinction the instantaneous growth rate is valid at a specific point in time. This growth rate is dependent on the division times of all the cells in the population and it is ever changing with time. The time-independent specific growth rate is calculated from the growth of a population over a certain time period by considering that the logarithm of the cell density versus time is linear. For this calculation the specific growth rate is assumed to be independent of time.

The simulations of Fig. 2 and Fig. 3 demonstrate that the variance of the instantaneous specific growth rate decreases with time, due to the increase in the number of cells, as formulated by Eq. (9). The variance of the time-independent specific growth rate on the other hand is dependent on the range of cell densities considered during the growth of the population. It is the instantaneous specific growth rate that represents the variability of the growth of a population and it is the effect of the variance of this growth rate that should be studied by researchers who are interested in providing probability distributions for the number of cells in a population as a function of time (contrary to what has been done by, e.g., Koutsoumanis and Lianou (2013)). The growth rate that is studied in this research, on the other hand, is the time-independent growth rate. It can be determined for each simulation by estimating the slope of the curves in Fig. 3 (b). The mean of these growth rates is $1.37\ h^{-1}$ with a variance of just $9.41 \cdot 10^{-7}\ h^{-2}$. This very low variance demonstrates that the variability of the growth rate of the population itself can be neglected during conventional growth experiments. The variance on the growth rate that is found is thus due to the experimental uncertainty on the measurements of the cell density. This experimental uncertainty is studied in the next section.

Uncertainty of the cell density measurements

Based on the experimental protocol (explained in the Materials and Methods section), the cell density measurements with experimental uncertainty are simulated. For this simulation, an experiment is considered where cells are grown from a concentration of 7 to $19\ ln(CFU/mL)$ at a growth rate of $1\ h^{-1}$. To obtain the experimental uncertainties, the necessary probability

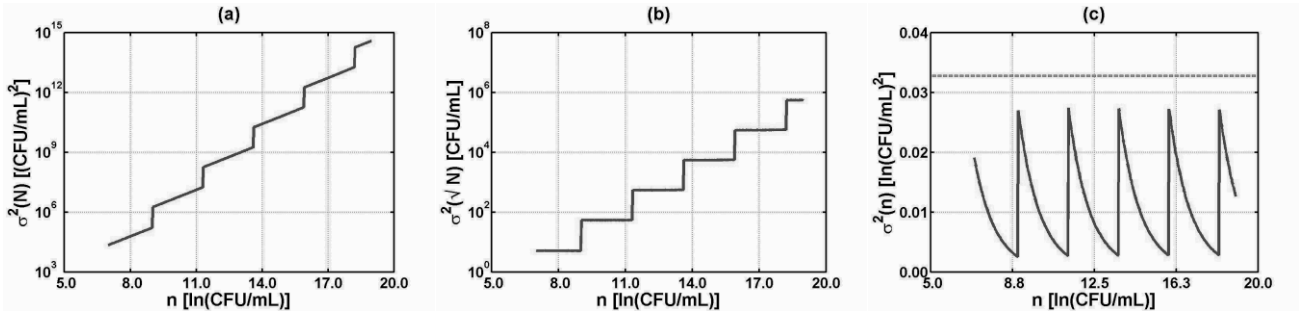

Fig. 4: Variance of (a) the cell density and its (b) square root and (c) logarithmic transformation with the experimentally determined variance from Van Derlinden et al. (2008) (- -).

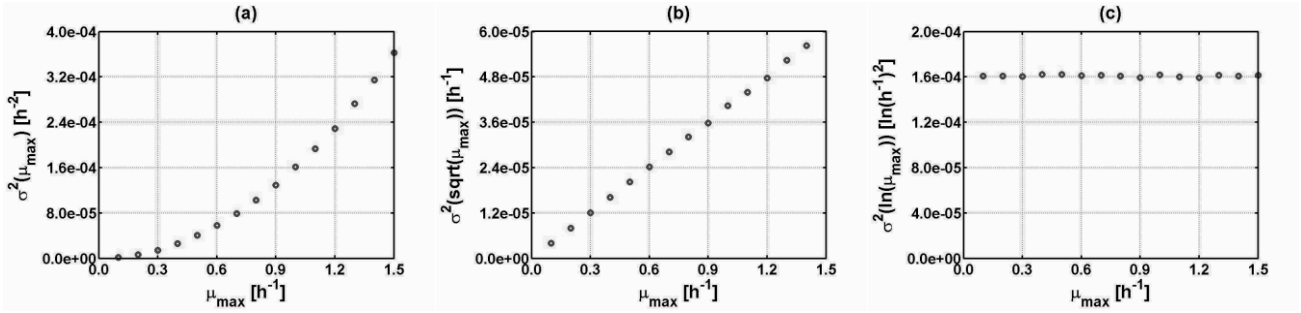

Fig. 5: The variance of (a) the growth rate and its (b) square root and (c) logarithmic transformation versus the growth rate.

distributions are included in the calculation. Pipetted volumes of 100 and 900 µL to make the dilution series are assigned a normal distribution with a standard deviation of respectively 0.3 and 1.8 µL, based on the manufacturer's specifications (Biohit, Sartorius AG). The amount of cells contained in a sample when making dilutions and when plating are determined by a Poisson distribution. To determine the variance of the measurements of the cell density, a Monte Carlo simulation with 50,000 iterations is performed at every cell density. The resulting variance is plotted as a function of the logarithm of the cell density in Fig. 4 (a). This figure illustrates how the variance increases exponentially with the amount of cells plated, due to the variance of the Poisson distribution, which increases with the mean. It also demonstrates that the error increases stepwise with every additional dilution, since the error is multiplied by 10 for each dilution when calculating the cell density in the undiluted sample. If the square root of the cell density is used, the variance is stabilized within the same dilution but still increases with every dilution (Fig. 4 (b)). When taking the logarithm of the cell density, the variance decreases with an increasing number of cells within the same dilution (Fig. 4 (c)). In this way, it compensates for the increase of the variance with every additional dilution. Thus, taking the logarithm of the cell density doesn't completely stabilize the variance but it prevents making a systematic error during fitting, and that is what matters most. Fig. 4 (c) also indicates the experimentally determined variance of the logarithm of the cell density that was reported by Van Derlinden et al. (2008) for the same experimental procedure. By nature, this experimentally determined value is higher than the ideal values of the current study.

These results demonstrate that the necessary variance stabilizing transformation is dependent on the experimental protocol used. Care should be taken not to make a logarithmic transformation of (a measure of) the cell density without considering if it is a valid procedure for the given experimental protocol. The same type of simulations is used in the next section to generate in silico results at different growth rates.

Experimental uncertainty of the growth rate

Since it has been established in the previous section that logarithmic transformations of the cell density measurements are acceptable for the considered experimental protocol, parameter estimations are performed on such data to estimate the growth rate. Measurements are simulated for experiments with growth rates between 0.1 and 2.0 h^{-1}. For each experiment, 10 samples are taken at the same concentrations. The distribution of the cell density measurements is identical to the distribution described in the previous section. The logarithmic form of the simple primary model described in Eq. (2) is fitted to these cell densities to find the growth rate. This procedure is repeated 50,000 times at every growth rate, to obtain an accurate estimate of the variance.

Fig. 5 (a) represents the relationship between the growth rate and its variance. These results prove that the variance on the experimentally determined growth rate is much higher at high growth rates than at low growth rates. Therefore, when fitting a secondary model on untransformed growth rate data with an unweighted least squares method, too much confidence is placed in the results at high growth rates in comparison with the results at low growth rates. This leads to inaccurate predictions of the microbial growth at low growth rates. Performing a weighted least squares estimation is often not a good solution because too much experimental data is required to obtain an accurate estimation of the variance on the growth rate (as demonstrated previously). The square root

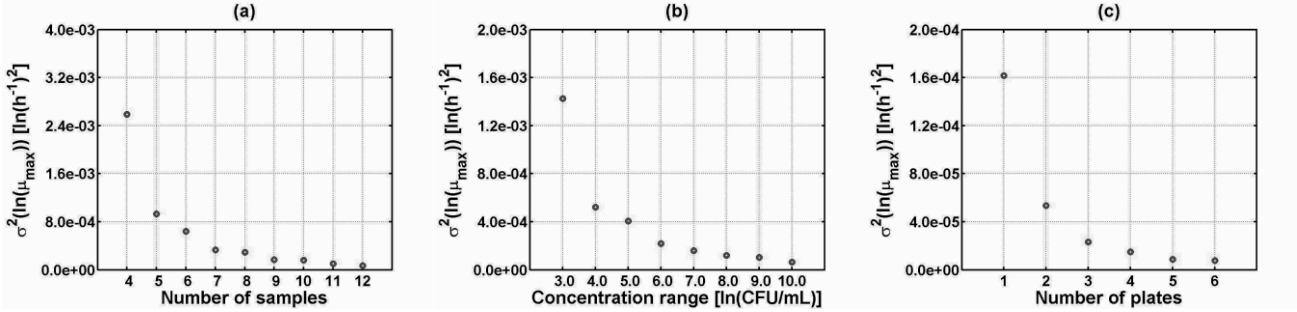

Fig. 6: Dependency of the variance of the logarithm of the growth rate on (a) the number of samples, (b) the concentration range and (c) the number of plates for each sample.

transformation of the growth rate is often suggested as a variance stabilizing transformation but the results of Fig. 5 (b) illustrate that this is not the case in the current study. This transformation only transforms the exponential relationship into a linear relationship. The logarithmic transformation on the other hand does result in a homoscedastic variance (Fig. 5 (c)). This transformation is therefore most suitable for researchers who wish to apply the two-step modeling method for the considered experimental protocol. It can even be demonstrated that for the very strict experimental protocol used in these simulations, the two-step method with logarithmically transformed growth rates has an objective function that is equivalent to that of the one-step method and therefore leads to the exact same combination of parameter estimates. The experimental protocol assumed for the simulations is however unrealistically strict. The following section therefore evaluates the effect of changes in the experimental protocol on the variance of the growth rate.

Applicability of the two-step method

The simulations made in the previous section demonstrated that it is possible to stabilize the variance on the experimentally determined growth rates by making a logarithmic transformation. However, a constant variance is only obtained if measurements are taken according to a very strict experimental protocol. First of all, the analysis is made for a situation in which only experimental results of the exponential phase of growth are considered. In practice this would mean that the lag and stationary phase have to be omitted during sampling or that the results of these phases of growth have to be removed from the results. It is however preferred not to exclude these phases of growth to avoid the modeler having to make decisions on when the lag phase ends and when the stationary phase begins.

The logarithmic transformations of the growth rate can only be homoscedastic if the same amount of samples are taken, at the same concentrations and with the same number of plates for each sample in every experiment. This is, however, a very unlikely scenario and experimenters will often choose to change the sample frequency, the amount of plates made per sample, the amount of experiments at some conditions and the range of concentrations included in an experiment. All these changes in the experimental protocol have a significant effect on the variance of the growth rate, as demonstrated in Fig. 6. The variance of the logarithm of the cell density decays exponentially with an increase of (*i*) the number of samples, (*ii*) the concentration range and (*iii*) the number of plates. This means that, in practice, the variance of the growth rates still varies, even if the correct variance stabilizing transformation is applied.

Calculation of confidence intervals

Apart from estimating the model parameters, also confidence bounds of these parameters should be provided. These confidence bounds give an indication of the amount of confidence that can be placed in the parameter estimates for a given set of experimental data and they can be used to produce confidence intervals on the model predictions. However, obtaining accurate confidence intervals is often not possible when applying the two-step method since a large number of measurements is necessary. There are two important reasons why a large amount of data is needed. The first reason is that in the calculation of the confidence bounds, according to the procedure described in Eq. (3) – (8), the MSE is used as an approximation of the variance on the measurements. As explained before, a large amount of measurements is needed to obtain an accurate estimate of the variance. This means that if, e.g., 100 measurements are needed to obtain a sufficiently accurate estimate of the measurement variance, the two-step method would require 100 experiments where the one-step method only needs 100 samples spread over a much smaller number of experiments. The second reason is that the Cramér-Rao bound states that the inverse of the Fisher information matrix provides the lower bound of the variance on the model parameters. For maximum likelihood estimators, such as least squares optimizations, the Cramér-Rao bound is only reached for an infinite amount of measurements (Walter and Pronzato, 1997). Consequently, the two-step method results in a larger underestimation of the variance on the model parameters due to the smaller amount of measurements, compared to the one-step method. Apart from these technical motivations, it is also conceptually more appealing to obtain uncertainties based on the cell evolution data for the prediction of uncertainties on such an evolution of cells. The one-step method always has a much larger amount of measurements at its disposal than the two-step method and therefore leads to a more accurate determination of the confidence intervals of the parameter estimates.

CONCLUSIONS

The first important conclusion of this work is that the variability between individual cells can generally be neglected when studying the variability of the growth rate, since the large amount of cells in the considered populations causes there to be very little variability in the growth rate of the entire population. Therefore, the variability that is found on the growth rate is a consequence of experimental errors. By simulating this variability, it is confirmed that the logarithmic transformation of the cell densities should be taken when working with dilutions and a plate count method. But it is also important to remember that the necessary transformation is clearly dependent on the chosen experimental protocol. Based on the same simulations, it is demonstrated that the logarithmic transformation is most suitable to stabilize the variance on the measured growth rate. However, this variance is proven to be highly dependent on the specifications of the applied experimental protocol, which means that the individual growth rate measurements can in practice not be weighted correctly. Finally, it is concluded that the one-step method will result in a more accurate determination of the confidence intervals of the parameter estimates than the two-step method. Based on all these findings it can be concluded that the one-step modeling method is more suitable for the estimation of parameters of secondary models.

Guidelines for building secondary models:

- Measures of variation (i.e., standard error, variance, confidence intervals, …) shouldn't be trusted if small amounts of data are used.
- The variance on the growth rate is almost entirely determined by experimental uncertainty and can thus be minimized by obtaining more (accurate) measurements.
- Choose the one-step method to avoid statistical errors during the parameter estimation.
- Choose the one-step method to obtain a better approximation of the confidence bounds of the parameter estimates.

ACKNOWLEDGEMENTS

This work was supported by project PFV/10/002 (Center of Excellence OPTEC-Optimization in Engineering) of the KU Leuven Research Fund, projects G.0930.13 and KAN.15189.13 of the Fund for Scientific Research-Flanders, and the Belgian Program on Interuniversity Poles of Attraction, initiated by the Belgian Federal Science Policy Office (IAP Phase VII/19 DYSCO).

REFERENCES

Alber, S.A. and D.W. Schaffner. 1992. Evaluation of data transformations used with the square root and Schoolfield models for predicting bacterial growth rate. *Applied and Environmental Microbiology*, 58(10): 3337-3342.

Augustin, J.-C. and V. Carlier. 2000. Modelling the growth rate of *Listeria monocytogenes* with a multiplicative type model including interactions between environmental factors. *International Journal of Food Microbiology*, 56: 53-70.

Coroller, L.; V. Guerrot; V. Huchet; Y. Le Marc; P. Mafart; D. Sohier; D. Thuault. 2005. Modelling the influence of single acid and mixture on bacterial growth. *International Journal of Food Microbiology*, 100: 167-178.

Francois, K.; F. Devlieghere; K. Smet; A.R. Standaert; A.H. Geeraerd; J.F. Van Impe; J. Debevere. 2005. Modelling the individual cell lag phase: Effect of temperature and pH on the individual cell lag distribution of *Listeria monocytogenes*. *International Journal of Food Microbiology*, 100: 41-53.

Koutsoumanis, K.P. and A. Lianou. 2013. Stochasticity in colonial growth dynamics of individual bacterial cells. *Applied and Environmental Microbiology,* 79 (9): 2294-2301.

Masana, M.O. and J. Baranyi. 2000. Adding new factors to predictive models: the effect on the risk of extrapolation. *Food Microbiology*, 17: 367-374.

Metris, A.; Y. Le Marc; A. Elfwing; A. Ballagi and J. Baranyi. 2005. Modelling the variability of lag times and the first generation times of single cells of *E. coli*. *International Journal of Food Microbiology*, 100: 13-19.

Neter, J.; W. Wasseman and M.H. Kutner. 1990. *Applied linear statistical models*. CRC Press, Boca Raton, USA.

Pin, C. and J. Baranyi. 2006. Kinetics of single cells: Observations and modelling of a stochastic process. *Applied and Environmental Microbiology*, 72 (3): 2163-2169.

Ratkowsky, D.A.; T. Ross; T.A. McMeekin and J. Olley. 1991. Comparison of Arrhenius-type and Belehradek-type models for prediction of bacterial growth in foods. *Journal of Applied Bacteriology*, 71: 452-459.

Schaffner, D.W. 1998. Predictive food microbiology Gedanke experiment: why do microbial growth data require a transformation? *Food Microbiology*, 15: 185-189.

te Giffel, M.C. and M.H. Zwietering. 1999. Validation of predictive models describing the growth of *Listeria monocytogenes*. *International Journal of Food Microbiology*, 46: 135-149.

Van Derlinden, E.; K. Bernaerts; J.F. Van Impe. 2008. Accurate estimation of cardinal growth temperatures of *Escherichia coli* from optimal dynamic experiments. *International Journal of Food Microbiology*. 128: 89-100.

Versyck, K.J.; K. Bernaerts; A.H. Geeraerd; J.F. Van Impe. 1999. Introducing optimal experimental design in predictive modeling: A motivating example. *International Journal of Food Microbiology*, 51: 39-51.

Walter, E. and L. Pronzato. 1997. *Identification of parametric models from experimental data.* Springer, Germany, Berlin.

Whiting, R.C. and R.L Buchanan. 1993. "A classification of models for predictive microbiology." *Food Microbiology*, 10: 175-177.

Zwietering, M.H.; H.G.A.M. Cuppens; J.C. De Wit; K. Van 't Riet. 1992. Evaluation of data transformations and validation of a model for the effect of temperature on bacterial growth. *Applied and Environmental Microbiology*, 60(1): 195-203.

RECENT EU-INITIATIVES IN FOOD MODELING AND SIMULATION

FoodMC: A European COST Action on Food Modelling

Alberto Tonda
UMR 782 GMPA, Team MALICES, INRA
1 av. Lucien Brétignières, 78850, Thiverval-Grignon, France
email: alberto.tonda@grignon.inra.fr

KEYWORDS
Food process modelling, European project, COST

ABSTRACT

Methodologies and tools from Maths and Computer Science (MCS) are emerging as key contributors to modernization and optimization of processes in various disciplines: the agri-food sector, however, is not a traditional domain of application for MCS, and at the moment there is no community organized around solving the issues of this field. The COST Action FoodMC brings together scientists and practitioners from MCS and agri-food domains, stimulating the emergence of new research, and structuring a new community to coordinate further investigation efforts. Exploiting approaches originating at different sub-fields of MCS, from applied mathematical models to knowledge engineering, this COST Action will cover two main topics: understanding and controlling agri-food processes; and eco-design of agri-food products.

INTRODUCTION

European Cooperation in Science and Technology (COST) is Europe's longest-running intergovernmental framework for cooperation in science and technology. Founded in 1971, COST holds a successful history of funding science and technology networks for over 40 years, offering scientists the opportunity to embark upon bottom-up, multidisciplinary cooperation across all science and technology domains.

Also known as COST Actions, these science and technology networks allow scientists to grow their ideas by sharing them with their peers. This gives impetus to their research, career and innovation. Researchers, engineers and scholars from both public and private sectors can set up their own network in any field of science and technology.

COST Actions grow throughout a funding period of 4 years. The funding covers networking activities such as meetings (e.g. travel, subsistence, local organiser support), conferences, workshops, short-term scientific missions (STSMs), training schools, publications and dissemination activities. COST does not fund research itself.

CHALLENGE

Food processing and agricultural products catering companies are one of the major employers and economic forces in the EU, representing both a central component of the agro-food system, and a crucial provider of biomaterials and biofuels. In recent years, this strategic industry has been facing unprecedented challenges, mainly concerning food security and the threat of climate change. Additionally, the production of processed agricultural products needs to adopt and comply with several new regulations, aiming at reducing waste, improving re-utilization of by-products, limiting energy consumption and lowering the overall environmental impact. These demanding objectives can only be achieved through appropriate adaptation and innovation in the food processing activity. Disruptive innovations, however, require considerable economic efforts and the development of new skills not readily available in the agro-food domain, especially in small and medium enterprises (SMEs). A considerable number of unsustainable practices are still in place, due to the high cost of experimenting with new techniques on existing production/supply chains and validating scale-up.

There is evidence that developing Mathematical and Computer Science (MCS) models for the target processes can contribute to solving the issue (Trystram (2012)), allowing even SMEs to optimize resource management and economic outputs, while guaranteeing the current levels of quality and availability of products. The agro-food industry, however, is not a traditional application domain for MCS: at the moment, there is no structured community around this issue, nor a coordinated effort to advance the state of the art; and building adequate mathematical models for specific applications is extremely knowledge and labour intensive. It is the role of academic research to initiate the development of methods, functional models, software or technologies, which will be critical to guide the evolution of the food processing industry with regards to the grand challenges of the future.

MCS researchers and practitioners can also benefit from working on agro-products industry applications, since the field provides considerable challenges to existing methodologies in MCS: uncertainty of the data, multi-scale description of the systems, coupling of models, rep-

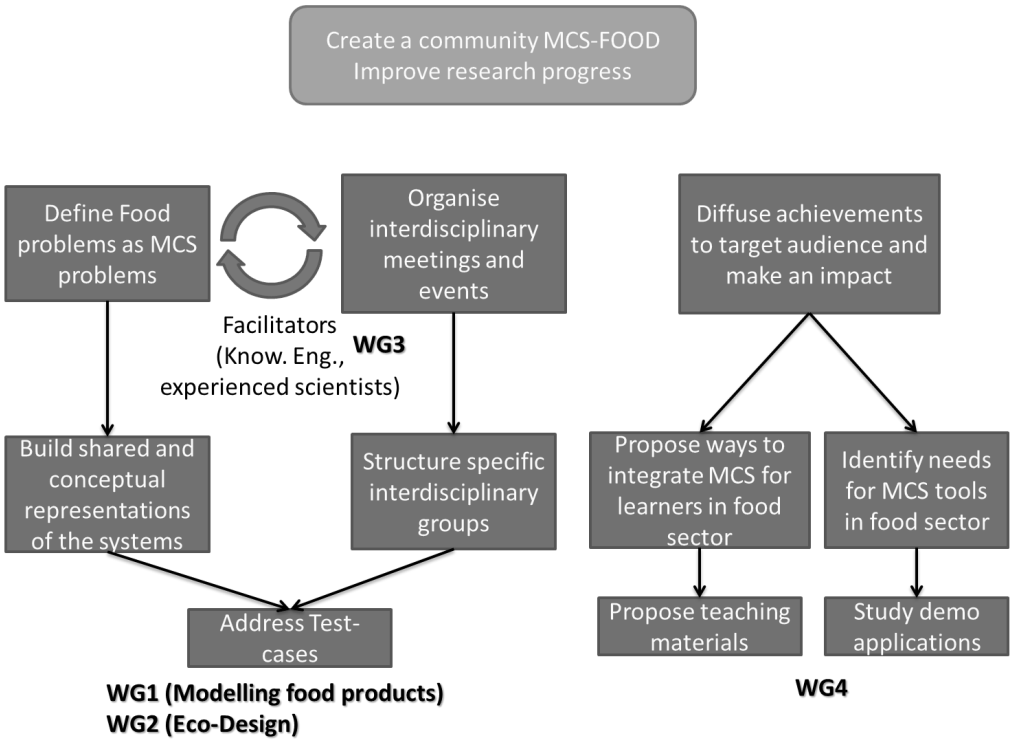

Figure 1: Organization of the Working Groups envisioned in the Action.

resentation of expert knowledge, etc. As the upcoming challenges for the industry grow more pressing, promoting cooperation between agro-food and applied mathematics becomes more and more urgent. The aim of this COST Action is thus to create a community of scientists and practitioners from the two different domains, stimulating the emergence of new research and ideas tackling these ambitious topics.

The development of novel mathematical and computer models, following the complex systems and knowledge engineering paradigms, has been slowly gaining support in the agro-food community over the last two decades (Van Mil et al. (2014), Perrot et al. (2016)). Existing projects, however, are scattered and uncoordinated, focusing more on the solutions to specific issues than on an organized collection of demands and techniques in the field: for these reasons, major methodological breakthroughs, even stemming from applications, are still extremely rare. Although food production is a major industry in most countries, the number of publications dedicated to the treatment of food industry problems by means of innovative MCS modelling is well below that of other types of industries. Coordinating the currently divided research efforts is crucial to avoid re-discoveries and dispersion of useful data, and at the same time promoting the sharing of theoretical and experimental results. Moreover, the application domain of agro-food products is rich and multi-faceted, and research efforts so far have not been balanced over all aspects. As a result, several features of the considered challenges are not well understood, while the expertise around others should be further developed. Significant progress in the domain can be obtained by providing a roadmap with well-defined MCS problems, addressing critical issues in food processing, in particular food security and sustainability. This issue calls for the close collaboration of domain specialists with mathematicians and computer scientists.

ACTION ORGANIZATION

FoodMC is going to officially start on **April 11, 2016** and currently includes researchers from 21 different European nations and partner countries (Bosnia and Herzegovina, Belgium, Bulgaria, Croatia, Denmark, Germany, Greece, Ireland, Italy, former Yugoslav republic of Macedonia, France, Malta, The Netherlands, Norway, Poland, Portugal, Romania, Serbia, Slovenia, Spain, United Kingdom).

The Action is tentatively divided into four Working Groups (WGs), organized as in Figure 1. Each WG is going to focus on a specific aspect of the network, ranging from exploring suitable real-world case studies, to discussing industrials' and practitioners' needs for efficient modelling tools, to gathering and sharing information.

WG 1: Modelling food products and processes

This group is focused on MCS solutions for modelling food properties and food processes. As the domain is very large, the group will identify the opportunities susceptible to lead to breakthroughs and to meet stakeholders needs, and will focus the work on the description of benchmark case-studies. This WG will produce a state-of-the-art review of food products and food process modelling, an overview of the scientific challenges and finally identify stakeholders concerns. WG 1 will provide guidelines for research at both the fundamental and the applicative level. The WG members will be in charge of identifying modelling approaches with a potential high impact on food sector activities, and define benchmark case-studies that will be addressed during Action workshops and STSMs. Finally, this WG will promote the use of MCS solutions in the food sector through the creation of training schools.

WG 2: Eco-design of food processes

This group will describe the kind of systems to be addressed by eco-design, the appropriate MCS techniques and tools to be used, it will propose illustrative/pedagogical case-studies and define the boundaries of this interdisciplinary research, that will lead to the delivery of suitable methods and tools in the future. Mirroring the actions on WG 1, WG 2 will describe the state of the art for modelling in eco-design, addressing the complex network of interactions linking the agro-food activities together, which grows more intricate with system size (local, regional, international). To do so, the WG will collect and integrate inputs from involved stakeholders and specialists from different disciplines, through dedicated meetings, workshops and STSM. Finally, it will identify a few representative case studies that the scientific community could efficiently address.

WG 3: From scientific results to tools

The WG has the objective to promote the development of computer applications, allowing a larger audience of users to exploit scientific results. Expert knowledge, experimental data and mathematical models will be used to answer the users' needs. WG 3 will address the problem of the low delivery of operational tools based on food science research results. Existing applications, such as web semantic applications, knowledge-based systems, simulation tools, will be adapted to the food sector. The WG will identify the main needs of the users that can benefit the most from the development of such tools. A limited number of case-studies will be identified and addressed during the Action, through specific workshops and STSMs, from the second year. At the end of the Action, results will be disseminated to interested users through a comprehensive report, and a training school will be organized with the gathered materials.

WG 4: Knowledge acquisition and diffusion

The WG's objective is to promote dissemination of the Action results, via the design and maintenance of the Action website. More than a support to convey related information and deliverables, the Action website will stimulate knowledge transfer. This WG's activity will also favor communication, as successful interdisciplinary research requires a mutual understanding between participants with different backgrounds. Face-to-face meetings of specialists from distant disciplines are generally insufficient to reach this point, because a typical expert relies on a great deal of tacit and implicit knowledge. Shared understanding can be promoted by formalization of tacit knowledge and participatory modelling using, for example, visualization techniques that support acquisition of knowledge. WG members will work with the other WGs leaders to take part into activities that require strong interdisciplinary exchange, and organize the co-construction of knowledge models.

CONCLUSIONS

While the topic of food modelling has been partially explored in several applied European-level projects, FoodMC aims at creating a European network dedicated to a high-level discussion on the current state and future of food modelling, and its repercussions on supply chains and eco-design of processes. Ideally, this COST Action could be a great think tank to devise and propose new research project, and explore cooperation with private companies. As it is always possible to join a COST Action in its first years, I encourage the reader to seek further information and, if interested, contact the main proposer or the participants, on the COST Action website[1].

REFERENCES

Perrot N.; De Vries H.; Lutton E.; van Mil H.G.; Donner M.; Tonda A.; Martin S.; Alvarez I.; Bourgine P.; van der Linden E.; et al., 2016. *Some remarks on computational approaches towards sustainable complex agri-food systems. Trends in Food Science & Technology*, 48, 88–101.

Trystram G., 2012. *Modelling of food and food processes. Journal of Food Engineering*, 110, no. 2, 269–277.

Van Mil H.G.; Foegeding E.A.; Windhab E.J.; Perrot N.; and Van Der Linden E., 2014. *A complex system approach to address world challenges in food and agriculture. Trends in Food Science & Technology*, 40, no. 1, 20–32.

[1] http://www.cost.eu/COST_Actions/ca/CA15118

Q-SAFE ERASMUS TRAINING PROGRAMME – TEACHING AND STUDENT LEARNING EXPERIENCES

Enda Cummins
School of Biosystems and Food Engineering
University College Dublin
Dublin
Ireland
E-mail: enda.cummins@ucd.ie

Jeanne-Marie Membré
Food Safey and Microbiology
ONIRIS
La Chantrerie
France

Jan Van Impe
Department of Chemical Engineering,
KU Leuven
Gebroeders De Smetstraat 1, B-9000
Gent
Belgium

Kostas Koutsoumanis
Department of Food Science and Technology
Thessaloniki
Aristotle University of Thessaloniki
Greece

Serafim Bakalis
School of Chemical Engineering
University of Birminghan
Birminghan
UK

Aludena Hospido
Department of Chemical Engineering
University of Santiago de Compostela
15782 - Santiago de Compostela
Spain

Ismael Martínez Lede
Dept. I+D+i FEIRACO S. Coop. Galega
Spain

Vasilis Valdramidis
Department of Food Studies and Environmental Health
Msida MSD 2080
University of Malta
Malta
E-mail: vasilis.valdramidis@um.edu.mt

KEYWORDS
Quantitative tools, ERASMUS, sustainability, Food.

ABSTRACT

Erasmus+ Programmes (Key Action 2: Strategic partnerships in the Field of education, training and youth) are funded by the European Commission as part of an EU lifelong learning initiative. This paper reports on a 10 day intensive teaching programme as part a Earmsus + on Quantitative Tools for Sustainable Food and Energy in the food chain with 7 international third level institutions and 1 industrial partner. This paper describes the development of the teaching activity, including programme aims and design, and our experience in implementing it. The study highlights the objectives and programme of study for students and the need to recognise learning achievement. Evaluation, based on student feedback and on students' performance suggests overall success of the programme. On a satisfaction rating scale of 1 - 5, 44% of students (n = 18) regarded the experience as "excellent" and awarded a top score of 5 (56% awarding a score of 4); 84% of students awarded a score of 4 and 5 when asked about the importance of the course to further their careers. The programme was particularly useful for promoting intercultural communication and collaboration. In addition to detailing the Erasmus paradigm adopted, through lessons learned, it is hoped this paper will help to improve good international collaborative teaching practices.

INTRODUCTION

With increased globalisation of trade in goods and services, cross-border cooperation in education seems a logical and natural progression (Ekti 2013). Educational cooperation has remained a top priority for many international organisations, including the Organisation for Economic Co-operation and Development (OECD) and United Nations Educational, Scientific and Cultural Organisation (UNESCO) (Jallade 2011). It is therefore critical to promote mutual exchange through interdisciplinary innovative programmes. In this context the European Union aims to be the global leader in developing a knowledge-based economy (Molle 2007).

EU mobility and exchange has been facilitated by the EU Lifelong Learning (LLL) Programme (2007–2013) and subsequently Erasmus + (2014-2020) providing learning opportunities for young and old alike (Jallade 2011). These mobilities are something all people should be encouraged to participate in, as we never stop learning throughout our lives (Laal and Laal 2012). The EU has set Lifelong Learning as one of its key strategic objectives (Pépin 2007), with international student exchanges and Erasmus programmes becoming a central pillar for globalisation of third level education within the EU. It has been shown that students who have participated in an Erasmus programme have a comparative advantage with a higher rate of international career placement experience (James 2013; European Union 2013a). ERASMUS has become the most successful student exchange programme in the world with more than 230,000 students studying abroad under the Erasmus programme (European Union 2013b, 2013c). Erasmus has also led to the development of a more integrated European higher education and research community (Beerkens 2008). The ERASMUS Lifelong Learning Programme (Decision No 1720/2006/EC) and the Eramsus + were developed to promote collaborative and multidisciplinary teaching programmes and to foster increased cultural understanding within Europe. The ERASMUS LLP and Erasmus + also addresses the goals set out in EU 2020 by rejuvenating and transforming education systems in participating countries (Com 2010) and 'aims to

foster interchange, co-operation and mobility between education and training institutions and systems within the EU so that they may become a world quality reference' (European Union 2013d).

Erasmus + (strategic partnerships) focuses on sharing, developing and transferring innovative practices between participating countries. Partnerships foster cooperation between organisations in different countries engaged in youth work and non-formal learning for young people. The organisations involved are expected to develop new approaches to youth work and encourage cooperation over longer periods (European Union 2016).

Europe has long been associated with the production of high quality foods, safety and control of environmental standards. In order to maintain this status it is important that we are proactive in our approaches for quality surveillance in foods while making improvements to the food chain. Food safety and energy sustainability has become a priority research area worldwide as the global food supply evolves. For example food safety is amongst the top eleven organisational priorities identified by the World Health Organisation. Recent health scares, including the outbreak of Shiga toxin-producing *E. coli* (STEC) O104:H4, BSE crisis, growth hormones in meat, dioxin, sudan red and avian flue scares, have made consumers more wary about the origin, traceability and safety of the food they eat. At the same time, making improvements to the food chain to reduce energy consumption and to prolong shelf life is essential for food security and sustainability but represents a significant challenge for the industry.

It's within this context of globalised education and globalisation of the food chain that idea for an ERASMUS + programme on Quantitative Tools for Sustainable Food and Energy in the food chain (Q SAFE) was born. Components of predictive modelling, risk assessment and LCA are taught under different guises in a number of different institutions; however no one programme covers all components. This collaborative and multidisciplinary programme, brings together food scientists, microbiologists, statisticians and engineers with complementary expertise, this ensures wide appeal across the disciplines and the engagement of multidisciplinary students. This Erasmus + brings together international experts and encourages collaborations with industry and international scientists for the benefit of the public good. The Erasmus + increases the international profile of European early stage researchers in the area of predictive modelling and quantitative risk assessment in food and biosciences. Consequently the Erasmus + contributes to the development of a European dimension in lifelong learning and the support of a European knowledge based economy.

This paper reports on the design and implementation of the Q-Safe ERASMUS + in Quantitative Tools for Sustainable Food and Energy in the food chain and details the paradigm adopted, including organisation, programme development, assessment and evaluation stages. This paper explores the challenges posed and lessons learned by the programme, while using student feedback to enhance the programme design. It is hoped the paper will assist in promoting good international collaborative teaching practices.

MATERIALS AND METHODS

The mission of the IP programme on Quantitative Tools for Sustainable Food and Energy in the food chain is to explore new advances in modelling practices, to present the concepts and tools of analysis and to finally deliver applied mathematical knowledge to the research field of Food and Biosciences, while remaining true to the overall EU aims of an Erasmus + intensitve teaching activity. In the development of the ERASMUS +, a paradigm was adopted which consisted of a 6 stage cyclical process (Figure 1). The paradigm considers the initial objectives of the programme, followed by the programme design, content development, implementation, evaluation and enhancement stages. The cyclical paradigm ensures a feedback loop to improve the programme.

Figure 1: Proposed paradigm for ERASMUS + Q-Safe intenstive study programme

Programme objectives

The specific objectives of this IP (thematic area of Predictive Modelling, Quantitative Risk Assessment and LCA) were:
(i) to develop each participants capacity to design and generate informative experimental data,
(ii) to build skills in developing or selecting modelling structures appropriate to describe quantitatively chemical, microbiological and physical phenomena and develop capabilities for quantifying accurately the sources of stochasticity,
(iii) to make participants familiar with optimisation software and model simulation in research, that can be exploited for developing decision-making, quantitative risk assessment and life cycle analysis tools.

Programm design

Critical thinking has become the most prized student outcome at all levels of education (Gallego et al. 2013). A learning process which is based on critical thinking is problem-based learning (PBL). In PBL students are active participants in their own learning and they engage in the

problem-solving process while the teachers have to assess the process that the students follow to reach a solution. One of the main advantages of the case study method is that it allows the combination of theory and practice in order to produce graduates able to find an expert solution (Ng et al. 2011). Therefore, PBL practises in an inter-professional education (IPE) environment were proposed for this IP. More specifically, PBL pedagogical tools were proposed in which students worked in groups to solve realistic multifaceted problems with the use of programming tools.
The involvement of academic professionals from the areas of Food Microbiology, Statistics and Engineering was seen as important in creating a stimulating IPE environment as professions with different expertise will learn with, from and about each other to improve collaboration and the quality of teaching. It was anticipated that these innovative practises would contribute to developing students' skills on defining problem objectives in realistic and dynamic food environments and to critically assess the application of mathematical knowledge to particular contexts. The programme was designed to accommodate a significant proportion of PBL group activities and autonomous student learning as shown in Figure 2.

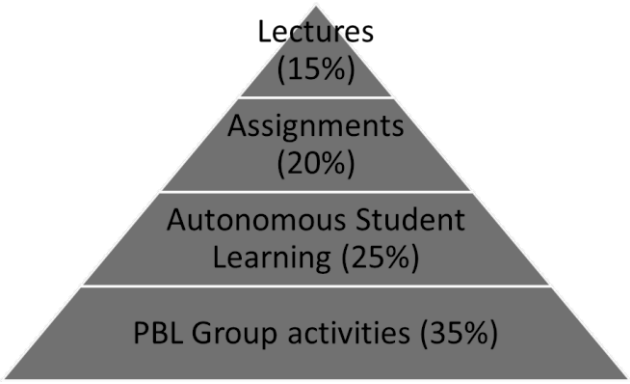

Figure 2: Programme design with approximate percentage time allocation

Content development

Student activities revolved around a series of seven key specialist topics representing central food safety topics and the teaching and research expertise of each of the partner institutions. These were:

1) Experimental design and model development
2) Risk Analysis
3) Microbial Risk assessment
4) Predictive Microbiology
5) Optimisation and design of food processes
6) Life cycle analysis
7) Integrating process modelling approaches

Implementation & Assessment

Successful implementation of the programme on site required all teachers to be actively engaged in all stages of the process while been cognisant of differing student abilities and cultural differences. In particular, students from different disciplines had varying experience with the topics and tools covered. In addition, the different language skills of students needed careful consideration.

The seven key topics covered a series of introduction lectures, case studies and project tasks. Details of these are provided for the six key topics.: 1) Experimental design and model development, 2) Risk Analysis, 3) Microbial Risk assessment 4) Predictive Microbiology 5) Optimisation and design of food processes 6) Life cycle analysis 7) Integrating process modelling approaches.

Evaluation & Enhancement

Evaluation of the programme is essential for the continued improvement of the programme and to ensure the programme remains relevant to student needs. The best way to evaluate the success of a programme is invariably through student feedback questionnaires. For this IP students provided written anonymous feedback for each of the 6 key topics. This was important for individual teachers to highlight problem/difficult areas or areas of misunderstanding within their topic.

DISCUSSION AND RESULTS

The paradigm worked well for the IP on Quantitative Tools for Sustainable Food and Energy in the food chain with positive feedback from students. In the student evaluation survey the overriding motivation for participation in the course was academic, but it is noteworthy that developing career plans and the European experience were also an important consideration (Figure 3). In terms of academic activities and the pedagogical aspects of the IP, overall students were very satisfied (Figure 4).

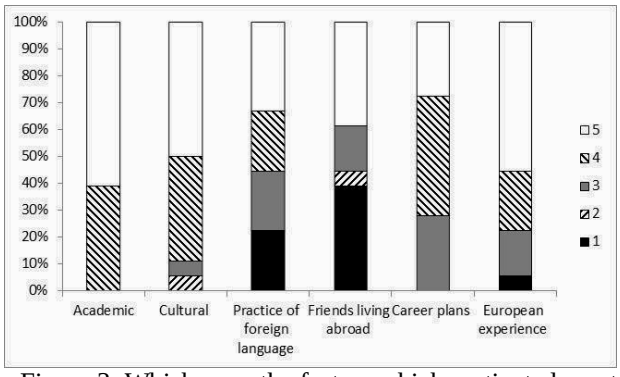

Figure 3: Which were the factors which motivated you to participate? (n = 18)

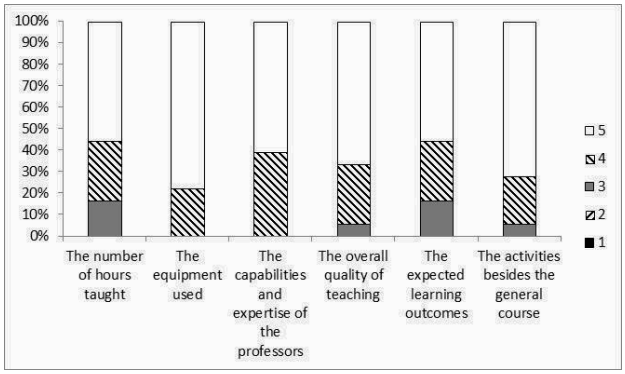

Figure 4: How satisfied were you with the academic activities and the pedagogical aspects of the IP in terms of the following aspects? (n = 18)

Figure 5 highlights that 84% of students gave a score of 4 and 5 when asked if the IP participation would help them to further their studies/career. It is worthy of note that the majority of the attendees were PhD students working in food safety / food protection / food engineering but having limited experience of the quantitative techniques and tools provided during the IP course. While building their capability in such techniques and tools during the course, students realised how they could use what they have learnt in their own studies.

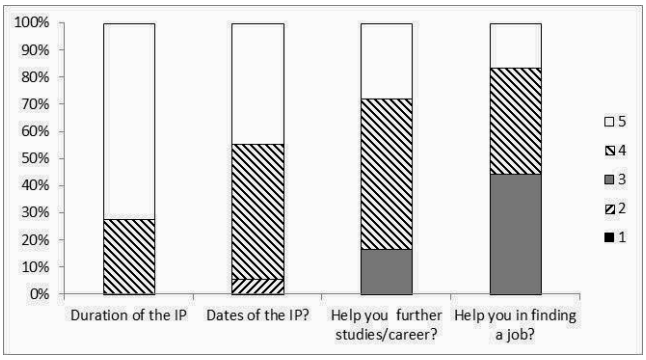

Figure 5: Student satisfaction rating (n = 18)

The students emphasised the interaction of professors as being critical to their learning and the importance of the practical problem based learning initiatives used in the programme. Overall student satisfaction was very high, with the majority awarding a score of 5 (excellent) for achieving academic/learning outcomes and personal outcomes of the IP (Figure 6)

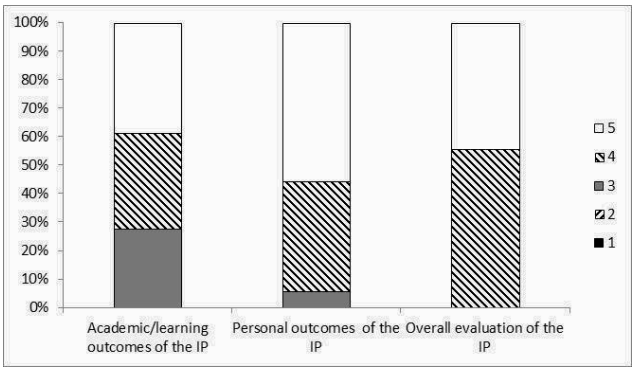

Figure 6: Student outcomes satisfaction rating (n = 18)

CONCLUSIONS

The ERASMUS + Q-Safe Intensive Programme is an innovative programme created out of the desire for intra-European cooperation and internationalisation of third level education. The ERASMUS + Q-Safe Intensive Programme proved valuable for students to participate in an international programme and increase their intercultural awareness and communication with partner countries. From the student feedback it was evident the programme had a beneficial impact on the university students. The academic institution involved benefited from the internationalisation of their teaching, while cultural integration and intercultural communication will benefit the European community as a whole. With the European Union's goal of becoming a leading knowledge economy the globalisation of student education must be viewed as a positive development. The success of this programme illustrated the willingness for student mobility and intercultural contact while learning key competency skills. Students also develop their language (both technical and non-technical) skills. They were exposed to different cultures, particularly at the host country, this enhances the participants' intercultural communication competencies.

The formation of revolving working groups enabled students and teachers to intermingle and cooperate as a multinational unit, providing an international perspective on each problem. The prospect of studying abroad for a short period appealed to students and provided them with intercultural competencies.

Evaluation sheets from students involved in the IP reported that the IP was very worthwhile and facilitated networking opportunities with peers. The IP helped their development of intercultural skills and given teachers a new perspective on international collaborations in teaching and learning. These findings are also supported by the scientific literature (James 2013; Civzele and Turusheva 2012). The IP also provided an opportunity to test new pedagogical approaches, which can positively influence teaching and learning strategies in partner institutions, a strategy which is strongly encouraged by the European Commission (Clough et al. 2012). Student and teacher feedback on their experiences was overwhelmingly positive.

The IP helped to focus on the exchange of knowledge between R&D divisions of Universities and food enterprises and all participating institutions, which will lead to successful cooperation between the higher education institutions and further dissemination to collaborative companies. The cooperation in the IP programme resulted in a knowledge transfer between participating institutions and facilitated the exchange of students for practical training in companies between the countries. Therefore, this IP promoted diverse cross-section cooperation of international: academic, industrial, government and healthcare professionals. The activities of the IP also contributed to research collaborations between the institutions involved and other EU Institutes by preparing research projects in the area of food and Biosciences.

FUNDING

The financial support of the European Commissions through the Q-Safe Erasmus+ programme of the European Union is acknowledged.

REFERENCES

Beerkens, E. (2008). The Emergence and Institutionalisation of the European Higher Education and Research Area. European Journal of Education 43(4), 407-423.

Com. (2010). EU 2020. Communication from the Commission: Europe 2020 – A Strategy for Smart, Sustainable and Inclusive Growth.

Ekti, M. (2013). An Evaluation Regarding to the Gains of Erasmus Program in Terms of Language and Science. Procedia - Social and Behavioral Sciences 70, 1800 – 1809.

Gallego, A., Fortunato, M.S., Rossi, S.L., Korol, S.E. & Moretton, J.A. (2013). Case Method in the Teaching of Food Safety. Journal of Food Science Education, 12(3), 42-47.

Jallade, J.P. (2011). International Approaches to Education: A review of some major cooperative programmes. European Journal of Education, 46 (1), 7-24.

James, C. (2013). Enhancing the QLD: internationalisation and employability: the benefits of Erasmus Intensive Programmes. The Law Teacher, 47(1), 64–82.

Laal, M. & Laal, A. (2012). Challenges for lifelong learning. Procedia - Social and Behavioral Sciences, 47, 1539 – 1544.

Molle, W. (2007). European Cohesion Policy. New York: Routledge Publishers.

Ng, B.L.L., Yap, K.C. & Hoh, Y.K. (2011). Students' perception of interdisciplinary, problem-based learning in a food biotechnology course. Journal of Food science Education, 10, 4-8.

Pepin, L. (2007). The History of EU Cooperation in the Field of Education and Training: how lifelong learning became a strategic objective. European Journal of Education, 42, 121-132.

WEB REFERENCES

Clough, N., Tarr, J., Macedo, E. & Cortesao, L. (2010). Testing the Impact of Innovative Pedagogies for Higher Education. European Conference on Educational Research, Helsinki. Retrieved from http://eprints.uwe.ac.uk/12926/2/Clough2010Testingtheimpact.pdf.

Civzele, O. & Turusheva, L. (2013). Intensive Programmes as a means of multinational collaboration and development of students' skills, INTED2012 Proceedings, 1608–1615. Retrieved from http://library.iated.org/view/CIVZELE2012INT.

European Union (2013a). The ERASMUS Programme – studying in Europe and more. Retrieved from http://ec.europa.eu/education/lifelong-learning-programme/erasmus_en.htm.

European Union (2013b). ERASMUS Intensive programmes. Retrieved from http://ec.europa.eu/education/erasmus/ip_en.htm

European Union (2013c). European Commission – Education & Training – lifelong learning programme – Erasmus – Statistics. Retrieved from http://ec.europa.eu/education/erasmus/statistics_en.htm.

European union (2013d) Lifelong Learning Programme 2007-13. Retrieved from http://europa.eu/legislation_summaries/education_training_youth/general_framework/c11082_en.htm

European union (2016) Erasmus + programme guide. Retrieved from http://ec.europa.eu/programmes/erasmus-plus/documents/erasmus-plus-programme-guide_en.pdf

Q-SAFE QUANTITATIVE TOOLS FOR SUSTAINABLE FOOD & ENERGY IN THE FOOD CHAIN

EFFECT OF ULTRASOUND ON RECOVERY KINETICS OF *ALICYCLOBACILLUS ACIDOTERRESTRIS* SPORES

Myrsini N. Kakagianni[1], Konstantinos P. Koutsoumanis[1]
[1]Department of Food Science and Technology
School of Agriculture
Faculty of Agriculture, Forestry and Natural Environment
Aristotle University of Thessaloniki
GR57001, Thessaloniki,
Greece
E-mail: mkakagianni@agro.auth.gr, kkoutsou@agro.auth.gr

Vasilis P. Valdramidis[2]
[2]Department of Food Studies and Environmental Health
Faculty of Health Sciences
University of Malta
MSD2080, Msida
Malta
E-mail: vasilis.valdaramidis@um.edu.mt

KEYWORDS
Alicyclobacillus acidoterrestris, ultrasound, microbial growth.

ABSTRACT

Consumer demand for healthy, safe and minimally processed foods with high-quality attributes has increased in the last decades. Increased consumption of fruit juices has direct influence on economy in positive way but in negative way also when spoilage problems occur. In recent years, *Alicyclobacillus acidoterrestris* has emerged as a new thermoacidophilic, endospore-forming spoilage bacterium for commercialized fruit juices that can survive pasteurization and spoil heat treated fruit juices by the production of taint compounds (e.g. guaiacol). Non-thermal technologies, such as ultrasound, are receiving good attention as an alternative because of their potential for quality and safety improvement of food. In this study, the objective was to investigate the effect of the ultrasound on the kinetic growth of *Alicyclobacillus acidoterrestris* spores at the population and individual level. The effectiveness of the ultrasound process on the lag phase was increased with the higher processing time duration (from 5 to 15 min) and the lower incubation growth temperature (from 45 to 35°C). Furthermore, the heat combined with ultrasound treatment could work synergistically on delaying the germination and outgrowth of the tested bacterial spores.

INTRODUCTION

Increased consumption of fruit juices has direct influence on economy in positive way but in negative way also when food borne disease outbreaks and spoilage problems occur. Conventional thermal processing is widely used for the inactivation of microorganisms' spores and enzymes in food products resulting in the increase of their shelf life. However, the thermal methods adversely affect the sensory qualities and nutritional quality of the processed foods (Lee et al. 2009). Consumer demand for healthy, safe and minimally processed foods (natural products and fewer chemicals) with high-quality attributes has increased in the last decades, leading to the development of non-thermal process technologies (Jiménez-Sánchez et al. 2015; Wang et al. 2010). Compared with the thermal treatments, non-thermal technologies, such as ultrasound (US) processing, or a combination of preservation methods are receiving good attention as an alternative processing option because of their potential for quality and safety improvement of food increasing the retention of flavors, colour and nutrient compositions (Piyasena et al. 2003).

It has been known that the type of microorganism, the ultrasonic waves, the power level, time of exposure to ultrasound, the volume of food to be processed and composition of food are critical processing factors of ultrasound treatment (Hoover 2000; Lee et al. 2009). The ultrasonic inactivation mechanism of microorganisms may be due to the effect of cavitation generated by ultrasound. According to this, microbubbles of gas are generated within a liquid, undergo a violent collapse during succeeding compression cycles of propagated ultrasonic waves and, consequently, due to a localized heating and intracellular micro-mechanical stress (Mukhopadhyay and Ramaswamy 2012). Consequently, an alteration in the cell membrane integration occurs, which can result in their disruption (Koda et al. 2009). The production of H- and OH- free radicals from the dissociation of water molecules could lead to adverse oxidative damage to DNA or alternatevily US would induce the protein denaturation and produce free radicals (Chemat and Khan 2011; Gogate and Kabadi 2009).

Since 1982, thermo-acidophilic endospore-forming *Alicyclobacillus acidoterrestris* isolated and identified as a new type of spoilage bacterium from aseptically packaged apple juice in Germany (Cerny et al. 1984), it is regarded as a major potential quality concern for the fruit juice industry (Steyn et al. 2011). The elimination and control of this microorganism from the processing environment is of great importance, as its endospores are difficult to detect before consumption (Silva et al. 2012), are able to survive the pasteurization processes, germinate, outgrow and transform to vegetative form and reach a spoilage level. This is associated with off-flavours or -odours attributed to the production, predominantly, of chemical metabolite guaiacol causing "smoky, medicinal, antiseptic disinfectant" (Bevilacqua et al. 2009; Pettipher et al. 1997), that reduces the shelf-life of the acidic fruit juices and acidic beverages (pH<4) during distribution and storage (Pettipher et al. 1997; Silva et al. 2015).

In general, bacterial spores, consisted of a complicated structure and chemistry including dipicolinic acid and calcium ions, are much more resistant than vegetative ones. So far, few papers have been published on the inactivation of the *A. acidoterrestris* spores exposed to ultrasound (Ferrario

et al. 2015; Groenewald et al. 2012; Yuan et al. 2009; Wang et al. 2010). Furthermore, *A. acidoterrestris* growth or recovery kinetic studies following the application of ultrasound are still missing in the literature.
Based on the above, the aim of this work was to investigate the ability of different ultrasonic treatments combined with heat stress to the kinetic growth of *Alicyclobacillus acidoterrestris* spores at the population and individual level.

MATERIALS AND METHODS

Bacterial strain and culture conditions

The type strain *Alicyclobacillus acidoterrestris* ATCC 49025 was used for all experiments in the present study. The working culture was grown in K broth (2.5g/l yeast extract; 5g/l peptone; 1g/l glucose; 1g/l tween 80), adjusted to pH=4.0 with filtered 25% (w/v) citric acid, and incubating at 45°C for 48h.

Ultrasonic treatments at the population level

For the experiments conducted in K broth (pH=4.5), the 48-h cultures in K broth (pH=4.0) of the strain were inoculated into the K broth samples (200ml) in order to obtain an initial concentration of *ca.* 10^3 CFU/ml. After inoculation, K broth samples were either only treated with an ultrasound probe system or treated with ultrasound and then heated (at 80°C for 10 min). Ultrasound treatment was applied with an ultrasonic system (UP 200ST, Hielscher Ultrasonic, Teltow, Germany) operating at 26 kHz, 90 μm, 200 W attached with a probe of 14 mm Ø that was submerged (3 cm) into the K broth samples. Different processing time durations (5, 10 and 15 min) were applied in a continuous mode. After the ultrasonic treatments, the samples were rapidly cooled down to room temperature and immediately were heat shocked at 80°C for 10 min (IFU 2007), in order to eliminate any vegetative cell and obtain uniform activation and germination of dormant *Alicyclobacillus* endospores (Goto 2007). As control samples were considered the only heat treated (at 80°C for 10 min) samples. All experiments were performed in duplicate with 2 replications (n=4). The number of viable cells before and after ultrasonic treatments was determined with the plate count method. The plates were incubated at 45°C for 48 h before enumeration. The growth data (log cfu/ml) in K broth stored under isothermal temperatures (35 and 45°C) were fitted to the primary model of Baranyi and Roberts (1994) in order to estimate the kinetic parameters for growth, i.e., maximum specific growth rate, μ_{max}, and lag phase.

Ultrasonic treatments at the individual spore level

Moreover, aiming at evaluating the lag time derived from single spores either with the application of ultrasound (10 min) and/or thermal treatment (at 80°C for 10 min), the tested strain was assessed in K broth, adjusted to pH=4.5 with filtered 25% (w/v) citric acid, at incubation isothermal temperature 40°C, using the microplate absorbance reader TECAN Xfluor 4. The optical density (OD) measurements were taken at 600 nm. The microplates were placed in the spectrophotometer at an incubation temperature of 40°C and OD measurements were taken at 15-min intervals after agitation of the microplates for 15s at medium amplitude.
The single-spore lag time (λ) values of the tested organism were estimated based on turbidity growth curves, according to a previously developed methodology (Aguirre et al. 2011; Baranyi and Pin 1999; Baranyi et al. 2009). The culture was decimally diluted in the treatment medium (Control, K broth-pH=4.5) to a concentration of ca. 10^0 CFU/ml, and 300-μl aliquots of this dilution were dispensed in the 96 wells of a microplate. The average number of cells per microplate well was estimated based on the assumption that the probability of having one cell per well is described by the Poisson distribution (Baranyi et al., 2009). More specifically, the equation correlating the average number of cells per well (m) with the probability of no growth occurring in a well (P_0) is the following:

$$m = - \mathrm{Ln} P_0 \quad (1)$$

with m being obtained, based on the calculated P_0 values, from Poisson distribution tables.

In this context, single-spore λ values were estimated using the following equation (Baranyi and Pin 1999):

$$Lag = T_{\mathrm{det}} - \frac{Ln(N_{\mathrm{det}}) - Ln(N_0)}{\mu_{\mathrm{max}}} \quad (2)$$

where T_{det} is defined as thetime required for an OD measurement of 0.2 to be obtained (correspondingto a bacterial concentration of ca. 10^7 cfu/well), N_{det} is the bacterial concentration at T_{det}, N_0 is the number of cells initiating growth in each microplate well, and μ_{max} is the maximum specific growth rate of the bacterial strain.

The experiments were replicated as many times needed for obtainining at least 200 values approximately of λ for each treatment.

Determination of energy levels

The energy level of ultrasound operation was expressed in ultrasound intensity (UI). This parameter was determined calorimetrically using the following equations described by Mason (1990).

$$UI = 4P/\pi d^2 \quad (3)$$

where d [cm] is the diameter of the sonotrode and P [W] represents the absolute ultrasonic power and can be defined as:

$$P = m\, C_p\, (dT/dt) \quad (4)$$

where, m[g] is themass, Cp [$J \cdot g^{-1} \cdot K^{-1}$] is the specific heat capacity of the liquid medium and dT/dt [$K \cdot s^{-1}$] is the temperature rate change during sonication.

The changes of the temperature were recorded and plot against the time for all the tested treatments for a mass of 200 ml of K broth. Hereafter, a linear regression was performed to estimate the dT/dt in Equation (4) that was used to obtain the UI (Equation (3)).

RESULTS AND DISCUSSION

Table 1 shows the average lag time of *A. acidoterrestris* spores in K broth at population level (initial cell counts at the level of 10^3 cfu/ml) at 35°C, after ultrasonic treatment at 100% amplitude for different durations and heat treatment (at 80°C for 10min). An increase in the lag phase was observed when the exposure time to ultrasound was increasing (from 5 to 15 min). As can be seen in Table 1, the combination of ultrasound and heat treatment resulted in a further increase of lag phase compared to that after the single application of an ultrasonic treatment.

Table 1: Average lag time of *Alicyclobacillus acidoterrestris* spores in K broth adjusted to pH=4.5 with filtered 25% (w/v) citric acid at 35°C, using the ultrasound or the combination of ultrasound and heat treatment.

Treatments	Lag (h) ± sd[a]
Control (80°C/10min)	5.679 ± 0.363
100%Amplitude/5min	7.176 ± 1.458
100%Amplitude/10min	11.126 ± 1.250
100%Amplitude/15min	11.465 ± 0.805
100%Amplitude/5min-80°C/10min	7.589 ± 1.528
100%Amplitude/10min-80°C/10min	5.947 ± 1.974
100%Amplitude/15min-80°C/10min	15.602 ± 1.193

[a] Average lag time (±: standard deviation)

Similarly, the growth delay of the tested microorganism at 45°C increased with the ultrasonic treatment time (Table 2). The lag phase durations were also higher under the application of ultrasonic and heat treatment than those when ultrasound was applied alone.

Table 2: Average lag time of *Alicyclobacillus acidoterrestris* spores in K broth adjusted to pH=4.5 with filtered 25% (w/v) citric acid at 45°C, using the ultrasound or the combination of ultrasound and heat treatment.

Treatments	Lag (h) ± sd[a]
Control (80°C/10min)	2.248 ± 0.610
100%Amplitude/5min	3.915 ± 0.056
100%Amplitude/10min	5.541 ± 2.036
100%Amplitude/15min	5.006 ± 0.499
100%Amplitude/5min-80°C/10min	4.476 ± 1.875
100%Amplitude/10min-80°C/10min	7.329 ± 1.114
100%Amplitude/15min-80°C/10min	8.966 ± 0.860

[a] Average lag time (±: standard deviation)

Accordingly, it can be concluded that increasing the treatment time of ultrasound and applying both ultrasonic and thermal treatment can increase the lag phase of *A. acidoterrestris* in K broth at the population level. Given the estimated theoretical minimum (close to 20°C) and optimum (approximately 48°C) growth temperature for this specific strain (data not shown), is is obvious from the Tables 1 and 2 that the microorganism needs more time to adjust to its new environment at 35°C compared to 45°C.

In the turbidity experiments in which a microplate absorbance reader TECAN Xfluor 4 was used, there was considerable heterogeneity in the lag times derived from individual spores at both cases. Under the growth conditions tested in this experiment, the mean lag time derived from ultrasound and heat treated samples (29.5 h) was much longer than the mean lag time derived from only heat treated samples (12.1 h). As also illustrated by the probability distributions (Fig. 1), the single-spore variability of λ was substantially increased in samples treated with ultrasound and heat compared to the those only treated with heat. As demonstrated by the comparative evaluation of the distributions corresponding to both treatments, the way in which each treatment affected the position and the shape of the single-spore λ distributions was dependent on the application of ultrasound before the heat stress. Ultrasound appears to work synergistically with the heat treatment affecting largely the distribution of lag times, with the histograms becoming very broad with extended tails (Fig. 1). These findings support the widely recognized importance of individual spore lag time distributions for applications in risk assessment and prediction of shelf life (Ross and McMeekin, 2003). The need of evaluating the behavior of single cells/spores (or small populations/sub-populations) and describing its variability through the use of stochastic modeling approaches (Koutsoumanis and Lianou, 2013) is also evident in this study.

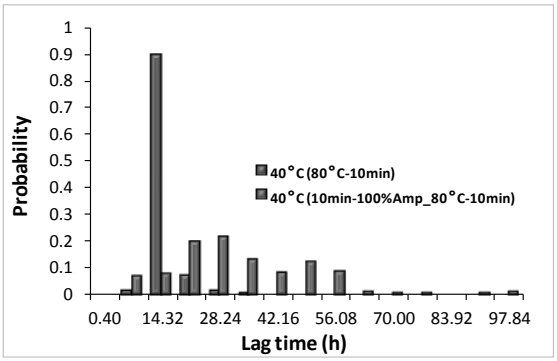

Figure 1: Probability distributions of the single-spore lag time values of *Alicyclobacillus acidoterrestris* in K broth adjusted to pH=4.5 with filtered 25% (w/v) citric acid containing microbial supernatant that was subjected to heat treatment or to ultrasound and then to heat treatment.

CONCLUSIONS

This work provides useful information on the efficiency of the ultrasound and its combination with the heat in delaying *Alicyclobacillus* spores to germinate and outgrow in a laboratory medium at population and individual level. This would help for a better understanding of the response to the proposed combined treatments, since there was a synergistic interaction in increasing microbial lag phase between ultrasound and heat treatment. Further research should be performed on investigating the effectiveness of the ultrasound process on microbial growth of endospore-forming bacteria in order to control in a more precisely way the consequent food spoilage and prolong the shelf life of food products.

ACKNOWLEDGEMENTS

This research was funded with the support of the Erasmus+ programme of the European Union (Project No. 2014-1-MT01-KA200-000327).

REFERENCES

Aguirre, J.S., Rodríguez M.R. and García de Fernando G.D. 2011. "Effects of electron beam irradiation on the variability in survivor number and duration of lag phase of four food-borne organisms". *International Journal of Food Microbiology* No. 149, 236–246.

Baranyi J., George S.M. and Kutalik Z. 2009. "Parameter estimation for the distribution of single cell lag times". *Journal of Theoretical Biology* No. 259, 24–30.

Baranyi J. and Pin, C. 1999. "Estimating bacterial growth parameters by means of detection times". *Applied and Environmental Microbiology* No.65, 732–736.

Baranyi J. and Roberts T.A. 1994. "Review: A dynamic approach to predicting bacterial growth in food". *International Journal of Food Microbiology* No. 23, 277-294.

Bevilacqua A., Sinigaglia M., and Corbo M. 2009. "Effects of pH, cinnamaldehyde and heat-treatment time on spore viability of *Alicyclobacillus acidoterrestris". International Journal of Food Science and Technology* No. 44, 340-385.

Cerny G., Hennlich W. and Poralla K. 1984. "Spoilage of fruit juice by *Bacilli*: isolation and characterization of the spoilage organism". *Z Lebens Unters Forschung* No. 179, 224-227.

Chemat F. and Khan M.K. 2011. "Applications of ultrasound in food technology: Processing, preservation and extraction". *Ultrasonics Sonochemistry* No. 18, 813–835.

Ferrario, M., Alzamora S.M. and Guerrero S. 2015. "Study of the inactivation of spoilage microorganisms in apple juice by pulsed light and ultrasound". *Food Microbiology* No. 46, 635-642.

Gogate P.R. and Kabadi A.M. 2009. "A review of applications of cavitation in biochemical engineering/biotechnology". *Biochemical Engineering Journal* No. 44, 60–72.

Goto K. 2007. "Parameters for detection of *Alicyclobacillus* and test methods". In: *Alicyclobacillus: Thermophillic Acidophilic Bacilli*, A. Yokota, T. Fujii and K. Goto (Eds.). Springer, Shinano Inc., Japan, 49–69.

Groenewald W.H., Gouws P.A., Cilliers F.P. and Witthuhn R.C. 2013. "The use of ultraviolet radiation as a non-thermal treatment for the inactivation of alicyclobacillus spores in water, wash water from a fruit processing plant and grape juice concentrate".

Hoover D.G. (2000). "Kinetics of microbial inactivation for alternative food processing technologies ultrasound". *Journal of Food Science* (Supplement), 93–95.

International Federation of Fruit Juice Producers (IFU) 2007. "Method on the Detection of Taint Producing *Alicyclobacillus* in Fruit Juices". *IFU Method No. 12. IFU*, Paris, 1-11.

Jiménez-Sánchez C., Lozano-Sánchez J., Segura-Carretero A. and Fernández-Gutiérrez A. 2015. "Review: Alternatives to Conventional Thermal Treatments in Fruit-juice Processing. Part 1: Techniques and Applications". *Critical Reviews in Food Science and Nutrition* (just-accepted), 00-00.

Koda S., Miyamoto M., Toma M., Matsuoka T., Maebayashi M. 2009. "Inactivation of *Escherichia coli* and *Streptococcus mutans* by ultrasound at 500 kHz". *Ultrasonics Sonochemistry* No. 16, 655–659.

Koutsoumanis K.P. and Lianou A. 2013. "Stochasticity in colonial growth dynamics of individual bacterial cells". *Applied and Environmental Microbiology* No. 79, 2294–2301.

Lee H., Zhou B., Liang W., Feng H., Martin S.E. 2009. "Inactivation of *Escherichia coli* cells with sonication, manosonication, thermosonication, and manothermosonication: microbial responses and kinetics modeling". *Journal of Food Engineering* No. 93, 354–364.

Mason T.J. 1990. "Sonochemistry: The uses of ultrasound in chemistry". Cambridge, England: Royal Society of Chemistry.

Mukhopadhyay S. and Ramaswamy R. 2012. "Application of emerging technologies to control *Salmonella* in foods: A review". *Food Research International* No. 45, 666–677.

Pettipher G.L., Osmundson M.E. and Murphy J.M. 1997. "Methods for the detection and enumeration of *Alicyclobacillus acidoterrestris* and investigation of growth and production of taint in fruit juice and fruit juice-containing drinks". *Letters in Applied Microbiology* No. 24, 185-189.

Piyasena P., Mohareb E. and McKellar R.C. 2003. "Inactivation of microbes using ultrasound: a review". *International Journal of Food Microbiology* No. 87, 207–216.

Ross T. and McMeekin T.A. 2003. "Modeling microbial growth within food safety risk assessments". *Risk Analysis* No.23, 179–197.

Silva L.P., Golzales-Barron U., Cadavez V. and Sant' Ana A.S. 2015. "Modeling the effects of temperature and pH on the resistance of *Alicyclobacillus acidoterrestris* in conventional heat-treated fruit beverages through a meta-analysis approach". *Food Microbiology* No. 46, 541-546.

Silva F.V.M., Tan E.K. and Farid M. 2012. "Bacterial spore inactivation at 45-65°C using high pressure processing: Study of *Alicyclobacillus acidoterrestris* in orange juice". *Food Microbiology* No. 32, 206-211.

Steyn C.E., Cameron M. and Witthuhn R.C. 2011. "Occurrence of *Alicyclobacillus* in the fruit processing environment — A review". *International Journal of Food Microbiology* No. 147, 1-11.

Yuan Y., Hu Y., Yue T., Chen T. and Martin Lo Y. 2009. "Effect of ultrasonic treatments on thermoacidophilic *Alicyclobacillus acidoterrestris* in apple juice". *Journal of Food Processing and Preservation* No. 33, 370-383.

Wang J., Hu X. and Wang Z. (2010). "Kinetics models for the inactivation of *Alicyclobacillus acidiphilus* DSM14558T and *Alicyclobacillus acidoterrestris* DSM 3922T in apple juice by ultrasound". *International Journal of Food Microbiology* No. 139, 177-181.

AUTHOR BIOGRAPHIES

MYRSINI KAKAGIANNI was born in Athens, Greece and went to the Aristotle University of Thessaloniki (A.U.Th.), where she studied Biology and obtained her degree in 2008. Afterwards, she received her M.Sc. degree in 2010 from the Department of Food Science and Technology of School of Agriculture (A.U.Th.). She is currently a PhD candidate in the same department. During her graduate studies in A.U.Th., she participated also in 5 research projects as a research assistant in the Laboratory of Food Microbiology and Hygiene with research objectives-responsibilities: the study of growth behavior of foodborne pathogens in beef meat, the study of growth behavior of spoilage endospore-former microorganisms in milk products and fruit juices during chill chain, the microencapsulation of probiotics in dairy and meat products and data analyses. Her research interests include a wide range of Food Quality and Safety, particularly on applications of Predictive Microbiology, Quantitative Microbial Risk Assessment and Food Microbiology.

KOSTANTINOS KOUTSOUMANIS is currently serving as an Associate Professor at the Department of Food Science and Technology, Faculty of Agriculture, Aristotle University of Thessaloniki, Greece. Currently, he teaches several graduate and MSc courses including General Microbiology, Food Quality and Safety Assurance, Predictive Microbiology and Risk Assessment and Applied Statistics in Food Science. From 2011 he is a member and from 2015 the vice-Chair of the Biohazard panel of the European Food Safety Authority (EFSA). He is Associate editor in the journal Frontiers in Microbiology and member of the editorial boards of the Journal of Food Protection, International Journal of Food Microbiology, Food Microbiology and Current Opinion in Food Science. Recent research efforts have centered on the microbiological quality and safety of fresh and processed food products, predictive microbiology, microbial risk assessment, stochastic modeling approaches in food safety and quality, development and application of Time Temperature Indicators (TTI) for monitoring food quality and safety, etc.

VASILIS VALDRAMIDIS is a member of the Faculty of Health Sciences at the University of Malta. He is leading the research group on the Food Sciences and Environmental Health (FSEH) at the Unviersity of Malta http://www.um.edu.mt/healthsciences/research/fseh He is the coordinator of the education programme Erasmus + : Cooperation for innovation and the exchange of good practices. Strategic Partnerships. Quantitative Tools for Sustainable Food and Energy in the food chain, Q-SAFE https://www.um.edu.mt/healthsciences/projects/q-safe 2014-2017. He is member of the International Committee on Food Microbiology and Hygiene of the IUMS and member of the International Committee of Predictive Modelling in Food since 2011.

ARTIFICIAL NEURAL NETWORKS AS A TOOL TO PREDICT THE MIGRATION OF SILVER FROM ANTIMICROBIAL NANO-COATED LDPE FILMS

Joseph C. Hannon
Enda Cummins
School of Biosystems and Food Engineering,
University College Dublin,
Dublin,
Ireland
E-mail: enda.cummins@ucd.ie

Joseph P. Kerry
Malco Cruz-Romero
Shafrina Azlin-Hasim
School of Food & Nutritional Sciences,
University College Cork,
Cork,
Ireland

Michael Morris
Department of Chemistry,
University College Cork,
Cork,
Ireland

KEYWORDS
Neural Networks, NeuralTools, Nanoparticles, Nanomaterial, Nanosilver, Antimicrobial Packaging, Migration, Food Packaging, Food Simulant, ICP-AES.

ABSTRACT

Antimicrobial nanocomposite silver (Ag) coated LDPE films were developed using a number of surface treatments to enhance attachment of Ag nanoparticles (NPs) and reduce potential migration of NPs into food. The migration of NPs into food has caused concern regarding the safety of NP food packaging, mainly surrounding human exposure and potential toxicity. Due to the complexity of the NP migration mechanisms, artificial neural networks (ANNs) were investigated as an alternative methodology to conventional mathematical models for migration prediction. Two ANNs were investigated; generalised regression neural network (GRNN) and multilayer perceptron neural network (MLPNN). The migration of total Ag from an experimental AgNP coated LDPE food packaging material following incubation for two storage conditions was found to range from 1.1 – 72 μg/dm^2. Twenty percent of the dataset from the migration experiments was excluded from the ANN training set to allow for the model to be validated. Both ANNs were found to predict migration with R^2 values ranging from 0.76 – 0.91 (GRNN) and 0.76 – 0.94 (MLPNN).

INTRODUCTION

Novel materials incorporating small particles in the size range 1-100 nm are proving revolutionary in a number of industries, including the food industry (Hannon et al 2015a). Nanoparticles (NPs) have been included within the walls and at the surface of food packaging to provide antimicrobial, gas barrier, UV barrier, improved biodegradability, improved strength, improved thermal properties, and gas scavenging properties. Despite the many benefits that nanotechnology can offer in the food packaging industry, there are concerns related to the potential migration of NPs from food packaging into food, and the subsequent human exposure and toxicity. These concerns are magnified when focusing on NP food packaging coatings in particular, due to the heightened ability for attached NPs to migrate from packaging coatings into food (Hannon et al. 2015b). In addition, there is added uncertainty due to the lack of studies that have investigated NP migration from NP food packaging coatings (Hannon et al. 2015b, Nobile et al. 2004, Smirnova et al. 2012). In the literature, only one study has quantified human exposure to NPs from food packaging coatings (Smirnova et a. 2012). With increasing numbers of commercially available products on the world market utilising NP coatings (Maynard and Michelson, 2014), it has never been more important to assess the safety of these novel products. In the light of this, current migration test methods are costly and time consuming, particularly when NP food packaging must be assessed on a case-by-case basis. One solution to this problem is migration predictive modelling. In the literature, migration models have been developed for packaging materials incorporating NPs within their walls (Cushen et al. 2013, Cushen et al. 2014, Simon et al. 2008, bott et al. 2014a, bott et al. 2014b, Huang et al. 2014). However, to the best of the authors' knowledge there are no existing migration models for NP food packaging coatings. The lack of models in the literature could be attributed to difficulties modelling complex desorption mechanisms of NPs on packaging surfaces with conventional mathematical models.
A novel predictive modelling technique based on machine learning involving ANNs that mimics neurons in the brain could provide a solution to this issue. ANNs can be used to model complex non-linear systems, while considering numerous influencing factors that may be difficult to include in conventional mathematical models (Siripatrawan et al. 2008). The structure of the ANNs involves an input layer, a neuron layer dependent on the ANN used, and an output layer. Information inputted to the neurons undergoes a weighted process over a number of iterations. The iterative behaviour of the ANN contributes to its ability to model a given system. With each iteration the neurons in the ANN undergoes a change in transfer function, altering the output to fit the dependent variable being modelled. Additionally, the quality and quantity of the input dataset will significantly affect the ability of the ANN to accurately simulate the system. Too few datapoints limits the ability of the ANN to accurately simulate the system.
This paper presents methodologies for the modelling of Ag migration from nano coated LDPE films using novel

generalised regression and multilayer perceptron neural networks.

MATERIALS AND METHODS

Artificial Neural Network

In general, ANNs are comprised of an input layer, multiple neurons and an output layer. The basic function of the neurons is to perform as a weighted transfer function, processing the input parameters with each iteration and producing an output. The basic equation which describes how a neuron functions can be seen in Equation (1) and equation (2) (Siripatrawan et al. 2008).

$$u_k = \sum_{j=1}^{m} w_{kj}\, x_j \quad (1)$$

where u_k is the output as a result of the input signal, x_j is the input signal and w_{kj} is the function weight of the neuron (subscript k). The output of the neuron is performed using Equation (2).

$$y_k = \varphi(u_k + b_k) \quad (2)$$

where φ is the activation function, b_k is the bias and y_k is the output of the neuron.

Generalised Regression/Probabilistic Neural Network

The probabilistic neural network was first proposed by Specht (1990). The ANN involves an architecture with four layers of parallel neurons (see Figure 1) and has significant time saving benefits over ANNs which involve back propagation.

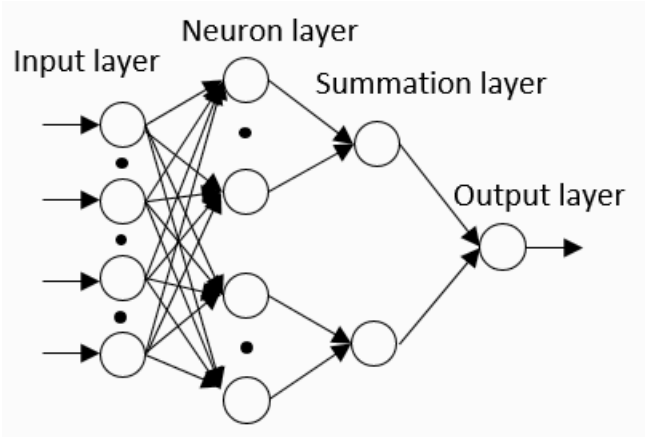

Figure 1: Probabilistic Neural Network Architecture adapted from Specht (1990)

The configuration of this ANN is chosen based on whether the input data is numeric (GRNN) or categorical (PNN). Irrespective of the nature of the input, both perform in a similar manner.

Multilayer Perceptron Feedforward Neural Network

The most commonly applied ANN is the MLPNN (Siripatrawan et al. 2008). It comprises of an input layer, multiple neuron hidden layers and an output layer (see Figure 2).

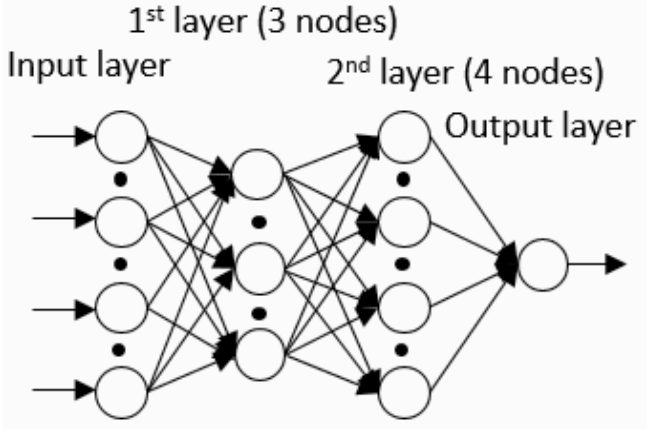

Figure 2: Multilayer Perceptron Neural Network Architecture

Nanocomposite Manufacture

Commercial LDPE films with a thickness of 0.04 mm were immersed in ethanol for 3 min, drained and dried at 60 °C in an oven (Memmert, Germany). In order to modify the surface of one side of the cleaned LDPE films the following surface treatments were used: UV treatment, UV + pluronic treatment or UV + pluronic + PS-*b*-PEO treatment. For the UV-treated samples, LDPE films were exposed to UV/ozone in a Digital UV Ozone System (PSD Pro Series, UV source: 180 - 254 nm) for 30 min with 0.5 L/min flow of O_2. For the pluronic non-ionic copolymer surfactant treatment, LDPE films were spray coated with pluronic solution (0.2 wt.%) using an air brush compressor (Model AS 18-2, Air Brush Pro, UK) fitted with Airbrush BD-128P Kit and dried in an oven at 60 °C for 2 hr. For the PS-*b*-PEO treatment, LDPE film with a modified surface was spray coated with solutions of PS-*b*-PEO in toluene (0.4 or 0.85 wt.%) and then spray coated with an ethanolic solution of $AgNO_3$ (2 wt.%). The uncoated and coated films were exposed to UV light in an environmental chamber (Binder, Germany) integrated with UV light at 25 °C and 50% RH for 2 hr. In order to cross-link the coating materials with the surface modified LDPE films, treated LDPE films were placed in an oven at 60 °C for 18 hr. To oxidise the Ag^+ to Ag°, the LDPE films were exposed to UV light for 18 min in a laminar flow (Airclean 600 PCR Workstation STAR LAB). For 2 wt.% $AgNO_3$ control samples, no surface modification of the LDPE films were carried out and the ethanolic solution of $AgNO_3$ was directly spray coated on the LDPE films after the cleaning process with ethanol.

ICP-AES Analysis

Due to the inability of the ICP-AES technique to distinguish between Ag^+ and AgNPs, the total Ag found in food

simulants following migration studies, and the initial concentration of Ag in the Ag coated LDPE films was quantified by ICP-AES analysis using the operating conditions shown in Table 1. For each analytical run the ICP-AES was calibrated using a blank and four standards (10, 100, 1000 and 5000 µg/l, or 1, 5, 10 and 20 µg/l for the migration studies or total digestions, respectively) diluted volumetrically from a stock Ag standard (1000 mg/l Ag^+,

Table 1: ICP-AES Operating Conditions

Operating conditions	
Power (kW)	1.2
Auxiliary gas flow (l/min)	1.5
Nebuliser gas flow (l/min)	1
Torch gas flow (l/min)	15
Nebuliser pressure (kPa)	200
Torch orientation	Radial
Viewing height	8
Pump rate (rpm)	15
Replicate read time (s)	10
Sample uptake delay (s)	15
Rinse time (s)	60

Elementec, Ireland). To reduce spectral interference due to matrix effects, all samples and standards were spiked with an internal standard (1000 mg/l yttrium, Elementec, Ireland). Any potential effects on the ICP readings due to cross-over contamination was quantified by running a blank between samples. In order to reduce contamination from the spray chamber and nebuliser, prior to analysis both were soaked in 25% RBS detergent in distilled water for 12 hours. The ICP inlet tubing was replaced before each analytical run.

Nanocomposite Total Digestion

To determine the Ag loading in each of the Ag coated LDPE films a total digestion was carried out using a method outlined by Bott et al. (2014) with some modifications. Total digestion was performed by cutting larger samples into approximately 1 × 1 mm^2 pieces. These pieces were then placed in an individual PTFE vessel with 10 ml of 69% nitric acid (69% HNO_3, VWR International, Ireland). The vessels were sealed with a rupture membrane in place, and incubated in an oven (Plus II Oven Gallenkamp, UK) for 5 hours at 120 ˚C. Before ICP-AES analysis, 100 µl of the concentrated digestate was diluted in 9.9 ml Millipore water.

Migration Experiments

Migration studies were carried out according to European Commission (2011) Regulation No. 10/2011. To simulate worst case migration, 2.5 × 2.5 cm^2 coated packaging samples were immersed in 10 ml of 3% acetic acid (prepared volumetrically with >99% HAc, Sigma-Aldrich, Arklow Ireland) and incubated in an oven for one of the two temperature / time scenarios (70 ˚C for 2 hours or 60 ˚C for 10 days). Once the incubation time elapsed, samples were removed from sample pots and 5 ml of the food simulant was transferred to a pyrex tube for digestion. Simulants were digested with 100 µl of HNO_3 and 50 µl of HCL (37% HCL, Sigma-Aldrich, Ireland) at 95 ± 5 ˚C for 2.5 hours (Palintest Digital Tubetest Heater, Gateshead, UK). Food simulants were allowed to cool down for 30 minutes before ICP-AES analysis. To avoid contamination from glassware and sample containers, all materials that contacted the food simulant and ICP-AES calibration standards were soaked in 5% HNO_3 for 12 hours and then cleaned for 30 minutes in an ultrasonicator bath, before being dried in a closed glassware drier.

Neural Network Execution

The performance of two ANNs (GRNN and MLPNN) was assessed using the NeuralTools programme (Palisade, UK). The two models were trained on the dataset found in Table 2. This dataset is broken into six variables that are related to the surface treatments applied during the manufacture of the coatings, the actual concentration of the Ag absorbed to the coating during the coating manufacture determined by total digestion and the time/temperature conditions used to test NP migration from the packaging material. The three surface treatment variables which were examined for their ability to improve the attachment of NPs in the coating were; UV treatment (independent categorical: 2 levels) and the addition of two copolymers during the coating process; PS-*b*-PEO (polystyrene-*b*-polyethylene oxide) (independent numeric, 3 levels) and pluronic (a non-ionic triblock copolymer) (independent categorical, 2 levels). To assess the effect of time and temperature on migration a time/temperature variable was included, having two categorical levels representing the two worst case accelerated migration conditions; 10 days at 60 ˚C and 2 hours at 70 ˚C according to European Commission (2011) Regulation No. 10/2011. The final variable included was the initial concentration variable (ICV) (independent numeric, continuous) of Ag in the coating prior to migration studies. To examine the effect of the ICV on the predictive ability of both the GRNN and MLPNN, the ICV was included in one dataset (Table 2) used to train the MLPNN and GRNN and then excluded from the same dataset to train both ANNs again for comparison. For the MLP model, training was carried out for 1,000,000 iterations, as no change in error was witnessed beyond this point. The network configuration relating to the number of nodes and layers in each MLPNN carried out was optimised by the programme automatically. In all cases, there was only one hidden layer, with two and three neurons used

Table 2: ANN Training and Testing Parameters

Samples	PS-*b*-PEO (%)	UV	Pluronic	Migration (mg/dm^2) (n = 3) 2 hours 70˚C	Migration (mg/dm^2) (n = 3) 10 days 60˚C	Initial concentration (mg/dm^2) (n = 2)
2% Ag	0	No	No	0.059±0.0018	0.036±0.014	-
2% Ag + UV	0	Yes	No	0.055±0.0143	0.038±0.0081	0.069±0.0082
2% Ag + UV + PS-*b*-PEO	0.4	Yes	No	0.04±0.0062	0.027[a]	0.055±0.0174
2% Ag + UV + PS-*b*-PEO	0.85	Yes	No	0.0406±0.0009	0.015±0.0043	0.064±0.0159
2% Ag + PL + PS-*b*-PEO	0.4	No	Yes	0.0369±0.0037	0.005±0.0052	0.045±0.0323
2% Ag + PL + UV + PS-*b*-PEO	0.4	Yes	Yes	0.045[a]	0.012±0.0074	0.045±0.0257

[a] Only one sample tested

for the ANNs without the ICV and with the ICV, respectively. The ANNs were tested using leave-one-out cross validation method with 20% of the datapoints in Table 2 which were excluded from the training dataset and comprised of the other 80% of the dataset. The results were fit using a regression function within the Microsoft Analysis ToolPak addin (Microsoft, USA).

DISCUSSION AND RESULTS

Experimental Migration

From the results obtained from the migration studies (Figure 3), it can be seen that the migration levels exceed the European Commission (2011) migration limit for unauthorised substances of 0.01 mg/kg.

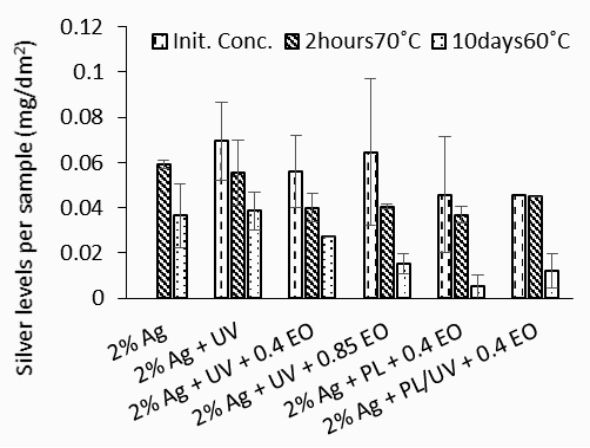

Figure 3: Silver levels present in each of the packaging samples tested and migration results for both time/temperature scenarios

This is assuming that the packaging material is used to package one cubic kg of food on all six sides, with a food product density of ~ 1 kg/l w/v. It must be noted that in this study the packaging samples have been optimised for antimicrobial activity by increasing Ag precursor concentration during the coating process to 2% $AgNO_3$ w/v. If this experimental material were to be used as a food contact material, the concentration of Ag in the coating could be reduced due to the good antimicrobial activity exhibited at lower precursor concentrations (Azlin-Hasim et al. 2015).

Despite the high migration observed, this study demonstrates the effect of different treatments on migration reduction. Although the initial Ag precursor concentration used in the coating of the LDPE films had a substantial effect on the migration levels, when observing the differences between initial concentration and migration values in Figure 3, it was observed that the treatments involving higher PS-*b*-PEO levels and pluronic treatment showed greater attachment when compared to ultraviolet treatment for surface modification alone. These findings suggest that migration levels could be reduced by optimising the levels of PS-*b*-PEO used in the coating process, while also using non-ionic copolymer surfactant treatment pluronic as a surface treatment.

GRNN Performance

On inspection of the residual plots for the GRNN in Figure 4 in can be deduced that the residuals are equally distributed and symmetrical around the x-axis. This suggests that the GRNN performs well when predicting migration of NPs from food packaging coatings and does not favour positive or negative errors. With the exception of one outlier in the residual plot generated from GRNN that included the ICV, the training residuals (RMSE = 0.91) are only marginally smaller and testing residuals are considerably smaller (RMSE = 0.87) than the GRNN that did not include initial concentration (RMSE = 0.83 for training and RMSE = 0.76 for testing). This suggested that the inclusion of the ICV may improve the performance of the GRNN model when predicting migration. This trend is also reflected in the predicted vs observed migration plots which show more clustering around the central line in the GRNN with the ICV

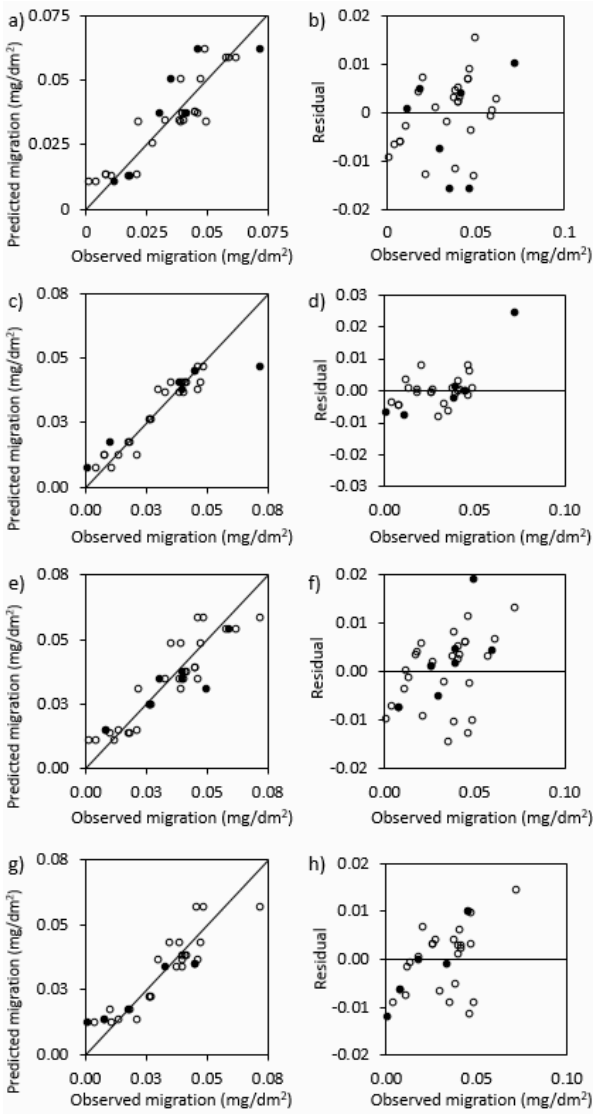

Figure 4: ANN predicted vs observed migration for; a) GRNN without ICV c) GRNN with ICV, e) MLPNN without ICV, g) MLPNN with ICV and the related residual plots (b, d, f and h).

than the one without. Additionally, the R^2 values are higher for the ANN that includes the ICV (R^2 = 0.917 (Training) and R^2 = 0.877 (Testing)) than the ANN that does not (R^2 = 0.837 (Training) and R^2 = 0.762 (Testing)). These findings demonstrate the importance of the ICV when developing ANNs for NP migration prediction.

MLPNN Performance

Similar observations were made for the MLPNN in comparison to the GRNN. For the MLPNN model which included the ICV, R^2 values were higher (R^2 = 0.829 (Training) and R^2 = 0.94 (Testing)) than the model without the ICV included. When comparing the residuals for both MLPNNs there was no noticeable difference between the residuals magnitude and spread around the x-axis.

Of the R^2 values obtained for all four of the ANNs conducted, the ANN which produced the most accurate predictions was the GRNN that included the ICV, having a collective R^2 = 0.87 (training and testing combined) when compared to the MLPNN with an R^2 = 0.82 (training and testing combined). These findings in combination with the significantly lower training and testing times of the GRNN propose that it outperforms the MLPNN when used to predict the migration of NPs from antimicrobial coated LDPE films.

CONCLUSIONS

Accelerated migration studies on antimicrobial coated LDPE films showed that migration of Ag occurred in the range 1.1 – 72 µg/dm^2. The addition of PS-*b*-PEO and pluronic surfactant surface treatment during the coating process was found to decrease migration from the nanocoated materials. Both GRNN and MLPNN were found to accurately predict Ag migration with R^2 values of 0.81 (GRNN without ICV), 0.87 (GRNN with ICV), 0.81 (MLPNN without ICV) and 0.72 (MLPNN with ICV). The best ANN methodology to simulate migration of Ag from nanocoated LDPE films was the GRNN with the ICV included.

While good prediction of Ag migration from nanocoated LDPE films was obtained, further research is necessary to validate the ANNs and test the applicability of ANNs as a predictive modelling tool on migration of NPs from other coated packaging materials.

FUNDING

This work was funded under the Food Industrial Research Measure (FIRM) as administered by the Irish Department of Agriculture, Food and the Marine.

REFERENCES

Azlin-Hasim, S., Cruz-Romero, M., Cummins, E., Kerry, J. P., and Morris, M. A. 2015. "Application of silver nanodots for potential use in antimicrobial packaging applications." Innovative Food Science & Emerging Technologies, 27, 136-143.

Bott, J., Störmer, A., and Franz, R. 2014a. "A Comprehensive Study into the Migration Potential of Nano Silver Particles from Food Contact Polyolefins." *Chemistry of Food, Food Supplements, and Food Contact Materials: From Production to Plate,* 1159(1), 51-70.

Bott, J., Störmer, A., and Franz, R. 2014b. "A model study into the migration potential of nanoparticles from plastics nanocomposites for food contact." *Food Packaging and Shelf Life, 2*(2), 73-80.

Cushen, M., Kerry, J., Morris, M., Cruz-Romero, M., and Cummins, E. 2013. "Migration and exposure assessment of silver from a PVC nanocomposite." *Food Chemistry, 139*(1–4), 389-397.

Cushen, M., Kerry, J., Morris, M., Cruz-Romero, M., and Cummins, E. 2014. "Evaluation and Simulation of Silver and Copper Nanoparticle Migration from Polyethylene Nanocomposites to Food and an Associated Exposure Assessment." *Journal of Agricultural and Food Chemistry,* 62(6), 1403-1411.

European Commission. 2011. “Regulation (EU) No. 10/2011 of 14 January 2011 on plastic materials and articles intended to come into contact with food.” *Official Journal of European Union*. 54, 1-38.

Hannon, J. C., Kerry, J., Cruz-Romero, M., Morris, M., and Cummins, E. 2015a. “Advances and challenges for the use of engineered nanoparticles in food contact materials.” *Trends in Food Science & Technology, 43*(1), 43-62.

Hannon, J. C., Kerry, J. P., Cruz-Romero, M., Azlin-Hasim, S., Morris, M., and Cummins, E. 2015b. “Assessment of the migration potential of nanosilver from nanoparticle coated low density polyethylene food packaging into food simulants.” *Food Additives & Contaminants: Part A*, Available online doi: 10.1080/19440049.2015.1114184.

Huang, J. Y., Chieng, Y. Y., Li, X., and Zhou, W. 2014. “Experimental and Mathematical Assessment of Migration from Multilayer Food Packaging Containing a Novel Clay/Polymer Nanocomposite.” *Food and Bioprocess Technology*, 8(2), 382-393.

Nobile, M. A. d., Cannarsi, M., Altieri, C., Sinigaglia, M., Favia, P., Iacoviello, G., and D'Agostino, R. 2004. “Effect of Ag-containing Nano-composite Active Packaging System on Survival of Alicyclobacillus acidoterrestris.” *Journal of Food Science, 69*(8), 379-383.

Simon, P., Chaudhry, Q., and Bakos, D. 2008. “Migration of Engineered Nanoparticles from Polymer Packaging to Food - A Physicochemical View.” *Journal of Food and Nutritional Research, 47*(3), 105-113.

Siripatrawan, U., and Jantawat, P. 2008. “A novel method for shelf life prediction of a packaged moisture sensitive snack using multilayer perceptron neural network.” *Expert Systems with Applications, 34*(2), 1562-1567.

Smirnova, V. V., Krasnoiarova, O. V., Pridvorova, S. M., Zherdev, A. V., Gmoshinskiĭ, I. V., Kazydub, G. V., . . . Khotimchenko, S. A. 2012. “Characterization of silver nanoparticles migration from package materials destined for contact with foods.” *Voprosy pitaniia, 81*(2), 34-39.

Specht, D. F. 1990. “Probabilistic neural networks.” *Neural Networks, 3*(1), 109-118.

WEB REFERENCES

1. Maynard, A., and Michelson, E. 2014. The Nanotechnology Consumer Products Inventory. Retrieved from http://www.nanotechproject.org/cpi/

BIOGRAPHY

Joseph C Hannon was born in County Meath, Ireland and went to Dublin Institute of technology where he obtained his degree in mechanical engineering in 2013. He is currently carrying out a PhD in the area of nanoparticle food packaging risk assessment in University College Dublin, Ireland and expects to graduate in 2016/17

Second order Monte Carlo simulation to characterize the health impact of different infant feeding strategies

Géraldine BOUÉ[1,2], Sandrine GUILLOU[1,2], Jeanne-Marie MEMBRÉ[2,1]*
[1]LUNAM University, Oniris, UMR1014 Secalim, F-44307 Nantes, France.
[2] INRA, F-44307 Nantes, France.
*Jeanne-marie.membre@oniris-nantes.fr
+33 240 684 058

Jean-Philippe ANTIGNAC[3,2], Bruno LE BIZEC[3]
[3]LUNAM University, Oniris, USC 1329 Laboratoire d'Etude des Résidus et Contaminants dans les Aliments (LABERCA), F-44307 Nantes, France.

Enda CUMMINS[4]
[4]UCD School of Biosystems and Food Engineering, Dublin, Ireland.

KEYWORDS
Probabilistic model, food safety, risk-benefit assessment, breast milk and infant formula.

ABSTRACT

The quantification of the overall health impact of different infant feeding strategies requires an integrated Risk-Benefit Assessment (RBA), including different consumption scenarios and chemical, microbiological and nutritional components of food. In this comprehensive approach, the intra-populational variability must be taken into account to capture all the potential individual health impacts. Uncertainty appears as a second parameter that must also be considered and characterised to interpret better the outputs, to select whether there are significant differences between scenarios and/or to identify a need for more data. To progress further on the RBA methodology, a probabilistic second order model was developed and applied to the assessment of breast milk and infant formula feeding strategies. The first model focused on factors known to cause health effects for each field, namely *Cronobacter sakazakii* for microbiology, dioxin-like polychlorobiphenyls for chemistry and docosahexaenoic and arachidonic acids for nutrition. The overall health impact has been estimated through second order Monde Carlo simulation for a set of five scenarios of consumption.

INTRODUCTION

Infant feeding is a major concern for parents and public health authorities because the first months of life are crucial for short and long term healthy physiological development (Horta *et al*., 2007; Horta and Victoria, 2013). Breast milk is the main recommendation for infants during the first 6 months of life (WHO, 2014). However, infant formula is the main alternative taken in western countries (OECD, 2009). Both diets were intensively investigated with regard to microbiological, chemical and nutritional aspects. Nevertheless, the overall impact of each diet has not yet been quantified. Moreover, milk preparation can also have an impact on infant health balance and should be considered to underpin guidance on different recommendations. In this context, the present paper aims to document the developed probabilistic RBA model applied to the assessment of different infant feeding strategies.

RISK-BENEFIT ASSESSMENT OF INFANT FEEDING STRATEGIES: SCOPE AND FRAMEWORK

The proposed approach is focused on the development of an integrated RBA probabilistic model. One factor known to contribute to health effects was selected per field based on their scientific interest, originality and feasibility:

- Microbiology: *Cronobacter sakazakii* was selected as the main hazard associated with powder infant formula (PIF) consumption, leading to meningitis, bacteremia and urinary tract infection.
- Nutrition: two fatty acids were considered, docosahexaenoic acid (DHA) and arachidonic acid (ARA). They play a role in the cognitive development that is measured with intellectual quotient tests. Both can be found in breast milk or supplemented PIF.
- Chemistry: dioxin-like polychlorobiphenyls (dl-PCB) were prioritized considering both exposure and hazard characterization data. They have been classified as carcinogen, linked to melanoma, lymphoma non Hodgkin and breast cancer.

Infant feeding strategies are susceptible to have a different health balance, according to the milk consumed and the type of preparation. To evaluate such strategies, different scenarios of consumption were determined and assessed, including two diets: six months of consumption of exclusive PIF and six months of exclusive breast milk.

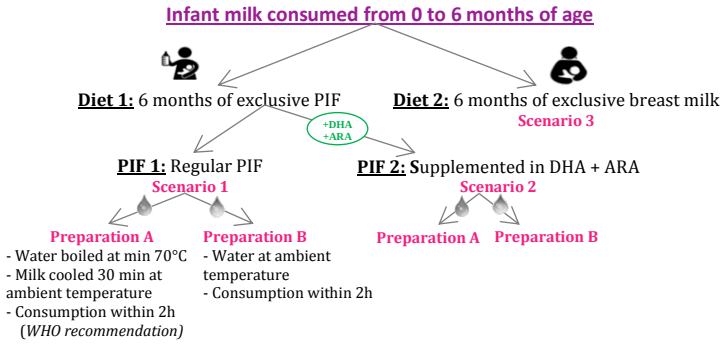

Figure 1: Definition of scenarios implemented and tested

Two different PIF formulas were considered, the regular formula and the fatty acids supplemented formula. Two different PIF preparations were also assessed. One preparation corresponds to the main recommendation (FAO/WHO, 2007) involving the addition of boiled water to the powder followed by half an hour of cooling and a

consumption within two hours. The other preparation considered the addition of water at ambient temperature to the powder and a consumption of the milk within two hours. These different options were distinguished with five different scenarios (Figure 1) and assessed for the French population.

The multidisciplinary Risk-Benefit Assessment (RBA) is an emerging approach from the beginning of the 21st century that includes an individual assessment of risks and benefits in each field and a comparison of the estimated health impacts (Boué *et al.,* 2015). This comparison involves the conversion of the risks and benefits in a composite metric to balance the impacts of all the different diseases. The Disability Adjusted Life Year, DALY (Murray, 1994), a public health indicator, allows to integrate the mortality due to a disease by estimating the years of life lost due to premature death and also the morbidity by weighting the quality of life lost during the years lived with the disease. One DALY is equivalent to one year of perfect life lost. For an individual of a certain age, the DALY associated with a particular disease is calculated with equation 1 (Hoekstra *et al.,* 2012) with P_{eff} the probability of onset of the disease, P_{rec} the probability of recovery and P_{die} the probability of death. YLD_{rec} and YLD_{die} correspond to the duration of the disease when recovering and when die. LE is the expected life expectancy at the current age CA at the disease onset and w is the disability weight of the disease, ranging from 0 a perfect health state to 1 corresponding to the death.

$$DALY = P_{eff}.[(P_{rec}.YLD_{rec}.w + P_{die}(YLD_{die}.w + LE–CA-YLD_{die}) + (1–P_{die}–P_{rec}).(LE–CA).w] \quad \textbf{(1)}$$

METHOD

A probabilistic RBA model was developed to estimate the health impact associated with each factor selected (*Cronobacter sakazakii*, DHA/ARA and dl-PCB).
Data was collected in France when available or in western countries from the scientific literature, reports of food safety agencies and/or other national data sources.

In this model, second order Monte Carlo simulation was run to distinguish between inherent differences in values among members of a population (i.e. variability) versus lack of knowledge (i.e. uncertainty). More precisely, a variability analysis for different uncertainty realizations (Mokhtari *et al.* 2005) was set up: 10 000 iterations in the variability dimension were generated for each of the 100 realizations of uncertainty.

RBA model and second order Monte Carlo simulations were implemented in Excel 2010 using the @Risk software (version 6.3.1).

INDIVIDUAL RISK AND BENEFIT ASSESSMENTS

Microbiology: *Cronobacter sakazakii*

Cronobacter sakazakii is the main bacteria found in PIF but was not associated with breast milk (Jones, 2001; Cossey *et al.,* 2011) so the scenario of exclusive breast milk consumption (scenario 3) was not assessed by this model. The initial level of *Cronobacter sakazakii* at the manufacturing step, N_0, was implemented by bootstrapping data reported in the literature (FAO/WHO, 2006). The storage duration, $t_{storage}$, including the transportation and storage in the supermarket and at home is taken into account. During this period a decrease of the level of bacteria is calculated with equation 2, for a can of 1000 g, given the level at the time of preparation, N_{f1} in log/g of powder (Figure 2). Dr is the decrease rate of the bacteria per day in log units/day (FAO/WHO, 2006).

$$N_{f1} = N_0 . 1000 - t_{storage} . Dr \quad \textbf{(2)}$$

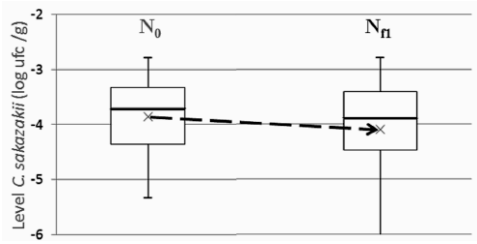

Figure 2: Level of *Cronobacter sakazakii* at the manufacturing step (N_0) and at the time of preparation (N_{f1})

Then, at the step of preparation the prevalence of bottle contaminated is calculated. Each bottle contains a certain portion of powder that is calculated for each gender (i) and age (j) in month according to the specific nutritional requirements (Butte, 2005) and baby weight (Scherdel *et al.,* 2015). Based on this portion and the partitioning law (Nauta, 2005), equation 3 is used to estimate the prevalence of bottle contaminated at the time of preparation. The prevalence of bottle contaminated varies between 0.01% and 5% and is in average at 2%.

$$Prevalence(i,j) = 1-\exp(-Portion(i,j)/(1000.10^{Nf1})) \quad \textbf{(3)}$$

For bottle contaminated the growth and/or inactivation is calculated for both preparations A and B (Figure 1). However, for preparation A the thermal inactivation induced by the addition of boiled water is expected to be effective and avoids the risk associated with *Cronobacter sakazakii*. Indeed, this bacteria has a low thermal resistance (Edelson-Mammel *et al.,* 2004; Iversen *et al*., 2004; Osaili *et al.,* 2009) and even the most resistant strain has a D-value of 3.9 seconds at 70°C (Edelson-Mammel *et al.,* 2004). In addition, the preparation B with water at ambient temperature is not subject of growth because the lag phase is higher than the 2h of consumption set in the scenarios (Kandhai *et al.,* 2006).

At this stage, only preparation B, can contain *Cronobacter sakazakii* at the level estimated at the time of preparation, N_{f1}. For this scenario, the probability of illness was estimated with an exponential dose-response model, equations 4, with r the dose-response parameter (FAO/WHO, 2006).

$$P_{ill} = (1- \exp(-r . 10^{N_{f1}})) \quad \textbf{(4)}$$

The number of illness per 100 000 infants following this preparation during 6 months, $n_{ill}(i,j)$, is calculated per gender (i) and per age (j) going from 1 to 6 months with equation 5, considering 30 days per month.

The cumulated number of contaminated portions per month, per gender, N(i,j), equals 100 000 times 30 days times Prevalence(i,j). N(ij) is large (> 10 000) while the probability of illness, P_{ill}, is small (< 10^{-6}). Then, $n_{ill}(i,j)$ is derived from a Binomial distribution which was approximated by a Poisson distribution to avoid numerical problem (Mendenhall *et al.,* 1990):

$$n_{ill}(i,j) \sim \text{Poisson}\,(N(I,j).P_{ill}) \qquad \textbf{(5)}$$

At the population scale, the average number of illness is 1 per 100 000 infants, varying between 0 and 4 when considering the uncertainty.

Finally, the risk is converted in DALY with the data given in (Reij *et al.*, 2009). On average 37 DALY/100 000 infants were estimated, going from 0 up to 170 DALY.

Nutrition: Docosahexaenoic and Arachidonic acids

In nutrition, both fatty acids DHA and ARA were linked to the improvement of the cognitive development. This development is measured by intellectual quotient (IQ) tests. At the population scale the IQ level follows a normal distribution with a standard deviation of 15 (Neisser *et al.,* 1996) and a mean between 98 and 101 in France (Christainsen, 2012). This distribution is assumed as the reference scenario, the current situation of the population. It was associated with the six months of regular formula feeding scenario because the breastfeeding rate is low in France (Salanave *et al.,* 2014) and only one in third products are supplemented (Briend *et al.,* 2014).
The benefit considered in this case is a potential improvement of IQ for someone who had intellectual disability. A limit was set at 70 IQ points by sociologist to diagnose intellectual disability and is used in the WHO burden of disease study (WHO, 2013). Below this limit, different ranges were defined according to the level of assistance required.
The higher IQ gain associated with supplemented formula and breast milk diets were considered to estimate if there is a significant difference between scenarios. Indeed, an extensive approach including all the published dose-responses would be required to estimate this gain but the net benefit is not obvious regarding the very low disability weight associated with this health state.
For supplemented infant formula, a potential gain of 6.5 points (Birch *et al.,* 2007) was compared with the reference scenario. For breastfeeding the gain was calculated with equation 6 (Gustafsson *et al.,* 2004), taken into account the ratio of DHA and ARA in breast milk (Bernard *et al.,* 2015) and the duration of 6 months (26 weeks). The IQ distribution of the population with intellectual disability for each scenario is represented in Figure 3.

$$\text{Gain} = (0{,}5\ .\ \text{DHA/ARA} + 0{,}528\ .\ 26) \qquad \textbf{(6)}$$

The part of the population with intellectual disability decreases in scenarios 2 and 3 compared with the reference scenario 1, going from 2.4% up to 0.8% for scenario 2 (supplemented PIF) and 0.1% for scenario 3 (breast milk).

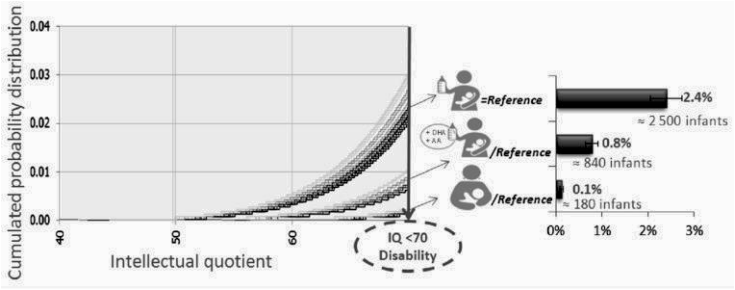

Figure 3: Output distributions of the number of infant with intellectual disability for each scenario

The DALY calculation integrates only the morbidity with this health effect. For each person with intellectual disability, the average burden is estimated at 3.5 DALY. At the population level, scenario 2 and scenario 3 can save in average 6000 and 8000 DALY when compared with the reference scenario.

Chemistry: Dioxin-Like Polychlorinated Biphenyls

Dioxin-like polychlorobiphenyls is a family of 12 congeners that have a similar structure and toxicology than dioxins, and classified as carcinogens (IARC, 2015).
The reference concentration of dl-PCB in French breast milk, $[BM_{TEQ}]$, was calculated with equation 7 based on available exposure data at French level C(k) (Focant *et al.,* 2013; INVS, 2007), the toxic equivalent factor of each congener $WHO_{TEF}(k)$ (van den Berg *et al.,* 2006) and the fatty acid level [FA]. A typical high variability among the population levels is observed, ranging from 0 up to 2 pg/ml.

$$[BM_{TEQ}] = \sum_{k=1}^{n12} WHO_{TEF(k)}.C(k).[Fat] \qquad \textbf{(7)}$$

The reference level in PIF, $[PIF_{TEQ}]$, was deduced from European data (EFSA, 2012). As these reported data are often below the limit of detection (LOD), a worst case approach was applied using a uniform distribution between LOD/2 and the maximum value of 0.02 pg/ml obtained in reconstituted milk.
Infant exposure was then calculated according to equation 8 for formula fed infants by integrating the inter absorption factor of contaminants, AF, and the milk intake varying for each gender (i) and age (j).

$$\text{Exposure}_{PIF}(i,j) = AF\ .\ \text{Intake}_{PIF}(i,j)\ .\ [PIF_{TEQ}] \qquad \textbf{(8)}$$

For breastfed infants, the decrease of the level of contaminants in breast milk during the lactation period was additionally integrated in equation 9 (Ulaszewska *et al.,* 2011).

$$\text{Exposure}_{BM}(i,j) = \left(AF.\text{Intake}_{BM}(i,j).[BM_{TEQ}].\int_0^t e^{-Dft}\,dt\right) \qquad \textbf{(9)}$$

Both diets exhibit distinct exposure trends. The exposure of formula fed infant varies between 0 and 2 pg/bw per day and for breastfed infants between 9 and 66 pg/bw. The comparison of the level of exposure with the safety reference value of 2 pg/bw per day, when converted in daily intake (SCF, 2001), point out that the risk cannot be excluded for breastfed infants.

The assessment was stopped at the exposure step because of a particularly complex issue related to the "late effect of early exposure" problematic, and the high uncertainty associated to this programming effects associated with this particular window of life.

COMPARISON OF SCENARIOS

The five scenarios were compared at this stage with regard to our initial objective. The preparation A with boiled water is a good way to protect formula fed infants against *Cronobacter sakazakii* coming from the powder intrinsic contamination. For preparation B, the burden of disease was estimated in average at 37 DALY for 100 000 infants and more precisely causes 1 case of illness. In comparison, in nutrition, the individual burden of disease associated with intellectual disability is lower, on average 3.5 DALY per case, but it affects a higher part of the population, leading to a potential saving of 6000 and 8000 DALY for scenarios 2 (supplemented PIF) and scenario 3 (breast milk) respectively, by comparison with Scenario 1. Regarding finally the chemical component, the risk associated with dl-PCB cannot be ruled out especially for breastfed infants.
In this first approach where three factors where considered, six months of consumption of supplemented infant formula prepared with boiled water, scenario 2A, appears as a good alternative to avoid the microbiological risk associated with *Cronobacter sakazakii*, to decrease the burden of disease due to intellectual disability and to minimise the exposure to dl-PCB.

CONCLUSION AND PERSPECTIVES

The present case study investigating different infant feeding strategies, pointed out the necessity to undertake a probabilistic approach in Risk-Benefit assessment to detect all the potential health effects that affect only the tails of the distributions. Additionally, the separated characterisation of variability and uncertainty strengthens the analysis by enabling to interpret better the outputs. Indeed, it is a way to see if we have differences between scenarios and also to identify where more data is needed.
To improve the model, accurate the dose-response on the improvement of cognitive development linked with DHA/ARA by integrating lower dose-responses is required. A remaining bottleneck is to link early chemical exposure in life with potential late effects, a big challenge in chemistry.

REFERENCES

Bernard, J. Y.; M. Armand; C. Garcia; A. Forhan; M. De Agostini; M-A. Charles and B. Heude. 2015. "The association between linoleic acid levels in colostrum and child cognition at 2 and 3y in the EDEN cohort." *Pediatric Research,* 77(6), 829-835.

Birch, E. E.; S. Garfield; Y. Castaneda; D. Hughbanks-Wheaton; R. Uauy and D. Hoffman. 2007. "Visual acuity and cognitive outcomes at 4 years of age in a double-blind, randomized trial of long-chain polyunsaturated fatty acid-supplemented infant formula." *Early Human Development*, 83(5), 279-284.

Boué, G.; S. Guillou; J-P. Antignac; B. Le Bizec and J-M. Membré. 2015. "Public Health Risk-Benefit Assessment Associated with Food Consumption – A Review". *European Journal of Food Safety and Nutrition.* 5, 32-58.

Briend, A.; P. Legrand; A. Bocquet; J. Girardet; J. Bresson; J. Chouraqui; D. Darmaun; C. Dupont; M. Frelut and O. Goulet. 2014. "Les apports en lipides chez l'enfant de moins de 3 ans en France. Mise au point et recommandations du Comité de nutrition de la Société Française de Pédiatrie."

Butte, N. F. 2005. "Energy requirements of infants". *Public Health Nutrition*. 8, 953-967.

Christainsen, G. B. 2013. "IQ and the wealth of nations: How much reverse causality?". *Intelligence*, 41(5), 688-698.

Cossey, V.; A. Jeurissen; M.J. Thelissen; C. Vanhole and A. Schuermans. 2011. "Expressed breast milk on a neonatal unit: a hazard analysis and critical control points approach." *American Journal of Infection Control,* 39(10), 832-838.

Edelson-Mammel, S.G. and R.L. Buchanan. 2004. "Thermal inactivation of *Enterobacter sakazakii* in rehydrated infant formula." *Journal of Food Protection*, 67(1), 60-63.

FAO/WHO. 2006. "*Enterobacter sakazakii* and *Salmonella* in powdered infant formula": Meeting report. In: Microbiological Risk Assessment Series, p. 95. Rome, Italy.

FAO/WHO. 2007. "How to Prepare Formula for Bottle-Feeding at Home". Available at http://www.who.int/foodsafety/publications/micro/PIF_Bottle_en.pdf. Accessed on January 7, 2015.

Gustafsson, P.; K. Duchén; U. Birberg and T. Karlsson. 2004. "Breastfeeding, very long polyunsaturated fatty acids (PUFA) and IQ at 6 1/2 years of age". *Acta Paediatrica*, 93(10), 1280-1287.

Hoekstra, J.; A. Hart; A. Boobis; E. Claupein; A. Cockburn; A. Hunt; I. Knudseng; D. Richardsonh, B. Schilteri; K. Schüttej and P.R. Torgerson. 2012. "BRAFO tiered approach for benefit–risk assessment of foods". *Food and Chemical Toxicology*, 50, 684-698.

Horta, B.L.; R. Bahl; J.C. Martines and C.G. Victora. 2007. "Evidence on the long-term effects of breastfeeding: Systematic reviews and meta-analyses". *WHO Press*, Switzerland.

Horta, B.L. and C.G. Victora. 2013. "Short-term effects of breastfeeding: A systematic review on the benefits of breastfeeding on diarrhoea and pneumonia mortality". *WHO Press*, Switzerland.

Focant, J.F.; N. Fréry; M.L. Bidondo; G. Eppe; G. Scholl, A. Saoudi; A. Oleko and S. Vandentorren. 2013. "Levels of polychlorinated dibenzo-p-dioxins, polychlorinated dibenzofurans and polychlorinated biphenyls in human milk from different regions of France". *Science of the Total Environment*, 452, 155-162.

IARC Working Group on the Evaluation of Carcinogenic Risks to Humans (2015). Polychlorinated biphenyls and polybrominated biphenyls, 107.

INVS. 2007. "Dosage des biomarqueurs en maternité dans le cadre de l'enquête Elfe (Étude longitudinale française depuis l'enfance) ".

Iversen, C.; M. Lane and S.J. Forsythe. 2004. "The growth profile, thermotolerance and biofilm formation of *Enterobacter sakazakii* grown in infant formula milk." *Letters in Applied Microbiology*, 38(5), 378-382.

Jones, C.A. 2001. "Maternal transmission of infectious pathogens in breast milk." *Journal of Paediatrics and Child Health,* 37(6), 576-582.

Kandhai, M.; M. Reij; C. Grognou; M. Van Schothorst; L. Gorris and M. Zwietering. 2006. "Effects of preculturing conditions on lag time and specific growth rate of *Enterobacter sakazakii* in reconstituted powdered infant formula". *Applied and environmental microbiology.* 72, 2721-2729.

Mendenhall, W., D. D. Wackerly, and R. L. Scheaffer. 1990. "Discrete random variables and their probability distributions". p. 116–118. In Mathematical statistics with applications. PWS-Kent Publishing Co., Boston.

Mokhtari, A., and H. C. Frey, 2005. "Sensitivity analysis of a two-dimensional probabilistic risk assessment model using analysis of variance". *Risk analysis*. 25, 1511-1529.

Murray, CJ. 1994. "Quantifying the burden of disease: the technical basis for disability-adjusted life years". *Bulletin of the World Health Organization.* 72(3), 429-445.

Nauta, M. J. (2005). "Microbiological risk assessment models for partitioning and mixing during food handling." *International Journal of Food Microbiology*. 100, 311-322.

Neisser, U; G. Boodoo; T.J. Bouchard; A.W. Boykin; N. Brody; S.J. Ceci; D.F. Halpern; J.C. Loehlin; R. Perloff; R.J. Sternberg and S. Urbina. 1996. "Intelligence: knowns and unknowns". *American psychologist*, 51(2), 77-101.

OECD. 2014. OECD Family database. Available at www.oecd.org/els/social/family/database. Accessed on November 18, 2014.

Osaili, T.M.; R.R. Shaker; M.S. Al-Haddaq; A.A. Al-Nabulsi and R.A. Holley. 2009. "Heat resistance of *Cronobacter* species (*Enterobacter sakazakii*) in milk and special feeding formula". *Journal of applied microbiology*, 107(3), 928-935.

Reij, M.W.; I. Jongenburger; E. Gkogka, L.G. Gorris and M. Zwietering. 2009. "Perspective on the risk to infants in the Netherlands associated with *Cronobacter* spp. occurring in powdered infant formula". *International journal of food microbiology*, 136(2), 232-237.

Salanave, B.; C. de Launay; J. Boudet-Berquier and K. Castetbon. 2014. "Durée de l'allaitement maternel en France (Épifane 2012-2013)". *Bulletin épidémiologique hebdomadaire*. 27, 450-457.

SCF (Scientific Committee on Food), 2001. "Opinion of the Scientific Committee on Food on the Risk Assessment of Dioxins and Dioxin-like PCBs in Food". Adopted on 30 May 2001. European Commission, Brussels. Available at: http://europa.eu.int/comm/food/fs/sc/scf/outcome_en.html

Scherdel P.; J. Botton; M.F. Rolland-Cachera; J. Leger; F. Pele; P.Y. Ancel; C. Simon; K. Castetbon; B. Salanave; H. Thibault; S. Lioret; S. Peneau; G. Gusto; M.A. Charles and B. Heude. 2015. "Should the WHO growth charts be used in France?" *PLoS One*. 10(3).

Ulaszewska, M.M.; E. Zuccato and E. Davoli. 2011. "PCDD/Fs and dioxin-like PCBs in human milk and estimation of infants' daily intake: A review". *Chemosphere*. 83, 774-782.

Van den Berg, M.; L.S. Birnbaum; M. Denison; M. De Vito; W. Farland; M. Feeley; H. Fiedler; H. Hakansson; L. Haws; M. Rose; S. Safe; D. Schrenk; C. Tohyama; A. Tritscher; J. Tuomisto; M. Tysklind; N. Walker and R.E. Peterson. 2006. "The 2005 World Health Organization reevaluation of human and mammalian toxic equivalency factors for dioxins and dioxin-like compounds". *Toxicological sciences*, 93(2), 223-241.

WHO. 2013. "WHO methods and data sources for global burden of disease estimates 2000-2011". Global Health Estimates Technical Paper WHO/HIS/HSI/GHE.

WHO. 2014. 10 facts on breastfeeding. Available at http://www.who.int/features/factfiles/breastfeeding/en/#. Accessed on December 2, 2014.

ACKNOWLEDGEMENTS

The authors would like to acknowledge the technical training from the Erasmus+ Intensive Programme Q-Safe, "Quantitative Tools for Sustainable Food and Energy in the food chain" of the European Union, Project No: 2014-1-MT01-KA200-000327 and the scientific contribution from the MAN-IMAL (ANR-11-IDFI-0003) higher education degree programme of Oniris, the Nantes Atlantic College of Veterinary Medicine, Food Science and Engineering, France.

MODELLING THE MYCELIUM FORMATION ABILITY OF PENICILLIUM EXPANSUM AS A FUNCTION OF PROPOLIS, pH AND NaCl

Arianne Muscat[a]
Ioannis Mourtzinos[b]
Maria Gougouli[b,c]
Vasilis Valdramidis[a]
Konstantinos P. Koutsoumanis[b]

[a]University of Malta,
Faculty of Health Sciences,
Department of Food Studies and Environmental Health,
Msida MSD 2080,
Malta
[b]Aristotle University of Thessaloniki,
School of Agriculture, Forestry and Natural Environment,
Department of Food Science and Technology,
Thessaloniki 54124,
Greece
[c]American Farm School,
Perrotis College, Department of Food Science and Technology
Thessaloniki 55102,
Greece
E-mail: kkoutsou@agro.auth.gr

KEYWORDS
Growth-No Growth Model, moulds, propolis, pH, NaCl.

ABSTRACT

The effect of propolis, pH and NaCl on the formation of visible mycelia by *Penicillium expansum*, previously identified as a spoiler of dairy products, was assessed. Mycelium formation was evaluated in tryptone soy broth at 25°C and at different combinations of propolis (0 - 300 μl/ml) , pH (3 – 5) and NaCl concentrations (0%, 12% w/v). In total, 625 visble mycelium formation tests in 125 propolis, pH and NaCl combinations were carried out in polystyrene microtiter plates. A probabilistic model predicting the *P.expansum* mycelium formation boundaries was developed. The information provided from the developed model can be used as useful tool in order to control the growth of moulds in foods with specific characteristics (pH, a_w) with the use of a natural substances like propolis.

INTRODUCTION

Although industrial standards have been greatly improved in the last years, food spoilage by fungi is still a major concern for the food industry (Dantigny et al. 2005; Garcia et al. 2009). Fungal presence in food may adversely affect not only the organoleptic value of the commodity, but most importantly its nutritional value (Gougouli and Koutsoumanis 2012). Furthermore, the development of visible mycelia is one of the most significant quality problems in dairy products with important economic implications for the food industry (Gougouli et al. 2011).
The consumers demand for more healthy foods without preservatives have been increased the last years. The assurance of food safety by controlling the growth of food-borne and food-spoilage microorganisms, while reducing the use of synthetic preservatives that are associated with health risks and microbial resistance, is increased (Naidu, 2000). A new trend in food preservation consists of the use of natural antimicrobial. One prosmising substance for this purpose can be considered propolis.
Propolis is a resinous substance, collected by honeybees (Apismellifera L.) (Marcucci 1995). It is responsible for the lower incidence of bacteria and moulds within the hive than in the surrounding atmosphere. Besides its antibacterial, anti-fungal and anti-viral properties, propolis possesses many other beneficial biological activities such as anti-oxidant, anti-inflammatory, anti-tumour, hepatoprotective, local anaesthetic, immunostimulatory, antimutagenic, etc (Orsia et al. 2005, Marquele et al. 2006). More than 150 bioactive ingredients, among which polyphenols, and terpenoids, have been detected in raw propolis (Ahn et al. 2007). Formation of inclusion complexes between active indgredients and cyclodextrins provides advantages, such as increase in water solubility, protection against oxidation and protection against decomposition by heat or light (Kalogeropoulos et al. 2009). The complexity of the propolis composition, the low solubility of its components in water, make the formation of inclusion complexes an ideal technique for increasing the extraction efficiency.The formation of inclusion complexes during extraction increases the solubility of propolis active components in the extraction medium, providing at the same time a stable extract, since the entrapped components are protected against oxidation and decomposition.
In this study, the combined effect of propolis, pH and NaCl on the mycelium formation of *Penicillium expansum* was studied. More specifically a growth-no growth model was developed incorporating all the above parameters. This kind of models, probability-of-growth modes can help to describe the ability of microorganisms to initiate growth in response to several intrinsic and extrinsic factors (Skandamis et al. 2013). Given that probability models commonly used to link a range of factors (i.e. pH, a_w, temperature, antimicrobials,

atmosphere) to the likelihood of growth, these models can be used as a useful tool for preventing the growth of a biological hazard or of the dominant spoilage microorganism.

MATERIALS AND METHODS

Fungal Strain and Preparation of the Inoculum

P. expansum (strain PE-YV1) examined in this study were isolated from the environment of a yogurt production unit (Gougouli et al., 2011). The above isolate, which is deposited in the strain collection of the Laboratory of Food Microbiology and Hygiene of Aristotle University of Thessaloniki, were maintained on sterile distilled water containing 0.1% (vol/vol) wetting agent (Tween 80; Merck, Darmstadt, Germany) at 5°C and were subcultured bimonthly.
P. expansum was routinely grown at 25°C on malt extract agar (MEA; LAB M Limited, Lancashire, United Kingdom) for 7 to obtain heavily sporulating cultures. Spores were then suspended in sterile distilled water containing 0.1% (vol/vol) of Tween 80 by gently scraping the surface of the medium with a sterile spatula. After filtering the spores' suspensions through four layers of sterile medical tissue (Aseptica, Athens, Greece) in order to remove any debris (mostly mycelial fragments), their final concentration was determined using a Neubauer counting chamber (Precicolor, HBG, Germany). Immediately after preparation, the spore suspension the fungal strain tested was diluted in Ringer's solution (Lab M Limited) to yield an inoculum count of approximately 10^5 spores/ml and used as quickly as possible.

Preparation of Propolis Extract

Extraction Procedure
Grounded propolis was mixed with 2.5% aqueous solution of HP-β-cyclodextrin (liquid-to-solid ratio 1:1), in a stoppered glass bottle. The material was subjected to extraction under stirring at 600 rpm, at room temperature for 2 weeks. Following extraction, samples were filtrated and centrifuged in a table centrifuge (Hermle Z300K, Germany) at 5,000 rpm for 10 min. The clear supernatant was a stored at −20 °C until used for further analysis.

Chracterization of the Extract
Determination of total polyphenol yield (Y_{TP}). The concentration of total polyphenols in the extracts (C_{TP}) was determined using the Folin-Ciocalteu methodology. Yield in total polyphenols (Y_{TP}) was expressed as mg gallic acid/L.
Determination of the antiradical activity (A_{AR}). An aliquot of 0.025 mL of sample was added to 0.975 mL DPPH$^{\bullet}$ solution (100 μM in MeOH) and the absorbance was read at t = 0 and t = 30 min. Trolox™ equivalents (mMTRE) were determined from linear regression, after plotting $\%\Delta A_{515}$ of known solutions of trolox™.
Determination of the reducing power (P_R). A Sample aliquot(0.05 mL) was mixed with 0.05 mL $FeCl_3$ solution (4 mM in 0.05 M HCl), and incubated for 30 min in a water bath at 37 °C. Following this, 0.9 mL TPTZ solution (1 mM in 0.05 M HCl) wasadded, and the absorbance was recorded at 620 nm after exactly 5 min. P_R was determined as mM ascorbic acid equivalents (mM AAE).

Growth-No Growth Assays

Environmental conditions
The mycelium-forming ability of the tested *P. expansum* was evaluated in tryptone soy broth (TSB, LabM Limited) at 25°C, in high-precision (±0.2 C) incubator (Sanyo MIR 153, Sanyo MIR 253, Sanyo Electic Co., Ora - Gun, Japan), and at different combinations of pH values, propolis and NaCl concentrations. More specifically, five pH values (3, 3,5, 4, 4,5 and 5), five different concentrations of propolis (0, 50, 100, 200 and 300μl/ml) and five different NaCl concentrations (0%, 3%, 6%, 9% and 12% w/v) were evaluated. The pH of TSB was adjusted to the above values with 10% (vol/vol) lactic acid (Fluka, Buchs, Germany) using a digital pH meter with an epoxy refillable pH probe (Thermo Electron Corporation, Beverly, MA, USA). The abovementioned salt concentrations were achieved by adding to the medium appropriate amounts of NaCl (Merck, Darmstadt, Germany). The pH values of the substrates were also measured after sterilization and those were used for modeling purposes. Aqueous solution of propolis were added in the TSB after sterilization in order to achieve the aforementioned concentrations. Five replicates for each pH, propolis and NaCl combination were tested resulting in a total of 625 tested samples from pH, propolis and NaCl.
Mycelium formation was evaluated macroscopically in microtiter plate wells. 20-ml aliquots of the *P. expansum* spore suspension (with the characteristics described previously) dispensed in 100-well polystyrene microtiter plates (Oy Growth Curves Ab Ltd., Raisio, Finland), while negative control wells (i.e. containing broth only) also were included. The microtiter plates were incubated statically at 25°C for 17 d, and then the plates were observed for any visble mycelium formation.

Modelling the boundaries of mycelium formation

The collected macroscopical data, corresponding to different conditions, were converted into binary data. Then, a logistic polynomial regression model was fitted to the binary data using Minitab ver. 16 (Minitab Inc., State College,PA, USA), based on the approach described by Ratkowsky and Ross
(1995). The model's equation is shown below:

$$\text{Logit}(P) = \alpha_0+\alpha_1\cdot pr+\alpha_2\cdot NaCl+\alpha_3\cdot pH+\alpha_4\cdot pr\cdot NaCl+\alpha_5\cdot pH\cdot NaCl \quad (1)$$

where Logit (P) is an abbreviation of ln[P/(1-P)], P is the probability of biofilm formation (in the range of 0-1) and a_i are the coefficients to be estimated.
The automatic variable selection option with a stepwise selection method was used to choose the most significant effects ($P \geq 0.05$). The predicted mycelium formation/no formation interfaces for P = 0.1, 0.5 and 0.9 were calculated using Excel Solver (Microsoft Corp., Redmond, WA, USA).

RESULTS AND DISCUSSION

The presence of active ingredients as polyphenols in propolis, varies and being influenced by botanical and geographical factors, as well as with collection season. Three photometric tests selected as parameters to characterize the propolis extract. A standarized extract with certain specifications could be produced using different types of propolis. Results of photometric tests of propolis extract presented in Table 1.

Table 1:Values of Photometric tests of Propolis Extract

Photemertic test	**Value**
Total polyphenol yield (Y_{TP})	3700 mg gallic acid/ L
Antiradical activity (A_{AR})	13.4 mM TRE
Reducing power (P_R)	1.04 mM AAE

An increased number of probabilistic models predicting microbial growth/no growth boundaries have been developed until now in both liquid and solid substrates and at various environmental conditions such as pH, temperature and a_w for bacterial (Koutsoumanis and Sofos, 2004, 2005; Koutsoumanis et al. 2004; Lanciotti et al. 2001; Presser et al. 1998; Valero et al. 2010; Yoon et al. 2012). Nonetheless, no attempt has been made so far, to our knowledge, towards the development of mathematical models for the description of the mycelium formation boundaries of spoilage moulds. In this study, a probabilistic model was developed predicting the propolis, pH and a_w boundaries of *P. expansum* visible mycelium formation. For this purpose, the collected macroscopical measurements, corresponding to different environmental conditions, were converted into binary data. Among the 125 combination treatments of propolis pH and a_w tested in the present study, mycelium formation of *P. expansum* was observed in 56 conditions and no mycelium formation in 69.

The raw data revealed that in absence of propolis the tested mould can grow almost in all combinations of pH and concentrations of NaCl, even at very low pH values and/or high concsntrations of salt. However, with the addition of a small amount of propolis (50 μl/ml) the mould loses its ability in forming mycelium at concentrations of NaCl equal or higher to 6%. At propolis concentrations equal to 200 μl/ml, it was observed that the mould grows and forms visible mycelia only in the absence of NaCl, while at 300 μl/ml the growth is prevented even after 60 days of storage at 25°C.

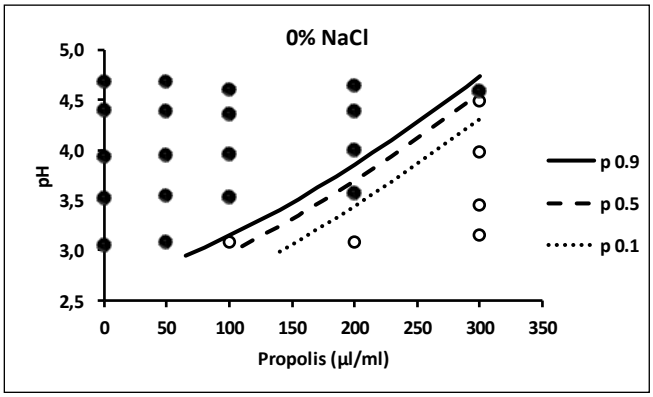

Figure 1: Growth (Mycelium Formation) Boundaries of *Penicillium expansum* at 25°C as afunction of Propolis and pH predicted by the Model (equation (1)) Compared with the Data used to Generate the Model. (Black symbols: mycelium formation in all replicates; empty symbols: no mycelium formation in all replicates; lower dashed line: P = 0.1; interim solid line: P = 0.5; upper dashed line: P = 0.9).

In the absence of NaCl, as it is illustrated in Figure 1, propolis is effective in inhibiting *P. expansum* growth at concentrations higher than 100 μl/ml, especially at low pH values.

The binary data were further fitted to a polynomial model using logistic regression. The estimated parameters of the logistic regression model are shown in Table 2. The parameters with no significant effect ($P \geq 0.05$) were removed from the model. The concordance index and the Hosmere-Lemeshow goodness-of-fit statistic were used as measures of the goodness-of-fit of the developed model. The predictions at probabilities of 0.1, 0.5 and 0.9 with the corresponding observed data from which the predictions were derived. As can be seen in Figure 1, where the growth boundaries of *P. expansum* are presented for 0%NaCl, only one condition fell outside the prediction probability range (from 0.1 to 0.9).

Table 2. Parameter Estimates of the Logistic Regression Model for the Boundaries of Mycelium Formation.

Cofficients	**Estimated values**	**Standard error**	***P* value**
constant	-15.346	3.167	0.000
pr	-0.054	0.008	0.000
NaCl	1.033	0.387	0.008
pH	7.113	1.135	0.000
pr·NaCl	-0.006	0.001	0.000
pH·NaCl	-0.447	0.121	0.000

In conclusion, the results of the present study demonstrated that this physical substance can be effective in managing the fungal growth alone or in combination with low pH and with the presence of NaCl. The ability of above factors in inhibiting the mould growth was quantified and expressed as probability of growth with the aid of a Growth-No Growth model. The model developed in this work, although based on simplified growth medium, constitutes a good basis towards the quantification of the overall interactions of mycelium formation factors and can, thus, provide useful information for controlling similar moulds in food systems. Further research objectives of great value for the control of moulds in foods, especially with the use of biological compounds include the incorporation of these in edible films or coatings.

This research was funded with the support of the Erasmus+ programme of the European Union (Project No. 2014-1-MT01-KA200-000327).

REFERENCES

Garcia, D., Ramos, A.J., Sanchis, V. and Marín, S. (2009). "Predicting mycotoxins in foods: a review." Food Microbiology 26, p. 757–769.

Gougouli, M. and Koutsoumanis, K. (2012). "Modeling germination of fungal spores at constant and fluctuating temperature conditions." International Journal of Food Microbiology 152, p. 153-161.

Gougouli, M., Kalantzi, K., Beletsiotis, E. And Koutsoumanis, K.P. (2011). "Development and application of predictive models for fungal growth at tolls to improve quality control in yogurt production." Food Microbiology 28, p. 1453–1462.

Koutsoumanis, K., and Sofos, J.N. 2004. "A comparative study on growth limits of *Listeria monocytogenes* as affected by temperature, pH and aw when grown in suspension or on a solid surface." Food Microbiol. 21, 415-422.

Koutsoumanis, K.P., Kendall, P.A., Sofos, J.N. 2004. "Modeling the boundaries of growth of *Salmonella* Typhimurium in broth as a function of temperature, water activity and pH." J. Food Prot. 67, 53-59.

Lanciotti, R., Sinigaglia, M., Gardini, F., Vannini, L., Guerzoni, M.E. 2001. "Growth/no growth interfaces of *Bacillus cereus*, *Staphylococcus aureus* and *Salmonella enteritidis* in model systems based on water activity, pH, temperature and ethanol concentration." Food Microbiol. 18, 659-668.

Marquele FD, Oliveira ARM, Bonato PS, Lara MG. Fonseca MJV. 2006. "Propolis extract release evaluation from topical formulations by chemiluminescence and HPLC." J Pharm Biomed Anal 41,461-468.

Microbiology 100, p. 187-196.

Naidu, A. S. (2000). "Natural food antimicrobial systems." Boca Raton, FL: CRC Press.

Nick Kalogeropoulos N, Konteles S, Ioannis Mourtzinos I, Troullidou E, Chiou A, Karathanos V.T. 2009. "Encapsulation of complex extracts in β-cyclodextrin:An application to propolisethanolic extract." Journal of Microencapsulation, 2009; 26(7), 603–613

Orsia OR, Sforcin JM, Funaria SRC, Bankova V. 2005. "Effects of Brazilian and Bulgarian propolis on bactericidal activity of macrophages against *Salmonella* Typhimurium." Int Immunopharmacol 5,359-368.

Presser, K.A., Ross, T., Ratkowsky, D.A. 1998. "Modelling the growth limits (growth/no growth interface) of *Escherichia coli* as a function of temperature, pH, lactic acid concentration, and water activity." Appl. Environ. Microbiol. 64, 1773-1779.

Presser, K.A., Ross, T., Ratkowsky, D.A. 1998. "Modelling the growth limits (growth/no growth interface) of *Escherichia coli* as a function of temperature, pH, lactic acid concentration, and water activity." Appl. Environ. Microbiol. 64, 1773-1779.

Ratkowsky, D.A., Ross, T. 1995. "Modelling the bacterial growth/no growth interface." Lett. Appl. Microbiol. 20, 29-33.

Skandamis, P.N, Mataragas, M., Lambert, M.R. 2013. Primary Model fitting and probabilistic modes. In Dantigny, P., Panagou, E.Z. (Eds.), Predictive Mycology. Nova Science Publishers, Inc. NY, USA. pp:221-247.

Yoon, H., Lee, J.-Y., Suk, H.-J., Lee, S., Lee, H., Lee, S., Yoon, Y. 2012. "Modeling to predict growth/no growth boundaries and kinetic behavior of *Salmonella* on cutting board surfaces." J. Food Prot. 75, 2116-2121.

MODELLING OF A NUTRIENT FEEDBACK MECHANISM DURING HUMAN DIGESTION OF CARBOHYDRATES

Tom Moxon[1], Philippe Nimmegeers[2], Dries Telen[2], Jan Van Impe[2], Serafim Bakalis[1]

[1]Chemical engineering,
The University of Birmingham
Edgbaston, Birmingham, United Kingdom, B15 2TT,
E-mail: TEM801@bham.ac.uk

[2]KU Leuven, Department of Chemical Engineering,
BioTeC+ & OPTEC,
Gebroeders De Smetstraat 1, 9000 Ghent, Belgium
E-mail: jan.vanimpe@cit.kuleuven.be

KEYWORDS

Optimization, PDEs, Model Design, Dynamic Modelling, Monte Carlo

ABSTRACT

The paper builds on previous work (Moxon *et al.* 2016), to add a nutrient based feedback mechanism to a model of gastric and intestinal nutrient transport during human digestion. The mechanism operates as an 'on-off' switch, whereby if the maximum absorption rate is reached, the gastric emptying rate is set to zero. The model parameters were estimated against *in vivo* results from literature, followed by a Monte Carlo simulation to see how the parameter estimates are affected by the random noise in the experimental data, where the parameter estimates for high viscosity solutions show more sensitivity to experimental noise. A sensitivity analysis on the gastric content showed that the system is most sensitive to changes in parameters when high glucose, high viscosity liquids are consumed.

INTRODUCTION

Diet related diseases such as obesity, type 2 diabetes, and heart disease are becoming a major problem in the developed world (HSCIC 2014). This increase has been linked to changes in diet and physical activity, with a greater abundance of energy-dense and processed food being available for consumption (Haslam and James 2005). The addition of fiber to foods has been shown to have positive effects upon health which are linked to the fibers effect upon viscosity, solubility and fermentation ability (Gidley 2013).
Numerical modelling of the gastrointestinal tract has been carried out in both pharmacokinetic (Peng and Cheung 2009; Stoll *et al.* 2000) and food related research (Moxon *et al.* 2016; Taghipoor *et al.* 2012), to try and gain a greater understanding of the processes involved during drug or food consumption.
The gut can be thought of as a series of ideal reactor systems (Penry and Jumars 1986), and models are developed from this starting point with an understanding of the gut physiology.

Digestion in the human gut

The digestion of liquid solutions will be considered in this paper; this starts in the mouth, whereby food is mixed with saliva containing α-amylase, which initiates the chemical breakdown of carbohydrates. After swallowing, the food moves through the oesophagus to the stomach. The stomach acts as a reservoir to store the food and control the release to the small intestine (Kong and Singh 2008). Whilst in the stomach the food will be mixed with gastric juices to produce chyme.
The stomach can be thought of as analogous to engineering unit processes, whereby the stomach acts as a reservoir, a mixer, a grinder, and a pump (Kong and Singh 2009).
There is also evidence of a nutrient controlled feedback mechanism where the rate of gastric emptying is influenced by the amount of nutrient within the small intestine (Brener *et al.* 1983; Calbet and MacLean 1997).
The small intestine is the main site of nutrient absorption. This work will focus on the absorption of glucose, which takes place by active transport through sodium dependent glucose co-transporter (SGLT1). Along with the presence of proteins for the absorption of glucose there will be taste receptors, such as T1R2/R3 (Hass *et al.* 2010), which will detect sugars and initiate a feedback mechanism to inhibit glucose production and food intake (Breen *et al.* 2013). This sensing of nutrients could also explain the nutrient controlled feedback mechanism, whereby nutrients in the duodenum lead to a decrease in the gastric emptying rate (Brener *et al.* 1983; Calbet and MacLean 1997).

Scope

In this work a grey-box model is developed for stomach emptying and the intestinal absorption of glucose. A nutrient controlled feedback mechanism, that expresses the influence of the amount of nutrient within the small intestine on the rate of gastric emptying, is incorporated in the model.
A model structure, based on previously published work (Moxon et al., 2016), is extended and two non-measurable model parameters have to be estimated: the maximum rate of absorption before the feedback mechanism begins inhibition of gastric emptying, $A_{\max}$, and the initial gastric emptying rate γ_0.

PROBLEM FORMULATION

In this section, the model structure and mathematical problem formulations for parameter estimation are presented.

Model structure

The model will assume the stomach can be described as a continuous stirred tank reactor (CSTR) and the small intestine will be described as a plug flow reactor (PFR), as shown in Figure 1. The effect on the structure (chemical or physical) of the food is not considered.
The ingestion of liquid solutions will be modelled, but the effect of secretions upon the digestion will not be considered. It will be assumed that upon consumption the entire liquid meal will enter the stomach at the initial time

(t=0s), and emptying will occur over the temporal domain $t \in [0, t_f]$, where t_f is the final measurement time.

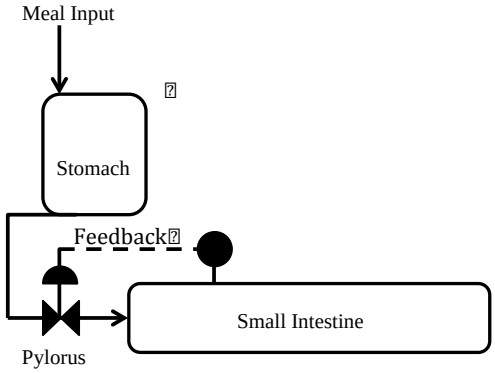

Figure 1 Schematic of the stomach and small intestine represented by a series of reactors with a feedback mechanism from intestinal to stomach compartment.

The mass balance on the stomach glucose mass, G_S (g) gives:

$$\frac{\partial G_s(t)}{\partial t} = -\gamma G_s(t)$$
$$G_s(0) = G_{s0}$$

Where G_{s0} is the initial input of glucose to the stomach and, γ, is the gastric emptying rate (s^{-1}).
The glucose mass in the small intestine is modelled by taking the effect of mass transfer on glucose absorption in the small intestine into account, together with an input from the gastric emptying. The movement of the mass along the small intestine and the absorption will be modelled using a one dimensional advection-reaction equation. The glucose mass (g) in the small intestine $G(z,t)$ will be described by a partial differential equation (PDE), with the spatial domain $z \in [0, L]$, where L (m) is the total length of the small intestine:

$$\frac{\partial G(z,t)}{\partial t} = \begin{cases} \gamma G_s(t) - \bar{u}\frac{\partial G(z,t)}{\partial z} - \frac{2f}{r_m} KG(z,t), & if\ z = l_0 \\ -\bar{u}\frac{\partial G(z,t)}{\partial z} - \frac{2f}{r_m} KG(z,t), & otherwise \end{cases}$$

$$G(z,0) = 0$$

$$\left.\frac{\partial G}{\partial z}\right|_{z=0} = \left.\frac{\partial G}{\partial z}\right|_{z=L} = 0$$

The point of input l_0 will be equal to the radius of the mass entering the small intestine from the stomach at time, t. Assuming that the mass enters as a spherical bolus, the absorption (g/s) $A(t)$ will be modelled as:

$$A(t) = \sum_{z=0}^{L} K_a G\,(z,t)$$

$$K_a = \frac{2f}{r_m} K$$

Where K_a is the absorption rate (s^{-1}) and K is the mass transfer coefficient (m/s).
It is assumed that the gastric emptying rate is related to the absorption rate of glucose:

$$\gamma = \begin{cases} 0 & if\ A(t) > A_{\max} \\ \gamma_0 & otherwise \end{cases}$$

Here, γ_0 is the initial rate of gastric emptying, $A(t)$ is the absorption rate of glucose, and $A_{\max}$ is the maximum rate of absorption (g/s) before the feedback mechanism initiates inhibition of gastric emptying.

Table 1 List of parameters used in the models that are fixed.

Parameter	Value	Reference
Velocity ($\bar{u}$)	1.7e-4 ($m.s^{-1}$)	(Ganong 2005; Stoll *et al.* 2000)
Mean intestinal radius (r_m)	1.75 (cm)	(Ganong 2005; Stoll *et al.* 2000)
Length of intestine	2.85 (m)	(Ganong 2005; Stoll *et al.* 2000)
Protrusion factor (f)	12	(Moxon et al. 2016)

The model equations will be solved in MATLAB (R2014a). The PDEs will be discretised backwards in space as follows, where the spatial step used is Δz:

$$\frac{\partial G(z,t)}{\partial z} = \frac{G(z,t) - G(z-\Delta z, t)}{\Delta z}$$

Consequently, by discretizing the spatial domain, the PDE model is approximated by a system of ordinary differential equations (ODEs) in time. For use of the model in an optimisation setting, e.g., for parameter estimation, the ODE model is reformulated as:

$$\begin{cases} \dot{\mathbf{x}} = \mathbf{f}(\mathbf{x}, \mathbf{u}, \boldsymbol{\theta}, t) \\ \mathbf{y} = \mathbf{h}(\mathbf{x}, \mathbf{u}, \boldsymbol{\theta}, t) \\ \mathbf{x_0} = \mathbf{x}(0) \end{cases}$$

With $\dot{\mathbf{x}} \in \mathbb{R}^{n_x}$ the time derivative of the state vector $\mathbf{x} \in \mathbb{R}^{n_x}$, $\mathbf{u} \in \mathbb{R}^{n_u}$ the control vector, $\mathbf{y} \in \mathbb{R}^{n_y}$ the measurement or output vector and $\mathbf{x_0} \in \mathbb{R}^{n_x}$ the initial condition vector. Depending on the number of discretisation steps taken in space n_z, there are n_z states for the glucose content in the small intestine and 1 state for the glucose content in the stomach G_s: $\mathbf{x} = [G_s(t) \quad G(0,t) \quad \ldots \quad G(n_z \Delta z, t)]^T$. The controls are the initial glucose content G_{s0} fed to the stomach and viscosity μ: $\mathbf{u} = [G_{s0} \quad \mu]^T$. The parameters that are considered to be estimated in this paper are the maximum absorption rate before the feedback mechanism begins inhibition of gastric emptying A_{max} and the initial gastric emptying rate γ_0: $\boldsymbol{\theta} = [A_{\max} \quad \gamma_0]^T$.
For the actual simulation and optimisation, the ODEs will be discretized in the temporal domain using forward Euler method, with time step Δt.

MATERIALS AND METHODS

Experimental data

Experimental data will be taken from literature, for the gastric emptying of a variety of glucose solutions. Three different sets of experimental results will be used, all using the aspiration method for measuring the gastric content, to ensure consistency between the measurements, as different methods (scintigraphy and C-13 breath test) differ in the magnitude of measurements (Becker *et al.* 1992) and glucose as the source of calories. The first runs a single low glucose

solution (Calbet and MacLean 1997), the second runs three different concentrations of glucose solutions (Brener *et al.* 1983), and the third runs high and low concentrations of glucose both at high and low polymer concentrations (Vist and Maughan 1995).

Parameter estimation

The aim of a parameter estimation procedure is to find the set of model parameter values (i.e., the model parameter vector **θ)** that predicts the experimental data as closely as possible. The parameter estimation problem can be seen as an optimisation problem, in which the cost function expresses the difference between the model predictions $y_{i_y}(t_{i_t}, \boldsymbol{\theta})$ and the measurements $y_{\text{meas},i_y}(t_{i_t})$, with $i_y = 1, \dots, n_y$ and $i_t = 1, \dots, n_t$. In this work a sum of squared errors cost function J_{SSE} will be minimised.

$$\min_{\boldsymbol{\theta}} \sum_{i_y=1}^{n_y} \sum_{i_t}^{n_t} \left(y_{\text{meas},i_y}(t_{i_t}) - y_{i_y}(t_{i_t}, \boldsymbol{\theta}) \right)^2$$

subject to:

$$\begin{cases} \dot{\mathbf{x}} = \mathbf{f}(\mathbf{x}, \mathbf{u}, \boldsymbol{\theta}, t) \\ \mathbf{y} = \mathbf{h}(\mathbf{x}, \mathbf{u}, \boldsymbol{\theta}, t) \\ \mathbf{x_0} = \mathbf{x}(0) \end{cases}$$

With n_y, n_t the number of outputs and measurement time points and t_{i_t} the sampling times.

Monte Carlo simulations

To assess the quality of the parameter estimates, a Monte Carlo resampling analysis is performed with *lsqnonlin* in MATLAB R2014b. The rationale is that on a set of measurements a particular random noise realisation with prespecified standard deviation is superimposed. For the quantification of the quality of the parameter estimates, the mean and standard deviation will be calculated.

Sensitivity analysis

To investigate the effect of the parameters upon the output behavior, a parameter sensitivity analysis is carried out.

Due to the large number ordinary differential equations resulting from the PDE system, a finite differences approach is followed to avoid the computation of the system's sensitivity equations. In this approach the effect of a small perturbation applied to the parameter value θ_i on the output is analysed by comparing the nominal state $\mathbf{x_{nom}}$ to the states computed with the perturbed parameter value $\mathbf{x_{pert}}$:

$$\frac{d\mathbf{x}}{d\theta_i} \approx \frac{\mathbf{x_{nom}} - \mathbf{x_{pert}}}{(1-\varepsilon)\theta_i}$$

RESULTS AND DISCUSSION

Parameter Estimation

Table 2 shows the estimated values for the parameters for the different sets of experiments and conditions. Figures 2 and 3 show the results for the mass of glucose in the stomach during digestion. The solid lines show simulated results implementing a feedback loop, from the simulated absorbed glucose and gastric emptying rate. The points show the experimental data from different literature sources that were used to estimate the values of parameters.

Table 2 Experimental data used from literature with the estimated parameters. (HP- high polymer concentration)

Input mass	$\gamma_0(s^{-1})$	$A_{max}\left(\frac{g}{s}\right)$	$K_a(s^{-1})$	Experimental data reference
15g	0.0012	-	-	(Calbet and MacLean 1997)
20g	0.0008	0.007	0.0009	(Brener *et al.* 1983)
50g				
100g				
24g	0.0016	0.01	0.0014	(Vist and Maughen 1995)
112.8g				
24g HP	0.0004	0.01	0.0004	
112.8g HP				

It can be seen in plots (a) and (b) of both figures, that the glucose mass in the stomach empties via exponential decay, when the initial glucose mass in the stomach is low. This could be explained by the fact that nutrients in the intestine are not reaching a great enough bioaccessibility to trigger the feedback mechanism. The difference in the emptying rate of the 4 plots may be due to the different volumes used in the liquid meals (Hunt & Stubbs 1975), different secretions rates of gastric juices due to compositions of the meals (Marciani *et al.* 2000), differences in rheological properties of the liquids (Marciani *et al.* 2001), or variation between people tested. These factors were not considered in the model but could have an influence upon the emptying rate γ_0.

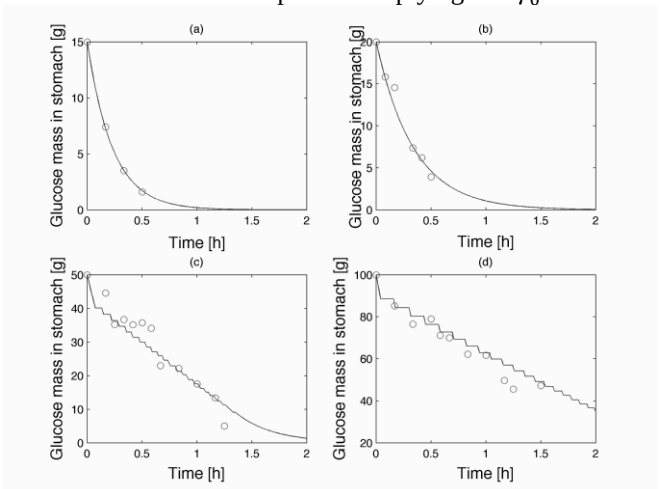

Figure 2 Graphs showing the mass of glucose in the stomach over time as emptying occurs, with simulated (solid line) and experimental results (dots). The four plots are glucose solutions with different initial glucose masses (a) 15g (Calbet and MacLean,1997), (b) 20g (Brener *et al.*, 1983), (c) 50g (Brener *et al.*, 1983), (d) 100g (Brener *et al.* 1983).

When the mass is increased the glucose seems to empty in a more linear fashion. This is shown in both the simulated and experimental results shown in plots (c) and (d) in both Figures 2 and 3. The simulated results show a step like decrease as the emptying from the gastric compartment is prevented. This is due to the bioaccessibility of glucose in the small intestine been too high, leading to a constant calorific emptying rate described in literature (Brener *et al.* 1983; Calbet and MacLean 1997). The number of temporal

discretisation points (after each time step, the gastric emptying rate is re-evaluated) will have an effect upon this.

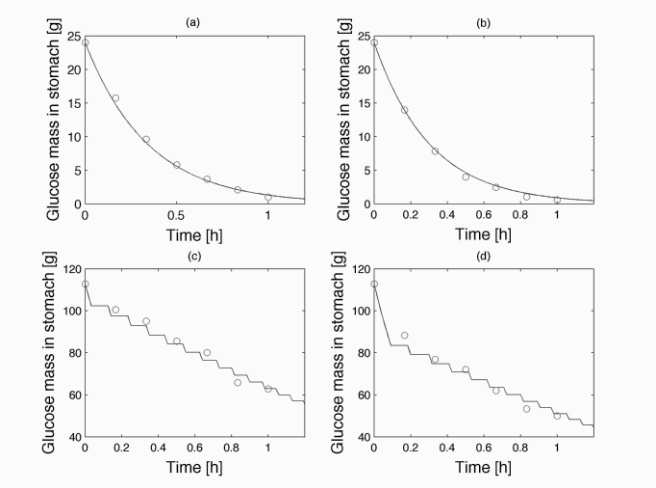

Figure 3 Graphs showing the mass of glucose in the stomach over time as emptying occurs. Simulated results (solid line), and experimental results (dots) (Vist and Maughan 1995) for glucose solutions with (a) Low glucose, low polymer, (b) Low glucose, high polymer, (c) High glucose, low polymer, (d) High glucose, high polymer.

Monte Carlo simulations

To analyse the quality of the estimated parameter values a Monte Carlo simulation was carried out on the data, whereby random noise was added to the experimental data before the model was fitted. The noise was taken as the range of the maximum deviation from the mean for the experimental repetitions from the experimental data. The simulation was carried out for the high glucose concentrations with high and low polymer concentration (Vist and Maughen 1995). The initial empty rate, γ_0, and the maximum absorption rate before feedback initiates, $A_{\max}$, were estimated using fixed values for the mass transfer rate. 1000 iterations were carried out and the resulting parameter values are plotted in Figure 4 along with the 95% confidence regime.

The results in Figure 4 show how the noise in the experimental data (Vist and Maughen 1995) will affect the parameters γ_0 and $A_{\max}$. For plot (a) which is the parameter estimations for the high glucose, low polymer solutions, and plot (b) is the parameter estimations for high glucose high polymer solutions.

In plot (a) most of the parameter values fall within the 95% confidence interval, with random outliers outside the area, the confidence ellipse is longer in than wider meaning the noise affects the estimation of $A_{\max}$ more than γ_0. With the higher viscosity solutions (plot (b)) a larger range of $A_{\max}$ values is seen, and a wider ellipse meaning more variation in the estimation of γ_0 than for the low viscosity solution, again most of the points again falling into the 95% confidence interval with some falling outside with greater $A_{\max}$ or γ_0 estimations.

The histogram plots allow for a better view of the distribution of the parameters when noise is added to the system. Figure 5 shows the histograms for the 2 parameters fitted for high glucose and low polymer solutions. Plot (a) shows the distribution for γ_0, in which there is a tight range around a value of $9e^{-4}$ s^{-1} with a quarter of the simulations giving values of exactly $9e^{-4}$ s^{-1}. Plot (b) shows the distribution of the $A_{\max}$ values where the greatest occurance is around a value of $8e^{-3}$ $g.s^{-1}$, with few estimates below that value, but values occurring up to $8.5e^{-3}$ g/s^{-3} with some frequency.

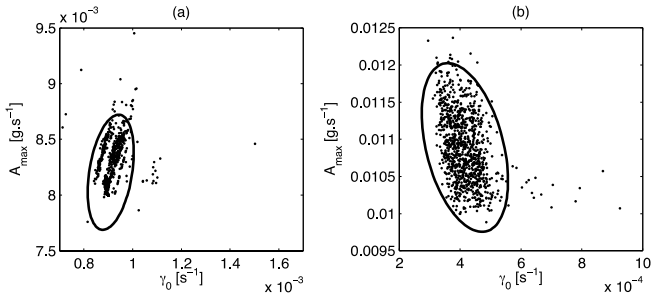

Figure 4 parameter value distribution from Monte Carlo simuation 95% confidence ellipse for (a) high glucose, low polymer solutions, and (b) high glucose, high polymer solutions.

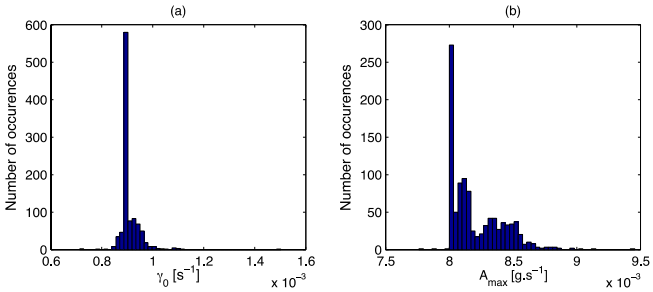

Figure 5 Histogram plots of estimated parameter γ_0 and A_{max} from the Monte Carlo simulation of high glucose, low viscosity solutions.

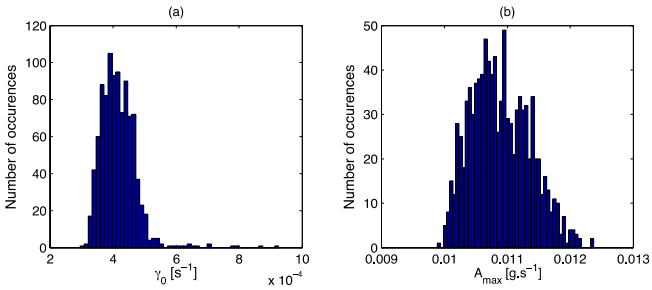

Figure 6 Histogram plots of estimated parameters from Monte Carlo plot of high viscosity high glucose solutions.

Figure 6 shows the histogram plots for high glucose and high polymer solutions parameter estimations. The two plots show a more Gaussian distribution that the low polymer solution with a peak around $4e^{-4}$ s^{-1} for γ_0 and 0.0107 $g.s^{-1}$ for the $A_{\max}$ value.

The parameter estimates for the high and low polymer solution show different values. These could be explained by some of the phenomena that are not included in the model such as the effect of gastric and intestinal secretions upon the viscosity of the meal. This may have a greater effect upon the high polymer solution, which is likely to stimulate greater gastric secretion (Marciani *et al.* 2000) and lead to more noise in the gastric emptying data due to the additional volume added to the stomach and its influence upon the dilution of nutrients and the rheological properties of the meal.

Sensitivity analysis

To investigate the effect of the parameters upon the gastric content a sensitivity analysis was carried out, where by small perturbations are applied to the parameter value then the

output is compared to the nominal state. This was carried out using the data from Table 2.

At low glucose concentraitons the sensitivity of the output to γ_0 is low, with small variations in between the two simulations, as the feedback mechanism is not initiated hence the difference represents the change in the decay constant of the exponential emptying curve.

At higher concentrations a different sensitivity is seen as the rate of absorption reaches the maximum and the feedback mechanism is intiatied, hence a step like sensitivity is seen when the emptying is inhibited the sensitivity is constant. The sensitivity to perpertations is highest for high glucose, high viscosity solutions. This is also seen in the histogram plots Figure 5 (a) and Figure 6 (a) where there high viscosity plot (Figure 6) shows greater sensitivity to the random noise in the system than the low visocity plot.

The low glucose concentration solutions show no sensitivity to the perturbations of A_{max}, this is due to the feedback mechanism not been initiated, at higher concentrations the gastric content shows some variation as the A_{max} is changed but the highest sensitivity is seen when high glucose, high viscosity solutions are tested. This is in agreement with Figure 6 plot (b), where the histogram shows large variablility in the optimised parameter estimation when noise is added to the system. This could be due to the effect of the high viscosity slowing the mass transfer within the small intestine. Changes in the maximum absorption rate along with the reduction in bioaccessibility resulting in greater variability in the gastric content.

This seems to show high glucose and high viscosity solutions will have greater sensitivity to small perturbations to the parameters. Variation of these parameters between people and due to other factors will lead to different results especially within normal meals that tend to have greater nutrient concentration and more complex rheological properties than low concentration glucose liquids.

CONCLUSIONS

This work presents a model to implement the effect of a nutrient induced feedback mechanism during the consumption of glucose solutions. The results show that it is possible to link the nutrient content in the small intestine to the emptying rate of stomach. This was evaluated against data from literature for emptying of different glucose concentration (Brener *et al.* 1983) and for different viscosities (Vist and Maughen 1995) with the estimated model parameters showing good confidence with the experimental data. The model highlights the importance of bioaccessibility of the nutrient within the small intestine upon the emptying rate.

Further work will be carried out to include an optimal experimental design step and develop a more mechanistic approach to the feedback mechanism by modelling the hormonal pathways involved with the proteins which sense the sugar within the small intestine.

REFERENCES

Breen, DM; BA Rasmussen; CD Cote; VM Jackson and TKT Lam. 2013. Nutrient-sensing mechanisms in the gut as therapeutic targets for diabetes. *Diabetes*. 62: 3005-3013.

Brener, W; T R Hendrix and P R McHugh. 1983. Regulation of the gastric emptying of glucose. *Gastroenterology*, 85: 76-82.

Calbet, J A L and D A MacLean. 1997. Role of caloric content on gastric emptying in humans. *J. Physiol.*, 498(2): 553-559.

Ganong, W. 2005 gastrointestinal physiology. In *ganong's review of medical physiology*, 429-486. The McGraw-Hill Companies.

Gidley, M J. 2013. Hydrocolloids in the digestive tract and related health implications. *Curr. Opin. colloid interface sci*. 18: 371-378.

Haslam, DW and WPT James. 2005. Obestiy, *Lancet*. 366: 1197-1209

Hass, N; K Schwarzenbacher; H Breer. 2010. T1R3 is expressed in brush cells and gherlin-producing cells of murine stomach. *Cell tissue res.* 339: 493-504.

HSCIC, 2014. Statistics on obesity, physical activity and diet: England. *Health and social care information centre*.

Hunt, JN and DF Stubbs. 1975. The Volume and Energy Content of Meals as Determinants of Gastric Emptying. *J. Physiol.* 245: 209–225.

Kong, F and RP Singh. 2009. Modes of disintegration of solid foods in simulated gastric environment. *Food Biophys*. 4: 180-190

Kong, F and RP Singh. 2008. Disintegration of solid foods in human stomach. *J. Food Sci.* 73(5): R67-R80.

Marciani, L; PA Gowland; RC Spiller; P Manoj; RJ Moore; P Young and AJ Fillery-Travis. 2001. Effect of Meal Viscosity and Nutrients on Satiety, Intragastric Dilution, and Emptying Assessed by MRI. *Am. J. Physiol. Gastrointest. Liver Physiol*. 280 (6): G1227–G1233.

Marciani, L; PA Gowland; RC Spiller; P Manoj; RJ Moore; P Young; S Al-Sahab; D Bush; J Wright and AJ Fillery-Travis. 2000. Gastric Response to Increased Meal Viscosity Assessed by Echo-Planar Magnetic Resonance Imaging in Humans, *J. Nutr*. 130(1): 122-7.

Moxon, TE; O Gouseti and S Bakalis. 2016. In silico modelling of mass transfer & absorption in the human gut. *J. Food Eng*, 176: 110-120.

Peng, H and B Cheung. 2009. *A review on pharmacokinetic modeling and the effects of environmental stressors on pharmacokinetics for operational medicine.* Toronto: Defence R&D Canada.

Penry, DL and PA Jumars. 1986. Chemical reactor analysis and optimal digestion. *BioScience* 36(5): 310-315.

Stoll, BR; RP Batycky; HR Leipold; S Milstein and DA Edwards. 2000. A theory of molecular absorption from the small intestine. *Chem. Eng. Sci*. 55: 473-489.

Taghipoor, M; P Lescoat; J-R Licois; C Georgelin and G Barles. 2012. Mathematical modeling of transport and degradation of feedstuffs in the small intestine. *J. Theor. Biol*. 294: 114-121.

Vist, GE and RJ Maughan. 1995. The effect of osmolality and carbohydrate content on the rate of gastric emptying of liquids in man. *J. Physiol*. 486(2): 523-531

MODELLING IN FOOD ENGINEERING AND FOOD TECHNOLOGY

MODELING THE DRYING OF A FOOD PROCESSING PLANT

Logan Lecoq (1), Onrawee Laguerre (1), Evelyne Derens (1) Hong-Minh Hoang (1) and Denis Flick (2*)
(1) Irstea UR GPAN 1 rue Pierre-Gilles de Gennes, 92761 Antony, France
(2) UMR Ingénierie Procédés Aliments, AgroParisTech, INRA, Université Paris-Saclay, 91300 Massy, France

(*) corresponding author, address:
AgroParisTech, Dept. MMIP, 16 rue Claude Bernard, 75231 Paris CEDEX 5
E-mail: denis.flick@agroparistech.fr

KEYWORDS

Model, Drying, Food processing plant, Evaporation, Heat transfer, Mass transfer

ABSTRACT

After cleaning, food processing plants have to be dried as quickly as possible to avoid bacteria growth in zones of high humidity. In order to predict the drying of the different wet surfaces (equipment, floor, wall) in function of the operating conditions (air flow rate, temperature and humidity of blown air…), a simplified heat and mass transfer model was developed. Validation was performed by comparing the predicted water mass evolutions with the ones measured in a food processing plant. The influence of blown air humidity, heating of the equipment and air flow rate on evaporation rate was numerically studied.

NOMENCLATURE

C_{pa} Specific heat capacity of air ($J.kg^{-1}.K^{-1}$)
h Heat transfer coefficient ($W.m^{-2}.K^{-1}$)
k Mass transfer coefficient ($m.s^{-1}$)
m Mass of water (kg)
$\dot{m}$ Air mass flow rate ($kg.s^{-1}$)
mC Heat capacity ($J.K^{-1}$)
RH Relative humidity (-)
S Surface area (m^2)
T Temperature (°C or K)
X Water content in air ($kg_{water}.kg_{dry\ air}^{-1}$)
α, γ Air distribution coefficient (-)
β Percentage of wet surface (-)
ρ Air density ($kg.m^{-3}$)
ΔH_v Latent heat of water vaporization ($J.kg^{-1}$)

Subscripts:
a: air;
ext: external;
w: wall;
e: equipment;
f: floor;
0: initial time

INTRODUCTION

The ambient condition of a food factory can be favorable for the growth of food-borne pathogens. *Listeria monocytogenes* is able to resist against the disinfection (Holah et al. 2004), thus, this operation must be performed in an efficient way. This bacteria can "refuge" inside holes on damaged equipment, cracked floors or even complex machinery where stagnant water with nutrient could remain (Carpentier and Cerf 2011). Stagnant water or high air relative humidity (Likotrafiti et al. 2013) are favorable conditions for bacterial growth. Therefore air dehumidification and water evaporation must be performed properly during the drying process just after cleaning to limit the contamination.
When water droplets are deposited on solid surfaces, different steps occur during evaporation. First the contact angle (air/water/solid) decreases while the surface occupied by water on the solid stays constant. Once this angle reaches a minimal value called "receding angle", it stays constant while the water surface decreases until the end of the evaporation process (Chandra et al. 1996, D'agaro et al. 2006). Therefore, the change of evaporation rate when the water surface decreases has to be considered (Vik and Reif 2011).
The main objective of this study is to develop a simplified heat and mass transfer model for the drying process in a food plant. This model allows the prediction of the evaporation rate at different positions in the plant (wall, floor and equipment) according to the operating conditions such as temperature, velocity and humidity of the inlet blown air, the initial temperature and water load inside the plant. In the future, this model will be combined with microbiology models to predict the evolution of the population of pathogens.

EXPERIMENT IN A FOOD FACTORY

The experiment was carried out in a production room of chilled foods: 17.1m long, 8.2m wide and 3.6m high (Figure 1). Low temperature was maintained in this room using 3 evaporators located at the ceiling. Air was blown from the center both to the left and the right, the return air was at the bottom of the evaporator. The configuration was almost the same along the room; therefore in the development of a simplified model, a depth of 1 m long was considered. In this section, the air flow rate was 8600 $m^3.h^{-1}$ (cross section of the inlet air 1.2 m^2 and average inlet velocity 2.0 $m.s^{-1}$).

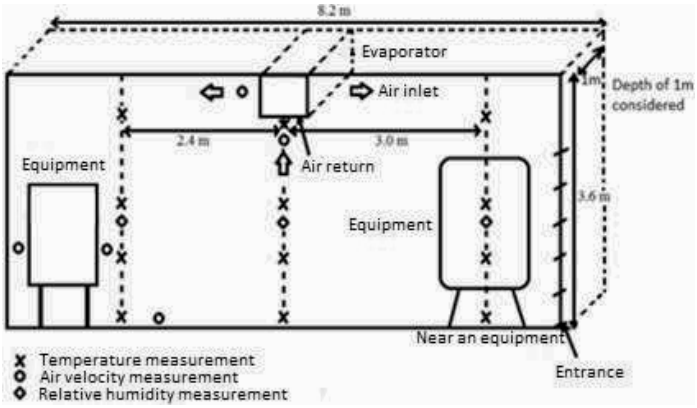

Figure 1: Food production room
(side view, with the measurement points)

The cleaning was carried out by warm water (40°C) added with disinfectant. After that, drying was performed thanks to the air blown from the evaporators during 2 hours. During this period, different measurements were carried out (temperature, relative humidity, air velocity, water weight). To evaluate the drying process, the water weight at different times was measured on various surfaces: wall, floor and equipment. For this measurement, paper towelettes were used to wipe a 50cm x 50cm surface area. The same manipulation was repeated about every 30 min on neighboring surfaces. More details can be found in Lecoq *et al* (2016)

SIMPLIFIED HEAT AND MASS TRANSFER MODEL

The model structure based on the data collected from the factory (geometry, air velocity, temperature, humidity, water weight, materials…) is shown in Figure 2.

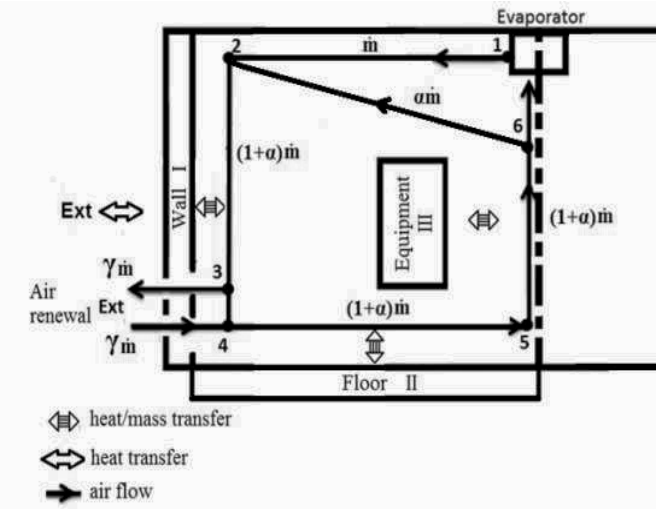

Figure 2: Simplified airflow, heat and mass transfer model in a food factory (side view)

This model allows the prediction of the temperature and water weight evolutions. Only a half of the room is studied considering the same phenomena in the other half (symmetry). Air is blown from the evaporator located on the ceiling, it flows downward near the wall (I) then toward the center along the floor (II) and finally upward to the return air grill (under the evaporator) along the equipment (III). The entrainment of air by the blown air (which constitutes a wall jet in front of the evaporator) is characterized by the coefficient of air distribution α. The air renewal is characterized by the coefficient γ.

Heat exchange between the air and the wall

Convective exchange (heat transfer coefficient h_w) takes place between the air (temperature T_2) and the wall (temperature T_w). After this exchange, the air temperature is T_3:

$$T_w - T_3 = e^{-\frac{h_w S_w}{(1+\alpha)\dot{m}C_{pa}}}(T_w - T_2)$$

The same kind of heat balance was applied from point 1 to 6 (Figure 2).

Water exchange between the air and the wall

The evaporation rate is assumed to be proportional to the wet surface area and the difference between water content of the air in equilibrium with water (at surface temperature) and the air circulating in the vicinity of the surface. The water content of saturated air X_w near the wall is estimated by a linear relation ($X_w = a_w T_w + b_w$) where the values of a_w and b_w are deduced from Antoine's equation.

$$X_w - X_3 = e^{-\frac{k_w \beta_w S_w \rho}{(1+\alpha)\dot{m}}}(X_w - T_2)$$

The same kind of mass balance was applied from the point 1 to 6 (Figure 2).

Temperature evolution of the wall

The variation of the internal energy of the wall depends on the heat exchange by convection with air outside the room and the heat and water exchanges with the air inside the room.

$$\frac{dT_w}{dt} = \frac{h_{ext} S_{ext}}{(mC)_w}(T_{ext} - T_w) - \frac{(1+\alpha)\dot{m}C_{pa}}{(mC)_w}(T_3 - T_2) - \frac{(1+\alpha)\dot{m}\Delta H_v}{(mC)_w}(X_3 - X_2)$$

The same kind of heat balance was applied to the floor and equipment.

Water weight evolution on the wall

$$\frac{dm_w}{dt} = -(1+\alpha)\dot{m}(X_3 - X_2)$$

The same mass balance was applied to the floor and equipment.

The relative humidity of the inlet air RH_1 (coming from the evaporator) is assumed to be known (in absence of air dehumidifier, RH_1 is often around 85%) and the return air temperature is either fixed at a certain value (T_{set}=5°C) or fixed by the maximal power the evaporator can reach (3000W in the studied room).

This system of equations was solved using Matlab software (vR2012a; The MathWorks Inc., Natick, MA, USA, Runge-Kutta 2nd order method).

RESULTS AND DISCUSSION

Comparison between the experimental and the predicted results

The comparison of the evolutions of the mass of water on the wall, floor and equipment obtained with the simplified model and the experimental results obtained in the food production plant shows a relative good agreement (Figure 3). The initial mass of water on the floor is much more significant than that on the wall and equipment. Because of a high thermal inertia, the floor temperature decreases slowly. Therefore the temperature difference between the floor and the air remains significant during a long period, inducing a high evaporation rate. For the equipment made of stainless steel, because of a much lower thermal inertia, its temperature decreases faster, inducing a low evaporation rate.

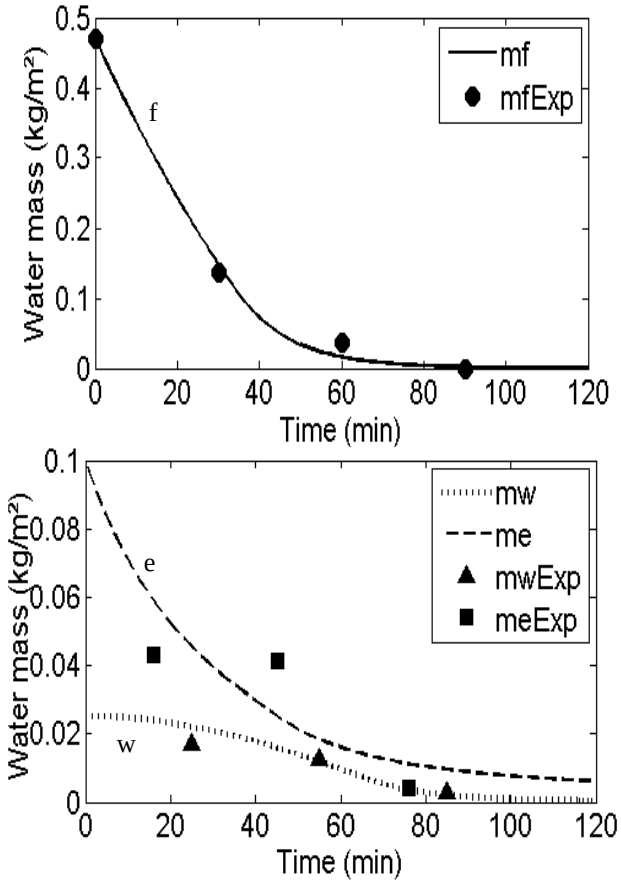

Figure 3: Measured and calculated mass of water located on the floor (f) on the wall (w) and equipment (e) during the drying process (relative humidity of blown air 85%)

Numerical study of the influence of supply air humidity

The results previously shown indicate that at the end of the drying period (for 85% relative humidity of blown air), water can still remain in the plant. Even if the amount of water is small, it may present a risk of bacterial growth. Thanks to the simplified model, the evolution of mass of water in the room can be studied with other ambient conditions. The comparison of water mass evolutions for 50% and 85% relative humidity at the air inlet is shown in Figure 4. The results show that for 50% relative humidity, water evaporation is faster and surfaces are entirely dried after 120 min (end of the drying period). This shows the interest of the use of a drying device to dehydrate the supply air.

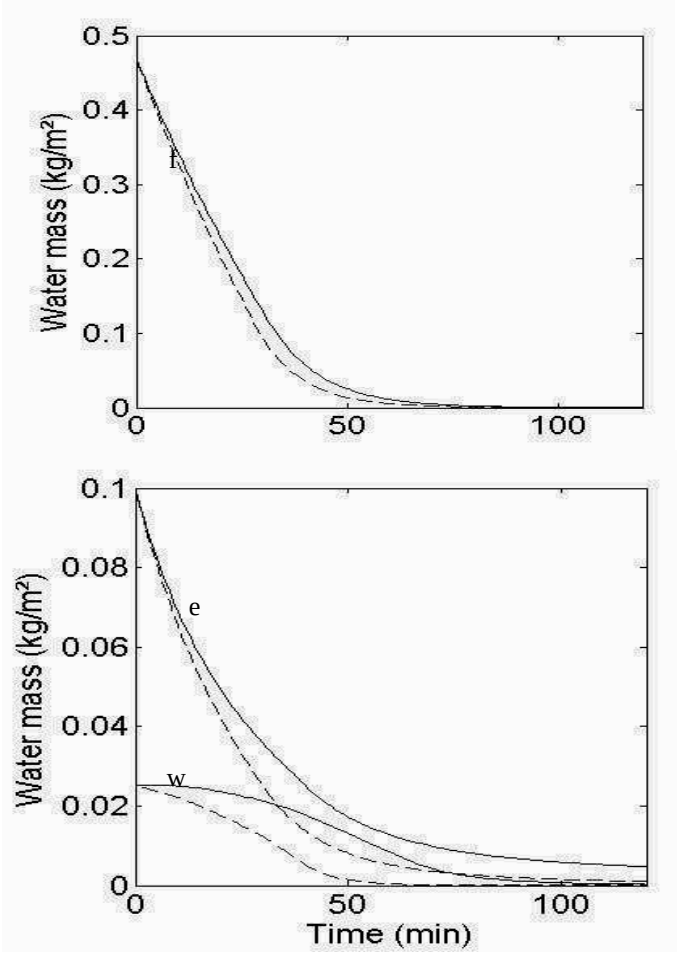

Figure 4: Calculated mass of water located on the floor (f), wall (w) and equipment (e) during the drying process with a relative humidity of blown air of 85% (continuous line) or 50% (dotted line)

Numerical study of the influence of heating the equipment

Because of its low thermal inertia, the drying of the equipment requires a long time. Therefore it should be interesting to slightly heat the equipment in order to accelerate the drying. Figure 5 compares the water mass evolutions in the reference case (without heating) and the case where the equipment is heated with a moderate heating power of 100W (for the equipment located in the 1 meter long section which is considered in the model) with the same relative humidity of blown air (85%) .

The results show that, even with a high humidity (85% RH) of the supply air, using a moderate heating of the equipment allows to dry it in a reasonable time (2h).

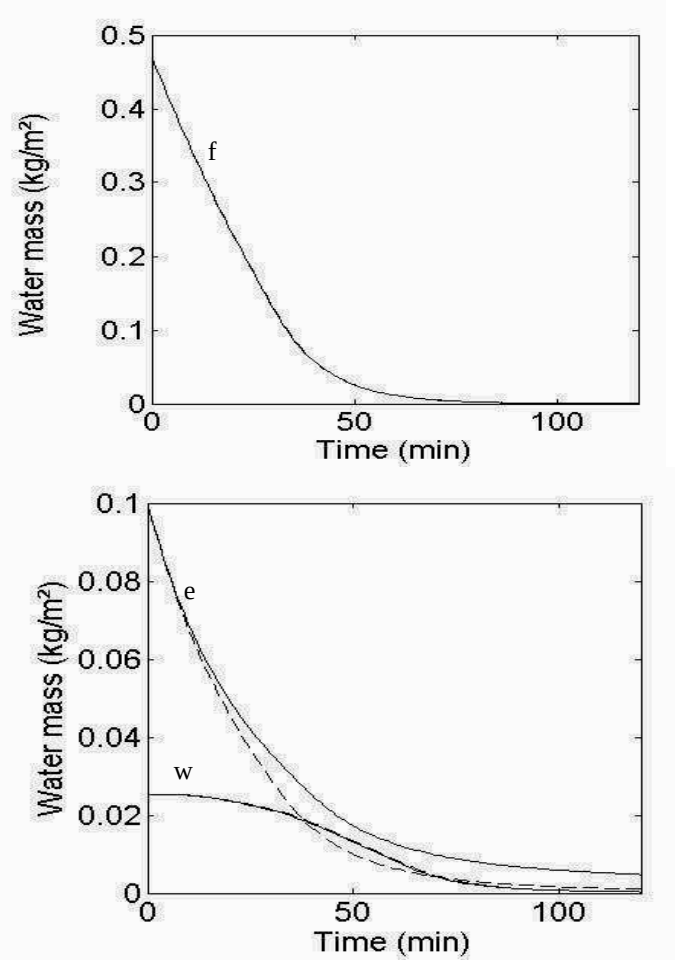

Figure 5: Calculated mass of water located on the floor (f), wall (w) and equipment (e) during the drying process without heating (continuous line) or with 100 W heating of the equipment (dotted line) (relative humidity of blown air 85%) (no difference with or without heating for the water mass on the floor)

Numerical study of the influence of air flow rate on the evaporation time

The numerical model allows also to investigate the influence of air flow rate. Rise of air flow rate limits the increase of temperature and humidity from supply to return of the evaporator. It also leads to intensify the convective heat and mass transfers; the transfer coefficients are approximately proportional to the square root of the velocity which in turn is almost proportional to the air flow rate. The comparison of the water mass evolutions for the reference case (air flow rate of 8600 $m^3.h^{-1}$) and for the case where the air flow rate was doubled is shown in Figure 6 (blown air relative humidity 85%). The results show that the floor and equipment drying rates are increased. But the mass of water on the equipment decreases very slowly after about one hour and, as for the reference case, water remains on the equipment after two hours. For the equipment, the limiting factor seems to be the required heat of vaporization.

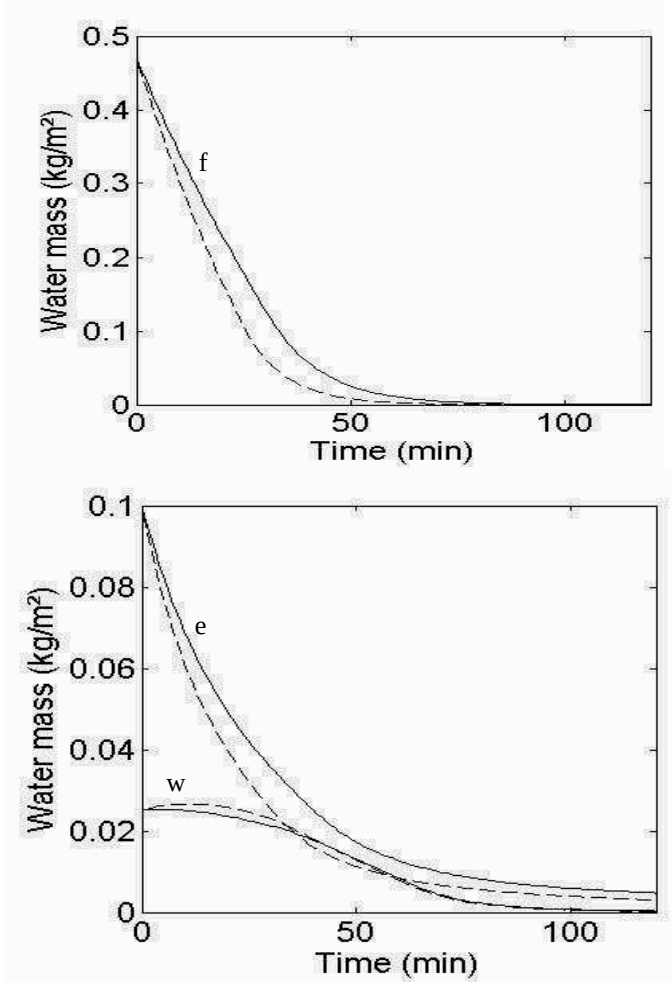

Figure 6: Calculated mass of water located on the floor (f), wall (w) and equipment (e) during the drying process using normal or increased (+100%) air flow rate (relative humidity of blown air 85%).

CONCLUSION

A simplified model was developed to predict the drying of a food production plant after cleaning. It takes into account the heat and mass exchanges between the air and the wall, floor and equipment. It allows the prediction of water mass, temperature of air and solid surfaces, relative humidity and water content of air during the whole drying process. This model, validated by an experiment in a food factory for given operating conditions, can be applied to other conditions to optimize the drying process and to prevent bacterial growth. Reducing the humidity of blown air or heating slightly the equipment could improve the drying.

ACKNOWLEDGEMENT

The research leading to this result has received funding from the French National Research Agency (EcoSec Project, ANR-12-ALID-0005-04). The authors would like to thanks to Labeyrie Fine Foods for their participation of experimentation in plant.

REFERENCES

Carpentier, B.,; and O. Cerf O. 2011. "Review - Persistence of Listeria monocytogenes in food industry equipment and premises". *International Journal of Food Microbiology*, 145, 1-8

Chandra S.; M.D. Marzo; Y.M. Qiao; and P. Tartarini P. 1996. "Effect of liquid-solid contact angle on droplet evaporation". *Fire Safety Journal*, 27, 141-58

Chaturongakul S.; S. Raengpradub; M. Wiedmann and K. Boor. 2008. "Modulation of stress and virulence in Listeria monocytogenes". *Trends in Microbiology*, 16, 388–96

D'agaro P.; G. Croce; and G. Cortella. 2006. "Numerical simulation of glass doors fogging and defogging in refrigerated display cabinets". *Applied Thermal Engineering*, 26, 1927–34

Holah J.; J. Bird and K. Hall. 2004. "The microbial ecology of high-risk, chilled food factories; evidence for persistent Listeria spp. and Escherichia coli strains". *Journal of Applied Microbiology*, 97, 68–77

Lecoq L.; D. Flick; E. Derens; H.M. Hoang; and O. Laguerre. 2016. "Simplified heat and mass transfer modeling in a food processing plant". *Journal of Food Engineering*, 171,1-13.

Likotrafiti E.; P. Smirniotis; A. Nastou; and J. Rhoades. 2013. "Effect of relative humidity and storage temperature on the behavior of Listeria Monocytogenes on fresh vegetables". *Journal of Food Safety*, 33, 545-51

Vik T.; and B.A.P Reif. 2011. "Modeling the evaporation from a thin liquid surface beneath a turbulent boundary layer". *International Journal of Thermal Sciences*, 50, 2311–17

BIOGRAPHIES

LOGAN LECOQ is engineer, he is conducting a PhD work on experimental and numerical characterization of fluid flow, temperature and humidity in cold rooms at Irstea.

ONRAWEE LAGUERRE is research director at Irstea, she is working on heat and mass transfer in cold chain equipments in relation with food quality and security.

EVELYNE DERENS is refrigeration engineer at Irstea, she is working on the equipments and the logistic of the cold chain.

HONG-MINH HOANG is researcher at Irstea, she is working on experimental characterization and modeling of different refrigeration equipments.

DENIS FLICK is professor at AgroParisTech, he is working on modeling of coupled phenomena occurring in food processing : fluid flow, transfers and food transformation.

PREDICTION OF MATERIAL BEHAVIOUR AND FLOWS IN INDUSTRIAL FOOD PROCESSING

Benoit Debbaut
Ansys Belgium s.a.
Avenue Pasteur 4
B 1300 Wavre
Belgium
E-mail: Benoit.Debbaut@ansys.com

KEYWORDS
Modelling, numerical simulation, constitutive equations, boundary conditions, viscoelasticity, thixotropy

ABSTRACT

Food products are known to exhibit complex behaviours in industrial processing, which originate from the kinematics involved or structural changes. Hence, prediction or numerical simulation of complex behaviours in industrial food processing can be challenging. Indeed, it involves the transcription of complex properties and operating conditions into mathematical models. In this contribution, we propose a quick overview of available modelling tools which, hopefully, can assist the process engineer in making appropriate decisions. A few applications are also selected; they will allow us to suggest a reasonable methodology for performing an analysis of complex flow behaviours and for obtaining added value simulation results.

INTRODUCTION

Food processing is probably as old as the invention of fire: However, it is mainly in modern times that food processing has transitioned from a delicate art to an industrial activity endowed with increased systematic and scientific approach. However, contrary to other industrial activities, the material involved, food ingredients, often exhibit less stable physical, chemical or biological properties. And so, for example, next to usually admitted dependences of flow properties with respect to temperature and kinematics, food products under processing may also exhibit physical or chemical changes, which affect the local behaviour.

The improvement or development of a new food product, a process; or an equipment usually requires a trial-and-error procedure in order to fulfil the several technological, economical and health requirements. Often, just-in-time delivery requires squeezing development timelines. Those are generic situations where modelling can bring a useful contribution by enabling preliminary virtual analyses. Yet, before performing a simulation of a process or a segment of a process, relevant data are needed about the material involved. Here, measurements of flow properties are often a first step towards a material characterization, before considering subsequent simulations (Debbaut and Burhin 2002; Macosko 1994; Steffe 1993; Walters 1975).

When observing food products one sometimes witnesses the development of interesting and often anomalous effects which exhibit similarities with observations done with polymers (Boger and Walters 1993; Giesekus 1965). Shear thinning, strain hardening, extrudate swelling, rod climbing, tubeless syphon, are features of viscoelasticity. They are often the fingerprint of specific macromolecular architecture and topology (see e.g. Steffe 1993).

Viscous and viscoelastic effects develop with an intensity that depends on the process and operating conditions. Next to those effects which are more or less easily connected to the flow kinematics, other mechanisms also develop, which are often related to the intrinsic nature of food materials. Indeed, the physical structure and chemical composition can make food materials quite sensitive to their environment. The large number of possibilities makes it difficult to characterize a food material, and phenomenological approaches can be considered.

Next to bulk properties, there are also surface or interface properties. Surface tension easily pops up in mind, however, behaviour along channel walls, from slipping to adhesion, are nonetheless equally important.

As suggested, we are facing a broad scientific context, which offers many experimentation opportunities in terms of modelling. Our purpose in the present contribution is to provide a few guidelines for using modelling as a bridge between process and simulation in food industry. In the next sections, we give an overview of modelling capabilities for viscoelasticity and thixotropy, and we provide comments on boundary conditions as well. The subsequent section is dedicated to the numerical simulation, with a special emphasis on the treatment of non-linearities. Eventually, in the last three sections, we apply the modelling and solver tools to the prediction of conchiglia (pasta) extrusion and to the simulation of specific behaviours in flow distributors.

CONSTITUTIVE MODELLING

Let p, $\underline{\underline{T}}$ and $\underline{v}$ respectively denote the pressure, the extra-stress tensor and the velocity, and let $\underline{\underline{D}}$ denote the rate-of-deformation tensor, or the symmetric part of the velocity gradient. For the sake of facility, we omit temperature effects. Flow of food materials can be considered within

the context of continuum mechanics. With the assumption of incompressibility, the momentum equations is given by

$$-\nabla p + \nabla\cdot\underline{\underline{T}} = \rho\, D\underline{u}/Dt \qquad (1)$$

Here ρ is the fluid density, while D/Dt is the material derivative operator with respect to time. Next, for describing the material behaviour, a constitutive equation must be selected. The simplest constitutive model is an algebraic relationship which relates $\underline{\underline{T}}$ to $\underline{\underline{D}}$ as follows:

$$\underline{\underline{T}} = 2\eta\underline{\underline{D}} \qquad (2)$$

In equation (2) η is the shear viscosity, which can be a function of the local kinematics (see e.g. Macosko 1994) or of a suitable state variable, as will be shown below. The algebraic nature of equation (2) enables its substitution into the momentum equation (1), so that the extra-stress tensor $\underline{\underline{T}}$ does no longer to be calculated simultaneously.

Often the material exhibits a transient response to a kinematic change, and a differential constitutive equation needs to be considered in order to mimic such a behaviour. Constitutive equations of the so-called Oldroyd family (Oldroyd 1958) can be considered here. The general form of such equation is written as:

$$\underline{\underline{T}}\cdot\underline{\underline{G}}(\underline{\underline{T}}) + \lambda\,\delta\underline{\underline{T}}/\delta t = 2\eta\underline{\underline{D}} \qquad (3)$$

In equation (3), λ and η are material parameters, namely a relaxation time and a viscosity factor; they dictate the linear response of the material. Combining several modes endows the rheological model with a relaxation spectrum. The (scalar or tensorial) function $\underline{\underline{G}}(\underline{\underline{T}})$ controls non-linear properties (Giesekus 1982; Johnson and Segalman 1977; Phan Thien 1978; Phan Thien and Tanner 1977). Finally, the term $\delta/\delta t$ stands for a time-derivative operator (contravariant, covariant, etc.), which satisfies the basic objectivity and invariance requirements.

In other situations, the material behaviour is best described with a thixotropic model. This can be achieved e.g. via a dependence of the viscosity in equation (2) upon a state variable χ, which in turn obeys a transport equation:

$$D\chi/Dt = f(\chi,\underline{\underline{D}}) \qquad (4)$$

In equation (4), f is a source term which may typically depend on χ and on the kinematics. This approach is very versatile. Indeed, one can easily build a phenomenological model where the viscosity increases with time by assigning the role of residence time to the variable χ by selecting a unit source term in equation (4) and an appropriate dependence of the viscosity with respect to χ in equation (2). This will be illustrated in a subsequent section.

BOUNDARY CONDITIONS

The momentum equation (1) as well as the constitutive equations (2), (3) or (4) require appropriate boundary conditions. In simple words, they describe the process that is considered as well as the flow domain. For example, an extrusion process for pasta involves an assigned flow rate at the inlet, and a stress free jet (extrudate). It is often assumed that velocities vanish along the channel walls. However, there are situations where wall slipping should be considered. The simplest model for slipping obeys the Navier's law, which relates the tangential force $\underline{f}_s$ to the tangential velocity $\underline{v}_s$ as follows

$$\underline{f}_s = -k\underline{v}_s$$

where k is a coefficient to be experimentally determined. Some materials may exhibit slipping along a wall when the tangential stress exceeds a given value, also to be determined experimentally. Such a behaviour can be described with an asymptotic law, whose scalar form can be written as follows:

$$f_s = -\sigma_w[1 - exp(-v_s/v_c)] \qquad (5)$$

where σ_w and v_c are respectively the upper stress value at the wall and a scaling velocity.

Free surface boundary condition is rather specific. Not only does it assumes zero force on the boundary, but it also relates the motion of material points to the velocity. In other words, this boundary condition is suitable e.g. for extrusion simulation. Selecting this boundary condition also means that the boundary shape is a priori unknown and it will be calculated together with the other flow unknowns. Eventually, it involves a deformation of the calculation domain, and techniques such as remeshing or adaptive meshing are therefore invoked.

NUMERICAL SIMULATION

As has been introduced above, the flow governing equations and the boundary conditions are often non-linear. In addition, flow domains are usually complex, and with the exception of a few cases, analytical solutions can no longer be obtained. Hence, numerical simulation tools are invoked (Keunings, 1989; Owens and Phillips, 2002; Strang and Fix, 1973). In a few words, the principle consists of discretising the flow domain with e.g. finite elements or finite volumes, integrating and assembling the system of equations, and solving the non-linear system with an appropriate solver.

Considering the non-linearities involved and in view of the mixed elliptic/hyperbolic nature of the equations, a Newton iteration is a good candidate for solving the non-linearities, while the use of a direct solver is often recommended for solving the linearized system.

TRANSIENT EXTRUSION OF A SINGLE CONCHIGLIA PASTA

In order to illustrate the potentialities of modelling in food processing industry, let us consider the production of

conchiglie paste made of dough. They are produced via extrusion, and the die must be designed in such a way that the item is properly curled. An additional criterion is the residence time distribution along walls and in dead zones. It can be often critical in food processing, and appropriate warnings about process duration must then be given in the usage notice. In Figure 1(left), we display a typical sketch of a conchiglie die. A single unit consists successively of a feeding channel, a flat distributor and the die lips. In actual (artisanal) process, four to six units are circumferentially connected together as suggested in Figure 1(right) and fed upstream via a single screw extruder. The conchiglie are extruded in a continuous fashion and a blade cuts the extrudates at appropriate length. For scaling the image displayed, the height of the die lips is 4 mm, while the diameter of the feeding channel is 6.5 mm.

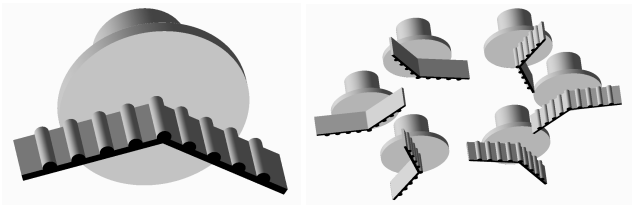

Figure 1. Extrusion of a conchiglia pasta: flow channel of a single unit (left) and geometry of a multiple unit (right)

In the present application, we focus on the development of the conchiglia vs. time; hence we consider simple fluid parameters: the density is 1 g/cm^3, while the viscosity is 10 Pa.s. The actual dough viscosity data exhibits a broad scattering (de la Peña et al. 2014). In terms of boundary conditions, we assume a flow rate of 0.1 cm^3/s at the inlet to a single feeding channel and that the dough sticks at the wall of the device. At the exit of the die, we assume free surface conditions. Since the present application is transient in nature, the calculation for a single unit starts with (nearly) no dough at the die exit, so that the entire transient development of the extruded conchiglia can be predicted. For achieving this, boundary condition for transient free surface is imposed, and it is combined with an appropriate adaptive meshing algorithm for creating additional elements when the calculation domain grows. For simulating an individual unit, symmetry could have been taken into account.

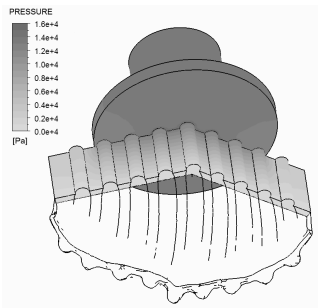

Figure 2. Extrusion of a conchiglia pasta: Pressure distribution and trace of the extruded conchiglia.

As stated above, an important criterion for the process is the absence of dead zones. They can be located by examining the pressure distribution and the trajectories. When inspecting the pressure distribution shown in Figure 2, we see a visible gradient from the entry to the exit of the die. In the present case, the absolute values of the pressure field are not so relevant, and they are obviously affected by the selected rheological model. Pressure changes are very moderate in the flat distributor, and this section deserves a further inspection.

In Figure 3 we display dough trajectories from the entry to the exit. Tracking these trajectories is very instructive. Indeed, they indicate how the dough is being spread within the distributor and the die. Trajectories suggest that the dough is relatively well distributed; a focus into zones which are not really seen by trajectories may reveal further information about the design. An additional output of such analysis is the velocity along trajectories. Quite obviously, trajectories with low velocity should be carefully watched.

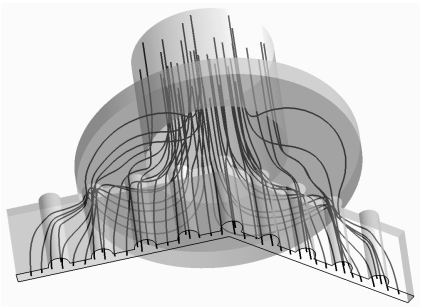

Figure 3. Extrusion of a conchiglia pasta: Dough trajectories.

Eventually, it is important to check whether the conchiglia can be properly extruded, i.e. whether curling develops with time. In Figure 4 we display the shape of the conchiglia at various time during extrusion: we clearly see the development of the shape during the allocated time interval. Of course, this development depends on several factors, the most important ones are the viscosity and the boundary conditions along the die wall. They will actually dictate the velocity distribution, and the unbalance in velocity will produce the desired shape. A contrario, in the event of full slipping at the wall, there would be no curling at all.

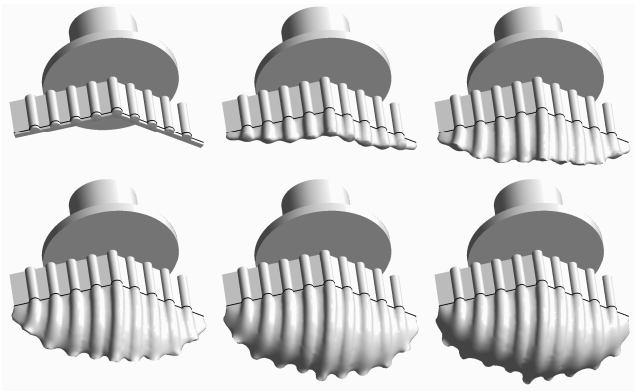

Figure 4. Extrusion of a conchiglia pasta: shape at various instants during extrusion. The black line marks the die exit.

INERTIA EFFECTS IN A FLOW DISTRIBUTOR

Let us consider a (fictive) situation involving a flow distributor with one entry and four exits, as displayed in Figure 5. For the sake of facility, the exits will be referred to by a number ranging from 1 to 4, from left to right. For scaling the flow domain, the diameter of the entry section is 1 cm. As can be seen, the material enters at the top, and the flow is split twice. If one considers a lineal representation of the flow domain, the path length from the entry to any exit is identical. This would suggest that the device is able to split the flow in equal parts. However, as will be shown, one can easily find situations where this is no true at all. Typical causes for asymmetric distributions are non-linear slipping boundary conditions, inertia effects, physical or chemical changes.

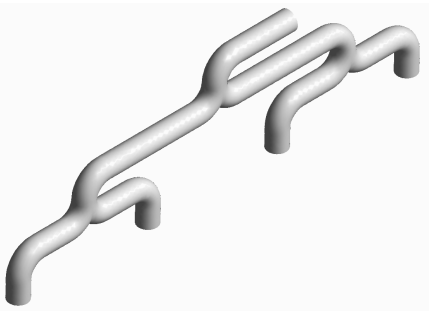

Figure 5. Flow distributor: geometry.

Let us first examine the effect of inertia on the flow splitting. We consider a food material whose properties are similar to honey, i.e. the density is 1g/cm^3, while the viscosity is 0.25 Pa.s. A volume flow rate of 50 g/s is assigned at the entry into the calculation domain. The Reynolds number is estimated at about 500, the flow is laminar, but it will be largely dominated by inertia. In Figure 6, we display velocity contours in the central cutting plane as well as at the entry and all exits, as obtained for the assigned flow rate. The flow splitting is visible.

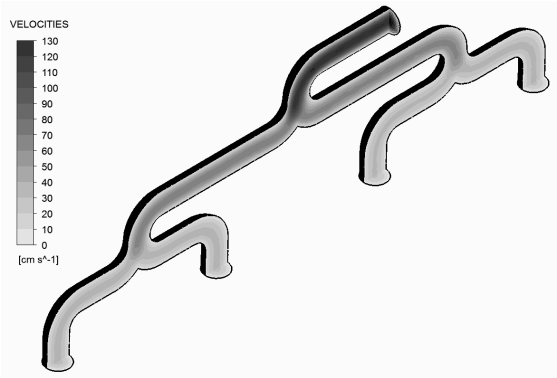

Figure 6. Flow distributor: contours of velocity magnitude in a central cutting plane and at the entry and all exits.

In order to evaluate the influence of inertia on the asymmetry of splitting, let us examine the exit flow rates vs. the inlet flow rate. In Figure 7, we display the relative flow rate at all four exits vs. inlet flow rate. As can be seen, asymmetry develops when the inlet flow rate increases, suggesting that inertia plays an increasing role. For example, the highest flow rate is observed at exit 1 on the left-hand side of the distributor: this originates from the fact that material flowing from the entry to this exit undergoes the least change in momentum. On the contrary, the flow rate at exit 3 is the lowest and is about 10% lower than the flow rate at exit 1. This originates from the fact that material flowing from the entry to exit 3 undergoes two changes of momentum.

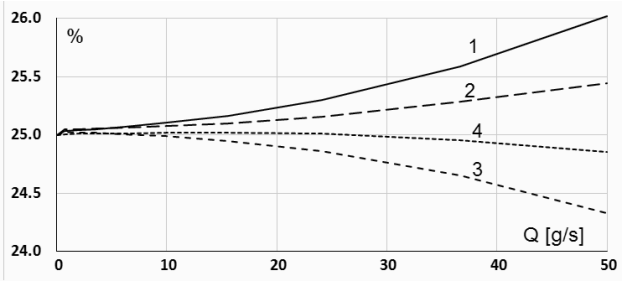

Figure 7. Flow distributor: relative flow rates at all four exits (numbered from left to right) vs. inlet flow rate Q.

PHYSICAL CHANGES IN A FLOW DISTRIBUTOR

Let us consider the same flow channel as in the previous section and displayed in Figure 5. We consider now a situation involving a relatively viscous food material whose chemical composition rapidly changes throughout the flow. Describing chemical reactions in food processing can be rather intricate, and it may require a broad series of measurements. In order to circumvent this challenge, we define a phenomenological thixotropic model which mimics the changes. In this context we propose a model where the viscosity η is affected by the residence time τ selected as a state variable. We write:

$$\eta(\tau) = \eta_0 \, [a - b.exp(-\tau/\tau_c)] \qquad (6)$$

where the residence time τ obeys the transport equation $D\tau/Dt = 1$ with $\tau = 0$ as initial condition at the entry to the flow domain. Equation (6) involves four parameters, namely η_0, a, b and τ_c, whose respective values in the current application are 2 Pa.s, 10, 9, and 3.3 s. Equation (6) with the selected parameters suggests a viscosity increase from 2 up to 20 Pa.s within about 10 s.

In terms of boundary conditions, a flow rate of 20 g/s is assigned at the entry of the domain. Along the channel wall, slipping is assumed along with equation (5), where we have selected σ_w = 1000 Pa and v_c = 0.5 cm/s.

The first result of interest in the present application is the flow rate distribution across all four exits. When there is no change in the viscosity, the exit flow rates are all equal to about 5 g/s. When thixotropy is involved with equation (6), asymmetry is observed in the flow rate distribution. More precisely, the flow rates at exits 1 to 4 (from left to right in Figure 5) are respectively equal to about 4.5, 5.1, 5.3 and 4.9 g/s. In other words, both central exits 2 and 3 receive the highest flow rates, while the lowest flow rate is reported

at exit 1. As can be seen here, thixotropy has consequences that differ from inertia effects. This can be understood if one examines the viscosity distribution across the distributor. In Figure 8, we display contours of the viscosity in the central cutting plane of symmetry, as obtained for the assigned flow rate. We see that the viscosity increases along the wall of the flow device, and this is especially visible at the outer rim of both left- and right-hand exits. This results from the successive splittings which lead to asymmetry in the flow. Indeed, each bifurcation locally splits the flow in its middle, i.e. where the residence time is the lowest, while flow along walls is never split. In other words, the residence time for particles initially located along the wall will be the largest, while it will be somewhat shorter for particles that have come in the vicinity of the wall after a flow splitting. From there, we understand that the average residence time is lower for both central exits, and consequently the viscosity is also lower. More generally, it is certainly relevant to identify whether a device or a process would exhibit a risk of flow stoppage in one of the exit; numerical simulation can be useful here.

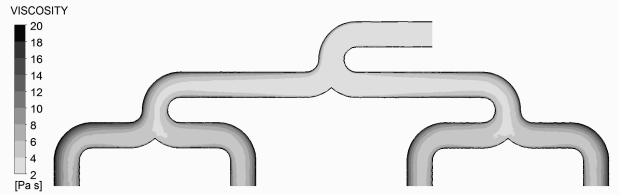

Figure 8. Flow distributor: viscosity contours for a thixotropic material in a central cutting plane.

CONCLUSIONS

Simulation of food processing is an activity endowed with many aspects, from property measurements to modelling and assumptions. Also, despite the geometric simplicity of flow domains, relatively complex material behaviours are found. They originate from intrinsic material properties, and develop in accordance with prescribed boundary conditions.

A few applications have been shown, in order to illustrate the potentialities of modelling and simulation. As has been shown, predictions are also relevant when the selected model is qualitative. This suggests that the lack of rheological data can be reasonably circumvented.

It is certainly true that the availability of constitutive equations with useful properties, such as shear thinning, thixotropy, is of great help. However, a careful identification of data, good engineering feeling, awareness of potentialities and limitations of models and solvers are necessary ingredients for achieving successful predictions.

ACKNOWLEDGEMENTS

The author wishes also to acknowledge the use of ANSYS POLYFLOW software of Ansys Inc. (ANSYS Inc. 2016; Crochet et al. 1992).

REFERENCES

ANSYS Inc. 2016. ANSYS POLYFLOW User's manual, version 17. Ansys Inc, Canonsburg, PA.

Boger, D.V.; and K. Walters. 1993. *Rheological phenomena in focus*. Elsevier, Amsterdam.

Crochet, M.J.; B. Debbaut; R. Keunings; and J.M. Marchal. 1992. "POLYFLOW: a multi-purpose finite element program for continuous polymer flows". In *Applications of CAE in Extrusion and Other Continuous Processes*, O'Brien K.T. (Ed.). Carl Hanser Verlag, München, 25-50.

Debbaut, B. and H. Burhin. 2002. "Large amplitude oscillatory shear and Fourier-transform rheology for a high-densi-ty polyethylene: experiments and numerical simulations." *J. Rheol.*, No.46, 1155-1176.

de la Peña, E.; F.A. Manthey; B.K. Patel and O.H. Campanella. 2014. "Rheological properties of pasta dough during pasta extrusion: effect of moisture and dough formulation." *J. Cereal Sci.*, No.60, 346-351.

Giesekus, H. 1965. "Sekundärströmungen in viskoelastischen Flüssigkeiten bei stationärer und periodischer Bewegung." *Rheol. Acta*, No.4, 85-101.

Giesekus, H. 1982. "A simple constitutive equation for polymer fluids based on the concept of deformation dependent tensorial mobility." *J. non-Newt. Fluid Mech.*, No.11, 69-102.

Johnson, M.W. Jr. and D. Segalman. 1977. "A model for viscoelastic fluid behaviour which allows non-affine deformation." *J. non-Newt. Fluid Mech.*, No.2, 255-270.

Keunings, R. 1989. "Simulation of viscoelastic fluid flow". In *Fundamentals of Computer Modeling for Polymer Processing*, Tucker III C.L. (Ed.). Carl Hanser Verlag, München, 402-470.

Macosko, C.W. 1994. *Rheology: principles, measurements, applications*. J. Wiley & sons, New York.

Oldroyd, J.G. 1958. "Non-Newtonian effects in steady motion of some idealized elastico-viscous liquids." *Proc. Roy. Soc.*, No.A245, 278-297.

Owens, R.G.; and T.N. Phillips. 2002. *Computational rheology*. Imperial College Press, London.

Phan Thien, N. 1978. "A nonlinear network viscoelastic model." *J. Rheol.*, No.22, 259-283.

Phan Thien, N. and R.I. Tanner. 1977. "A new constitutive equation derived from network theory." *J. non-Newt Fluid Mech.*, No.2, 353-365.

Steffe, J.F. 1992. *Rheological methods in food process engineering*. Freeman Press, East Lansing, MI.

Strang, G. and G.J. Fix. 1973. *An analysis of the finite element method*. Prentice-Hall, Englewood Cliffs, N.J.

Walters, K. 1975. *Rheometry*. Chapman and Hall, London.

AUTHOR BIOGRAPHY

BENOIT DEBBAUT obtained his Ph.D. degree in 1988 in the field of numerical simulation of viscoelastic flows, before joining Polyflow s.a. / ANSYS Belgium. Next to Product Support management activities, he is involved in software development, with a special emphasis on complex rheology, blow moulding and extrusion. He has a background of thirty years and has written about 70 scientific papers on viscoelastic flows and industrial process simulations, published in international journals and conference proceedings. He focuses often on model validations and comparisons with experimental observations. Feel free to discuss rheology with him in Dutch, German, French or English.

MODEL BASED PREVENTION OF POWDER BUILD-UP IN SPRAY DRIERS, INCLUDING VISUALIZATION

Kevin N. van Koerten
Martijn B. Fox
Han Straatsma
Maykel Verschueren
Coen Akkerman
NIZO food research
Kernhemseweg 2, 6718 ZB, Ede,
The Netherlands
E-mail:Kevin.vanKoerten@nizo.com

KEYWORDS
spray drying, modeling, online visualization

ABSTRACT

Model based control of spray dryers allows optimized processing conditions without powder build up and a maximum dryer capacity. A model has been developed, applying a near-equilibrium approach to predict conditions where fouling does not occur and thus a dryer can be operated. The model has been applied extensively in industry to optimize spray dryers. Recently, this model has been coupled to PLC systems, allowing online visualization and optimization.

INTRODUCTION

More and more spray-dried specialty products are developed, such as infant food products and whey derivatives, which are much more sticky by nature. Because of this stickiness, the risk of powder build-up inside a spray dryer increases, resulting in shorter runtimes and more cleaning cycles, resulting in a higher energy and increased use of chemicals. Therefore, it is important to limit powder build-up inside spray dryers.

However, product parameters, such as the sorption isotherm and stickiness curve, and process parameters, such as the inlet air humidity and feed dry solids content, are variable. Therefore, there is not one optimal setting for a spray dryer.

Predictive models are an important aid in improving spray dryer capacity (e.g. by Schuck et al.(2009)). NIZO regularly applies a predictive model to investigate whether a dryer is operated at settings which cause fouling. This model essentially solves the heat and mass balances of a dryer, which enable evaluation of the dryer operation. The model has recently been coupled to a dryer to enable online visualization. This is a powerful tool for operators running a dryer to check for optimal dryer settings.

RESULTS

NIZO has developed a dedicated model to describe spray drying processes, called DrySpec (Straatsma et al. 1991). In this model, product properties are coupled to process and equipment parameters. Using a near-equilibrium approach, these parameters can be coupled.

Product parameters

DrySpec requires two product properties as an input: the sorption isotherm and the stickiness curve. The sorption isotherm describes the powder moisture content at equilibrium as a function of the air temperature and relative humidity (water activity). In DrySpec, the sorption isotherm is implemented by a fitting measurement results to the GAB equation, which describes the powder moisture content (M_p, kg/kg DS) as a function of the water activity (a_w):

$$M_p = M_{p0} \cdot \left(\frac{(c_g - 1) \cdot K \cdot a_w}{1 + (c_g - 1) \cdot K \cdot a_w} + \frac{K \cdot a_w}{1 - K \cdot a_w} \right) \quad (1)$$

Where M_{p0}, K and c_g are the three GAB parameters. Usually, the sorption isotherm is measured at three relevant temperatures. Calculation of the equilibrium powder moisture content is done by interpolation.

Secondly, the stickiness curve is determined. A large variety of methods to determine the stickiness is available, each with its advantages and disadvantages. However, no standard method has been defined yet to define stickiness. NIZO applies a static method, where a layer of 5 mm powder is equilibrated at a given temperature and relative humidity. The relative humidity is increased step-wise until powder is judged sticky by the analyst. At sticky conditions, the powder is not free flowing anymore and it looks lumpy when putting it on a spatula. The stickiness point is usually determined at three relevant temperatures and subsequently fitted with an adapted Gordon-Taylor equation assuming a binary mixture of water and dry solids and an offset (ΔT_{st}, usually 20 °C is applied) from the glass transition temperature:

$$T_{st} = \Delta T_{st} + \frac{(1 - w) \cdot T_{g1} + k \cdot w \cdot T_{g2}}{(1 - w) + k \cdot w} \quad (2)$$

Where w is the powder moisture content of the stickiness point, T_{g1} the glass transition temperature of the dry solids, T_{g2} the glass transition temperature of water (-135 °C) and k

the Gordon-Taylor constant. The equation is fitted to the measurements by optimizing k and T_{g1}.

Product parameters

In essence, DrySpec solves the heat and mass balances for a spray dryer. The mass balance is described by

$$F_a \cdot X_{ai} + F_p \cdot M_{pi} = F_a \cdot X_{ao} + F_p \cdot M_{po} \qquad (3)$$

Where the air flow (F_a, kg dry air/h), the inlet and outlet air absolute humidity (X_{ai}/X_{ao}, kg water/kg dry air), the product flow (F_p, kg dry solids/h) and inlet and outlet product moisture content (M_{pi}/M_{po}, kg water/kg dry solids) are related.

The heat balance is described by

$$F_a \cdot H_{ai} + F_p \cdot H_{pi} = F_a \cdot H_{ao} + F_p \cdot H_{po} + Q \qquad (4)$$

Where the enthalpy of the inlet and outlet air and product (H_{ai}/H_{ao}, J/kg dry air, H_{pi}/H_{po}, J/kg dry solids) is based on dry air and product. The energy loss in the dryer due to heat loss is given by Q (J/h). To make calculations easier, it is assumed that the outlet powder and air temperature are equal.

In an ideal case, a droplet in a spray dryer would dry until an equilibrium condition with the air is reached. However, in practice the residence time is too short. Therefore, DrySpec assumes a near equilibrium approach to calculated process conditions. To calculate the near equilibrium, a small sub-model is assumed (Figure 1). A powder particle with a certain moisture content (M_p, kg/kg DS) and temperature (T_p, °C) would be at equilibrium with air at the same temperature resulting in a absolute moisture content (X, g/kg dry air). However, in practice, the outlet air with a given temperature (T_{ao},°C) and absolute humidity (X_{ao}, kg/kg dry air) is not at equilibrium. The offset, ΔX is assumed an equipment constant for a specific spray dryer.

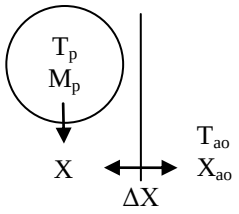

Figure 1: Schematic Representation of the Near Equilibrium Model

ΔX is described by:

$$\Delta X = DXA + DXB \cdot \Delta DS \qquad (5)$$

Where DXA and DXB are constants and ΔDS is the offset of the feed dry solids content compared to a reference point. In practice, DXA is kept at $1.5 \cdot 10^{-3}$ and DS_{ref} at 48% ($\Delta DS = DS - DS_{ref}$).

Calibration

When optimizing a dryer, the model needs to be calibrated once, using known process and product (sorption isotherm) properties. The parameters DXB (Eq. 5) and Q (Eq. 4) are fitted. After the calibration, these parameters are assumed constant for the specific dryer and not changed anymore.

Process optimization

To judge fouling, it is assumed that a droplet dries from the outside to the inside. The droplet will experience outlet air conditions (i.e. an ideally mixed reactor) in a large part of the dryer. Since convective drying processes are much quicker than the internal moisture diffusion, it is assumed that the outer shell of the particle will be in equilibrium with the surrounding air. When dryer conditions are such that the outer shell of a powder particle is in a sticky zone, it can be expected that the particle can attach to the dryer when hitting the wall.

DrySpec is often used for evaluation of dryer fouling problems (Figure 2). During a regular fouling optimization, a dryer is calibrated. Subsequently, the moisture content of the outer shell is calculated, based on the outlet temperature and humidity. The resulting moisture content and powder temperature is finally evaluated in a stickiness plot.

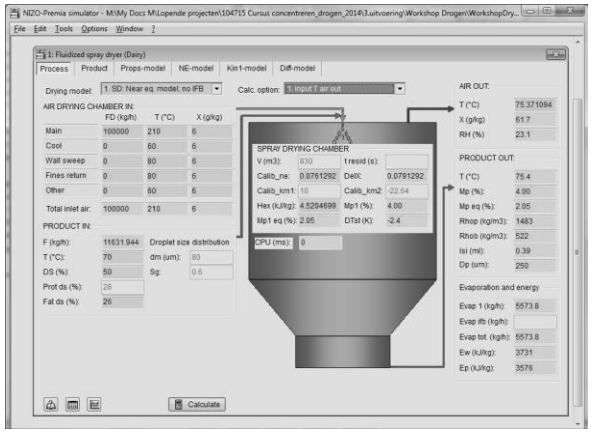

Figure 2 Screendump of DrySpec

An example of a process optimization is given in Figure 3. The stickiness curve of the product is given by the nose-shaped curve. This profile clearly shows that a product gets sticky at two different conditions at a similar absolute humidity: at a low temperature/high relative humidity condition and at a high temperature/low relative humidity condition. In between these two conditions, the powder is non-sticky, below the lower temperature and above the higher temperature, the powder is sticky.

Process calculations were performed for inlet air temperatures of 210 to 240 °C, at an outlet air temperature of 65 to 95 °C. The resulting lines in Figure 3 show that the outer shell of the particle at an air inlet temperature of 210 °C is within the non-sticky zone when operating at outlet air temperatures of 71 to 94 °C. At lower or higher temperatures, the outer shell of the particles is sticky, which can result in fouling of the spray dryer. Increasing the inlet temperature is very interesting from a capacity point of view. However, the margin for errors becomes smaller, and the outlet air temperature should be carefully chosen around 82 °C.

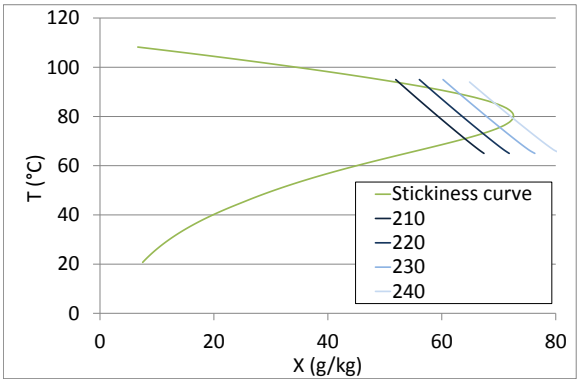

Figure 3: Stickiness Plot with Related Dryer Settings at Inlet Air Temperatures of 210 to 240 °C.

Using these kinds of simulations, it is possible to determine the room for operation of industrial spray dryers quickly without performing trials. Product properties, such as moisture content or an insolubility index can be implemented as well, allowing a careful selection of optimal properties.

Online visualization

Performing calculations offers a solution for one fixed inlet and outlet condition. However, in practice process parameters vary continuously, such as the feed temperature and dry solids content. But the inlet air absolute humidity is also highly variable. For example, in The Netherlands, the absolute humidity in 2012 varied between 1 and 17 g/kg of dry air. Often, spray dryers are operated at one, or a few fixed conditions. However, capacity is lost this way. An example calculation showed that 7 to 9 of capacity was lost in the week of 28 May when running it at the setting at maximal; inlet air humidity, compared to a continuous adjustment of the process settings towards maximal capacity.

A first step towards optimization of the process is to visualize process settings. Therefore, DrySpec has been coupled to a Programmable Logic Controller (PLC) via an Open Process control (OPC) server. Via this interface, it was possible to retrieve real-time process information while, allowing continuous visualization and optimization of the process. Several ways of visualization were implemented:

- The stickiness plot including the current condition of the dryer (Figure 4). Operators can adjust process settings such that the dryer is operated more towards the right area in the non-sticky zone
- A graph showing the offset towards the stickiness point in time
- A small window showing the optimal settings at the current conditions.

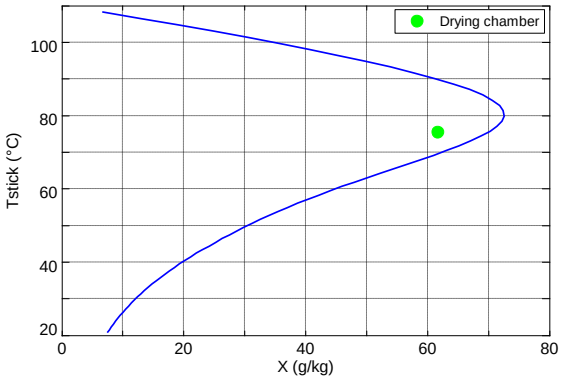

Figure 4: Stickiness Plot for Online Visualization.

CONCLUSIONS

Predictive calculations with DrySpec allow optimization of a spray dryer with regard to fouling and powder build up. This way capacity can be increased while avoiding fouling. This approach has been proved in industry in numerous cases.

Recently, DrySpec has been coupled to industrial PLC systems, allowing online visualization and optimization of spray dryers. In an ideal world, the whole dryer could be operated by model-based control, but online visualization is a powerful first step towards optimization, while staying in control.

NOMENCLATURE

a_w	water activity	-
c_g	GAB parameter	
F	flow	kg·h
H	Enthalpy	J/kg
K	GAB parameter	
M_{p0}	GAB parameter	
M_p	Powder moisture content	g/kg DS
Q	Heat loss	J/h
X	Absolute moisture content	g/kg

Subscripts

a	air
i	inlet
o	outlet
p	product

REFERENCES

Schuck, P., Dolivet, A., Méjean, S., Zhu, P., Blanchard, E., Jeantet, R. 2009. "Drying by desorption: A tool to determine spray drying parameters". *Journal of food engineering*, 94, 199-204

Straatsma, J., van Houwelingen, G., Meulman, A.P., Steenbergen, A.E. 1991. "DrySPEC2: a computer model of a two-stage dryer". *International Journal of Dairy Technology*, 44, 107–111.

SPATIO-TEMPORAL PREDICTIVE MODELLING IN FOODS

INDIVIDUAL-BASED MODELLING OF MICROBIAL COLONY DYNAMICS ON FOOD SURFACES IN A PARALLEL SIMULATOR

Ignace Tack[1], Fabrice Harrouet[2], Gireg Desmeulles[2], Filip Logist[1], Jan F.M. Van Impe[1]

[1]KU Leuven, Department of Chemical Engineering, BioTeC & OPTEC & CPMF[2], Gebroeders De Smetstraat 1, B-9000 Gent, Belgium
*E-mail address: Jan.VanImpe@cit.kuleuven.be

[2]Lab-STICC-UEB-ENIB, CNRS UMR 6285 CERV, 29280 Plouzané, France

KEYWORDS
Predictive Microbiology, Individual-Based Modelling, Surface Colony Growth, TransProg, MICRODIMS

ABSTRACT

Throughout the whole food processing and distribution chain, an accurate assessment and control of microbiological food safety is indispensable to avoid large outbreaks of foodborne diseases. For this reason, mathematical models are developed in predictive microbiology to describe the growth and survival of food spoiling and pathogenic microorganisms as a function of the environmental conditions during food processing and distribution.
Traditionally, these models are representative for the planktonic growth of axenic microbial cultures in perfectly mixed liquid media. However, most food products are characterised by a semi-solid structure, where the contaminating cells grow out as colonies. Diffusion limitations emerge in these colonies due to the high local cell density. Hence, it is most appropriate to simulate microbial colonies at a microscopic level, considering the cell as basic modelling unit in an individual-based modelling approach. Within this respect, the MICRODIMS model has been developed at the BioTeC+ research group. However, over the last years, it became clear that the implementation of this individual-based model in the standard Repast Simphony toolkit is rather slow for the simulation of mature colonies containing a large number of cells. For this reason, MICRODIMS has been ported to the TransProg library, which uses modern general-purpose multicore and multiprocessor computers to their fullest potential.
This transfer enables the simulation of mature colony dynamics in three dimensions. In this paper, the branched morphology of colonies growing on the surface of a food substrate is investigated. It is demonstrated that the emergence of this pattern is dependent on the thickness of the food substrate and structural heterogeneities at the food surface.

INTRODUCTION

Over the last decades, significant progress has been achieved in the predictive modelling of microbial pathogen behaviour in food products (McMeekin et al. 2008). These mathematical models are used to quantitatively link microbial hazard levels in food processing companies and the contamination levels to which consumers are exposed, in order to assess the risk of food poisoning.
Traditionally, models in predictive microbiology are based on experiments of axenic microbial populations in homogeneously mixed liquids. In these liquid media, the population dynamics are the result of the corporate behaviour of free-swimming cells that are barely interacting with each other and exposed to more or less the same environmental conditions. For this reason, it is reasonable to consider the integral population as a continuous modelling unit, allowing for a noncomplex description of the population dynamics by means of a limited set of coupled differential and/or algebraic equations – see, e.g., (Baranyi and Roberts 1994).
However, most food products exhibit a semi-solid structure, limiting the mobility of contaminating pathogenic microorganisms. Hence, colonies of related organisms emerge from the initial contaminating cells on the food surface (Wimpenny et al. 1995). In these surface colonies, overconsumption of nutrients/oxygen and secretion of weak acid cell products lead to chemical gradients in the colony environment due to diffusion limitations. Ultimately, this results in nutrient or oxygen depletion and a pH drop in the colony. In other words, the growth of the colony is inhibited through the creation of adverse conditions by the collective behaviour of its constituting cells.
Due to the chemical gradients in and around mature colonies, the colony cells exhibit strongly different metabolic behaviours according to their position along the colony radius. Therefore, the most appropriate modelling unit is the individual microbial cell. This modelling approach is in line with the individual-based modelling (IbM) paradigm, where the dynamics of the considered multiagent system implicitly emerge from the simulated behaviour and interactions of its constituting individuals. The IbM approach facilitates the incorporation of microscopic knowledge about the microbial cells and heterogeneities in the food structure. However, the simulation of the behaviour and interactions of each individual cell leads to long simulation times for mature colonies containing millions of cells.
Over the last two decades, individual-based models have been developed for the simulation of microbial colony behaviour, starting with the BacSim model of Kreft et al. (1998) and the INDISIM simulator of Ginovart et al. (2002a). BacSim is an extension of the Gecko ecosystems simulator which is also used for, e.g., the simulation of spider or tree populations (Booth 1997), implying that BacSim contains a myriad of superfluous functionality compromising its performance and clarity (Dens et al. 2005; Standaert 2007). For this reason, a new individual-based model, MICRODIMS, has been developed in the BioTeC+ research group and implemented in user-friendly software toolkits like NetLogo (Wilensky 1999), Repast Simphony (North et al. 2013), and MASON (Luke et al. 2003). However, it became clear that for mature colonies the

simulation time increased heavily due to the large number of spatial interactions between the colony cells. Therefore, the MICRODIMS model has been ported to the TransProg library in order to make use of modern general-purpose multicore and multiprocessor computers to their fullest potential (Harrouet 2012).
This transfer enables the simulation of mature surface colony dynamics in three dimensions, as elaborated in this paper. More specifically, this paper focuses on the formation of branched colony morphologies in nutrient-limited colonies. The influence of the food substrate thickness and food surface inhomogeneities on the colony morphology are investigated.

MATERIALS AND METHODS

The relevance of the considered microorganism is explained in this section. In addition, the MICRODIMS model and its TransProg-based revision are described in more detail.

Considered Model Organism

In this work, *Escherichia coli* K-12 MG1655 is used as the simulated microorganism. This nonvirulent *E. coli* substrain is frequently applied in experimental studies as a model organism for pathogenic strains of *E. coli* and *Shigella* (Hayashi et al. 2001; Jin et al. 2002). Infection with these pathogenic strains can result in severe gastrointestinal disorders, kidney failure, and even death. Pathogenic *E. coli* strains are particularly dangerous for young, elderly, and immunity-compromised people. Moreover, treatment with antibiotics increases the risk of haemolytic uraemic syndrome (HUS) and renal failure (Wong et al. 2000; Tarr et al. 2005). In the US, the annual cost of Shiga toxin-producing *E. coli* (STEC) infections amounts to hundreds of millions of dollars (Frenzen et al. 2005; Economic Research Service, USDA 2014).
As a facultative anaerobic organism, *E. coli* can survive on a wide variety of nutrition sources both in the presence and absence of oxygen, increasing the risk of proliferation in food products. In this paper, only aerobic colony dynamics are considered, as described in Tack et al. (2015a), eliminating the possibility that weak acid cell products are secreted into the environment as a result of the mixed acid fermentation metabolism of *E. coli*.

Model Description of MICRODIMS

The MICRODIMS model has been described in full detail in previous publications (Tack et al. 2014; Tack et al. 2015a). It considers two kinds of agents: the microbial cells and the food substrate. This food substrate is divided in discrete units to simulate diffusion processes of glucose through the food system. The implementation of this diffusion process is explained in the next section.
Diffusion of glucose through the environment is caused by glucose uptake of the colony cells from their local environment. This glucose uptake is used for cell growth and maintenance purposes, and is modelled by means of the Monod kinetic model (Monod 1942):

$$v_{k,(i,j)} = v_{k,\max} \cdot \frac{C_{S,(i,j)}}{K_S + C_{S,(i,j)}} = \frac{\mu_{k,\max}}{Y_{X/S}} \cdot \frac{C_{S,(i,j)}}{K_S + C_{S,(i,j)}} \cdot X_k. \quad (1)$$

In this formula, $C_{S,(i,j)}$ [fg/fL] is the glucose concentration of the environmental unit in which the microbial cell is situated, $v_{k,(i,j)}$ [fg/min] is the glucose uptake of cell k, $v_{k,max}$ [fg/min] is the maximum glucose uptake rate, K_S [fg/fL] the Monod half-saturation constant, $\mu_{k,max}$ [min^{-1}] the maximum specific cellular growth rate, $Y_{X/S}$ [fgDW/fg] the cellular yield coefficient of biomass on glucose, and X_k [fgDW] the mass of cell k. The cellular growth and maintenance behaviour are implemented as an exponential growth law, containing contributions of the Monod-type glucose uptake, and biomass degradation according to the Herbert model (Herbert 1958):

$$\frac{dX_k}{dt} = \mu_k \cdot X_k = v_{k,(i,j)} \cdot Y_{X/S} - m_S \cdot X_k \cdot Y_{X/S}, \quad (2)$$

with μ_k [min^{-1}] the specific cellular growth rate of microbial cell k, and m_S [fg/(fgDW·min)] the specific maintenance coefficient.
A microbial cell starves when its maintenance requirement is not met and, consequently, its specific growth rate is negative. In a starving cell, the DNA replication and cell division processes stop progressing. These processes are modelled by means of an adapted version of the Donachie model (Donachie 1968), elaborated in Tack et al. (2015). In this model, the DNA replication (*C*-phase) and chromosomal segregation (*D*-phase) take a fixed period of time as a function of the specific cellular growth rate:

$$C + D = 3.50 \cdot \mu_k^{-0.658} \text{ for } \mu_k < 0.011 \text{ min}, \quad (3a)$$
$$C + D = 67.92 \text{ min for } \mu_k \geq 0.011 \text{ min} \quad (3b).$$

This equation has been derived as a fit on data of Helmstetter (1996) and Michelsen et al. (2003).
According to Donachie (1968), DNA replication cycles are initiated at a critical ratio X_c [fgDW] of the cell mass to the number of ongoing DNA replications:

$$\frac{X_i}{n_i} = X_c \Rightarrow X_i = X_c \cdot n_i = X_c \cdot 2^j \text{ with } j = 0,1,2,\ldots \quad (4)$$

For exponentially growing cultures, the critical initiation ratio can be derived from the mean cell mass at division X_D^{m} [fgDW] (Dens et al. 2005):

$$X_D^{\mathrm{m}}(\mu_{\max}^{\mathrm{m}}) = X_c \cdot \exp\left(\mu_{\max}^{\mathrm{m}} \cdot (C + D)\right). \quad (5)$$

Although Donachie (1968) postulated that the critical ratio was a constant, Wold et al. (1994) observed a linear decrease of X_c as a function of the specific cellular growth rate:

$$X_c = A - B \cdot \mu_{\max}^{\mathrm{m}}. \quad (6)$$

The mathematical constants *A* and *B* can be estimated from experimental data of Volkmer and Heinemann (2011) on the mean cell mass at division as a function of the specific growth rate, after the substitution of the critical initiation ratio in Equation (5) by the expression in Equation (6).
Finally, cells avoid spatial overlap by shoving over the surface and forming layers on top of each other, as explained in the next section.
All parameter values in the previous equations can be found in Tack et al. (2015a).

Porting the Model to TransProg

The TransProg library is not by itself a simulation engine dedicated to bacteria. It is rather a set of facilities (multiplatform and written in C language) for a programmer to harness the full potential of modern general-purpose computers. However, it was designed with individual-based simulations in mind, and consequently makes use of multiple cores and processors (CPU) as well as graphical processing units (GPU) for both rendering and computing.

The simulation of the aforementioned MICRODIMS model involves many bacterial individuals and a food substrate containing glucose as the carbon nutrient source. Because the simulation of glucose diffusion through the substrate implies computing Fick's second law with a discrete Laplacian on a spatial grid, these computations are identical in each spatial cell and use a regular pattern; therefore they are suitable to GPU computing (with the Nvidia Cuda toolkit). On the other hand, each individual takes its own decisions (consume glucose, grow, start a new DNA replication cycle, divide, separate from neighbours…); CPUs can easily deal with this kind of irregular computations and we dedicate all of them in the computer to the behaviour of the bacteria. The workloads on these CPUs are dynamically balanced according to their cache memory hierarchy in order to preserve data locality and then maximise computing efficiency. For the same purpose, alignment, cache blocking, and vectorisation techniques, as summarised in Jeffers and Reinders (2013), are used where suitable.

In this model, bacteria stay on the surface of the food substrate, thus the only interface between these two distinct computations is the top plane of the substrate. Bacteria get to know the local concentration of glucose (computed on the GPU) by reading a bidimensional spatial grid describing local glucose concentrations in this plane. In a similar way, they express (on the CPUs) their local glucose consumption in another bidimensional spatial grid that will be provided to the substrate to be considered in the next diffusion computation. This is a synchronous approach in which, at each time step, every computation refers to a previous immutable global state to produce the next one. Because, on a hardware point of view, GPU and CPU computations are asynchronous, they can run simultaneously. For this opportunity to be fully exploited, the back and forth data transfer of the two previous bidimensional spatial grids must also overlap with the computations; this is achieved with a triple-buffer scheme as described in Hrabcak and Masserann (2012).

All the care taken to optimise the computer efficiency enables us to address larger simulations than those run with the original version of MICRODIMS. If the number of simulated bacteria increases, the thickness of the food substrate should also be considered in the simulation. For this purpose, a three-dimensional grid is used for the discrete Laplacian computation; it is solved (on the GPU) by Jacobi iterations around the backward Euler method (or alternatively Crank-Nicolson). The top layer, which is actually the only layer accessible to the bacteria, is fine grained and has the same thickness as its horizontal grid step. As layers stand deeper, they can get coarser without influencing the bacteria that much. Hence, the diffusion equations are adapted to a geometric progression of the layer thickness, as illustrated in Figure 1. This three-dimensional cut view is an informal example that shows a bacterial colony standing on top of a multi-layered substrate. The red to blue gradient depicts the glucose concentration from its initial value to zero (totally consumed). The discrete steps of this colour gradient highlights the various thicknesses amongst the substrate layers. The food substrate acts as a thick glucose buffer without using too many layers that would harm computing efficiency. However, a thick substrate is likely to facilitate the bacterial access to nutrient since glucose does not only diffuse from beside, where it is already partially consumed by other bacteria, but also from below, where there is no consumption. In these conditions, bacterial growth is sped up (glucose is the only limiting factor in this model), and mechanical repulsion between the cells in a monolayer is not fast enough to separate individuals.

Figure 1: Cut View Under a Colony of Bacteria

Therefore, we introduced a stacking algorithm for the bacteria that produces multi-layered colony shapes as visible on Figure 1; it simply depends on their local density. As placement at a stacking level relies on a discrete spatial grid (to ease inter-individual detection for neighbour repulsions), each spatial cell keeps track of its remaining space. When a bacterium does not fit in a full spatial cell, it is then placed in the spatial cell on the above stacking level. Although some bacteria appear on top of some others, they all still interact with the substrate through its top layer. The main goal of this stacking algorithm is not to make the simulated colony look like a real one but it prevents a computational overload of the mechanical repulsion between bacteria. Actually, these repulsions are computed independently at each stacking level, then, as the density is contained, each bacteria has only a few neighbours to consider during the repulsion.

RESULTS

The aim of the experiments described here is to investigate branched colony shapes, as observed in Fujikawa and Matsushita (1989) and simulated by Ginovart et al. (2002b) and Tack et al. (2015a). Although the main model parameters directly come from Tack et al. (2015a), a peculiar care was taken when choosing some of them in order to achieve a satisfying trade-off between numerical stability and simulation duration. We retained 4 μm as horizontal grid step for the substrate and 0.1 min for the time step. It was checked that a factor 2 in the geometric progression of the thickness of the substrate layers gave results similar to those obtained with regular layers. We also checked whether the application of the backward Euler method with the selected time step to simulate glucose diffusion was similar to using

the Crank-Nicolson method with a much smaller time step respecting the Courant-Friedrichs-Lewy (CFL) constraint. The substrate is a square with a side dimension of 4096 µm; its thickness changes over the various experiments. Its initial glucose concentration is 0.1 g/L; it is maintained constant at the square boundaries. The usual glucose diffusivity inside this substrate is $6.7925 \cdot 10^{-10}$ m^2/s, but a tenfold lower value has been used in some simulations. These experiments were run on a dual Intel E5-2697 computer (24 cores, 48 threads) with a Nvidia Titan GPU.

Figure 2 contains some views of the patterns obtained when running such simulations with various conditions of substrate thickness and glucose diffusivity. Figure 2-*a1* shows the whole 4096 µm wide substrate, while Figures 2-*a2* to 2-*g* give a closer view (Figures 2-*a1* and 2-*a2* both depict the same experiment in the exact same state). The simulation experiments are stopped before the colony (1.5 mm diameter) gets near to the constant borders (4 mm wide). The red to blue gradient depicts the glucose concentration varying from its initial value to zero.

In Figures 2-*a1*/*a2* to 2-*d*, the same tenfold lower diffusivity is used, but the substrate thickness is varied from 4 µm to 60 µm. Despite the fact that very sharp branched patterns resembling a diffusion-limited aggregation pattern appear quite easily on a very thin substrate – as in Tack et al. (2015a) – they get smoother and involve more bacteria on a thicker one. Figure 2-*a1*/*a2* contains $2 \cdot 10^5$ bacteria (97% starving after 34 simulated days) and took 57 minutes to obtain (nutrient depletion implies slow growth rate), while Figure 2-*d* contains $1 \cdot 10^6$ bacteria (92% starving after 9 simulated days) and took 27 minutes to obtain.

Figures 2-*e* and 2-*f* show the effect of a substrate with a usual diffusivity value and a thickness of respectively 4 µm and 12 µm. It is clear that when the diffusivity rises, branched patterns are much more difficult to obtain even with larger colonies: they hardly start to appear with $3.2 \cdot 10^6$ bacteria forming a 2 mm wide colony on Figure 2-*f*.

For all of these simulations, the main part of the colony contains starving (dark) bacteria; the colony only continues growing at its border (light bacteria). This makes the branches appear where the colony border becomes irregular. Actually, when some bacteria are accidentally placed slightly apart from the colony due to inter-individual repulsions, they get an easier access to glucose, thus they grow faster than the other cells which are enclosed into the colony. Consequently, they are likely to produce an offspring which would stand even farther from the colony center, and this self-maintained process goes on, leading to branches.

In Figure 2-*g*, the same settings are used as in Figure 2-*f* except that some irregularities are introduced in the glucose diffusivity by placing some 64 µm wide random plots with a tenfold lower value. Our intent was to alter the regular border of the colony in order to induce some early branch starts. The obtained Figure 2-*g* shows that when branches actually start, they tend to persist because the glucose depletion between them prevents the cells at the colony border from growing towards this gap.

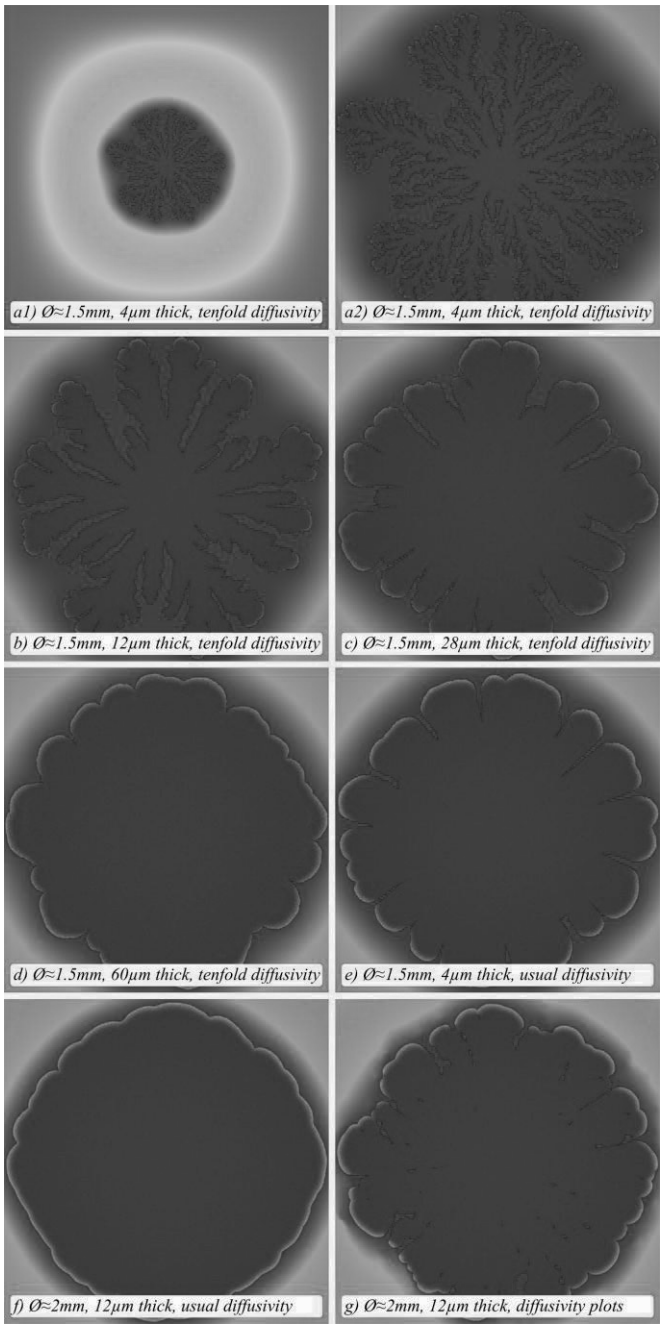

Figure 2: Colonies of Bacteria Labelled with their Diameter, the Substrate Thickness and Glucose Diffusivity

DISCUSSION

Optimising the computing efficiency of the simulation was an important step in this work. While several days where necessary in Tack et al. (2015a) to produce a 165 µm wide pattern involving around ten thousand bacteria, we now spend several dozens of minutes to a few hours to obtain colonies of many millions bacteria forming millimetre scale patterns. This enabled us to try and compare various sets of parameters in a decent time and to extend the simulation in the third dimension.

Actually, although it has been shown in Tack et al. (2015a) that nutrient depletion has a significant influence on the formation of branched colony shapes, this new version of the simulation helped to investigate this hypothesis further. These new results highlight that both the thickness of the

substrate and the diffusivity of glucose have a decisive impact on the ability to obtain such patterns. With no more new hypothesis than glucose depletion, it seems that millimetre scale branched colony shapes cannot be obtained with the usual diffusivity in a thick substrate. (This would probably require a much larger scale).
An alteration of the substrate with lower diffusivity plots was intended to reflect its natural heterogeneity. This led to early branch patterns on a thin substrate, but it is presumed that it would not be sufficient on a thick one. A new hypothesis to explain these patterns at the millimetre scale would be to consider the influence of oxygen diffusion in the colony. The inclusion of information from phenotypic phase plane analysis (Edwards et al. 2001) would enable the modelling of the whole spectrum from aerobic respiration to anaerobic fermentation, as described in a forthcoming publication (Tack et al. 2015b).
From a more technical point of view, we realised that the computing time was mainly spent to the calculation of the bacterial behaviours on the CPUs, while the GPU stays idle once the substrate is updated. It should be possible to assign the straightforward parts of these behaviours (consumption and growth) to the GPU and only use the CPUs for the division and spatial repulsion of the bacterial cells.

CONCLUSIONS

The previously implemented MICRODIMS individual-based model, dedicated to bacteria colony simulations, was rewritten on top of the TransProg library in order to maximise the computing efficiency. This speedup enables us to run larger simulations (several millions of individuals) and to extend the model in the third spatial dimension.
This new simulator helped investigate further the formation of branched colony shapes in relation with the role of the substrate in nutrient depletion. This led towards a new hypothesis implying both aerobic respiration and anaerobic fermentation.
Future efforts will both tend to further investigate this new hypothesis and to increase the GPU workload in order to raise the global computing efficiency.

ACKNOWLEDGEMENTS

The research of I. Tack was funded by PhD grant IWT SB-111565 of the Agency for Innovation by Science and Technology (IWT). This work was also supported by project PFV/10/002 (Center of Excellence OPTEC-Optimization in Engineering) of the KU Leuven Research Fund, projects G.0930.13 and KAN.15189.13 of the Fund for Scientific Research-Flanders, and the Belgian Program on Interuniversity Poles of Attraction, initiated by the Belgian Federal Science Policy Office (IAP Phase VII/19 DYSCO).

NOTE

This paper is the result of a collaboration between the BioTeC+ research group and the European Center for Virtual Reality (CERV). In fact, this collaboration started at the previous FOODSIM conference in Brest, where I. Tack and G. Desmeulles discovered common research interests. At that time, both researchers were involved in projects on the simulation of microbial colony dynamics. During a first research visit of I. Tack at CERV, G. Desmeulles introduced him to F. Harrouet to reimplement the BioTeC+ MICRODIMS model with the TransProg library. The idea to write a common paper came at a second meeting at BioTeC+ in Ghent.

REFERENCES

Baranyi J. and Roberts T.A. 1994. “A dynamic approach to predicting bacterial growth in food”. *International Journal of Food Microbiology*, 23, no. 3-4, 277-294.

Booth G. 1997. “Gecko: A continuous 2-D world for ecological modeling”. *Artificial Life*, 3, no. 3, 147-163.

Dens E.J.; Bernaerts K.; Standaert A.R.; Kreft J.U. and Van Impe J.F. 2005. “Cell division theory and individual-based modeling of microbial lag: Part II. Modeling lag phenomena induced by temperature shifts”. *International Journal of Food Microbiology*, 101, no. 3, 319-332.

Donachie W.D. 1968. “Relationship between cell size and time of initiation of DNA replication”. *Nature*, 219, 1077-1079.

Edwards J.S.; Ibarra R. and Palsson B.Ø. 2001. “In silico predictions of Escherichia coli metabolic capabilities are consistent with experimental data”. *Nature Biotechnology*, 19, no. 2, 125-130.

Frenzen P.D.; Drake A. and Angulo F.J. 2005. “Economic cost of illness due to Escherichia coli O157 infections in the United States”. *Journal of Food Protection*, 68, no. 12, 2623-2630.

Fujikawa H. and Matsushita M. 1989. “Fractal growth of Bacillus subtilis on agar plates”. *Journal of the Physical Society of Japan*, 58, no. 11, 3875-3878.

Ginovart M.; López D. and Valls J. 2002a. “INDISIM, an individual-based discrete simulation model to study bacterial cultures”. *Journal of Theoretical Biology*, 214, 305-319.

Ginovart M.; López D.; Valls J. and Silbert M. 2002b. “Individual based simulations of bacterial growth on agar plates”. *Physica A: Statistical Mechanics and its Applications*, 305, no. 3-4, 604-618.

Harrouet, F. 2012. “Designing a Multicore and Multiprocessor Individual-Based Simulation Engine”. *IEEE Micro*, 32, no 1, 54-65.

Hayashi T.; Makino K.; Ohnishi M.; Kurokawa K.; Ishii K.; Yokoyama K.; Han C.G.; Ohtsubo E.; Nakayama K.; Murata T.; Tanaka M.; Tobe T.; Iida T.; Takami H.; Honda T.; Sasakawa C.; Ogasawara N.; Yasunaga T.; Kuhara S.; Shiba T.; Hattori M. and Shinagawa H. 2001. “Complete genome sequence of enterohemorrhagic Escherichia coli O157: H7 and genomic comparison with a laboratory strain K-12”. *DNA Research*, 8, no. 1, 11-22.

Helmstetter C.E. 1996. “Timing of synthetic activities in the cell cycle”. In *Escherichia coli and Salmonella: Cellular and molecular biology*, F.C. Neidhardt; F. Curtiss III; R. Ingraham; J. Lin; E. Low; K. Maganasik; W. Reznikoff; M. Riley; M. Schaechter and H. Umbarger (Eds.), ASM Press, Washington, D.C. (United States), 1627-1637.

Herbert D. 1958. “Some principles of continuous culture”. In *Recent progress in microbiology, Symposia held at the VII International Congress on Microbiology*, G. Tunevall (Ed.), Almqvist & Wiksell, Uppsala (Sweden), 381-396.

Hrabcak L. and Masserann A. 2012. “Asynchronous Buffer Transfers”. In *OpenGL Insights*, P. Cozzi and C. Riccio (Eds.), CRC Press. ISBN 978-1439893760, 391-414.

Jeffers J. and Reinders J. 2013. *Intel ® Xeon Phi coprocessor high-performance programming*. Elsevier Waltham (Mass.), ISBN 978-0-12-410414-3.

Jin Q.; Yuan Z.; Xu J.; Wang Y.; Shen Y.; Lu W.; Wang J.; Liu H.; Yang J.; Yang F.; Zhang X.; Zhang J.; Yang G.; Wu H.; Qu D.; Dong J.; Sun L.; Xue Y.; Zhao A.; Gao Y.; Zhu J.; Kan B.; Ding K.; Chen S.; Cheng H.; Yao Z.; He B.; Chen R.; Ma D.; Qiang B.; Wen Y.; Hou Y. and Yu J. 2002. “Genome sequence of Shigella flexneri 2a: Insights into pathogenicity through

comparison with genomes of Escherichia coli K12 and O157". *Nucleic Acids Research*, 30, no. 20, 4432-4441.

Kreft, J.U.; Booth, G. and Wimpenny, J.W. 1998. "BacSim, a Simulator for Individual Based Modelling of Bacterial Colony Growth". *Microbiology*, 144, no. 12, 3275-3287.

Luke S.; Balan G.; Panait L.; Cioffi-Revilla C. and Paus S. 2003. "MASON: A Java multi-agent simulation library". In *Proceedings of the Agent 2003 Conference on Challenges in Social Simulation*. M. Clemmons (Ed.), Argonne National Laboratory, Chicago (Illinois, United States), 49-64.

McMeekin T.; Bowman J.; McQuestin O.; Mellefont L.; Ross T. and Tamplin M. 2008. "The future of predictive microbiology: Strategic research, innovative applications and great expectations". *International Journal of Food Microbiology*, 128, no. 1, 2-9.

Michelsen O.; Teixeira de Mattos M.J.; Jensen P.R. and Hansen F.G. 2003. "Precise determination of C and D periods by flow cytometry in *Escherichia coli* K-12 and B/r". *Microbiology*, 149, no. 4, 1001-1010.

Monod J. 1942. *Recherches sur la croissance des cultures bactériennes*. Hermann, Paris (France).

North M.J.; Collier N.T.; Ozik J.; Tatara E.R.; Altaweel M.; Macal C.M.; Bragen M. and Sydelko P. 2013. "Complex Adaptive Systems Modeling with Repast Simphony". *Complex Adaptive Systems Modeling*, 1, 3.

Standaert A. 2007. "From macroscopic to microscopic modelling methodologies in predictive microbiology". Ph.D. thesis, KU Leuven (Belgium).

Tack I.; Logist F.; Noriega Fernández E. and Van Impe J. 2014. "An individual-based model for anaerobic dynamics of Escherichia coli colonies". In *FOODSIM'2014*, A. Roudot (Ed.), Brest (France), 18-25.

Tack I.L.M.M.; Logist F.; Noriega Fernández E. and Van Impe J.F. 2015a. "An individual-based modeling approach to simulate the effects of cellular nutrient competition on Escherichia coli K-12 MG1655 colony behavior and interactions in aerobic structured food systems". *Food Microbiology*, 45B, 179-188.

Tack I.L.M.M.; Logist F.; Noriega Fernández E. and Van Impe J.F. 2015b. "A low-complexity model for the respiratory and fermentative metabolism of Escherichia coli based on genome-scale information and taking the synergistic effect of growth-inhibiting environmental conditions into account". *PloS Computational Biology*. Submitted.

Tarr P.I.; Gordon C.A. and Chandler W.L. 2005. "Shiga-toxin-producing *Escherichia coli* and haemolytic uraemic syndrome". *Lancet*, 365, no. 9464, 1073-1086.

Volkmer B. and Heinemann M. 2011. "Condition-dependent cell volume and concentration of *Escherichia coli* to facilitate data conversion for systems biology modeling". *PLoS ONE*, 6, no. 7.

Wimpenny J.W.T.; Leistner L.; Thomas L.V.; Mitchell A.J.; Katsaras K. and Peetz P. 1995. "Submerged bacterial colonies within food and model systems: their growth, distribution and interactions". *International Journal of Food Microbiology*, 28, no. 2, 299-315.

Wold S.; Skarstad K.; Steen H.B.; Stokke T. and Boye E. 1994. "The initiation mass for DNA replication in *Escherichia coli* K-12 is dependent on growth rate". *EMBO Journal*, 13, no. 9, 2097-2102.

Wong C.S.; Jelacic S.; Habeeb R.L.; Watkins S.L. and Tarr P.I. 2000. "The risk of hemolytic-uremic syndrome after antibiotic treatment of *Escherichia coli* O157:H7 infections". *The New England Journal of Medicine*, 342, no. 26, 1930-1936.

WEB REFERENCES

Economic Research Service, USDA, 2014.
Cost estimation of foodborne illnesses.
http://ers.usda.gov/dataproducts/cost-estimates-of-foodborne-illnesses.aspx. (accessed: 4 February, 2014).

Wilensky U. 1999. "NetLogo (and NetLogo User Manual)". Tech. report, Center for Connected Learning and Computer-Based Modeling, Northwestern University, Evanston (US). http://ccl.northwestern.edu/netlogo.

Supplemental material.
The TransProg Library.
http://www.enib.fr/~harrouet/transprog.html
(provides simulation source code and data).

BIOGRAPHIES

IGNACE TACK was born in Turnhout, Belgium. He graduated as Master of Chemical Engineering at the University of Leuven (KU Leuven) in 2011. After his graduation, he has been working on multiscale modelling techniques in predictive microbiology as a PhD researcher at the BioTeC+ division of KU Leuven.

FABRICE HARROUET was born in Nantes, France, graduated the ENIB engineering school in Brest, where he studied computer science, and obtained his PhD in 2000. He works as a lecturer in ENIB and does his research for the Lab-STICC. His research focuses on interactive individual based simulations; this mainly concerns parallel computing and 3D rendering.

GIREG DESMEULLES was born in Brest, France, graduated the ENIB engineering school in Brest, where he studied computer science, and obtained his PhD in 2006. He works as a lecturer in ENIB and does his research for the Lab-STICC. His research focuses on using virtual reality to help interdisciplinary modelling processes.

FILIP LOGIST was born in Wilrijk, Belgium. He graduated as Master of Chemical Engineering at the University of Leuven (KU Leuven) in 2003, and obtained his PhD in 2008. Currently, he works as a professor at the KU Leuven BioTeC+ division. His research interests are in process system engineering and more specifically in model-based optimization and control of dynamic (bio)chemical processes.

JAN VAN IMPE was born in Varsenare, Belgium. He graduated as Master of Electrical and Mechanical Engineering at the University of Ghent, and obtained his PhD from KU Leuven in 1993. He works as a professor at KU Leuven, and founded the BioTeC+ research group focusing on the modelling, optimization and control of (bio)chemical processes in reactors, waste-water treatment systems, and food systems.

TOWARDS AN INDIVIDUAL-BASED SIMULATOR OF THE YEAST *SACCHAROMYCES CEREVISIAE* FOR THE FOOD SCIENCE WITH PREDICTIVE CAPABILITIES

Xavier Portell
INRA AgroParisTech
UMR1402 ECOSYS
F-78850 Thiverval-Grignon, France
E-mail: xavier.portell-canal@grignon.inra.fr

Marta Ginovart
Department of Mathematics,
Universitat Politècnica de Catalunya,
08860-Castelldefels (Barcelona), Spain
E-mail: marta.ginovart@upc.edu

KEYWORDS
Individual-based simulator, *Saccharomyces cerevisiae*, aerobic and microaerophilic conditions.

ABSTRACT

A quantitative individual-based model to study the dynamics of *S. cerevisiae* fermentations was designed, implemented and it has been extended successfully to analyse the dynamics of *S. cerevisiae* cultures evolving in a liquid medium with oxygen by introducing the two sugar catabolic alternatives characteristic of this yeast: fermentative and respirative catabolism. Resulting methodology represents a further step to obtain a microbial individual-based model accounting for the whole set of metabolic alternatives experienced by *S. cerevisiae* cells in food processes. Potential benefits for the food science and the requirements for further developments of the approach are also briefly discussed.

INTRODUCTION

As opposed to the more traditional population-level approach of modelling, in which population parameters are modified directly by the model equations, Individual-based Models (IbMs, aka Agent-based Models within certain disciplines) explicitly simulate individuals, and the population behaviour emerges from their cumulative behaviour and interaction (Grimm and Railsback 2005; Railsback and Grimm 2012). In this context, a model that is individual-based means that the basic entities are the individual cells, each having its own properties that change during its life according to a set of rules. Unlike traditional top-down approaches, aiming to infer individual behaviour by describing population state, IbMs are bottom-up approaches, aiming to understand system behaviour from the behaviour of the individuals. IbMs already constitute a well-established modelling technique in ecological modelling where most applications have been geared to higher trophic levels. However, advances in microbiology and biochemistry have stimulated an increase in the application of IbMs to microbes as well (Ferrer et al. 2008; Hellweger and Bucci 2009; Kreft et al. 2013), where recognition of the role of the population heterogeneity, the existence of emergent phenomena and the absence of a continuum are capturing the interest of the scientific community. IbMs are important both for theory and management because they allow researchers to consider aspects usually ignored in analytical models: (i) variability among individuals, (ii) local interactions, (iii) complete life cycles and, in particular, (iv) individual behaviour adapting to the individual's changing internal and external environment. Nevertheless, the great potential of IbMs have a cost; IbMs are more intricate in structure than analytical models, they are more difficult to analyse, understand and communicate than analytical models. Consequently, the outcomes obtained from an IbM are not easily reproduced, and sometimes model assessment, model comparison and replication are very difficult to be carried out for this type of models (Müller et al. 2014). This drawback has been greatly mitigated with the proposition and posterior update of a standard protocol to describe IbMs, the ODD (Overview, Design concepts and Details) protocol (Grimm et al. 2010). The distinction of a conceptual model from the computer program that implements it is a crucial point, because usually the conceptual model is typically peer-reviewed, but the implementation (a translation of the conceptual model into code that a computer can read) is assumed to be well-done. Nevertheless, programming a model involves additional issues and challenges, approaches and methods for generating, verifying, and validating a conceptual model need to be considered (Scheller et al. 2010) and this could be transferred jointly with the simulations results.

Saccharomyces cerevisiae is one of the yeasts with a major economic, social and health significance in human culture. It is used in many industrial fields such as baking, food manufacturing, brewing and for the production of chemicals and heterologous proteins. Moreover, this yeast species is used as a model for understanding the cell cycle of eukaryotic cells. Consequently, this organism has been the subject of an enormous number of basic and applied studies, with an increasing number nowadays being centred on the individual level. The ample presence of this organism in such a variety of fields can be attributed, at least partially, to its sugar catabolism versatility. *S. cerevisiae* is a Crabtree-positive yeast and it is able to grow anoxically in a suitable medium, indicating that respiration is absolutely optional for it. Consequently, under aerobic growth conditions with glucose as an energy source, fermentation predominates over respiration. Depending on the growth conditions being

experienced by the cell, the cell growth can proceed via fermentative, respirative, or respirofermentative (a.k.a, oxido-reductive) metabolism. This variety of metabolic alternatives, the complexity of their regulation and the lack of knowledge of the precise mechanisms controlling them (Walker 1998) make it difficult to build a conceptual model suitable to work in the complete range of growth conditions faced by this yeast. Due to the specific properties of the individual-based approach, a model accounting for all these alternative metabolisms would potentially improve our knowledge of processes starting from few microbes, evolving close to the regulatory boundary limits and/or within changing or heterogeneous media. Other remarkable biological characteristics of *S. cerevisiae* are their budding reproduction, which leads to scar formation and unequal cell division, their limited replicative lifespan, and the increase in cell size with the cell's replicative age (Walker 1998). Besides potentially affecting the individual physiological state and subsequent performance of the bioprocesses, these peculiarities are all well suited to be incorporated and studied by means of an IbM.

The aim of our current research is to advance the development of an IbM methodology to tackle the study of microbial systems driven by the relevant yeast *S. cerevisiae*. In this contribution, we specifically aim to parameterize and calibrate an individual-based simulator to tackle the study of microbial systems driven by *S. cerevisiae* taking into account both the fermentative and respirative glucose metabolism. The long term purpose of the work is to obtain a quantitative simulator to be used as a tool with predictive capabilities for the food industry.

MATERIAL AND METHODS

A functional representation of the modelling cycle usually followed in building and using IbMs is shown in Fig. 1. It is essential to realise that the modelling is following its cycle iteratively; hence, there is no need for the entire cycle to be completed before a new iteration is undertaken, although it often makes smaller loops between two or more tasks. More details can be found in the work of Portell (Portell 2014).

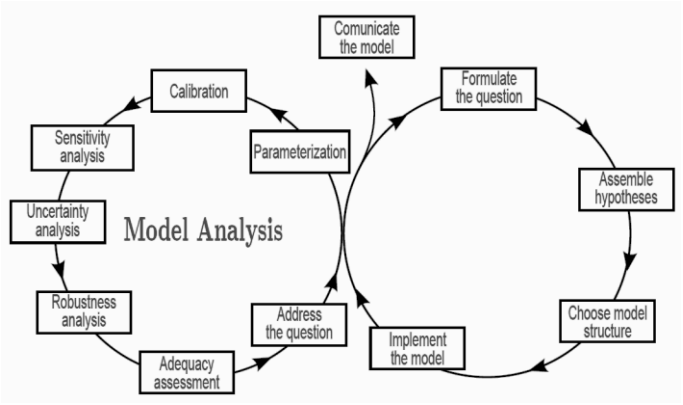

Figure 1: The Individual-based Model Modelling Cycle. Adapted from Grimm and Railsback (2005).

Of the microbial IbMs available at hand, we used the INDISIM (INDividual DIScrete SIMulations) methodology, the simulator developed by Ginovart et al. (2002), which has already been used to study different features of bacterial growth and providing a wide array of results. INDISIM is a methodology used for modelling and simulating microbial communities under different environmental conditions. It was developed by merging a discrete approach to ecosystems through individual-based modelling with the formalism used to model molecular dynamics in fluids (Ferrer et al. 2008). INDISIM settles and controls a group of bacterial cells in a discrete space: a regular lattice that consists of a group of spatial cells (subject to the appropriate boundary conditions). It models the global evolution of the group by governing the individual behaviour of each bacterium and spatial cell in discrete events (time steps) and using stochastic rules (for the introduction of variability). INDISIM-YEAST, which uses INDISIM as a core model, tackles the study of the specific characteristics of the yeast cell cycle, and is designed to deal with yeast populations growing in liquid media (Ginovart el al. 2011a; 2011b). INDISIM-YEAST models the evolution of a virtual generic budding yeast population by setting up rules of behaviour for each individual cell according to its own physiology (uptake, metabolism, reproduction, viability, etc.) and characteristics (biomass, genealogical age, state in the cellular reproduction cycle, etc.).

A quantitative model, termed INDISIM-*Saccha*, focused on the *S. cerevisiae* biology was built taking the generic qualitative yeast model INDISIM-YEAST as a starting point (Portell et al. 2014). Considering the great importance of the fermentative metabolism, which leads to ethanol formation, in classical and still dominant (at least mass-wise) biotechnologies worldwide, the implemented metabolism focused on fermentative processes. For a complete description of the implemented model, and the specific modelling steps of the modelling cycle (Fig. 1) see the paper and the supplementary material of Portell et al. (2014). Automation of the simulations to combine and select values for the model parameters was performed by using the programing language R (R Core Team 2013) under a Microsoft Windows environment. Parallel computing techniques provided by the parLapply function of the snow (small network of workstations) package were used in running the implemented simulator. Distance measures to take into account the agreement between simulated and experimental data were computed by using the R package qualV.

RESULTS AND DISCUSSION

An Extended Version of INDISIM-*Saccha*

An adaptation of INDISIM-*Saccha* (Portell et al. 2014) to deal with aerobic *S. cerevisiae* growth (Portell 2014), the dominant and desirable metabolism for, amongst others, biomass production (e.g., baker's yeast production), has been undertaken. The simulator has been implemented using Fortran 90 language specification and fully described

using the ODD protocol (Grimm et al. 2010). This seemingly unimportant step is crucial to document properly the model and to make the model easier to replicate, a must in science. This protocol has become the most currently accepted tool to facilitate communication of IbMs. A complete description of the model developed favours reproducibility of the simulation work, and therefore lends credibility to the model. New features of the extended version of the model are: (i) introduction of the oxygen as a metabolic substrate for the yeast; (ii) utilization of aerobic or anaerobic catabolic pathways according to the local environment of the individual; (iii) introduction of an individual adaptation time (individual lag); and (iv) actions on the medium adapted to the experimental setup of the data used to compare against simulated outputs (stirring, oxygen input, and oxygen reduction by external agents).

Verification of The Model

In line with the work of Scheller et al. (2010), which advocates increasing the reliability of computational models, we are convinced that much more effort must be done to show that the implementation of the model has been accurately perform, increasing hence, confidence in its outputs. A variety of measures and techniques, both informal and formal, have been used in order to make sure the model was accurately implemented. Informal verification was mainly performed by visual testing. Both system level outputs, the microscopic level with the distribution of individual characteristics for the yeast cells and the macroscopic level with state variables, were systematically collected through the simulation length and analysed (Portell 2014). Formal verification of the main parts of the simulator was undertaken by means of specifically built testing programs which allowed us to compare their output against an independent reimplementation of the submodel part on a different software platform (Fig 2) or, when appropriate, by testing statistically the output of the submodel being inspected. The generated files provides, therefore, convincing evidences of the correctness of the implementation (Portell 2014).

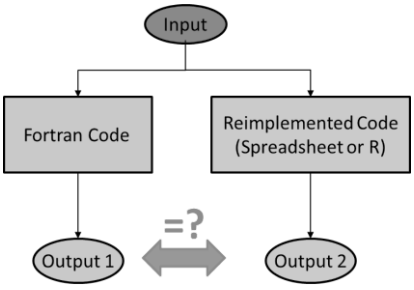

Figure 2: Formal Verification Using the Independent Reimplementation Technique.

Model Analysis

In order to evaluate the capability of the implemented metabolism to reproduce stirred laboratory experiments of *S. cerevisiae* with oxygen, the glucose, ethanol and cell density determinations collected in two experimental conditions with two different oxygen levels in the medium (aerobic and microaerophilic conditions) were used. The results achieved are shown in Figure 3.

Model parameterization was achieved tentatively by fixing or modifying model parameters until the experimental glucose, ethanol and cell density data were reproduced reasonably well. When possible, model parameter values were taken following the work of Portell et al. (2014). New parameters introduced here into INDISIM-*Saccha* are the respirative biomass yield, the mean individual lag time, the O_2 uptake coefficient, the respirative to fermentative energy relation, and the O_2 entrance rate to the medium. Considering that no formal calibration process to fit the experimental data available has been undertaken, this preliminary simulated results achieved with the extension of INDISIM-*Saccha* suggest that the approach holds potential to reproduce aerobic batch cultures of *S. cerevisiae*. At the same time, the ability to adapt the simulator to new hypotheses and questions is highly appreciated.

CONCLUSIONS AND FURTHER RESEARCH

A quantitative IbM to study the dynamics of *S. cerevisiae* fermentations was designed and it has been extended successfully to analyse the dynamics of *S. cerevisiae* cultures evolving in a liquid medium with oxygen by introducing the two sugar catabolic alternatives characteristic of this yeast: fermentative and respirative catabolism. Resulting methodology represents a further step to obtain a microbial IbM accounting for the whole set of metabolic alternatives experienced by *S. cerevisiae* cells in food processes. Successive descriptions and uses of the model developed favours reproducibility of the simulation work, and therefore lends credibility to the model. The ability that INDISIM-*Saccha* has to link population structure to macroscopic observations will clearly gain practical importance in the near future due to the likely availability of high-throughput devices (flow cytometers, and particle sizing and counting analysers) affordable for high and low added value bioindustries alike.

The production of research using IbMs in microbiology, and in food science in particular, has not been as effective as it could be desired. Reasons include that model assessment, replication, and comparison are not easily accomplished for these type of models. Nevertheless, and increasingly, the code developed for one project is reused for other closely related research, as this study, facilitating the constant improvement of the model and its implementation, and achieving different purposes in each stage. Until now, a significant way has been made in the development of individual-based simulators, however, greater collaboration between professionals of the sector and model developers is clearly needed in order for the approach can be eventually used successfully in the industry. In particular, it is necessary to design and carry out experimentation designed especially for the parameterization and calibration of these relatively new models in food science.

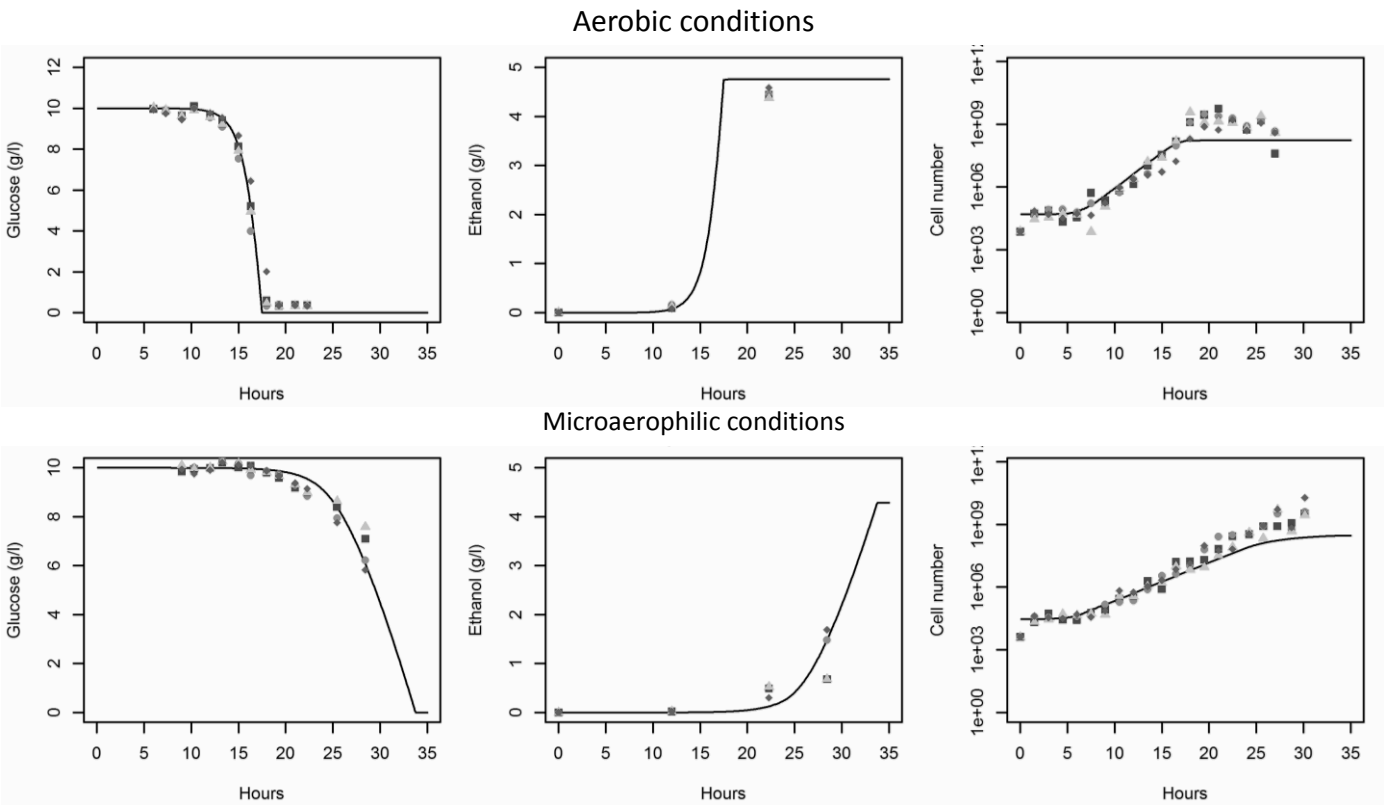

Figure 3: Experimental (points) versus Simulated (lines) Data.

REFERENCES

Ferrer, J.; C. Prats and D. López. 2008. "Individual-based modelling: an essential tool for microbiology." *J Biol Phys* 34, 19-37.

Ginovart, M., D. López and J. Valls. 2002. "INDISIM, an individual-based discrete simulation model to study bacterial cultures." *J Theor Biol* 214, 305-319.

Ginovart, M.; Prats, C.; Portell, X. and M. Silbert. .2011a. "Exploring the lag phase and growth initiation of a yeast culture by means of an individual-based model." *Food Microbiol* 28, 810-817.

Ginovart, M., Prats, C., Portell, X. and M. Silbert. 2011b. "Analysis of the effect of inoculum characteristics on the first stages of a growing yeast population in beer fermentations by means of an individual-based model." *J Ind Microb Biotechnol* 38, 153-165.

Grimm, V.; U. Berger; D.L. DeAngelis; J.G. Polhill; J. Giske and S.F. Railsback. 2010. "The ODD protocol: a review and first update." *Ecol Model* 221, 2760-2768.

Grimm, V. and S.F. Railsback. 2005. *Individual-based modeling and ecology*. Princeton university press, Princenton.

Hellweger, F.L. and V. Bucci. 2009. "A bunch of tiny individuals—Individual-based modeling for microbes." *Ecol Model* 220, 8-22.

Kreft, J.U.; C.M. Plugge; V. Grimm; C. Prats; J.H.J. Leveau; T. Banitz; S. Baines; J. Clark; A. Ros; I. Klapper; C.J. Topping; A.J. Field; A. Schuler; E. Litchman and F.L. Hellweger. 2013. "Mighty small: observing and modeling individual microbes becomes big science." *Proc Nat Acad Sci* 110, 18027-18028.

Müller B.; S. Balbi; C.M. Buchmann; L. de Sousa; G. Dressler; J. Groeneveld; C.J. Klassert; Q.B. Le; J.D.A. Millington; H. Nolzen; D.C. Parker; J.G. Polhill; M. Schlüter; J. Schulze, N. Schwarz; Z. Sun; P. Taillandier and H. Weise. 2014. "Standardised and transparent model descriptions for agent-based models: Current status and prospects." *Environ Modell Softw* 55, 156-163.

Portell X. 2014. *Individual-based observations and individual-based simulations to study Saccharomyces cerevisiae cultures*. PhD Thesis. Barcelona: Universitat Politècnica de Catalunya. Available online at: http://hdl.handle.net/10803/284741.

Portell X.; A. Gras and M. Ginovart. 2014. "INDISIM-Saccha, an individual-based model to tackle *Saccharomyces cerevisiae* fermentations." *Ecol Model* 279, 12-23.

R Core Team. 2013. R: A Language and Environment for Statistical Computing. R Foundation for Statistical Computing, Vienna, Austria, ISBN 3-900051-07-0, http://www.R-project.org/

Railsback, S.F. and V. Grimm. 2012. A*gent-based and individual-based modeling: a practical introduction*. Princeton University Press, Princenton.

Scheller, R.M.; B.R. Sturtevant; E.J. Gustafson; B.C. Ward and D.J. Mladenoff. 2010. "Increasing the reliability of ecological models using modern software engineering techniques." *Frontiers Ecol Environ* 8, 253-260.

Walker, G.M. 1998. *Yeast physiology and biotechnology*. John Wiley & Sons, Chichester.

XAVIER PORTELL CANAL was born in Berga (Barcelona), Spain. He is Agricultural Enginyer by the Universitat de Lleida and doctor in Agri-food Technology and Biotechnology from the Universitat Politècnica de Catalunya. He is currently working in the French Institute National de la Recherche Agronomique (INRA), where he is developing microbial individual-based models to improve the predictions of the emissions of CO_2 and N_2O from soils.

MODELLING SPATIOTEMPORAL DYNAMICS IN A FOOD MATRIX INITIATED BY INJECTED STARTER CULTURES

Thorsten Stefan
Institute of Applied Mathematics and Statistics
University of Hohenheim
Schloss Hohenheim, Westhof-Süd
D-70599 Stuttgart, Germany
E-mail: Thorsten.Stefan@uni-hohenheim.de

KEYWORDS
Spatiotemporal Predictive Modelling in Food, Partial Differential Equations, Reaction-Diffusion, Finite-Element-Method, Optimisation

ABSTRACT

We show how a spatiotemporal model that tracks changes in concentrations of microorganisms and their metabolites during cheese ripening, as well as their interactions, can be built by using a commercial software that includes a physics interfaces for handling CFD (computational fluid dynamics) in porous media. Such a model overcomes the main disadvantage of traditional models in predictive microbiology, namely their restricted use for food products that are not homogeneous, and their lack of a spatial component. We finally demonstrate how this model can be used to optimise parameters and thus increase the efficiency of the fermentation process.

INTRODUCTION

Modelling growth and resistance of microorganisms goes back to the 1920s (Esty and Meyer, 1922), but only in the 1970s the discipline of predictive microbiology, attempting to more fully understand growth and metabolism of microorganisms, began to establish itself as an independent research field (Bernaerts et al., 2004). Nevertheless, most of the models have been validated in homogeneous broth medium, and can therefore only be applied to most non-liquid food products with reservations. Critically, however, the vast majority of predictive models in microbiology lack a spatial component. While this might be a sufficient simplification in homogeneous environments, like broths and fluid foods, it nevertheless fails to make predictions of any accuracy when the food product is heterogeneous, diffusion limitations cause spatial gradients of metabolic products (Bernaerts et al., 2004), or the spatial positions of bacterial colonies are important. In these cases, predictions can only be made experimentally, which often comprises a lengthy incubation (Skinner et al., 1994) or ripening period. Such an experimental approach is therefore both time consuming and costly, and has to be repeated when external factors change (Baranyi and Roberts, 1995).

Spatially explicit models exist (Dens and Van Impe, 2000, 2001), but are in many cases restricted to special cases like biofilms (Eberl et al., 2001) or to areas outside the food context (Dens and Van Impe, 2000; Hellweger and Bucci, 2009). Therefore, the need for a spatially explicit transport model for microbes and chemical species related to microbial growth and metabolism in the context of food products is evident (Bernaerts et al., 2004; Dens and Van Impe, 2000).

Our work demonstrates how this gap can be closed by building a complex model of spatial and temporal changes in a food matrix with the commercial software COMSOL Multiphysics ®, which solves the emerging reaction-diffusion equations using the finite element method (FEM). This software has built-in physics interfaces for CFD (computational fluid dynamics) and diffusion processes in porous media.

We model the ripening period of cheeses of different shapes that were produced using a novel technology platform. This platform differs from traditional cheese-making procedures in that a solid, extruded cheese is inoculated with a starter culture of lactic acid bacteria in a number of different positions before the ripening period. This setup, with a number of centres of bacterial activity in an otherwise microbiologically inactive cheese, makes a spatially explicit model indispensable. The model aims to reproduce the main biochemical processes in the cheese together with the diffusion processes of bacteria and chemical species in order to identify the optimal injection strategy, which is not only defined by the injection pattern (i.e. the positions of the injections), but also by the amount and concentration of the bacterial suspension injected.

METHODS

While discretisation methods (as the FEM) are commonly used when modelling subsurface flow of liquids through porous soil layers, or characterising heat and mass transfer in food (Datta, 2007), such an approach has hardly been used in predictive microbiology, despite the growing awareness that classical well-mixed approaches are unsuitable for many food products (Bernaerts et al., 2004).

We used a commercial software (COMSOL Multiphysics ®) that includes a physics interface for handling reaction-diffusion equations in porous media. As cheese can be regarded as a porous medium, and estimates for the porosity of cheese exist (Kebary and Morris, 1990), this approach appears to be a promising alternative to classical models of predictive microbiology. We used the software to explicitly model the spatiotemporal dispersal of the starter cultures

within the three-dimensional porous food matrix while taking into account the temporal and spatial dynamics of substrate (lactose) and the metabolites lactic acid and lactate, as well as the concentrations of salt and buffer components, and the *pH*. We assume that the structure of the cheese does not vary over time, hence the porosity of the cheese and the effective diffusion coefficients stay constant during the ripening period.

Reaction-diffusion model and reaction terms

In our model, bacterial growth as well as spatiotemporal changes in the chemical species (all denoted with X) are governed by a system of nonlinear partial differential equations (PDEs) of reaction-diffusion type (1):

$$\frac{\partial X(x,t)}{\partial t} = D_X \nabla^2 X(x,t) + r_X(x,t) \tag{1}$$

The reaction terms $r_X(x,t)$ characterise the biochemical reactions, as the production of lactic acid from lactose by lactic acid bacteria or the dissociation of lactic acid into lactate and H^+. Furthermore, the reaction terms also specify bacterial growth according to equation (2):

$$r_B(x,t) = \mu_{\max} \cdot \frac{Q(t)}{1+Q(t)} \cdot cB(x,t) \cdot cS(x,t) \cdot f_{pH}\big(cH(x,t)\big) \cdot f_{aW}\big(cNaCl(x,t)\big) \tag{2}$$

In this equation, $\mu_{\max}$ is the maximum bacterial growth rate, $Q(t)$ is the physiological state of the lactic acid bacteria, $cB(x,t)$ and $cS(x,t)$ denote concentrations of bacteria and substrate (lactate), and $f_{pH}\big(cH(x,t)\big) \in [0,1]$ as well as $f_{aW}\big(cNaCl(x,t)\big) \in [0,1]$ are functions that specify the inhibiting effect of high concentrations of H^+ and low values of water activity (a_W) on bacterial growth. This reaction term is inspired by a general class of substrate- and product-limited microbial growth models (Van Impe et al., 2005; Poschet et al., 2005).

Initial conditions and boundary conditions

The bacterial concentration is at its maximum at the position of the inoculum and decreases in all directions according to a trivariate normal distribution. The model further assumes a boundary condition of no flux on all boundaries of the cheese matrix.

Optimisation of the injection strategy for various shapes

Different geometries of the food matrix, reflecting different cheese shapes (see figures 1 and 2 for two examples), were investigated by examining the effects of various injection strategies on the amount of substrate remaining and the homogeneity of the *pH* within the cheese matrix, both at the end of the ripening period. The number and positions of these inocula, together with the amount and concentration of the bacterial suspension injected (figures 1 and 2) ultimately determine whether the ripened cheese can be regarded as homogeneous enough in terms of its main chemical components. We determine the optimal injection strategy of the starter cultures using nonlinear optimisation procedures.

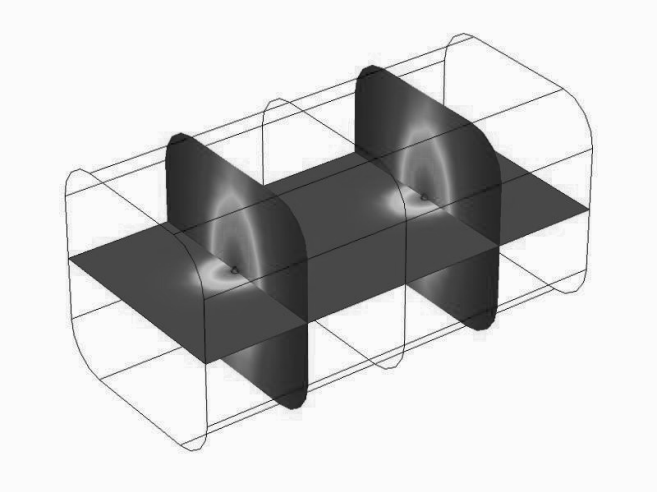

Figure 1: The Concentrations of Lactic Acid Bacteria (Shades of Red, Yellow and Light Blue, Horizontal Layer) and Lactic Acid Produced by These Bacteria (Shades of Red and White, Vertical Layers) in a Cheese Block
The two inocula where the starter culture was injected are in the centre of the intersections of the layers

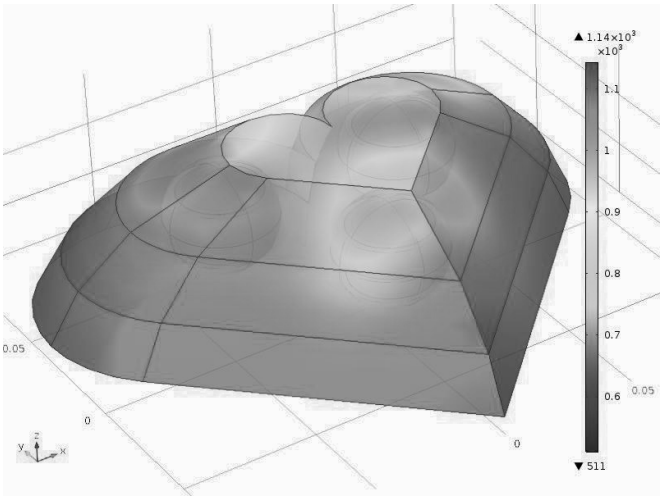

Figure 2: The Concentration of Lactose in a Heart-Shaped Cheese During Ripening
Here, starter culture has been injected in three locations (spheres within the cheese)

Modelling the processes related to the ripening of the cheese, as well as finding an optimal injection pattern helps to enormously save time compared to an experimental approach, as cheese ripening takes around 6 weeks. Furthermore, the potential complexity of the food matrix and the biological and biochemical processes make a purely experimental procedure infeasible. To solve the nonlinear optimisation problem, we use derivative-free procedures as well as gradient-based regularisation methods with stabilising effect. The latter calibrate the model simulation with the target distribution step by step, and this procedure ultimately leads to the optimal injection pattern that ensures a homogeneous distribution of metabolites within the cheese matrix at the end of the ripening period while minimising the number of starter culture injections.

RESULTS

Finding a suitable injection strategy

The right choice of the injection pattern can strongly influence the time required to achieve an even distribution of fermentation products in the cheese matrix, particularly for more complex geometries. This is true not only for the number and positions of the injections, but also for the amount of bacterial suspension injected, and the bacterial concentration of the suspension. While a higher number of injections and a higher volume of bacterial suspension improves homogeneity of the metabolic products and shortens the ripening time, it is nevertheless desirable to minimise both number of injections and injected volume, as they affect the quality of the cheese. Practical reasons further place an upper limit on the bacterial concentration of the injected suspension. The optimisation routines of our model predict the optimal injection pattern for every cheese geometry in terms of achieving a distribution of metabolites and substrate as even as possible while minimising the number of starter culture injections and the injected volume.

Parameter estimation and experimental validation

Most of the parameters used in the model had been taken from the literature, as experimental measurements were not yet available. Measurement of the effective diffusion coefficients were conducted in a diffusion chamber, but these are still ongoing.

The experimental validation of the model will be performed by analysing the local concentrations of the lactic acid bacteria and the modelled chemical species at different points in time during the ripening period. This might require more cheese blocks that ripen under equal conditions at the same time.

DISCUSSION

Our approach has several advantages over traditional approaches in predictive microbiology. By using a model based on reaction-diffusion equations that naturally takes the spatial component into account we were able to determine the spatiotemporal distribution of lactic acid bacteria, lactose, lactate and other chemical species that influence bacterial growth (as Na^+, Cl^- and H^+) during the ripening period of the cheese, which generally lasts for several weeks. This approach has the potential to substantially improve other predictive microbiological models in the food context, where ordinary differential equations might be equally unsuitable to model microbial growth in heterogeneous food products. Three-dimensional, spatially explicit models that take the dynamic changes in the concentrations of microorganisms and substrates, metabolites and other chemical species in time and space into account are to date rarely used in predictive microbiological models.
A challenge during modelling is the potentially complex food matrix geometry, and the uncertainty in some of the model parameters, as the movement of the microorganisms, the diffusion constants for metabolites and the functional dependencies of bacterial growth rates and metabolic activity on the other variables.

CONCLUSIONS

The benefits of spatiotemporal predictive modelling in foods were shown in an application where a novel technology platform for cheese production requires injecting starter cultures into an extruded, solid cheese block. This novel cheese-making procedure results in a food matrix with centres of bacterial metabolic activity, and a fermentation process that is highly localised. It was demonstrated that such a problem can be tackled with a commercial Multiphysics software package and a model that incorporates diffusion and the main reactions of the fermentation process.

REFERENCES

Baranyi, J., and Roberts, T.A. (1995). *Mathematics of predictive food microbiology*. Int. J. Food Microbiol. *26*, 199–218.

Bernaerts, K., Dens, E., Vereecken, K., Geeraerd, A.H., Standaert, A.R., Devlieghere, F., Debevere, J., and Van Impe, J.F. (2004). *Concepts and tools for predictive modeling of microbial dynamics*. J. Food Prot. *67*, 2041–2052.

Datta, A.K. (2007). *Porous media approaches to studying simultaneous heat and mass transfer in food processes. II: Property data and representative results*. J. Food Eng. *80*, 96–110.

Dens, E.J., and Van Impe, J.F. (2000). *On the importance of taking space into account when modeling microbial competition in structured food products*. Math. Comput. Simul. *53*, 443–448.

Dens, E.J., and Van Impe, J.F. (2001). *On the need for another type of predictive model in structured foods*. Int. J. Food Microbiol. *64*, 247–260.

Eberl, H.J., Parker, D.F., and Van Loosdrecht, M.C.M. (2001). A *New Deterministic Spatio-Temporal Continuum Model for Biofilm Development*. J. Theor. Med. *3*, 161–175.

Esty, J.R., and Meyer, K.F. (1922). *The heat resistance of the spores of B. Botulinus and allied anaerobes*. J. Infect. Dis. *31*, 650–663.

Hellweger, F.L., and Bucci, V. (2009). *A bunch of tiny individuals-Individual-based modeling for microbes*. Ecol. Modell. *220*, 8–22.

Van Impe, J.F., Poschet, F., Geeraerd, A.H., and Vereecken, K.M. (2005). *Towards a novel class of predictive microbial growth models*. Int. J. Food Microbiol. *100*, 97–105.

Kebary, K.M.K., and Morris, H.A. (1990). *Porosity, Specific Gravity and Air Content in Blue Cheeses*. Food Struct. *9*, 57–60.

Poschet, F., Vereecken, K.M., Geeraerd, A.H., Nicolaï, B.M., and Van Impe, J.F. (2005). *Analysis of a novel class of predictive microbial growth models and application to coculture growth*. Int. J. Food Microbiol. *100*, 107–124.

Skinner, G.E., Larkin, J.W., and Rhodehamel, E.J. (1994). *Mathematical Modeling of Microbial Growth: a Review*. J. Food Saf. *14*, 175–217.

BIOGRAPHY

THORSTEN STEFAN was born in Graz, Austria. He studied Mathematics and Chemistry at the University of Graz (Austria) and Mathematical Biology at the University of York (UK). He obtained his PhD at the University of Glasgow (UK) in 2016 with a thesis that investigated reasons for the diversity of the MHC, which is a genetic region in the vertebrate genome. While in Glasgow, he mostly worked at the interface of mathematical modelling, population genetics and immunology. In January 2015, he moved to the University of Hohenheim, Stuttgart (Germany), where he

started doing research in the area of predictive modelling in foods.

3D INDIVIDUAL BASED MODEL FOR BACTERIA GROWTH AND SPATIAL INTERACTIONS: APPLICATION TO THE CASE OF *LISTERIA MONOCYTOGENES* AND *CARNOBACTERIUM PISCICOLA*

Fabrice Harrouet,
Gireg Desmeulles
Lab-STICC-UEB-ENIB, CNRS UMR 6285
CERV, 25 rue Claude Chappe
29200 Plouzané, France
E-mail: desmeulles@enib.fr

Pascal Redou,
Laurent Gaubert
LATIM, INSERM UMR 1101
CERV, 25 rue Claude Chappe
29200 Plouzané, France

KEYWORDS
Predictive Microbiology, Bacterial Colony Growth Model, Spatialisation

ABSTRACT

By means of an interdisciplinary collaboration, we build a three dimensional individual-based model at the microscopic scale. This model is based on the cardinal model at the population scale, and aims at investigating the impact of spatialisation on the growth of bacterial colonies, in particular in the case of species in interaction. Our case of application is the influence of lactic acid bacteria on pathogens, which growth depends on pH evolution from lactic acid production and diffusion, according to carbohydrate concentration, temperature, water activity and ratio of both populations. We use our individual-based model to study and illustrate different and major effects of spatialisation on colonies growth. The last section presents some perspectives for the design of a continuous partial derivative equations-based companion model to our individual-based one.

INTRODUCTION

Nowadays, lactic acid bacteria (LAB) are not only considered for the production of fermented foods, but may be used as well to control the outgrowth of microbial pathogens – see (Matilla-Sandholm and Skyttä 1996) for an overview. Their presence can significantly modify a growth medium, by means of organic acids production which induces pH reduction, or through the increase of the medium solidity due to the presence of polysaccharides.
Recent numerical models in the area of food fermentation and biological preservation take into account the importance of these microbial metabolites, and not only the microbial growth. Moreover, they model the impact of these microbial metabolites on the growth medium in order to predict more accurately the microbial growth, but as well to enable medium-wise interactions between different species – see for example (Poschet et al. 2005). However, most of these models do not account for spatial effects, except in a few cases – see for instance (Kreft et al. 1998) for an individual based 2D model, or (Grimson and Barker 1994) for a continuous model.
In this paper, a model based on the cardinal model (Ellouze et al. 2008; Lobry et al. 1991) from literature is used to build a three dimensional individual-based model (IBM) at the microscopic scale, in order to investigate the impact of spatialisation. The metabolite taken into consideration is lactic acid, since it is the main end-product of LAB metabolism.
Our work can be subdivided in two main parts. A first part describes the modelling process itself since it is a deeply interdisciplinary project and because we believe that the development methods may be as important as the resulting model itself. The resulting model describes the concomitant growth of lactic acid bacteria, namely *Carnobacterium piscicola*, and pathogens, namely *Listeria monocytogenes*; these growths depend on pH evolution from lactic acid production and diffusion, according to carbohydrate concentration, temperature, water activity and ratio of both populations. In a second part, we use our IBM in order to study and illustrate a possible effect of spatialisation. We mainly investigate around the growth rate of a colony, into a virtual Petri dish, in relation with the spatial distribution of *C. piscicola* individuals. Then, we show that the resulting variability may have dramatic consequences on the final size of *L. monocytogenes* colony. The last section presents some promising perspectives, since we are currently designing a continuous partial derivative equations-based companion model to our IBM.

A Few Words About Interdisciplinarity

Although it is not the main purpose of this work, we want to stress the point that this study takes place in the context of an interdisciplinary project. Indeed, microbiologists, biologists, mathematicians and computer scientists were involved, so that nontrivial issues had to be addressed, in particular the collaborative construction of a relevant model. The steps of the project progress are reported on Figure 1.

1. This project first started by interdisciplinary exchanges, the development of collaborative web environments, and shared objectives definitions.
2. Based on Virtual Reality principles (Tisseau 2001), the *in virtuo* modelling step used a virtual laboratory to co-design a model, understood by all the participants of the project. This enabled us to tackle interdisciplinary issues: implicit knowledge, mutual understanding, science integration, etc., and to build a shared IBM.
3. Once the project consortium agreed on a shared model, it was thus possible to optimise this IBM and scale it up. This highly technical step excluded non experts.
4. Finally, mathematicians translated the IBM into a continuous partial derivative equations model, to reduce computation time. This step is still in progress and is briefly exposed in our perspectives.

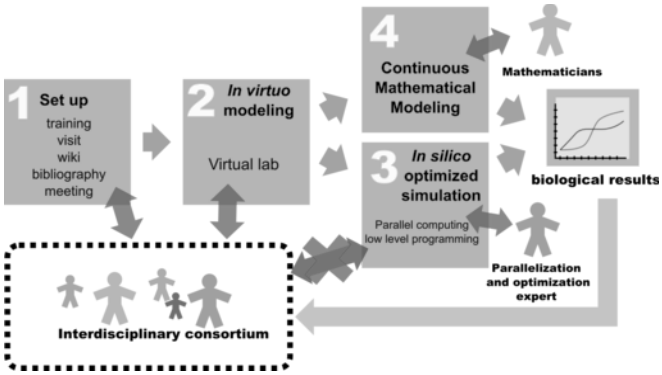

Figure 1: Four Step Interdisciplinary Project

INDIVIDUAL BASED MODEL

We built models of *C. piscicola* and *L. monocytogenes* interacting on a Petri dish. Bacteria shapes are 3D capsules that have mechanical interactions. Bacteria feed on glucose – and produce lactic acid –, and divide over time, depending on their local environment. The substrate was modelled as a 3D discrete reaction-diffusion system in which glucose and lactate diffuse. We made use of Unity3D to handle the graphical user interface that made it possible to see, experiment and modify the model during the simulation. Based on this *in virtuo* modelling, we used the TransProg C library (Harrouet 2012), so as to develop an optimised and parallel IBM, from the cardinal populational data and model. Spherical shapes for bacteria constitute the only simplification made to enable the simulation of hundred millions of individuals.

Development Methods

Two software tools were used to simulate the IBM.

RéISCOP for Interdisciplinary Co-Construction.
During the *in virtuo* experimentation step, we used the RéISCOP software (Figure 2), which is both a meta-model and a simulation engine (Desmeulles et al. 2009). It relies on the multi-interaction modelling paradigm which is dual and similar to the multi-agent paradigm. Multi-interaction model description is focused on interactions between components rather than on components themselves. This dual perspective is suitable for modelling complex and multi-model systems.
RéISCOP 2.0. was written with the C# language for this project, and was interfaced with the VR software Unity3D, to provide a graphical user interface (GUI).

TransProg for Optimisation and Parallelisation.
In order to achieve high computational loads we used the TransProg library (Harrouet 2012) to develop an optimised and parallel model. TransProg is a set of facilities (multi-platform and written in C language) for a programmer to harness the full potential of modern general purpose computers. It was designed with individual-based simulations in mind, and consequently makes use of multiple cores and processors, as well as graphical processing units for both rendering and computing. It is dedicated to interactive simulations of highly dynamic systems where entities can move, change, appear, disappear and interact with each other and the user at any time.

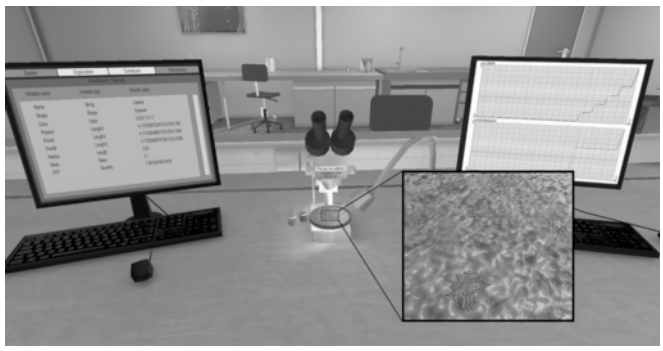

Figure 2: RéISCOP Based Virtual Laboratory

Model

The optimised IBM we used to produce our results is depicted on Figure 3. It consists in a diffusive substrate that simulates an agar-agar medium containing glucose and lactate, some pathogenic bacteria (*L. monocytogenes*) and some lactic acid bacteria (*C. piscicola*) – parameters are given in Tables 1 and 2. Each bacterium is modelled as an autonomous individual with its own behaviour.

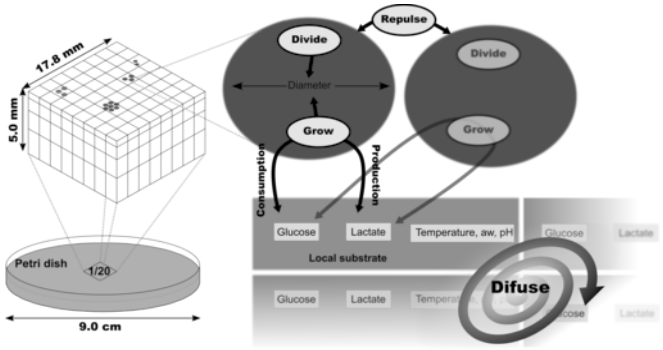

Figure 3: Individual Based Model Description

Substrate.
As shown on Figure 3, the simulated substrate represents *1/20* of the surface of a Petri dish and its full thickness (about *5 mm*). It consists in a 3D mesh of spatial cells maintaining concentrations of glucose and lactate. Although the horizontal grid step is regular, the vertical one uses a geometric progression in order limit the number of spatial cells while keeping a sufficient volume for a buffer effect. Because bacteria only interact with the top of the substrate, the coarse grained cells used at the bottom don't harm so much. We had to adapt the computation of Fick's second law with the Crank-Nicolson integration scheme for accuracy (Hairer et al. 1996), and its resolution with the Jacobi method, to this non isotropic 3D grid pattern.
Global substrate parameters are temperature and water activity. Local pH is calculated from local lactate concentration according to an empirical polynomial law:

$$pH = pH_0 + pH_1 \cdot [Lac] + pH_2 \cdot [Lac]^2$$

Growth, Lactic Acid Production.
The cardinal model (Ellouze et al. 2008) for colony growth μ was turned into individual bacteria behaviour based on individual generation time (t_g) and local parameters:

$$t_g = ln(2)/\mu$$

We estimate empirically the amount of glucose an individual consumes during a generation time. Thus, a bacterium, according to its local perception of the substrate, is able to determine its generation time and the corresponding amount of glucose to consume during the current simulation time step. Although bacteria metabolism is not modelled, this consumption yields a lactate production and raises the individual volume. Both phenomena are taken into account in our model.

Division.
When the radius of a bacterium reaches a limit (*1.5 µm* for *L. monocytogenes*, see Table 2), it splits into two halved volume individuals. One of them draws a new random perturbation for its optimal growth factor in order to desynchronise later divisions, otherwise the number of individual would always be a power-of-two.

Mechanics.
Because we planed to simulate millions of individuals in a 3D environment, collision detection and response are very critical considering computation time. As shown on Figure 4, we simplified this problem by turning bacillus shapes into spheres and we introduced a local density based stacking algorithm (not physically exact) to organise bacteria in distinct layers in which collision detection occurs.

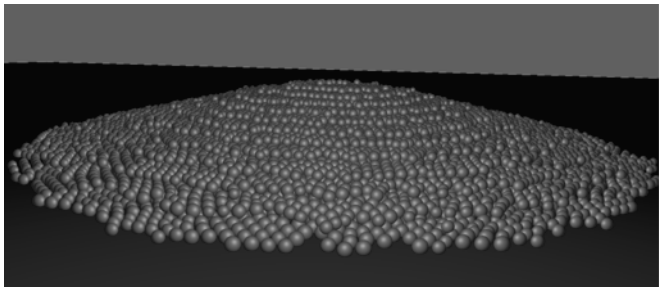

Figure 4: Multi-Layered Colony Shape

Validation

We validated our IBM on real data, provided by the ADRIA laboratory, Quimper, France. This validation was presented in (Desmeulles et al. 2015): the IBM parameters were adjusted by interpolating simulated data with real ones.

BENEFIT OF SPACIALISATION

As already explained in the introduction of this paper, cardinal models cannot account for the variations of bacteria spatial distribution observed on real food, or on Petri dishes. The main interest of our individual based simulation is its ability to achieve more realistic simulations, thanks to its 3D-spatialisation. In this section, we present two concrete cases which enlighten this ability.

Impact of Spatialisation on One Species Growth

We first simulate the temporal response of *C. piscicola* bacteria in a Petri dish for two distinct spatial distributions. Bacteria colonies grow on a $c * c * 5\ mm^3$ medium (sub-box of a virtual Petri dish), with $c = 17.836$. The environmental conditions are given in Table 1 and bacteria parameters in Table 2. All these parameters come from the actual experiments that were conducted by the ADRIA laboratory (see web references).

Table 1: Substrate Parameters

parameters	values	units
substrate size	17.836 x 17.836 x 5	*mm*
discretisation	89 x 89 x 8 (1.3 depth progr.)	–
substrate step	200	*µm*
diffusion time step	10	*s*
initial glucose	2	*g/l*
initial pH	7.2	–
pH_0	7.4	–
pH_1	-0.0758	–
pH_2	0.0004	–
glucose diffusivity	$6.7 \cdot 10^{-10}$	m^2/s
lactate diffusivity	$2.35 \cdot 10^{-10}$	m^2/s
temperature	8.0	*°C*
water activity	0.997	–

Table 2: Bacteria Parameters

parameters	Listeria	Carnobacterium	units
shoving factor	1.3	1.3	–
opt. growth rate (μ_{opt})	1.12	0.898	h^{-1}
division radius	$1.5 \cdot 10^{-6}$	$1.0 \cdot 10^{-6}$	*m*
div. glu. consum.	$13.5 \cdot 10^{-15}$	$13.5 \cdot 10^{-15}$	*Mole*
lactate yield	0.18	1.8	–
pH_{min}	4.21	5.12	–
pH_{opt}	7.21	7.27	–
pH_{max}	10.07	10.24	–
t_{min}	0.6	-5.42	*°C*
t_{opt}	37.4	31.6	*°C*
t_{max}	45.3	36.5	*°C*
aw_{min}	0.922	0.924	–
aw_{opt}	0.997	0.997	–
gamma pH exponent	1.68	7.77	–
Min inhib. concent.	6.4	0.48	*mMole/l*

Comparison of Two Spatial Distributions.

- **Case A:** we initialise our simulation with a packed configuration of 375 *C. piscicola* individuals. As depicted on Figure 5-A, all bacteria are uniformly distributed in a disk with diameter $c / 10$ (the size of a bacterium is approximately $c * 10^{-4}$).
- **Case B:** we initialise our simulation with a homogeneous distribution of 375 *C. piscicola* individuals. As depicted on Figure 5-B, all bacteria are uniformly distributed on the virtual Petri dish sub-box with dimensions $c * c * 5\ mm^3$.

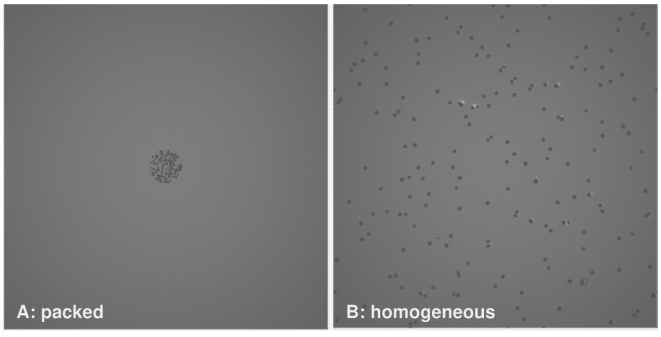

Figure 5: Two Spatial Distributions of *C. Piscicola*

Notice that the choice of 375 individuals on the sub-box considered here corresponds to 7500 CFU on a Petri dish which surface is about 20 times larger: these were the conditions of real data provided by the ADRIA laboratory.

Results.
These distinct spatial distributions highlight the importance of the spatial dimension for colony growth. Figure 6 shows how the same colony grows in drastically different ways, depending on its spatial distribution. These results are natural, since a high concentration of lactic bacteria induces a drastic decrease of pH, consequently a high self-inhibition.

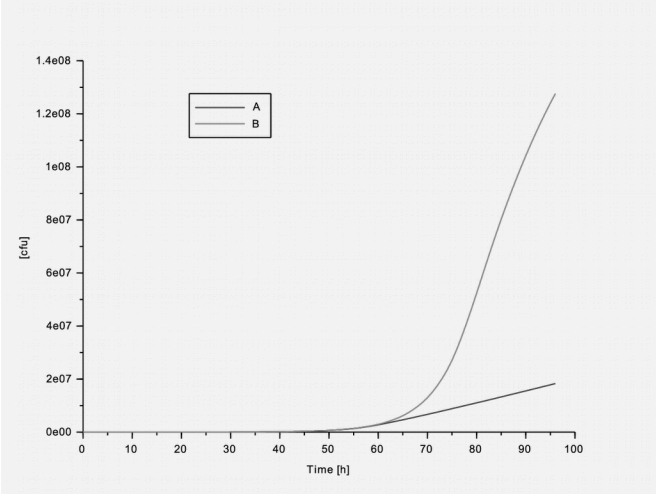

Figure 6: IBM Simulation of *C. Piscicola* Growth for Two Different Spatial Distributions (A: packed; B: homogeneous)

Impact of Spatialisation on Interacting Species

Comparison of Three Spatial Distributions.

- **Case A:** we initialise our simulation with a packed configuration of 375 *C. piscicola* individuals, and one *L. monocytogenes* individual. As depicted on Figure 7-A, *C. piscicola* bacteria are uniformly distributed in a disk with diameter *c / 4;* in the middle of this disk stands a *L. monocytogenes* bacterium.
- **Case B:** we initialise our simulation with a packed distribution of 375 *C. piscicola* individuals, and one isolated *L. monocytogenes* individual. As depicted on Figure 7-B, *C. piscicola* bacteria are uniformly distributed in a disk with diameter *c / 10;* this disk is placed in a corner of our virtual Petri dish subbox, in the opposite corner is placed a *L. monocytogenes* individual.
- **Case C:** our simulation is initialised with a homogeneous distribution of 375 *C. piscicola* individuals. As depicted on Figure 7-C, one *L. monocytogenes* individual is placed in the middle of the virtual Petri dish sub-box.

Results.
The results exposed for lactic acid bacteria without pathogens have emphasized the effect of spatial distribution on the self-inhibition mechanism. Figure 8 now illustrates how the inhibition of pathogens growth by lactic acid bacteria depends heavily on the spatial distributions of the different colonies. These results are once again natural: in case A, the inhibition is maximal, since the *L. monocytogenes* individuals stands where the lactic acid concentration is maximal, whereas in case B, the situation is reversed, and case C is intermediate. Note that these results strongly depend on the lactic acid diffusion coefficient. In case B, if the acid produced by *C. piscicola* had been more fastly diffused, the *L. monocytogenes* colony would obviously have grown slower.

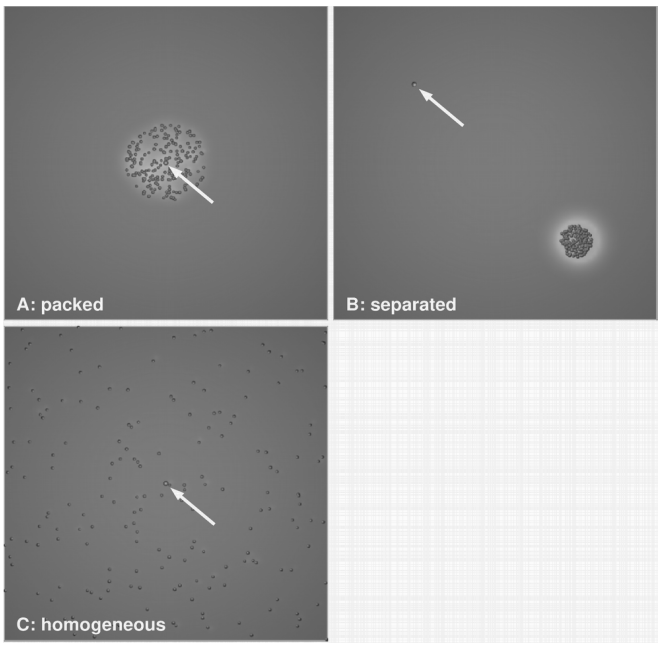

Figure 7: Three Spatial Distributions of *C. Piscicola* Around *L. Monocytogenes*

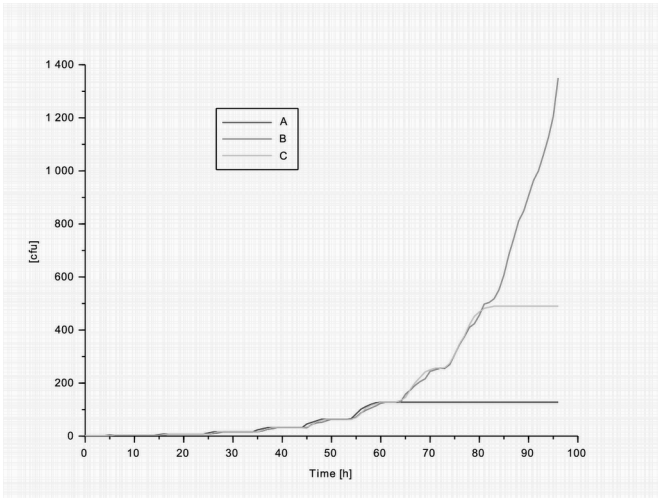

Figure 8: IBM Simulation of *L. Monocytogenes* Growth for Three Different Spatial Conditions Relative to *C. Piscicola* (A: packed; B: separated; C: homogeneous)

PERSPECTIVES

As described *supra*, the IBM we have developed is able to account for effects of spatialisation, such as diffusion, which the Cardinal models can obviously not consider. However, this IBM has a major flaw: its cost in terms of computation time can be huge when it comes to simulating a hundreds of millions of bacteria, particularly because of the collision process between individuals.
In order to supplement the IBM in cases where large colonies are formed and can be considered as "super

individuals", but also in order to be provided with a tool for parameters estimation, we have built a partial derivative equation model (PDE), which is briefly described here: the validation process for this model is not completed yet, so that precise developments will be exposed in a future work.
To understand our PDE model, we give a simplified version, in which only one population of bacteria is considered. We denote by $\rho(x, y, t)$ its density at the point (x, y) and at time t, γ_0 the threshold, for the norm of the density gradient, beyond which the population starts to move. Therefore, we name *truncated gradient* the vector field:

$$\overline{\nabla\rho} = \begin{cases} \nabla\rho \text{ if } \|\nabla\rho\| \geq \gamma_0 \\ 0 \text{ if not} \end{cases}$$

The density flow is given by $\emptyset = \rho V$ where V is the velocity field. We choose to consider that this velocity is proportional to the truncated gradient, rather than to the gradient, as usually used:

$$V = -K\overline{\nabla\rho}$$

This choice leads to a *modified transport equation*, that we complete by taking into account the population growth, here with a simple factor μ, so that we get:

$$\frac{\partial\rho}{\partial t} - K\nabla\cdot(\overline{\nabla\rho}\rho) = \mu\rho$$

We first checked that our continuous model could account for growth in layers, realistically, that is, in accordance with actual experiments. This verification was based on the work of (Su et al. 2012). We used the results exposed in this article to deduce our threshold for the truncation of the gradient norm: indeed, this threshold can simply be observed on the slope of a bacterial colony. We also used the same initial conditions as (Su et al. 2012), for instance sizes of bacteria and initial density.
Of course, this fitting with real growth-in-layers observations will have to be improved, and performed in our case of *C. piscicola* and *L. monocytogenes* colonies. However, the modest results exposed here seem rather promising.

CONCLUSION

We have presented an individual based model for bacteria colonies growth and inhibition by means of lactic acid production. This model enables a high level of description and a detailed co-construction of simulations by researchers from different domains. Even if we optimised the computing time of this IBM, when it comes to simulating hundreds of millions of bacteria, a partial derivative continuous model would enable faster simulations, but would suffer from a lack of accuracy in the description of local interactions. As a consequence, our aim is to make use of both IBM and PDE models. Although we have already built our PDE model, which gives in particular a realistic description of the layers which are observed in real growing colonies, we just briefly exposed it in this paper, since we have not completed its validation process.
Our next goal will be to make our IBM and PDE models involved in the same simulations, and interact in real time: the IBM will provide local precise results, transfer these results to the partial derivative equations model, which will fast give global results: these results will in turn be taken into account by the IBM.
Finally, the benefit of spatialisation which is provided by this IBM approach is currently exploited to investigate around the conditions leading to branched colony shapes in relation with local nutrient depletion.

ACKNOWLEDGEMENTS

This work was supported by PAO-Pôle Agronomique Ouest, Région Bretagne, and ADRIA Développement. The authors want to especially thank Dominique Thuault, Vincent Rodin and Marie-Pierre Cassagnes.

REFERENCES

Desmeulles, G.; Bonneaud, S.; Redou, P.; Rodin, V. and Tisseau, J. 2009. "In Virtuo Experiments Based on the Multi-Interaction System Framework: The Réiscop Meta-Model." *Computer Modeling in Engineering and Sciences (CEMS)*, 47, no. 3, 299-329.

Desmeulles, G.; Harrouet, F.; Thuault, D.; Huchet, V.; Redou, P.; Gaubert, L.; Pron, G.L.; Ballet, P. and Rodin V. 2015. "3D Individual Based Model for Simultaneous Growth and Interaction of L. Monocytogenes ans Lactic Acid Bacteria." In *International Conference on Predictive Modelling in Food (ICPMF'09)*, Rio, Brazil, page 003.02 Elsevier.

Ellouze, M.; Pichaud, M.; Bonaiti, C.; Coroller, L.; Couvert, O.; Thuault, D. and Vaillant, R. 2008. "Modelling pH Evolution and Lactic Acid Production in the Growth Medium of a Lactic acid Bacterium: Application to Set a Biological TTI." *International Journal of Food Microbiology*, 128, no. 1, 101-107.

Grimson, M. and Barker, G. 1994. "Continuum Model for the Spatiotemporal Growth of Bacterial Colonies". *Physical Review* E, 49, no. 2, 1680-1684.

Hairer, E.; Norsett, S. and Wanner, P. 1996. "Solving Ordinary Differential Equations II. Stiff and Differential-Algebraic Problems". Springer Series in Comput. Mathematics.

Harrouet, F. 2012. "Designing a Multicore and Multiprocessor Individual-Based Simulation Engine". *IEEE Micro*, 32, no. 1, 54-65.

Kreft, J.-U.; Booth, G. and Wimpenny, J. W. 1998. "BacSim, a Simulator for Individual Based Modelling of Bacterial Colony Growth". *Microbiology*, 144, no. 12, 3275-3287.

Lobry, J.; Rosso, L. and Flandrois, J.-P. 1991. "A FORTRAN Subroutine for the Determination of Parameter Confidence Limits in Non-Linear Models". *Binary*, 3, 86-93.

Matilla-Sandholm, T. and Skyttä, E. 1996. "The Role of Lactic Acid Bacteria as Protective Cultures". In *Second European Symposium on Sous Vide*, Alma Sous Vide Competence Centre, Leuven, Belgium, 209-221.

Poschet, F.; Vereecken, K.M.; Geeraerd, A.H.; Nicolaï, B.M. and Van Impe, J.F. 2005. "Analysis of a Novel Class of Predictive Microbial Growth Models and Application to Coculture Growth". International Journal of Food Microbiology, 100, no. 1-3, 107-24.

Su, P.T.; Liao, C.T.; Roan, J.R.; Wang, S.H.; Chiou, A. and Syu, W.J. 2012. "Bacterial Colony from Two-Dimensional Division to Three Dimensional Development". *PLoS ONE*, 7, no. 11.

Tisseau, J. 2001. "Virtual Reality - In Virtuo Autonomy". PhD thesis, Accreditation to direct research, Université de Rennes I, Rennes (France).

WEB REFERENCES

www.enib.fr/~harrouet/transprog.html
(provides simulation source code and data)

FOOD PRODUCT AND PROCESS MONITORING

ROLE OF DIFFERENTIAL PLATING-BASED METHODS IN THE DETECTION OF SUBLETHAL INJURY INDUCED TO *LISTERIA MONOCYTOGENES* BY NATURAL PLANT EXTRACTS

Davy Verheyen, Maria Baka, Estefanía Noriega, Jan F.M. Van Impe*

KU Leuven, Department of Chemical Engineering,
BioTeC - Chemical and Biochemical Process Technology and Control,
OPTEC - Optimization in Engineering Center-of-Excellence,
CPMF^2 - Flemish Cluster Predictive Microbiology in Foods,
Gebroeders De Smetstraat 1, B-9000 Gent, Belgium
*E-mail address: Jan.VanImpe@cit.kuleuven.be

KEYWORDS

Listeria monocytogenes, grape seed extract, garlic extract sublethal injury, thin agar layer

ABSTRACT

Recently, food researchers are investigating natural plant extracts as milder food preservation technologies. Milder treatments might cause sublethal injury (SI), which is a major food safety concern. This study demonstrates that both grape seed extract and garlic extract are suitable to inactivate *Listeria monocytogenes*. Both extracts cause a significant amount of SI, which increases at more severe treatments. Finally, experimental results indicated that the thin agar layer (TAL) method is a promising alternative to the traditional method, which uses the difference between plate counts on general and selective media to determine SI. The TAL method is unable to determine the total viable population of healthy and injured micro-organisms as adequately as the general medium in the traditional method, but can be used to determine SI in real food products.

INTRODUCTION

Listeria monocytogenes, causing listeriosis, is a dangerous foodborne pathogen due to its high fatality rate, e.g., 15.6% in Europe in 2013 (EFSA and ECDC, 2015). Symptoms of the disease range from mild clinical features like fever and diarrhea to severe infections like meningitis and septicemia (OIE, 2014). The disease is especially dangerous for pregnant women, the elderly population and persons with a compromised immune system (Farber and Peterkin, 1991).

Predictive microbiology is a discipline of food microbiology in which microbial responses in/on food products are studied under controlled intrinsic and extrinsic conditions to develop mathematical models. Well-developed models allow a realistic estimation of food safety risks, which leads to the development of production processes for safe food products (McMeekin et al., 2002). Recently, food researchers are investigating natural antimicrobial compounds like plant extracts (Devlieghere et al., 2004; Hintz et al., 2015). Grape seed extract (GSE) (Silván et al., 2013) and garlic extract (GarE) (Belguith et al., 2010; Marques et al., 2008) are examples of natural plant extracts, which have shown promising antimicrobial effects. GSE and GarE owe their antimicrobial properties to phenolic compounds and allicin (an oxygenated organic sulfur compound), respectively (Miron et al., 2000; Perumalla and Hettiarachchy, 2011).

The use of mild food preservation techniques possibly leads to difficulties in assessing the number of pathogenic micro-organisms in food products due to sublethal injury (SI) (Wu et al., 2001). Hurst (1977) defines SI as "a consequence of exposure to a chemical or physical process that damages but does not kill a micro-organism". SI is caused by the food environment, processing and preservation technologies. The injury can be structural (altered membrane permeability) or metabolic (damage to functional cell components) (Brashears et al, 2001). SI causes serious limitations in food diagnostics due to possible underestimation of contamination and false negative results as injured micro-organisms might be able to recover and exhibit enhanced resistance (Brashears et al., 2001; Jasson et al., 2007; Vermeiren et al., 2006). Traditional methods to quantify SI compare plate counts on a general and selective medium. Cells detected on the general medium correspond to the total viable population of healthy and injured cells, while cells on the selective medium correspond to the population of healthy cells (Busch and Donnelly, 1992; Wu, 2008). However, this technique is not optimal to quantify SI in real food products due to the presence of background microflora. For samples taken from real food products, counts on the general medium include the population of healthy background microflora. In order to quantify SI in real food products, injured cells must be allowed to resuscitate in a favorable environment first (Wu and Fung, 2001; Wu et al.; 2001). Several repair methods to asses SI in real food products exist, e.g., liquid-repair methods, surface-overlay plating, agar underlay method, thin agar layer method. The thin agar layer method (TAL) is promising, as it is a one-step method that requires no separate recovery step (as opposed to liquid-repair methods and the surface-overlay method) and is convenient to use and prepare (as opposed to the agar underlay method) (Wu, 2008). The TAL method was first developed by Kang and Fung (1999) and was optimized further over the years (Kang and Fung, 2000; Wu et al., 2001; Wu and Fung, 2001). The method uses plates in which a selective medium is overpoured with a general medium. The general medium allows the recovery of injured cells and the selective compounds, which diffuse into the general medium, inhibit the growth of background microflora (Wu, 2008).

In this study, the antlisterial activity of GSE and GarE is characterized, as well as the effect of the bioactive concentration and formulation of those extracts on the occurrence of SI. Furthermore, the TAL method is investigated as a means to quantify SI.

MATERIALS AND METHODS

Micro-organisms and preculture conditions

L. monocytogenes LMG 23775 strain, was acquired from the BCCM/LMG bacteria collection of Ghent University

in Belgium. A stock culture was stored at -80°C in Tryptone Soy Broth supplemented with 0.6% (w/v) yeast extract (TSBYE, Oxoid) and 20% (v/v) glycerol (Acros Organics). Inocula were prepared by transferring a loopful of the stock culture into 20 mL of TSBYE. After incubating for 9 h at 30°C under static conditions (Binder KB-series incubator; Binder Inc., NY, USA), 20 µL of the stationary-phase culture was inoculated into 20 mL of fresh TSBYE and incubated for 15 h under the same conditions. This resulted in a stationary-phase *L. monocytogenes* culture with an inoculum level of approximately 10^9 CFU/mL.

Preparation of bioactive extracts

The procedure to prepare GSE is based on the protocol reported by Silván et al. (2013). The total phenolic content (TPC) was equal to approximately 2500 mg gallic acid equivalents per L (mg GAE/L) (Silván et al., 2013). GSE tablets (Laboratories GSN, Madrid, Spain) were crushed using a pestle and mortar to obtain GSE powder. The powder (500 mg) was dissolved in 10 mL of distilled water and vortexed for 5 min at room temperature. Subsequently, the resulting suspension was centrifuged at 4,500 rpm for 10 min at 4°C. The supernatant was collected and filter-sterilized with a pore size membrane of 0.22 µm (TPP, Trasadingen, Switzerland). The aqueous GSE was immediately used or stored at room temperature in the dark.

The procedure to prepare GarE is a combination of the protocols reported by Prasad et al. (1995), Rees et al. (1993) and Singh et al. (2001). Solgar Garlic Powder 500 mg (Solgar inc., NJ, USA), provided by Farmacia International, was used as an allicin source. According to the product information, one Solgar capsule contains 750 µg of allicin (yield). The capsules were carefully opened and the powder was dissolved in distilled water (1 capsule per 5 mL). The suspensions were vortexed for 5 min and then centrifuged at 6,000 rpm for 10 min at 4°C. Afterwards, the supernatant was collected and centrifuged at the same conditions. The final supernatant was filter-sterilized. The resulting extract had a theoretical allicin concentration of 150 µg allicin/mL. The GarE was immediately used or stored at 4°C in the dark.

Preparation of TAL plates

To prepare the TAL plates, an adapted version of the method of Wu and Fung (2001) was used. 25 mL of selective medium was poured into a petri plate. Two different selective media for *Listeria* spp. were used to prepare plates: (i) *Listeria* selective agar - Oxford formulation (Oxford, VWR), and (ii) *Listeria* selective agar - Palcam formulation (Palcam, VWR). The plates were then allowed to solidify for approximately 24 h. Subsequently, a layer of 8.5 mL of general medium (TSAYE) was poured onto the selective medium. The new layer was then allowed to solidify for 1 min, after which a second layer of general medium was overpoured. When this layer was fully solidified, the plates were ready to be used.

Minimum Inhibitory Concentration (MIC)

The MIC of GSE was determined according to the protocol of Silván et al. (2013). The MIC of the bioactive compounds was defined as the lowest concentration that inflicts a significant quantitative decrease ($P \leq 0.05$) in viability of *L. monocytogenes* cells as compared to the control (TSBYE) after 24 h. Mixtures of GSE and TSBYE with different GSE concentrations (mg GAE/L) and a control in TSBYE were prepared. Each mixture was prepared containing a total volume of 20 mL in a 50 mL Erlenmeyer. For GSE concentrations lower than 20% of the TPC, the mixtures consisted of a combination of 4 mL of a GSE dilution (appropriately diluted with sterile distilled water) and 16 mL of a concentrated TSBYE solution. The final TSBYE concentration in the mixture was equal to the TSBYE concentration of the control. For GSE concentrations higher than 20% of the TPC, the volumes of pure GSE and TSBYE and the concentration of pure TSBYE were adapted, so that the final TSBYE concentration in the mixture was still equal to the one in the control. For the pure GSE, TSBYE powder was first heated at 105°C (Binder KB-series incubator; Binder Inc., NY, USA) for 20 min to eliminate the background microflora, and then directly added to the Erlenmeyer. GSE/TSBYE mixtures and the control in TSBYE were inoculated with 200 µL of a stationary-phase culture of *L. monocytogenes*. Bacterial cells were inoculated under aseptic conditions to yield a final concentration of about 10^7 CFU/mL. The mixtures were then incubated at 30°C and 180 rpm for 24 h. Afterwards, a sample from each mixture was taken and microbiologically analyzed. Each mixture was compared with the control (TSBYE) in order to evaluate the occurrence of significant differences. Experiments were conducted in duplicate.

A similar protocol was used for the MIC determination of GarE. Mixtures consisted of a combination of 15 mL of a GarE dilution and 5 mL of a concentrated TSBYE solution. The volumes of the pure GarE and the TSBYE were adapted for GarE concentrations higher than 75% of the allicin concentration of the pure GarE.

Challenge testing and estimation of sublethal injury

Five different mixtures (control in TSBYE, GSE-MIC, GarE-MIC, pure GSE and pure GarE) were inoculated with 200 µL of a stationary-phase culture of *L. monocytogenes* (to a concentration of approximately 10^7 CFU/mL), and incubated at 30°C while shaking at 180 rpm. GSE-MIC and GarE-MIC were prepared as mentioned before in the section 'Minimum inhibitory concentration (MIC)'. The pure extracts were prepared as mentioned in the section 'Preparation of bioactive extracts'. Samples were taken at different time intervals (in triplicate), and microbiologically analyzed using the different plating media. Since the maximum sampling time was 24 h, samples were taken in two batches. The experimental data were plotted as a function of time. To model the growth and inactivation of *L. monocytogenes*, the primary models of Baranyi and Roberts (1994) and Geeraerd et al. (2000) were fitted to the experimental data, respectively.

The theoretical data, obtained from the respective models, was used to calculate the percentage of sublethal injury (%SI) using Equation 1 according to the formula of Bush and Donnelly (1992).

$$\%SI = \frac{CFU\ on\ TSAYE - CFU\ on\ Oxford|Palcam}{CFU\ on\ TSAYE} \cdot 100 \qquad (1)$$

The %SI at the different exposure times was also determined with Equation 2, using the respective TAL medium as a general medium.

$$\%SI = \frac{CFU\ on\ TAL - CFU\ on\ Oxford|Palcam}{CFU\ on\ TAL} \cdot 100 \qquad (2)$$

Microbiological Analysis

Samples were first decimally diluted using an aqueous saline solution containing 0.9% (w/v) NaCl. Then, the different dilutions were plated using the drop technique. This method involves the careful deposit of 20 µL drops onto the corresponding agar plates (3 drops per dilution). Afterwards, the plates were incubated at 30°C for 24 h, after which the colonies were counted. Results were logarithmically transformed and expressed as ln CFU/mL in cases of growth or as log CFU/mL in cases of inactivation. The model of Baranyi and Roberts (1994), which was used to fit the data for growth, involves the natural exponential function to describe the growth phase. The model of Geeraerd et al. (2000), which was used to fit the inactivation data, as all inactivation models requires the reduction of micro-organisms to be expressed in log10 units.

Mathematical modeling

The model of Baranyi and Roberts (1994) is represented by Equations 1, 2 and 3.

$$\frac{dN}{dt} = \left(\frac{Q}{1+Q}\right)\mu_{max}\left(1 - \frac{N}{N_{max}}\right)N \qquad (1)$$

$$\frac{dQ}{dt} = \mu_{max} \cdot Q \qquad (2)$$

$$L_0 \cdot \mu_{max} = ln\left(1 + \frac{1}{Q(0)}\right) \qquad (3)$$

With N [CFU/mL], the cell density at time t; N_{max} [CFU/mL], the maximum cell density; μ_{max} [1/h], the maximum specific growth rate; Q [-], the physiological state of the cells; $Q(0)$, a measure of the initial physiological state of the cells; and L_0 [h], the lag time of the cells.

The model of Geeraerd et al. (2000) is represented by Equation 4, 5 and 6.

$$\frac{dN}{dt} = -\left(\frac{1}{1+C_c}\right)k_{max}\left(1 - \frac{N_{res}}{N}\right)N \qquad (4)$$

$$\frac{dC_C}{dt} = -k_{max} \cdot C_C \qquad (5)$$

$$C_C(0) = e^{k_{max}S_L} - 1 \qquad (6)$$

With N [CFU/mL], the cell density at time t; N_{res} [CFU/mL], the residual cell density; k_{max} [1/h], the maximum specific inactivation rate; C_C [-], the concentration of a critical component (intracellular or extracellular) for cell survival; $C_C(0)$ [-], the initial concentration of this critical component; and S_L [h], the shoulder length representing the period the cells need to adapt to the stress.

Statistical analysis

For the statistical analysis, significant differences between logarithmically transformed viable counts were determined using analysis of variance (ANOVA, single variance) test at a 95.0% confidence level (α = 0.05). Fisher's Least Significant Difference (LSD) test was used to distinguish which means were significantly different from others. The analyses were performed using the anova1 routine of the Statistical Toolbox of MatLab® version R2010b (The Mathworks, Inc., Natick, USA). Test statistics were regarded as significant when $P \leq 0.05$.

RESULTS AND DISCUSSION

Minimum inhibitory concentration (MIC)

For GSE, the statistical analysis shows a significant inhibition of *L. monocytogenes* compared to the control of pure TSBYE for concentrations equal to or higher than 500 mg GAE/L, which consequently is the MIC of GSE.

For GarE, the statistical analysis indicates a significant inhibition of *L. monocytogenes* for concentrations starting from 7.5 µg allicin/mL, which consequently is the MIC for GarE.

Challenge testing and estimation of sublethal injury

In Figure 1, the effect of bioactive compounds on *L. monocytogenes* kinetics is demonstrated using the different plating media. The TAL plates using Oxford as a selective medium were more practical to prepare than those using Palcam, as Oxford layers were spread more smoothly onto the general medium. Therefore, the methods involving Palcam were only used as an extra validation for the most extreme treatments (pure extracts) and the control.

Comparing the five conditions (A to E) in Figure 1, *L. monocytogenes* is able to grow in GSE-MIC and GarE-MIC. Compared to TSBYE (control), the maximum cell population reached at the stationary phase is slightly lower at GSE-MIC and GarE-MIC. Furthermore, the lag phase in GSE-MIC lasts longer than in TSBYE. For GarE-MIC, this phenomenon is even more pronounced. In pure GSE and pure GarE, *L. monocytogenes* is inactivated. It is important to mention that for pure GSE, the time range is only equal to 5 min instead of 24 h. Consequently, the inactivation in pure GSE is much more acute and rapid than in pure GarE.

The TAL media theoretically indicate the total viable population of *L. monocytogenes*, similarly to general media in the traditional method. When *Listeria* is grown in TSBYE, GSE-MIC and GarE-MIC, the differences between viable counts on the respective selective and TAL media are rather small. However, when *Listeria* cells are exposed to pure GSE and pure GarE, counts on the TAL

medium are significantly higher than on the respective selective medium, indicating the presence of SI.

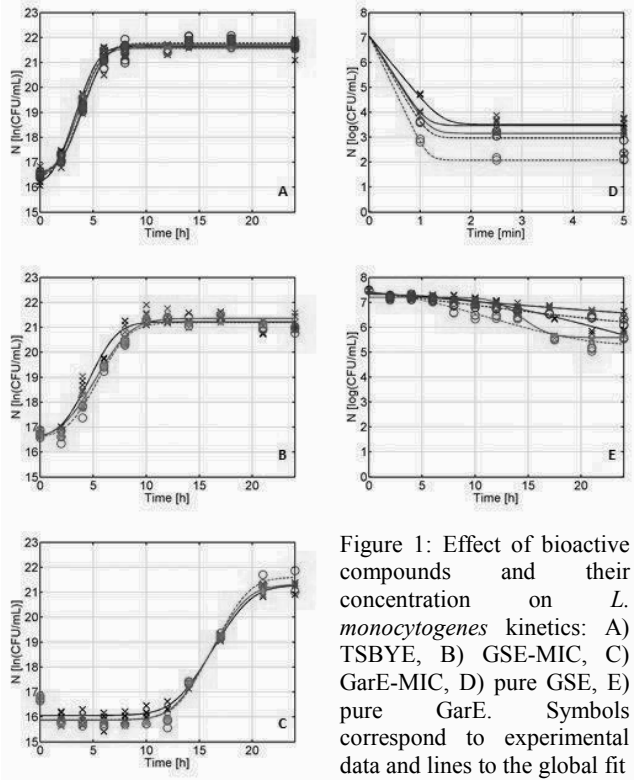

Figure 1: Effect of bioactive compounds and their concentration on *L. monocytogenes* kinetics: A) TSBYE, B) GSE-MIC, C) GarE-MIC, D) pure GSE, E) pure GarE. Symbols correspond to experimental data and lines to the global fit of the Baranyi and Roberts (1994) model for growth [ln(CFU/mL)] or the Geeraerd et al. (2000) model for inactivation [log(CFU/mL)]. Crosses and solid lines correspond to total viable population (TSAYE and TAL media) and circles and dashed lines correspond to uninjured viable subpopulation (selective media). The used media are TSAYE, Oxford-TAL Oxford and Palcam-TAL Palcam

Figure 2 illustrates the %SI induced to *L. monocytogenes* for all conditions. %SI was determined using Equation 1 (traditional method) and Equation 2 (TAL method) with the theoretical modeled values from Figure 1. The equations have two limiting cases. In the lower limit, the equations deliver a value of 0%, which means that no SI is present. In the upper limit, the equations deliver a value of 100%, which means that there are no uninjured cells. If the calculated %SI is negative, %SI has been assumed to be equal to 0%. A comparison of the different conditions presented in Figure 2 demonstrates that %SI of *L. monocytogenes* grown in TSBYE, GSE-MIC and GarE-MIC is significantly lower than in pure GSE and pure GarE. This observation indicates that higher concentrations of bioactive compounds also result in increased inactivation. A comparison of Figure 1 with Figure 2 demonstrates that, in the case of growth (in TSBYE, GSE-MIC and GarE-MIC), a peak in %SI always occurs when the cells are in their exponential growth phase. Since stress proteins are synthesized in the early stationary phase, cells at their stationary-phase are often more stress-resistant than exponentially growing cells (De Angelis et al., 2004; Dodd and Aldsworth, 2002). In the case of inactivation (pure GSE and pure GarE), the %SI increases during the exponential decay phase and decreases again in the stationary phase. This phenomenon is possibly caused by a mechanism of injury accumulation that culminates in cell death (Perni et al., 2007). A similar behavior was observed by Noriega et al. (2013) for *Listeria innocua* subjected to mild heating. In general, Figure 5 shows that %SI is higher in pure GSE than in pure GarE. Consequently, the antimicrobial treatment which causes a more evident and acute inactivation also causes a higher %SI.

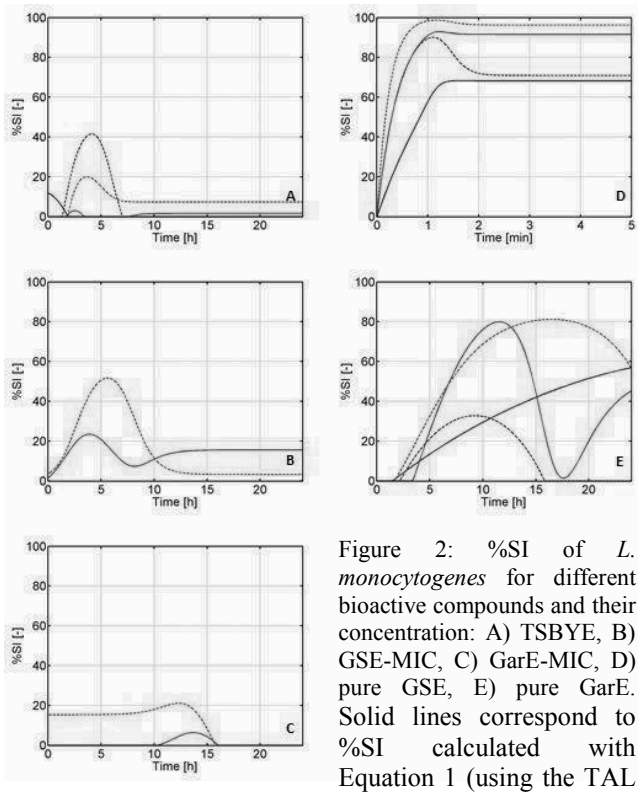

Figure 2: %SI of *L. monocytogenes* for different bioactive compounds and their concentration: A) TSBYE, B) GSE-MIC, C) GarE-MIC, D) pure GSE, E) pure GarE. Solid lines correspond to %SI calculated with Equation 1 (using the TAL and dashed lines correspond to %SI calculated with Equation 2 (using the traditional method). The used selective and TAL media are Oxford-TAL Oxford and Palcam-TAL Palcam

Overall, the methods using TAL media to represent the total viable cell population demonstrate a lower %SI than the traditional method. Therefore, TAL media are unable to show the total viable population of *L. monocytogenes* as adequately as general media. However, the results are still reasonably accurate, which is optimistic for the SI detection in food products. Normal general media cannot be used for SI detection in real food products as they are unable to inhibit the growth of background microflora. The TAL method involving Oxford provided results which were most similar to those from the traditional method. Oxford was also used as a selective medium for *Listeria* in other studies investigating the TAL method (Wu et al., 2008).

CONCLUSIONS

In this study, the antimicrobial activity of two natural plant extracts, i.e., GSE and GarE, against *L. monocytogenes* was characterized. Subsequently, the effect of the bioactive concentration and formulation of those extracts on the SI of *L. monocytogenes* was studied. In this regard, the TAL method was investigated as an alternative to calculate %SI in real food products containing background microflora. The results indicated that both extracts are effective on the inactivation or growth inhibition of *L. monocytogenes*. In general, microbial treatments which

caused a more severe inactivation also caused more SI. Additionally, it was concluded that the TAL method involving Oxford as a selective medium is suitable to quantify the total viable population of *L. monocytogenes* in SI determination studies, but significant differences with the general medium were observed for the pure extracts. However, as the traditional SI determination method cannot handle the presence of background microflora, results are promising for the SI determination in food.

ACKNOWLEDGEMENTS

This work was supported by project PFV/10/002 (Center of Excellence OPTEC-Optimization in Engineering) of the KU Leuven Research Fund, projects G.0930.13 and KAN.15189.13 of the Fund for Scientific Research-Flanders, and the Belgian Program on Interuniversity Poles of Attraction, initiated by the Belgian Federal Science Policy Office (IAP Phase VII/19 DYSCO).

REFERENCES

Baranyi, J. and T.A. Roberts. 1994. A dynamic approach to predicting bacterial growth in food. *International Journal of Food Microbiology*, 23: 277-294.

Belguith, H.; F. Kthiri; A. Chati; A. Abu Sofah; J. Ben Hamida; A. Landoulsi. 2010. Study of the effect of aqueous garlic extract (*Allium sativum*) on some *Salmonella* serovars isolates. *Emerates Journal of Food and Agriculture*, 22(3): 189-206.

Brashears, M.M.; A. Amezquita; J. Stratton. 2001. Validation of methods used to recover *Escherichia coli* O157:H7 and *Salmonella* spp. subjected to stress conditions. *Journal of Food Protection*, 64(10): 1466-1471.

Bush, S.V. and C.W. Donnelly. 1992. Development of a repair-enrichment broth for resuscitation of heat-injured *Listeria monocytogenes* and *Listeria innocua*. *Applied and Environmental Microbiology*, 58: 14-20.

De Angelis, M.: R. Di Cagno; C. Huet; C. Crecchio; P.F. Fox; M. Gobbetti. 2004. Heat shock response in *Lactobacillus plantarum*. *Applied and Environmental Microbiology*, 70(3): 1339-1346.

Devlieghere, F.; L. Vermeiren; J. Debevere. 2004. New preservation technologies: Possibilities and limitations. *International Dairy Journal*, 14: 273-285.

Dodd, C.E. and T.G. Aldsworth. 2002. The importance of RpoS in the survival of bacteria through food processing. *International Journal of Food Microbiology*, 74(3): 189-194.

EFSA (European Food Safety Authority) and ECDC (European Centre for Disease Prevention and Control). 2015. The European Union Summary Report on Trends and Sources of Zoonoses, Zoonotic Agents and Food-borne Outbreaks in 2013. *EFSA Journal 2015*, 13, 3991, 162 pp. doi:10.2903/j.efsa.2015.3991.

Farber, J.M. and P.I. Peterkin. 1991. *Listeria monocytogenes*, a Food-Borne pathogen. *Microbiological Reviews,* 55(3): 476-511.

Geeraerd, A.H.; C.H. Herremans; J.F.M. Van Impe. 2000. Structural model requirements to describe microbial inactivation during a mild heat treatment. *International Journal of Food Microbiology*, 59: 185-209.

Hintz, T.; K.K. Matthews; R. Di. 2015. The use of plant antimicrobial compounds for food preservation. *BioMed Research International*, accessible online at: http://dx.doi.org/10.1155/2015/246264

Hurst, A. 1977. Bacterial injury: A review. *Canadian Journal of Microbiology*, 23(8): 935-944.

Jasson, V.; M. Uyttendaele; A. Rajkovic; J. Debevere. 2007. Establishment of procedures provoking sub-lethal injury of *Listeria monocytogenes*, *Campylobacter jejuni* and *Escherichia coli* O157 to serve method performance testing. *International Journal of Food Microbiology*, 118: 241-249.

Kang, D.H. and D.Y.C. Fung. 1999. Thin agar layer method for recovery of heat-injured *Listeria monocytogenes*. *Journal of Food Protection*, 62: 1346-1349.

Kang, D.H. and D.Y.C. Fung. 2000. Application of thin agar layer method for recovery of injured *Salmonella* Typhimurium. *International Journal of Food Microbiology*, 54: 127-132.

Marques, A.; S. Encarnaçãu; S. Pedro; M.L. Nunes. 2008. In vitro antimicrobial activity of garlic, oregano and chitosan against *Salmonella enterica*. *World Journal of Microbiology and Biotechnology*, 24(2): 2357-2360.

McMeekin, T.A.; J. Olley; D.A. Ratkowsky; T. Ross. 2002. Predictive microbiology: towards the interface and beyond. *International Journal of Food Microbiology*, 73: 395-407.

Miron, T.; A. Rabinkov; D. Mirelman; M. Wilchek; L. Weiner. 2000. The mode of action of allicin: its ready permeability through phospholipid membranes may contribute to its biological activity. *Biochimica et Biophysica Acta*, 1463: 20-30.

Noriega, E.; E.G. Velliou; E. Van Derlinden; L. Mertens; J.F.M. Van Impe. 2013. Effect of cell immobilization on heat-induced sublethal injury of *Escherichia coli*, *Salmonella* Typhimurium and *Listeria innocua*. *Food Microbiology*, 36: 355-364.

OIE (World Organization for Animal Health). 2014. Manual of Diagnostic Tests and Vaccines for Terrestrial Animals. Chapter 2.9.7. *Listeria monocytogenes*, ISBN 978-92-9044-878-5.

Perni, S.; P.R. Chalise; G. Shama; M.G. Kong. 2007. Bacterial cells exposed to nanosecond pulsed electric field show lethal and sublethal effects. *International Journal of Food Microbiology*, 120(3): 311-314.

Perumalla, A.V.S. and N.S. Hettiarachchy. 2011. Green tea and grape seed extracts – Potential applications in food safety and quality. *Food Research International*, 44: 827-839.

Prasad, K.; V.A. Laxdal; M. Yu; B.L. Raney. 1995. Antioxidant activity of allicin, an active principle in garlic. *Molecular and Cellular Biochemistry*, 148: 183-189.

Rees, L.P.; S.F. Minney; N.T. Plummer; J.H. Slater; D.A. Skyrme. 1993. A quantitative assessment of the antimicrobial activity of garlic (*Allium sativum*). *World Journal of*

Silván, J.M.; E. Mingo; M. Hidalgo; S. de Pascual-Teresa; A.V. Carrascosa; A.J. Martinez-Rodriguez. 2013. Antibacterial activity of a grape seed extract and its fractions against *Campylobacter* spp. *Food Control*, 29: 25-31.

Singh, B.; M.B. Falahee; M.R. Adams. 2001. Synergistic inhibition of *Listeria monocytogenes* by nisin and garlic extract. *Food Microbiology*, 18: 133-139.

Vermeiren, L.; F. Devlieghere; I. Vandekinderen; U. Rajtak; J. Debevere. 2006. The sensory acceptability of cooked meat products treated with a protective culture depends on glucose content and buffering capacity: A case study with *Lactobacillus* sakei 10A. *Meat Science*, 74(3): 532-545.

Wu, V.C.H. 2008. A review of microbial injury and recovery methods in food. *Food Microbiology*, 25: 735-744.

Wu, V.C.H. and D.Y.C. Fung. 2001. Evaluation of thin agar layer method for recovery of heat-inured foodborne pathogens. *Journal of Food Science*, 66: 580-583.

Wu, V.C.H.; D.Y.C. Fung; D.H. Kang. 2001. Evaluation of thin agar layer method for recovery of cold-injured foodborne pathogens. *Journal of Rapid Methods and Automation in Microbiology*, 9: 11-25.

Wu, V.C.H.; X. Qiu; A. Bushway; L. Harper. 2008. Antibacterial effects of American cranberry (*Vaccinium macrocarpon*) concentrate on foodborne pathogens. *Food Science and Technology*, 41: 1834-1841.

APPLICATION OF NEAR-INFRARED TRANSMISSION (NIT) SPECTROSCOPY FOR DETERMINATION OF FAT AND PROTEIN IN QUINOA (*CHENOPODIUM QUINOA* Willd) GRAINS

Christian Encina-Zelada
José A. Teixeira
Department of Biological Engineering
School of Engineering
University of Minho
Portugal

Jorge Pereda
Faculty of Food Industries
National Agricultural University
La Molina
Peru

Luz Gómez-Pando
Martha Ibañez
Faculty of Agronomy
National Agricultural University
La Molina
Peru

Vasco Cadavez
Ursula Gonzales-Barron
CIMO Mountain Research Centre
School of Agriculture
Polytechnic Institute of Braganza
Portugal

E-mail: cencina@ipb.pt

KEYWORDS
Quinoa, chemometrics, spectrum, filters, pre-processing.

ABSTRACT
There is a need to speed up proximate analyses of quinoa by means of inexpensive, rapid and accurate methods such as those based on spectroscopy. Thus, the aim of this study was to assess the feasibility of using Near-Infrared Transmission (NIT) spectroscopy for precise and low-cost determinations of protein and fat contents of quinoa grains. NIT spectrum of Peruvian-origin quinoa grains of 73 different accessions were obtained while total protein and fat contents were determined by AOAC methods. To minimise the effects of changes in the baseline, spectra were pre-processed by separately applying a Savitzky-Golay algorithm first (SG1), second derivative (SG2), standard normal variate (SNV), multiplicative scatter correction (MSC) and Detrend (DT) filters. In addition, MSC filters were also applied in combination with SG1, SG2, SNV and DT. Best predictions for fat were obtained by extracting 16-18 partial least square (PLS) components from SNV, DT and SG2-treated spectra (mean square error of prediction, RMSEP=0.432-0.451; R^2=0.728-0.786) while best predictions for protein were attained by extracting 14-16 PLS components from DT, SG2+MSC and DT+MSC-treated spectra (RMSEP=0.545-598; R^2=0.833-0.862). Cross-validation run for ten-observation segments showed that model accuracy was slightly better for fat than for protein.

INTRODUCTION

Quinoa (*Chenopodium quinoa* Willd.) is a pseudo-cereal widely cultivated in South America which has lately gained worldwide attention due to its high nutritional value and protein quality (Ferreira et al. 2015). Despite being a less well-known plant, there has been increasing interest in quinoa for the past 15 years owing to its perceived superior nutritional quality in comparison with other grains. With the challenge of increasing the production of quality food to feed the world's population, considering climate change, quinoa represents an alternative crop for countries subject to insecurity in their food supplies (González-Martin et al. 2014).

Near infrared transmission (NIT) spectroscopy can presently provide whole kernel analysis of starch, moisture, protein, and oil percentages in cereals. In maize, for instance, the use of NIT technology for predicting extractable starch yields for wet milling provides the ability to select the most ideally suited maize lots and hybrids for wet milling use (Paulsen and Singh, 2004). Thus, the objective of this study was to assess the feasibility of accurately quantifying total protein and fat contents by rapid and low cost NIT spectroscopy.

MATERIALS AND METHODS

Samples
Quinoa crops (*Chenopodium quinoa* Willd.) harvested in Peru (from the National Agricultural University La Molina and Regional Development Centre – Highland), in different seasons between 2010 and 2012, were utilised. Quinoa grains samples amounted to 73 accessions which were of orange, beige and yellow colour.

Chemical analysis
Moisture, protein and crude fat contents were determined using the reference methods 925.10, 920.87 (conversion factor of 6.25) and 923.05 (FOSS Soxhtec), respectively, described in AOAC (2000). Determinations, done in triplicate, were averaged and converted to dry basis.

Near-infrared transmission (NIT) spectroscopy
NIT spectra were acquired by placing the grains directly in a Infratec 1241 grain analyzer (Module Foss Tecator), using 60-mm quartz cuvettes, and scanning the region 850-1050 nm

(wavenumber range of 11 765 - 9 524 cm^{-1}). The spectra were recorded at scanning step intervals of 2 nm to give 100 data points per sample. A total of 10 frequency scans were performed per sample, and carefully assessed for consistency. When present, outliers within the 10 frequency scans per sample were removed, and frequency scans were then averaged. All raw spectral data were then mean-centred and linked to the chemical analyses data in a spreadsheet. To correct for the non-linearity in the measure of transmittance, transmittance was transformed into absorbance by taking the base 10 logarithm of the reciprocal of the transmittance values. Different pre-processing filters were then applied to the raw spectra data, as described in the next subsection.

NIT pre-processing

Pre-processing filters were applied so as to reduce spectral noise and remove background effects of NIT data. It is known that variable spectral path length through the sample and chemical composition of the sample usually cause baseline shifting. Such multiplicative interference of scatter and particle size can be eliminated or minimised by applying smoothing techniques like Savitzky-Golay (SG), standard normal variate (SNV), Detrend (DT), multiplicative scatter correction (MSC), and other filters. SG smoothing (Savitzky and Golay, 1964) performs a piece-wise polynomial fitting with specified width and order to the spectrum. This smoothing method has been successfully adopted in chemometrics because it is able to reduce noise while keeping the meaningful variation that occurs at these wavelengths. SNV filter is designed to work on individual sample spectra. The transformation centers each spectrum and then scales it by its own standard deviation (Hadoux et al. 2014). The MSC is a transformation method used to compensate for additive and/or multiplicative effects in spectral data. It is a row-oriented transformation; thus, the contents of a cell are likely to be influenced by its horizontal neighbours. When one of the pre-processing steps used is the MSC, a separate model to calculate for MSC has to be derived from the data set (spectra) used during the calibration stage (Maleki et al. 2007). To minimise the effect of changes in the baseline, the raw spectra were firstly pre-processed using a combination of the above mathematical treatments: MSC, first and second derivatives using the Savitzky-Golay method (SG1, SG2), SNV and DT. In addition, combinations of filters with MSC were also tested: SG1+MSC, SG2+MSC, SNV+MSC and DT+MSC.

Statistical analysis

The extraction of information from quinoa grain's pre-processed spectra to estimate proten and fat contents was performed by Partial Least Squares (PLS) analysis. Separate PLS analyses were carried out with the measured fat and protein as dependent variables, and statistical inferences were computed using the jack-knife cross-validation method. For a specified number of PLS components, the cross-validation was set to randomly remove 10 samples at once (prediction set), and estimate the root mean square error of prediction (RMSEP) and the coefficient of determination (R^2) for the plot between the values predicted from the NIT model and the chemical analyses observations. For each of the nine pre-processing filters, RMSEP and R^2 statistics were obtained for a number of PLS components ranging from 10 to 20. Thus, the optimal numbers of Partial Least Squares (PLS) factors for fat and protein were assessed for every pre-processing filter. The entire NIT spectra analysis was conducted using the "pls" and the "prospectr" packages in R version 3.2.2 (R Development Core Team).

RESULTS AND DISCUSSION

Chemical analysis

Table 1 presents, in dry weight, the range, mean and standard deviation of the lipid and protein contents found using reference method. The standard deviation shows the variability of the quinoa grains samples from the accessions used, and also the degree of variability in fat and protein that are provided to the models. The values reported in this study for Peruvian quinoa were lower than those previously reported by Ferreira et al. (2015), who evaluated quinoa samples from Brazil, Peru and Bolivia with 6.19-15.52% lipid (db) and 11.40-36.10% protein (db). Gonzales-Martín et al. (2014) used quinoa samples cultivated in Chile, which presented higher protein content (16.0-20.2% db) and comparable fat content (4.4-7.5% db).

Table 1: Reference Chemical Data of Quinoa Samples (% dry basis)

Parameter	Min	Max	Mean±SD
Fat	5.67	7.56	6.59±0.42
Protein	8.33	11.38	9.88±0.77

SD=standard deviation.

NIT pre-processing

Applying the first and then the second derivative emphasized the peaks below and above the baseline, providing the best resolution for the expected signals (Fig. 1). SNV and MSC pretreatments corrected the multiplicative scattering effect and uneven particle size.

Nevertheless, while a pretreatment, such as a SG1, SG2, SNV or MSC is useful, the changes can usually be observed in the same regions in which the reconstructed signals from the particular coefficients wavelength show significant contributions. The main chemical constituents, especially those that contribute to these differences, are proteins, lipids and moisture, as pointed out by Cocchi et al. (2006) for durum wheat and wheat flour. Nonetheless, the best pre-processing filter cannot be determined by visualizing its resulting transformed spectral data, but by assessing its predictive capacity. The best filter or combination of filters will be the one that finally produces a robust model with the best predictive ability.

NIT Cross-Validation and Prediction for Fat and Protein

Table 2 and 3 compile the PLS prediction results of quinoa fat and protein, respectively. For fat, R^2 ranges from 0.588 to 0.815, while RMSEP ranges from 0.423 to 0.607%. For

protein, R^2 ranges from 0.681 to 0.897, while RMSEP ranges from 0.523 to 0.627%. For both protein and fat models, it was observed that as more PLS components were retained, higher R^2 were achieved (Tables 2 and 3). However, as the prediction ability of the model cannot be based on R^2 values, the RMSEP values were primarily evaluated. RMSEP was found to exhibit a different behaviour: in most cases RMSEP steadily decreased until attaining a minimum value (at an optimal number of PLS components), at which point they increased at a faster pace as more PLS components were retained. For instance, for fat content, the application of SG2 filter produced the lowest RMSEP between 8-18 PLS components (Fig. 2), while for protein, applying DT+MSC pre-processing rendered the lowest RMSEP values when only 10-16 components were retained (Fig. 3).

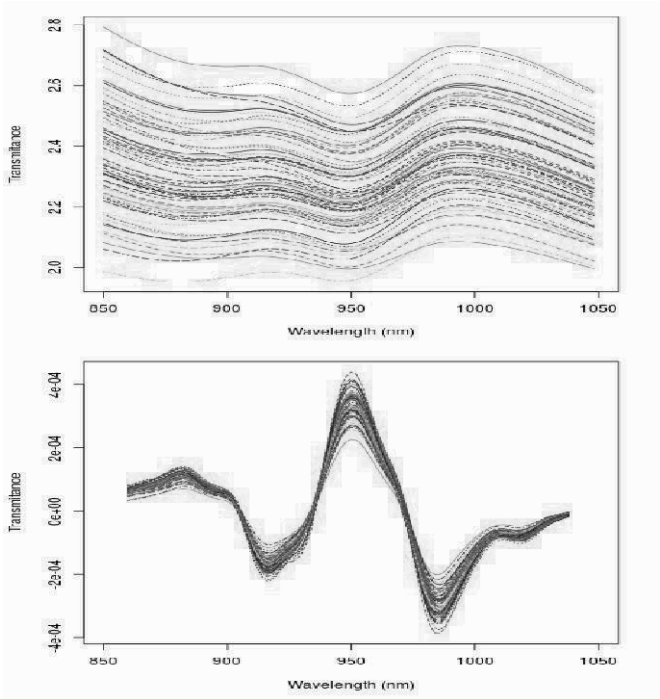

Figure 1: Untransformed- (top) and Savitzky-Golay Second Derivative Transformed- (bottom) Spectral Data From Quinoa Grains

Thus, plots of RMSEP versus extracted PLS number of components were evaluated for each of the nine filters in order to find an adequate range of PLS components. Subsequently, to find an optimal number of PLS components, RMSEP was kept to a minimum while R^2 was targeted to a reasonable value (R^2>0.70). Thus, in terms of model predictability for fat content, in general SG2, SNV and DT filters led to more accurate results than the other filters (Table 2). Specifically, extracting 18 PLS components from the SG2 pre-processed spectra (RMSEP=0.432; R^2=0.728) produced comparable results to extracting 16 PLS components from the SNV-processed spectra (RMSEP=0.438; R^2=0.754) and the DT-processed spectra (RMSEP=0.451; R^2=0.786). The DT+MSC filter however yielded the poorest prediction capacity among the filters shown in Table 2. Furthermore, MSC applied in combination with the other filters did not consistently enhance the prediction capacity of the models for fat determination.

Table 2: RMSEP adj (%) Statistic and R^2 (in Brackets) Obtained from Cross-Validation for Fat Quantification Using Individual and a Combination of Pre-Processing Filters: SG2 (Savitzky-Golay Second Derivative), SG2+MSC (Multiplicative Scattering Correction), SNV (Standard Normal Variate), DT (Detrend), DT+MSC, for 12 to 18 PLS Components (Best outcomes are shown in bold font)

Filter applied	Number of components			
	12	14	16	18
SG2	0.437 (0.588)	0.443 (0.641)	0.452 (0.703)	**0.432 (0.728)**
SG2 +MSC	0.429 (0.601)	0.444 (0.669)	0.472 (0.71)	0.496 (0.732)
SNV	0.449 (0.535)	0.437 (0.666)	**0.438 (0.754)**	0.460 (0.804)
DT	0.423 (0.635)	0.428 (0.722)	**0.451 (0.786)**	0.502 (0.828)
DT +MSC	0.505 (0.653)	0.542 (0.721)	0.592 (0.775)	0.607 (0.815)

Table 3: RMSEP adj (%) Statistic and R^2 (in brackets) Obtained from Cross-Validation for Protein Quantification Using Individual and a Combination of Pre-Processing Filters: SG1 (Savitzky-Golay First Derivative)+MSC (Multiplicative Scattering Correction), SG2 (Savitzky-Golay Second Derivative), SG2+MSC, DT (Detrend) and DT+MSC, for 10 to 16 PLS Components (Best outcomes are shown in bold font)

Filter applied	Number of components			
	10	12	14	16
SG1 +MSC	0.538 (0.695)	0.542 (0.716)	0.627 (0.754)	0.626 (0.813)
SG2	0.596 (0.693)	0.614 (0.757)	0.610 (0.777)	0.603 (0.796)
SG2 +MSC	0.523 (0.737)	0.556 (0.78)	0.606 (0.819)	**0.598 (0.859)**
DT	0.546 (0.695)	0.587 (0.7905)	**0.545 (0.833)**	0.619 (0.875)
DT +MSC	0.547 (0.681)	0.582 (0.816)	**0.597 (0.862)**	0.617 (0.897)

In the case of protein estimation, greater predictability of the models was generally achieved by the SG2 and DT filters (Table 3). Specifically, extracting 16 PLS components from the SG2+MSC pre-processed spectra produced statistics (RMSEP=0.598; R^2=0.859) that were comparable to the extraction of 14 components from the DT-processed spectra (RMSEP=0.545; R^2=0.833) and the DT+MSC-processed spectra (RMSEP=0.597; R^2=0.862). Unlike the models for fat estimations, the application of MSC in conjunction with other filters (SG2, DT) consistently enhanced the prediction capacity of the PLS models.

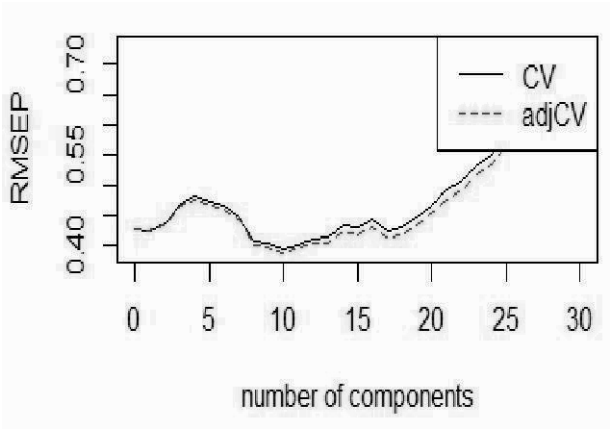

Figure 2: RMSEP Values as Affected by Number of PLS Components, Extracted from Spectra Pre-processed by Savitzky-Golay Second Derivative for Fat (CV: cross-validation estimated; adjCV: bias-corrected cross-validation estimated)

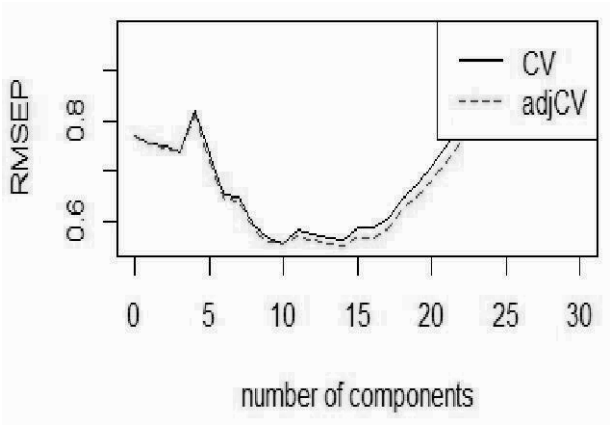

Figure 3: RMSEP Values as Affected by Number of PLS Components, Extracted from Spectra Pre-processed by Detrending and Multiplicative Scatter Correction for Protein (CV: cross-validation estimated; adjCV: bias-corrected cross-validation estimated)

It is noteworthy that although the R^2 values are overall higher for the protein estimation models (Table 3) than for the fat estimation models (Table 2), the PLS models estimating fat yielded overall greater accuracy, as indicated by their lower RMSEP values. Thus, the protein determination by NIT is subject to a slightly greater error than fat. The predictabilities of selected PLS models for fat and protein are shown in Figures 4 and 5, respectively. It can be seen that the degree of dispersion in both predictions is acceptable, considering that chemical analyses also have associated errors. For fat and protein estimation, it is inevitable that NIT errors are higher than those of the reference techniques, as the error of NIT technique contains both laboratory and NIT errors, although NIT procedures are often more repeatable than wet chemical methods.

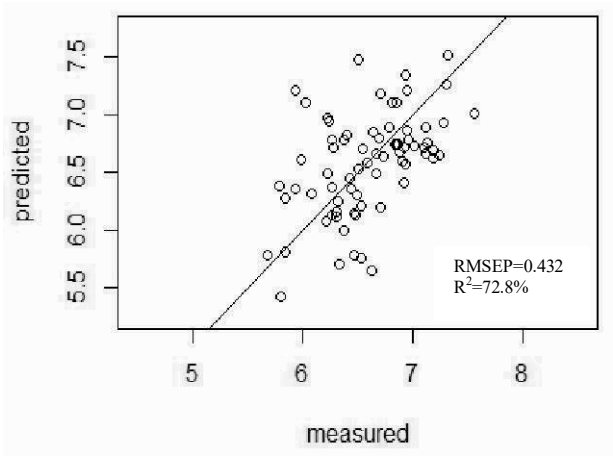

Figure 4: Measured vs Predicted Values for Fat Applying 18 Number of Components, Extracted From Spectra Pre-Processed by Savitzky-Golay Second Derivative

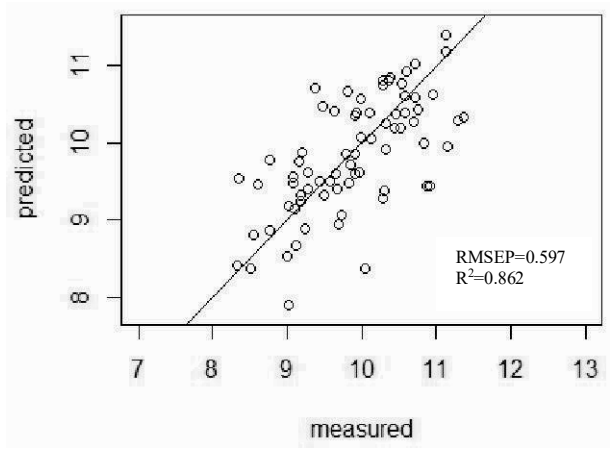

Figure 5: Measured vs Predicted Values for Protein Applying 14 Number of Components, Extracted from Spectra Pre-processed by Detrending and Multiplicative Scatter Correction

CONCLUSION

The NIT technique in conjunction with PLS modelling can be effectively used for predicting protein and fat of quinoa whole grains, although slightly better accuracy was obtained for fat content. A comparison of pre-processing filters through PLS cross-validation indicated that, in general, SNV, SG2 and DT are comparably good filters for fat estimation while DT and SG2 are better for protein estimation. Protein estimation can be enhanced by additionally applying MSC to the filtered signals. NIT technique with no waste generation, low cost, reduced time and no sample preparation can replace the laborious methods of analysis that are presently used for quantifying fat and protein of quinoa grains. In a future study, other filters will be evaluated in order to optimise RMSEP, R^2 and other statistics, for the estimation of fat, protein, moisture, ash and carbohydrates contents of quinoa grains and flour.

ACKNOWLEDGEMENT

Dr. Gonzales-Barron acknowledges the financial support provided by the Portuguese Foundation for Science and Technology (FCT) through the award of a 5-year Investigator Fellowship (IF) in the mode of Development Grants (IF/00570).

REFERENCES

AOAC. 2000. "Official methods of analysis of AOAC International". In W. Horwitz, & G. W. Latimer (Eds.), AOAC International (17th ed.) Gaithersbrug, Maryland.

Cocchi, M., C. Durante; G. Foca, A. Marchetti, L. Tassi and A. Ulrici. 2006. "Durum wheat adulteration detection by NIR spectroscopy multivariate calibration". *The International Journal of Pure and Applied Analytical Chemistry Talanta*, 68(5), 1505-1511.

Ferreira, D.S., J.A.L. Pallone and R.J. Poppi. 2015. "Direct analysis of the main chemical constituents in Chenopodium quinoa grain using Fourier transform near-infrared spectroscopy". *Food Control* (48), 91-95.

Gonzalez-Martın, M.I., G.W. Moncada, S. Fischer and O. Escuredo. 2014. "Chemical characteristics and mineral composition of quinoa by near-infrared spectroscopy"; *Journal of the Science of Food and Agriculture* 94, 876–881.

Hadoux X., N. Gorretta, J.M. Roger, R. Bendoula and G. Rabatel. 2014. "Comparison of the efficacy of spectral pre-treatments for wheat and weed discrimination in outdoor conditions". *Computers and Electronics in Agriculture* 108, 242-249.

Krishnan, A., L.J. Williams, A.R. McIntosh and H. Abdi. 2011. "Partial Least Squares (PLS) methods for neuroimaging: A tutorial and review". *NeuroImage* 56, 455–475

Maleki, M.R., A.M. Mouazen, H. Ramon and J. De Baerdemaeker. 2007. "Multiplicative Scatter Correction during On-line Measurement with Near Infrared Spectroscopy". *Biosystems Engineering* 96 (3), 427–433

Paulsen, M.R. and M. Singh. 2004. "Calibration of a Near-infrared Transmission Grain Analyser for Extractable Starchin Maize". *Biosystems Engineering* 89 (1), 79–83.

R Core Team. 2015. "R: A language and environment for statistical computing". R Foundation for Stastistical Computing, Vienna, Austria. URL http://www.R-project.org.

Savitzky, A. and M. Golay. 1964. "Smoothing and di_erentiation of data by simplied least squares procedures". *Analytical Chemistry* 36, 1627-1639.

Shenk, J.S., J.J.J. Workman and M.O. Westerhaus. 2007. "Application of NIR spectroscopy to agricultural products". In D. A. Burns, & Emil W. Ciurczak (Eds.), *Handbook of near-infrared analysis* (3rd ed.) (pp. 347-386). CRC Press.

BIOGRAPHIES

CHRISTIAN ENCINA-ZELADA, a Peruvian national, attended the National Agricultural University of La Molina (Lima, Peru), where he obtained his Bachelor degree and Food Industry Engineering title in 2003. Before obtaining his Master degree in Food Technology (2006), he started lecturing at the Food Technology Department of the UNALM since 2004. He is currently pursuing his PhD studies at the University of Minho, Portugal.

URSULA GONZALES-BARRON, a Peruvian-Irish national, graduated with first-class honours in the Faculty of Food Industries at the National Agricultural University La Molina, Peru (1999), and later on, she obtained her doctoral degree at the Biosystems Engineering Department of University College Dublin, Ireland (2006). Her expertise resides in diverse areas of food quality and safety, including mathematical modelling, predictive microbiology, risk assessment of pathogens, food traceability, shelf-life determination and sensory analysis. Dr. Gonzales-Barron has published over 52 peer-reviewed articles; and currently serves as Editor in the LWT – Food Science and Technology Journal.

VASCO CADAVEZ, a Portuguese national, obtained his first degree in Animal Science in 1993 at the Portuguese University of Trás-os-Montes e Alto Douro. After a novel research on carcass composition and quality using ultrasound, he obtained his PhD degree in 2004. He is currently a Professor at the Animal Science Department of the Polytechnic Institute of Braganza (IPB), Portugal. Dr. Cadavez is very knowledgeable in a wide range of mathematical and statistical modelling techniques applied agriculture, animal science, and food quality and safety.

Explorative MS-Fingerprinting to assess Novel Applications of Non-Thermal Plasma in Food Research

Jeroen Vandamme
Jim Van Durme
Department of Industrial Engineering sciences
KU Leuven
Gebroeders De Smetstraat, 1
9000, Ghent, Belgium
E-mail: jeroen.vandamme@kuleuven.be

KEYWORDS

Non-thermal plasma; lipid oxidation; GC-MS; MS-fingerprinting; SIMCA.

ABSTRACT

Several statistical tools such as Principal Component Analysis (PCA) and Soft Independent Modelling of Class Analogy (SIMCA) are often used in food research. In this study, the use of non-thermal plasma (NTP) as an accelerated lipid oxidation technique in food matrices was evaluated, using the abovementioned tools. First, a blend of vegetable oil was treated to evaluate the impact of NTP gas composition and treatment time. Secondly, oleic acid was used as food model matrix to undertake a profound parameter study and demonstrate the high steerability of NTP. Samples oxidized at room temperature for several months were used as reference. Results of the oil tests indicate significant differences in oxidized samples with different NTP conditions. The parameter study revealed highest correlation to oxidized samples at room temperature when Ar/O_2 (0.1%) NTP was used. Varying parameters such as oxygen concentration and treatment time indicate a good steerability of the NTP technique. Third, olive oil samples adulterated with cheap sunflower oil were detected through a unique pretreatment, using NTP. Adulterated olive oil samples could be identified through NTP pretreatment, even at the level of 1%.

INTRODUCTION

Statistical methods are important aids to detect trends, explore relationships and draw conclusions from experimental data (Granato et al. 2014). Several statistical tools such as Principal Component Analysis (PCA) and Soft Independent Modelling of Class Analogy (SIMCA) are often used in scientific research, including food research. For example, Barbaste et al. (2002) described the modelling of metal ion content in wine for denomination of origin of wines bottled in the Canary Islands. Classification studies in food research have been widely reported, among others for studies of cheese (De Sá Oliveira, et al. 2015), herbs (Yang et al. 2013), olive oil (Giacalone et al. 2015) and even medicine (Deconinck et al. 2012). In another study, detection and quantification of the adulteration of mincemeat with horse meat, fat beef trimmings, and textured soy protein was performed using SIMCA on infrared spectra data. From these studies it was clear that modelling techniques allow one not only to establish the characterization of different samples but also to establish the contribution of each variable to the model and its capacity to discriminate between one category and another. In this study, similar statistical tools are applied to explore the effectiveness and applications of a novel accelerated oxidation technique in food oil.

Oil and lipid oxidation is one of the most noticeable degradation processes in the food industry (Anbinder et al. 2015). This oxidative food deterioration negatively affects appearance, taste, odor and shelf life of food. Additionally, lipid oxidation degrades functional and nutritional compounds of food, damages essential fatty acids and produces oxidized polymers which could raise safety concerns (Wardhani et al. 2013). Lipid oxidation occurs through a well-known, however very complex mechanism that is referred as autoxidation (Erkan et al. 2009). During this autoxidation mechanism, hydroperoxides are formed as primary oxidation products. Degradation of these hydroperoxides leads to formation of a wide variety of low-molecular-weight compounds such as alkanes, alkenes, aldehydes, ketones, alcohols, esters, epoxides and carboxylic acids, each characterized by distinctive aromas (Gómez-Cortés et al. 2015). Numerous studies indicate the impact of oxidation in food products and its negative outcomes (Kerrihard et al. 2015; Vandamme et al., 2015; Huber et al. 2009; Estévez et al. 2007).

For food manufacturers it is of high importance to safeguard the initial nutritional and organoleptic characteristics during the shelf-life. Therefore, having more profound insights in the impact of oxidative variables and the determination of the oxidative stability is of great importance. Since lipid oxidation is a rather 'slow' process, accelerated oxidation tests are often applied. In practice, most of the accelerated oxidation techniques are based on increased temperatures, of which it is shown that they poorly correlate with realistic storage tests (Vandamme et al., 2015). For this reason, the development of innovative non-thermal accelerated oxidation techniques are required. In the recent study of Vandamme et al. (2015) and Van Durme et al. (2014) Non-Thermal Plasma (NTP) was already introduced as a highly innovative and challenging accelerated oxidation technique. Results from these promising studies show that NTP has great potential and could be steered towards a high correlation with the natural oxidation process.

In this work, the impact of some important plasma variables is explored on its lipid oxidation acceleration performance.

Experiments are done using a vegetable oil blend, pure oleic acid and olive oil respectively as matrices. NTP-treatments of the different matrices were evaluated by comparison with samples oxidized at room temperature. Results from these tests, more specific statistical data, were obtained by using MS-fingerprinting, combined with adapted software to execute PCA and SIMCA analyses.

MATERIALS AND METHODS

Lipid matrices oxidized by NTP treatment

First, a commercial blend of vegetable oil was used to evaluate natural oxidation, thermally accelerated oxidation and accelerated lipid oxidation through NTP. For natural aging (reference) this vegetable oil was stored at ambient conditions (dark, room temperature) for 5 years. To evaluate the performance of accelerated oxidation methods, a recent batch of the same fresh vegetable oil was used. One thermal accelerated oxidation test was performed by inserting ten mL of fresh vegetable oil in a 50 mL glass beaker, and heating to a constant temperature of 70 °C for 48 h using an autoclave (Hereaus instrument, function line B6). This temperature was chosen based on literature data (Martínez-Yusta et al. 2014). The heated oil was stirred using a twister stirbar with high velocity, in this way optimum transfer of atmospheric oxygen was guaranteed. NTP treatment was done for 20 minutes using either Ar/H_2O or Ar/O_2 plasma. Other specifications of the NTP treatments are described by Van Durme et al. (2014).

Secondly, pure oleic acid was used as a model matrix, in order to understand the underlying chemistry that is initiated by the NTP treatment. In this test, the steerability of NTP treatments towards the natural oxidation process was investigated (Vandamme et al., 2015).

Third, olive oil samples, either pure or adulterated with sunflower oil at different levels (1%, 2% and 3%) were submitted to an NTP treatment and compared to untreated samples (Van Durme et al., 2016).

Plasma reactor configuration

A dielectric barrier discharge (DBD) plasma source was used for Non-Thermal Plasma (NTP) treatments of oleic acid and olive oil samples. The plasma jet was operated with oxygen (Ar/O_2) gas mixture. The species generated in the active zone of the discharge located in between electrodes can be divided in (listed according to increasing reactivity): charged particles (electrons, positive and negative ions); neutral excited states of Ar (metastables, resonance states and electron excited states); UV and VUV photons (appearing due to excimer radiation, OH and NO bands emission); oxygenated species including O_3, O_2 singlet, and O. The production mechanisms of these different excited species have been intensively studied in the last decade worldwide (Knake et al. 2008; Sarani et al. 2010). Previous studies on the use of NTP (Ar/O_2) as an accelerated oxidation technique in food oils revealed that the effect of plasma treatment of liquid samples can be solely attributed to oxygenated species including mainly O_3, O_2 singlet, and atomic O in Ar/O_2 plasma. The plasma jet consists of a tungsten rod (energetic electrode) with a sharp tip, inserted in a quartz capillary with 1.3 mm inner diameter. The tungsten rod and quartz capillary together are centered inside a grounded aluminum tube (ground electrode). Alternating peak to peak voltage varying between 0 and 15 kV can be applied to the tungsten rod by a 50 kHz power supply (Bayerle, Germany). Gas is fed into the plasma jet through two separated lines each controlled by a mass flow controller (Bronckhorst, Belgium). A schematic setup can be found in Vandamme et al. (2015). A pure oxygen stream, controlled by mass-flow controller 1 (MF1) is mixed with the argon stream, controlled by MF2 and afterwards led through a 4m long tube to ensure sufficient mixing of both gases.

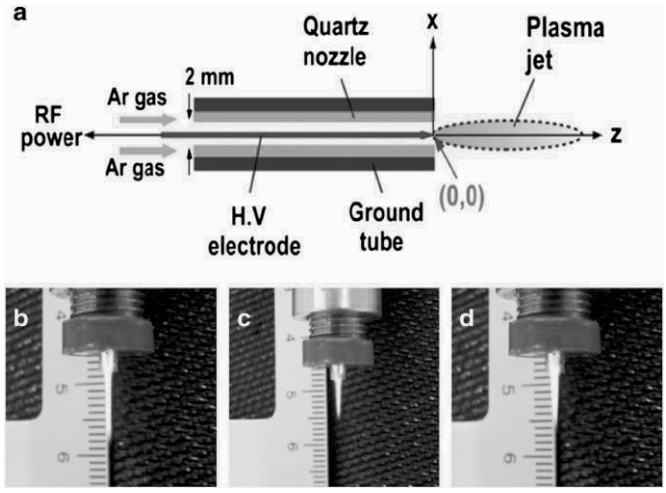

Figure 1: a) Schematic diagram of the RF plasma jet; b, c, d) high resolution digital camera (Panasonic Lumix FZ20) images of the RF discharge in Ar, 0.3% H_2O/Ar and 0.3% O_2/Ar mixtures, respectively.

Chemical analytical method

In this work, solely statistical results of the experiments are displayed and discussed. Other results, including identification and quantification of all secondary lipid oxidation volatiles, are described in the studies of Van Durme et al. (2014, 2015) and Vandamme et al. (2015).

During the MS-fingerprinting method, the GC temperature was held at 250 °C for 5 minutes, in order to avoid chromatographic separation of the analytes. Statistical processing on the obtained MS-Fingerprinting data was performed using 'Pirouette 3.11' software. Several multivariate statistical techniques such as Principal Compound analysis (PCA) and Hierarchical Cluster Analysis (HCA) were used to evaluate the treated samples.

RESULTS AND DISCUSSION

Vegetable oil blend – impact of gas composition and treatment time

In order to visualize to what degree the investigated accelerated oxidative techniques lead to the formation of relevant secondary products in close correlation with natural lipid oxidation, MS fingerprinting combined with multivariate statistics was applied. 3D-principal component analysis (PCA) score plot of the MS-fingerprinting data of the different

accelerated oxidation tests is presented in Fig. 2. The 3D-PCA-plot as presented in Fig. 2 explains 92.6% of the total variance. The first, second and third principal components each explain a variance of 71.8% (PC1), 12.4% (PC2) and 8.5% (PC3), respectively. Generally, the 3D-PCA-plot shows well clustered replicates for each type of oxidation experiment. As could be expected based on results of lipid oxidation volatiles (Van Durme et al., 2014), it can be seen that each type of treatment results in an oil sample that is clearly differentiated from one other. In Fig. 2 the fresh oil blend (V) is well differentiated form the naturally aged oil (O),which matches the findings discussed in the natural oxidized vegetable reference oil (Van Durme et al., 2014).

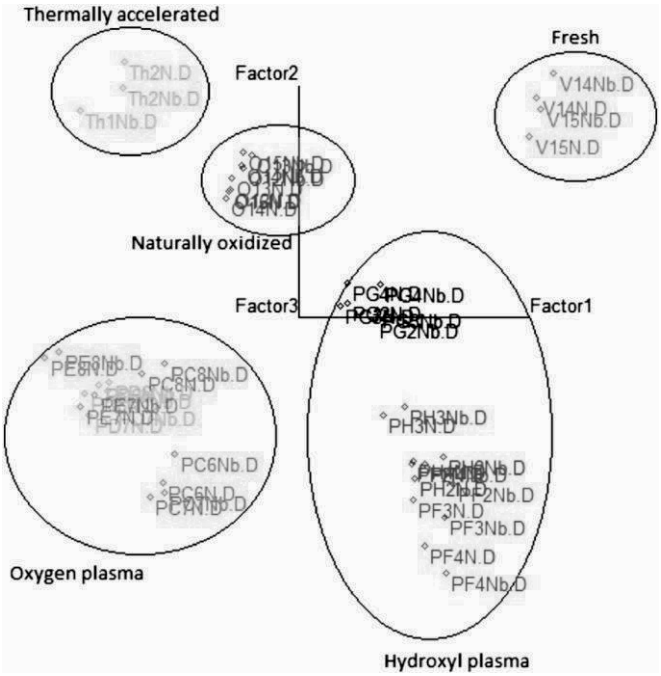

Figure 2: 3D-PCA plot of HS-SPME-MS-nose measurements on naturally aged (O), fresh (V), thermally induced (Th), oxygen plasma treated (PC — 10 min, PD — 15 min, PE — 20 min) and hydroxyl plasma treated (PF — 10min, PH — 15 min, PG — 20 min) vegetable oil (PC1: 71.8%, PC2: 12.4%, PC3: 8.5%).

From Fig. 2 it is observed that both the thermally accelerated, as well as the oxygen and hydroxyl exposed samples are classified separately. To evaluate which accelerated oxidation method correlates the best with the naturally aged oil, a statistical evaluation of the mass fingerprints by means of Soft Independent Modelling of Class Analogy (SIMCA) has been done (Table 1). In this approach, it is accepted that samples are significantly differentiated when interclass distances (IDs) are higher than 4. From Table 1, it can be concluded that interclass distances between the naturally aged oil and the other samples, are each time higher than 4. This is in agreement with the sensory results (Van Durme et al., 2014). Treating the oil during 20 min with the oxygen plasma, resulted in the largest interclass distance (27.1). This is in agreement with the described sensory evaluations for the oxygen plasma as being "extremely different from the reference" (Van Durme et al., 2014), and having a metallic off-flavor. Within the cluster of oxygen plasma experiments, relative low IDs ranging between 1.95 and 4.67 indicate that treatment time has no important effect on the type and concentration of volatile lipid oxidation products. Within the cluster of hydroxyl plasma experiments, all IDs obtained after 10, 15 and 20 minute treatment, proved to be typically higher than 4. It is noteworthy to mention that MS-fingerprinting techniques revealed that with prolonged hydroxyl plasma treatment, the volatile organic profile seems to change closer toward that of the naturally aged oil. These preliminary results indicate that Ar/H_2O NTP accelerated oxidation shows highest correlation with the natural oxidation mechanism. It should however be mentioned that in this study only gas composition and treatment time were varied. Since other important parameters such as voltage, oxygen and water concentration and surrounding atmosphere composition can be varied as well, more profound modelling studies are required to unravel the typical chemistry and interaction of this highly innovative and novel oxidation technique.

Oleic acid as model matrix

Since it was seen during the earlier discussed experiments on vegetable oil that plasma variables have a significant impact on the oxidation chemistry, a more profound parameter study was done, using a model matrix. Oleic acid was chosen to evaluate the impact of selected NTP parameters on the chemistry and effectiveness as an accelerated oxidation technique (Vandamme et al., 2015). Oleic acid (cis-9-octadecenoic acid) is a mono-unsaturated fatty acid that is present in many food products. From the parameter study performed by Vandamme et al. (2015) Argon NTP with 0.1% oxygen addition in argon atmosphere proved to have highest correlation with the oxidation mechanism at room temperature. This result is contrary to the statements made in the study of Van Durme et al. (2014). Presumably, since all experiments in the study of Van Durme et al. (2014) were performed in open air, all reactivity of the NTP was due to the presence of oxygen reactive species in the plasma, since oxygen from air can diffuse into the plasma jet. These findings

Table 1: Soft Independent Modelling of Class Analogy (SIMCA) between different oxidized vegetable oil samples**.**

Label	Description	n[a]	V	O	Th	PC	PD	PE	PF	PG	PH
V	Fresh vegetable oil	4	0	5.81	5.72	15.91	12.14	19.61	11.84	20.01	13.55
O	Naturally aged oil (>5 years)	8	5.81	0	7.42	19.97	14.95	27.16	16.48	23.40	14.87
Th	Thermally accelerated oxidation	3	5.72	7.42	0	18.80	15.61	23.59	15.33	24.54	12.90
PC	Oxygen plasma – 10 minute treatment	6	15.91	19.97	18.80	0	4.67	1.95	14.20	10.99	18.28
PD	Oxygen plasma – 15 minute treatment	6	12.14	14.95	15.61	4.67	0	4.32	8.55	9.24	13.58
PE	Oxygen plasma – 20 minute treatment	6	19.61	27.16	23.59	1.95	4.32	0	16.34	11.09	20.16
PF	Hydroxyl plasma – 10 minute treatment	6	11.84	16.48	15.33	14.20	8.55	16.34	0	16.76	10.64
PG	Hydroxyl plasma – 15 minute treatment	6	20.01	23.40	24.55	10.99	9.24	11.09	16.76	0	21.61
PH	Hydroxyl plasma – 20 minute treatment	6	13.55	14.87	12.90	18.28	13.58	20.16	10.64	21.61	0

Underlined values are lower than 4.
[a] Number of replicate MS-nose analyses for each vegetable oil sample.

were also supported by literature, which indicates the importance of (highly reactive) singlet oxygen in the lipid oxidation mechanism. 25 g of oleic acid was treated for 100 minutes, while measuring samples after 30, 60 and 100 minutes treatment. This treatment was performed in Argon doped with respectively 0.3 % O_2, 0.2 % O_2 and 0.1 % O_2. Distance between nozzle and sample was maintained at 5 mm. All samples were measured with MS-Fingerprinting and evaluated using SIMCA, and are shown in figure 3.

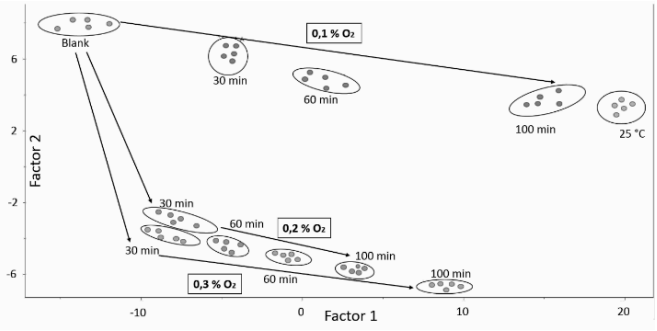

Figure 3: Soft Independent Modelling for Compound Analysis (SIMCA) for evaluation of the steerability of non-thermal plasma.

From figure 3 it can be derived that decreasing the oxygen concentration leads to a higher correlation with the naturally aged sample, especially after 100 minutes of treatment. From the Pirouette software it was calculated that Factor 1 (x-axis) explained 68.9 % of the total variance and Factor 2 explained 19.9 % of the total variance, meaning this plot explains over 88.8% of all variance. In this way, SIMCA is a very useful tool for the evaluation of the representativeness of the NTP treatments. Though the experiment with 100 minutes of Ar/O_2 (0.1%) is very close to the naturally aged oil sample, it should be pointed out that the relative concentrations of all oxidation compounds are still significantly different. Nonanal is still the main marker, followed by the other oxidation compounds which are less formed during the NTP treatment in comparison to the naturally aged sample (Vandamme et al., 2015).

Adulterated olive oil

Profiling of the headspace composition is an often applied approach to objectively assess product quality of food products. However despite the technological advances and low detection limits that can be achieved, the detection of adulteration in oil matrices cannot be achieved using state-of-the-art headspace analysis. In this work headspaces of untreated and NTP-treated oil samples were analyzed using MS-fingerprinting followed by a multivariate data processing. The headspaces were sampled by Solid-Phase MicroExtraction (SPME) using a CAR-PDMS fiber. As could be expected Figure 4 illustrates that authentic EVOO and up to 3% Sunflower Oil (SFO) adulterated EVOO samples cannot be classified from each other based on MS-fingerprinting data.

Next, samples of pure olive oil, 99% EVOO/1% SFO, 98% EVOO/2% SFO and 97% EVOO/3% SFO were each exposed to an identical NTP treatment. Based on previous works it was

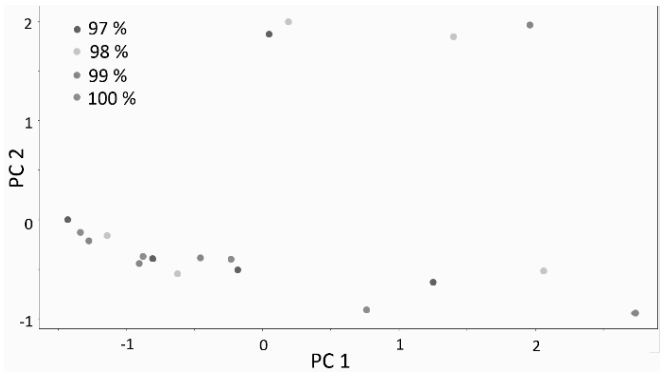

Figure 4: 2D-Principal component analysis (PCA) biplot of the HS-SPME-MS-fingerprint data (n = 5) on both authentic EVOO samples (100%) as EVOO samples increasingly adulterated with sunflower oil (99%, 98%, 97%) without sample pretreatment.

chosen to apply an O_2-doped (0.1 %) Ar-plasma (Vandamme et al., 2015; Van Durme et al., 2014). It was proven that such plasma configuration generates high concentrations of both atomic as singlet oxygen which are both highly oxidative species. Exposure of adulterated oil samples to these reactive species, might induces specific oxidation pathways which are adequately different than those induced in authentic EVOO. In order to verify this assumption, an identical MS-fingerprinting approach as discussed earlier was done for oil samples after these have been exposed to the NTP. Figure 5 illustrates that different clusters were measured, meaning that adulterated samples could be classified from authentic EVOO. The 2D-PCA-plot for NTP treated oil samples explains 97.53% (PC1: 93.01%, PC2: 4.52%) of the total variance. From Figure 5 it can be clearly seen that the 2D-PCA-plot shows well clustered replicates for each olive oil sample illustrating the reproducibility of the HS-SPME-MS-fingerprinting method. Importantly, it can be seen that a NTP pretreatment on the olive oil samples confirmed the formation of an unique headspace composition that can be used to differentiate samples. Interestingly, adulterated olive oil samples score positive on the first principal component, while pure EVOO scored negatively. Additionally, a trend can also be seen in relation to the degree of adulteration. Increasingly positive values for the second principal component are measured with increasing degree of SFO adulteration.

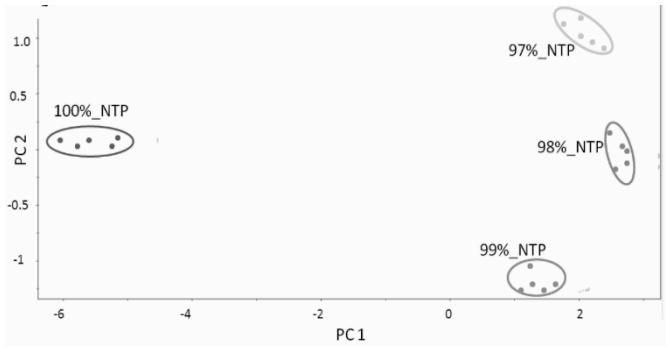

Figure 5: 2D-Principal component analysis (PCA) biplot of the HS-SPME-MS-fingerprint data (n = 5) on both authentic EVOO samples (100%) as EVOO samples increasingly adulterated with sunflower oil (99%, 98%, 97%) after sample pretreatment with NTP.

To confirm separate classification of NTP-pretreated adulterated olive oil samples, a statistical evaluation of the mass fingerprints by means of SIMCA has been done (Van Durme et al., 2016). Results confirmed the fact that no significant classification could be created between the untreated oil samples, since interclass distances were lower than 4 at all times. From the results it can be concluded that interclass distances between the extra virgin olive oil and the other samples, submitted to the NTP treatment, are mostly higher than 4. Interclass distances between 100% pure EVOO are in all cases higher than 19.5, confirming that even a 1% SFO addition results in significant changes of headspace composition enabling to detect a deviation from the pure olive oil. To the best of our knowledge, a detection limit of 1% SFO adulteration has never been achieved using headspace techniques. Next, it is clear from the relatively large interclass distances, that a NTP pretreatment will enable to detect SFO adulteration at even lower levels.

CONCLUSIONS

Results of the statistical tools used in this work show promising aspects of NTP to be used as an accelerated lipid oxidation technique in food oils. In all three cases, PCA and SIMCA analysis enabled a qualitative evaluation of different methods and comparison between different samples. However, the discussed results show the current NTP technology is not capable to mimic natural oxidation perfectly, due to the presence of several influencing variables each interacting with each other. In future research, well-thought Designs-of-experiments combined with appropriate modeling techniques are required in order to obtain clear insights in the underlying processes which are initiated by the NTP.

REFERENCES

Anbinder, P. S., Peruzzo, P. J., Martino, M. N., & Amalvy, J. I. (2015). Effect of antioxidant active films on the oxidation of soybean oil monitored by Fourier transform infrared spectroscopy. *Journal of Food Engineering*, *151*, 43–50.

Barbaste, M., Medina, B., Sarabia, L., Ortiz, M. ., & Pérez-Trujillo, J. . (2002). Analysis and comparison of SIMCA models for denominations of origin of wines from de Canary Islands (Spain) builds by means of their trace and ultratrace metals content. *Analytica Chimica Acta*, *472*(1-2), 161–174.

De Sá Oliveira, K., de Souza Callegaro, L., Stephani, R., Almeida, M. R., & de Oliveira, L. F. C. (2015). Analysis of Spreadable Cheese by Raman Spectroscopy and Chemometric Tools. *Food Chemistry*, *194*, 441–446.

Deconinck, E., Sacré, P. Y., Coomans, D., & De Beer, J. (2012). Classification trees based on infrared spectroscopic data to discriminate between genuine and counterfeit medicines. *Journal of Pharmaceutical and Biomedical Analysis*, *57*(1), 68–75.

Erkan, N., Ayranci, G., & Ayranci, E. (2009). A kinetic study of oxidation development in sunflower oil under microwave heating: Effect of natural antioxidants. *Food Research International*, *42*(8), 1171–1177.

Estévez, M., Ramírez, R., Ventanas, S., & Cava, R. (2007). Sage and rosemary essential oils versus BHT for the inhibition of lipid oxidative reactions in liver pâté. *LWT - Food Science and Technology*, *40*(1), 58–65.

Giacalone, R., Giuliano, S., Gulotta, E., Monfreda, M., & Presti, G. (2015). Origin assessment of {EV} olive oils by esterified sterols analysis. *Food Chemistry*, *188*, 279–285.

Gómez-Cortés, P., Sacks, G. L., & Brenna, J. T. (2015). Quantitative analysis of volatiles in edible oils following accelerated oxidation using broad spectrum isotope standards. *Food Chemistry*, *174*, 310–318.

Granato, D., de Araújo Calado, V. M., & Jarvis, B. (2014). Observations on the use of statistical methods in Food Science and Technology. *Food Research International*, *55*, 137–149.

Huber, G. M., Vasantha Rupasinghe, H. P., & Shahidi, F. (2009). Inhibition of oxidation of omega-3 polyunsaturated fatty acids and fish oil by quercetin glycosides. *Food Chemistry*, *117*(2), 290–295.

Kerrihard, A. L., Pegg, R. B., Sarkar, A., & Craft, B. D. (2015). Update on the methods for monitoring UFA oxidation in food products. *European Journal of Lipid Science and Technology*, *117*(1), 1–14.

Knake, N., Reuter, S., Niemi, K., der Gathen, V. S., & Winter, J. (2008). Absolute atomic oxygen density distributions in the effluent of a microscale atmospheric pressure plasma jet. *Journal of Physics D: Applied Physics*, *41*(19), 194006.

Martínez-Yusta, A., Goicoechea, E., & Guillén, M. D. (2014). A Review of Thermo-Oxidative Degradation of Food Lipids Studied by ^{1}H NMR Spectroscopy: Influence of Degradative Conditions and Food Lipid Nature. *Comprehensive Reviews in Food Science and Food Safety*, *13*(5), 838–859.

Sarani, A., Nikiforov, A. Y., & Leys, C. (2010). Atmospheric pressure plasma jet in Ar and Ar/H2O mixtures: Optical emission spectroscopy and temperature measurements. *Physics of Plasmas*, *17*(6), 063504.

Van Durme, J., Nikiforov, A., Vandamme, J., Leys, C., & De Winne, A. (2014). Accelerated lipid oxidation using non-thermal plasma technology: Evaluation of volatile compounds. *Food Research International*, *62*, 868–876.

Vandamme, J., Nikiforov, A., Dujardin, K., Leys, C., De Cooman, L., & Van Durme, J. (2015). Critical evaluation of non-thermal plasma as an innovative accelerated lipid oxidation technique in fish oil. *Food Research International*, *72*, 115–125.

Wardhani, D. H., Fuciños, P., Vázquez, J. A., & Pandiella, S. S. (2013). Inhibition kinetics of lipid oxidation of model foods by using antioxidant extract of fermented soybeans. *Food Chemistry*, *139*(1-4), 837–844.

Yang, I.-C., Tsai, C.-Y., Hsieh, K.-W., Yang, C.-W., Ouyang, F., Martin Lo, Y., & Chen, S. (2013). Integration of SIMCA and near-infrared spectroscopy for rapid and precise identification of herbal medicines. *Journal of Food and Drug Analysis*, *21*(3), 268–278.

AUTHOR BIOGRAPHIES

JEROEN VANDAMME is a fulltime PhD researcher at the research unit of Molecular Odor Chemistry, Department of Industrial Engineering Sciences, Technology Campus Ghent, KU Leuven, Belgium. Mr. Vandamme earned his master degree in industrial engineering sciences, option chemistry, at the before mentioned institute. He has published journal and conference papers and aims to obtain his doctoral degree in 2017. (jeroen.vandamme@kuleuven.be)

JIM VAN DURME is currently head of the research unit of Molecular Odor Chemistry, Department of Industrial Engineering Sciences, Technology Campus Ghent, KU Leuven, Belgium. Mr. Van Durme obtained his master degree in biological engineering. In 2008 he obtained his PhD at the university of Ghent, which included the application of non-thermal plasma technology for indoor air abatement. After a few years of gaining experience in the industry (Olfascan, Belgium), Dr. Van Durme started to lead the research unit of Molecular Odor chemistry in 2012. The research unit for Molecular Odor Chemistry is active in the domain of chemical-analytical and sensory research of food, as well as industrial products and processes. The main research mission of this laboratory is gaining insights in the chemical background of volatile fractions (scent, aroma) of food, non-food (packaging, material emissions) and processes (environmental aspects). Dr. Van Durme has published numerous journal and conference papers, which have gained a lot of interest at international level. (jim.vandurme@kuleuven.be)

PREDICTIVE FOOD MICROBIOLOGY

DEVELOPMENT OF VACUUM-PACKED MEAT-BASED MODEL SYSTEMS FOR THE EVALUATION OF THE FOOD INTRINSIC COMPLEXITY ON *LISTERIA MONOCYTOGENES* GROWTH AT REFRIGERATION AND ABUSE TEMPERATURES

Maria Baka, Estefanía Noriega, Kristof Van Langendonck, Jan F.M. Van Impe*
KU Leuven, Department of Chemical Engineering,
BioTeC - Chemical and Biochemical Process Technology and Control,
OPTEC - Optimization in Engineering Center-of-Excellence,
CPMF2 - Flemish Cluster Predictive Microbiology in Foods,
Gebroeders De Smetstraat 1, B-9000 Gent, Belgium
*E-mail address: Jan.VanImpe@cit.kuleuven.be

KEYWORDS

Listeria monocytogenes, food intrinsic factors, model systems, meat products, vacuum

ABSTRACT

Food intrinsic complexity ((micro)structure, composition and physicochemical characteristics) influences microbial growth. In this study, food (model) systems with variable (micro)structural complexity, compositional and physicochemical characteristics were developed. The model systems targeted the following (micro)structures: liquids, aqueous gels, emulsions, gelled emulsions, and canned meat, which is a food product, classified as a gelled emulsion. The growth dynamics of *Listeria monocytogenes* were studied at 4, 8 and 12°C in/on the developed model systems, which covered the whole spectrum of food (micro)structure. The composition and physicochemical characteristics of canned meat and gelled emulsions targeted Frankfurter sausages. Results indicated that *L. monocytogenes* grows faster on canned meat, indicating that microbial growth is possibly underestimated in/on model systems than real foods.

INTRODUCTION

Predictive microbiology describes microbial dynamics as a function of environmental factors, by means of mathematical models. So far, predictive models have been developed on the basis of experimental data collected either in liquid microbiological media or in/on real food products at various environmental conditions. Foods are not always liquid, but frequently possess a more complex (micro)structure, which is not considered in the models based on liquid microbiological media. Therefore, these models describe adequately microbial growth in liquid food products, but not necessarily in/on real, or more complex, food systems. Additionally, other food intrinsic factors, e.g., compositional and some physicochemical characteristics are not taken into account when working with liquid microbiological media. On the other hand, in challenge testing, the growth of target microorganisms is directly monitored in/on real food products, where the influence of food (micro)structure, compositional and physicochemical characteristics is intrinsically present, but it is expensive and time-consuming (Wareing & Komitopoulou, 2013).

In this study, the effect of food (micro)structure will be assessed, by means of model systems exhibiting variable (micro)structures. As a consequence of the food (micro)structure variability, compositional and physicochemical variations will occur. *L. monocytogenes* was selected as a target microorganism, as it is a foodborne pathogen with high fatality rate (15.6%) (EFSA and ECDC, 2015) and able to survive under harsh conditions. It is often related to cases of listeriosis in fish, ready-to-eat (RTE) and dairy products (EFSA and ECDC, 2015). Frankfurter sausages are RTE meat products, which were among the categories with the highest levels of non-compliance to the regulations (2.5 %) at the processing level in 2013, with respect to the presence of *L. monocytogenes* (EFSA and ECDC, 2015). Frankfurter sausages represent a complex (micro)structure of gelled emulsion systems and were selected as the target food products. The growth dynamics of *L. monocytogenes* will be studied in/on four model systems (liquids, aqueous gels, emulsions, gelled emulsions) and on a food product (canned meat), similar in composition to Frankfurter sausages, at refrigeration (4˚C) and suboptimal temperatures (8 and 12˚C) and under vacuum.

MATERIALS AND METHODS

Model systems preparation

The percentage of the ingredients used for the development of the model systems and the canned meat are provided in Table 1. For the preparation of the model systems, two aqueous solutions were produced. The 'solution 1', based on the heat-resistant components included NaCl, $NaNO_2$, pentasodium triphosphate, emulsifier, starch and agar, which were diluted in water and autoclaved. NaCl, $NaNO_2$ and pentasodium triphosphate, which are easily dissolved in water, were first added and stirred in cold water until they were dissolved. Then, the starch was added and stirred, while the temperature increased until it reached 80°C.

Table 1: Percentage of ingredients of the model systems

Ingredients (% w/w)	Liq.	Aq. Gel	Emul.	Gelled Emul.	Can. Meat
Water	84.9	84.4	65.9	65.4	65.4
Protein	12	12	12	12	12*
Fat	0	0	18	18	18
Starch	1	1	1	1	1
Agar	0.0	0.5	0.0	0.5	0.5
Emulsifier	0	0	1	1	1
Sodium Chloride	2	2	2	2	2
Sodium Nitrite	0.0011	0.0011	0.0011	0.0011	0.0011
Ascorbic acid	0.0056	0.0056	0.0056	0.0056	0.0056
Pentasodium Triphosphate	0.1	0.1	0.1	0.1	0.1

Further on, for the emulsion and gelled emulsion systems, the emulsifier was added and stirred, until it became

homogeneous, keeping the temperature constant at 80°C. Afterwards, the agar was added and stirred, until homogenisation at the same temperature (for the aqueous gel and gelled emulsion systems). The amount of water was
25.9, 25.4, 24.9 and 30.4 g for liquids, aqueous gels, emulsions and gelled emulsions, respectively. The 'solution 2' included the heat-sensitive compounds, protein and ascorbic acid, which were diluted in water and filter sterilised, by using a 0.22 µm filter (Filtertop, TPP, Switzerland). The amount of water was 59, 59, 41 and 35 g for liquids, aqueous gels, emulsions and gelled emulsions, respectively. Solutions 1 and 2 were mixed with a magnetic stirrer ('solution 3'), while the 'solution 1' was at 80°C. In the emulsions and gelled emulsions pork fat was also added. This was melted at 80°C in a water bath (GR150 S12; Grant, Shepreth, U.K.) and left at this temperature for 2 h to eliminate the background microflora and remain liquid. Fat was added to the 'solution 3' slowly, while being at a liquid state and homogenised with a homogenisation probe (S 18 N -19 G, IKA, Belgium) attached to the homogeniser (Ultra-Turrax, IKA, Belgium) at 24000 rpm for 6 min (3x2min). Breaks were made every 2 min in order to avoid overheating of the sample and the disperser. Aqueous gels and gelled emulsions were dispersed in sterile petri dishes (Ø 50mm, height 8mm, SIMPD210-14, VWR, Belgium) (7 mL/petri dish). The canned meat was produced in a laboratory-scale production line of meat products of KU Leuven Technology Campus of Ghent, Belgium. The composition was based on the chemical analysis of Frankfurter sausages, which has previously been characterised (Baka et al., 2015). Then, it was packaged in cans and autoclaved. The canned meat was sliced with thickness of < 4mm and then moulded by the round shape and size of small petri dishes.

(Pre)culture conditions and microbiological analysis

L. monocytogenes LMG 23775 strain was acquired from the BCCM/LMG bacteria collection of Ghent University in Belgium. A stock culture was stored at -80°C in Brain Heart Infusion broth (BHI, Oxoid, U.K.) supplemented with 25% (v/v) glycerol (Acros Organics, Belgium). For the inoculum preparation, a loopful of the stock culture was inoculated into a 100 mL Erlenmeyer flask containing 20 mL BHI, which was incubated in a temperature-controlled incubator at 30°C (Binder KB-series incubator; Binder Inc., NY, USA). After 22 h, 20 µL were transferred into 20 mL fresh BHI and again incubated at 30°C for 22 h. A target inoculum level of 10^2 CFU/g of *L. monocytogenes* cells was set for the model systems and the canned meat. Liquid and emulsion model systems were inoculated and mixed adequately until they become homogeneous. Then, 5 mL of the systems were transferred into vacuum bags of polyethylene/polyamine (PE/PA), vacuumed packed (Boxer 42, Henkelman, Netherlands) and incubated at 4, 8 and 12°C. Aqueous gels, gelled emulsions and canned meat were inoculated with the cell aliquot, which was homogeneously spread throughout the whole surface of each model system. Then, the Petri dishes were vacuum packaged separately, in vacuum bags and incubated at 4, 8 and 12°C. Evolution of *L. monocytogenes* concentration over time in the different model systems was monitored by viable plate counting. For liquid and emulsion systems, the corresponding serial decimal dilutions were directly prepared from an aliquot of the samples and plated with a Spiral Plate System (Eddy Jet IUL Instruments, Belgium) on BHI supplemented with agar (1.4% (w/v); Agar Technical No3, Oxoid, U.K.). For aqueous gels, gelled emulsions and canned meat, prior to making serial decimal dilutions and sample plating, the content of a Petri-dish and a standard volume of peptone water (10 g/L bacteriological peptone (Oxoid, U.K.) and 5 g/L NaCl (AnalaR, Normapur®, VWR, Belgium)) were aseptically transferred in a stomacher bag, and homogenised for 2 min (basic masticator, Led techno, Belgium). Plates were incubated at 30°C for 48 h before enumeration. Every experiment was independently performed in duplicate.

Modelling growth dynamics and parameter estimation

The model of Baranyi and Roberts (1994) is represented by Equations 1, 2 and 3 and was fitted to the experimental data.

$$\frac{dN}{dt} = lnN - lnN_0 = \left(\frac{Q}{1+Q}\right)\mu_{max}\left(1-\frac{N}{N_{max}}\right)N \quad (1)$$

$$\frac{dQ}{dt} = \mu_{max} \cdot Q \quad (2)$$

$$\lambda \cdot \mu_{max} = ln\left(1+\frac{1}{Q(0)}\right) \quad (3)$$

Growth parameters were estimated, i.e., N [CFU/g], the cell density at time t; N_0 [CFU/g], the initial cell density at time 0; N_{max} [CFU/g], the maximum cell density; μ_{max} [1/h], the maximum specific growth rate; Q [-], the physiological state of the cells; Q(0), a measure of the initial physiological state of the cells; and λ [h], the lag time of the cells.

RESULTS AND DISCUSSION

The physicochemical characteristics, i.e., pH and a_w, and their standard deviation of the model systems are provided in Table 2.

Table 2: Physicochemical characteristics (pH and a_w) and their standard deviation (SD) of the model systems.

Systems	pH ± SD(pH)	a_w ± SD(a_w)
Liquid	6.07 ± 0.05	0.9714 ± 0.0016
Aqueous gel	5.91 ± 0.30	0.9561 ± 0.0044
Emulsion	5.88 ± 0.03	0.9511 ± 0.0012
Gelled emulsion	5.69 ± 0.01	0.9460 ± 0.0030
Canned meat	5.58 ± 0.03	0.9770 ± 0.0040

In Figure 1, results illustrate the estimated growth parameters of *L. monocytogenes* in/on the different model systems at the three different storage temperatures. The influence of temperature on growth parameters is evident for all model systems. In this figure, it can be easily seen that *L. monocytogenes* grows faster (higher μ_{max}) at higher temperature, as already reported in literature (Ratkowsky et al., 1982). It is noteworthy that the range of temperature

considered in this study is very narrow and belongs to the suboptimal temperature for growth of *L. monocytogenes*. Nevertheless, the key results of this study are the growth dynamics of *L. monocytogenes* in/on the different model systems and canned meat, which is the scope of this paper. The growth parameters of *L. monocytogenes* are being compared and discussed.

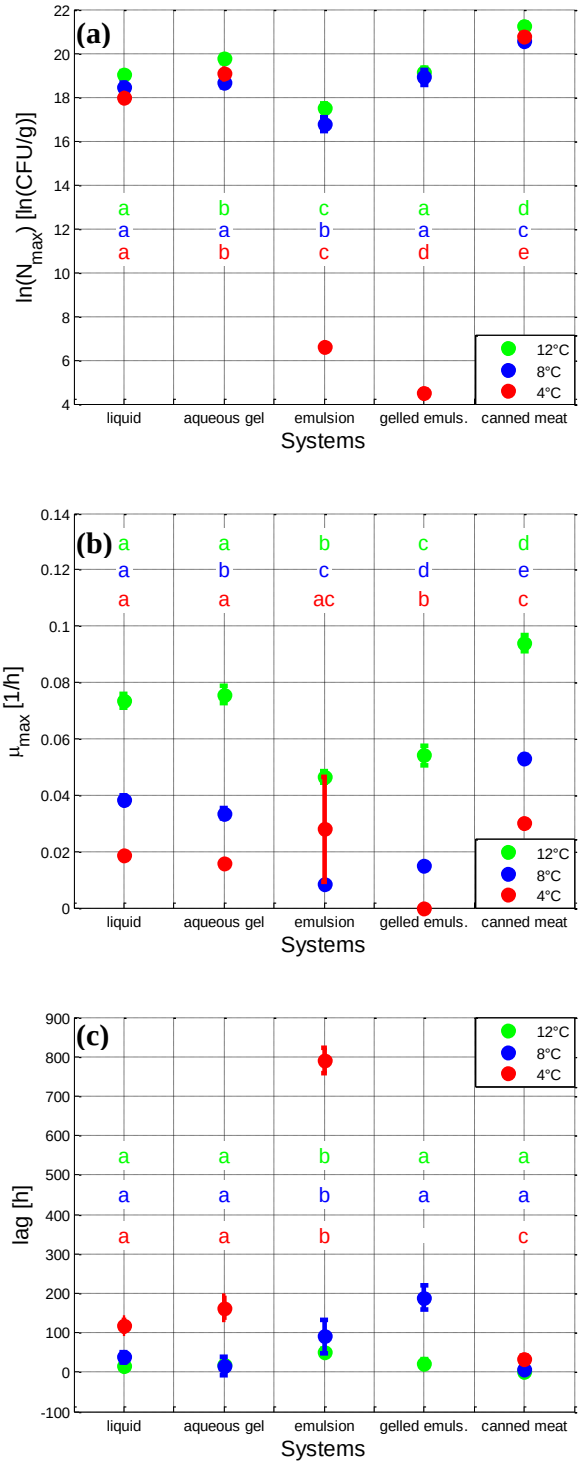

Figure 1: Growth parameters of *L. monocytogenes* (a) ln (N_{max}), (b) μ_{max} and (c) lag, and their standard error (error bars) for the different model systems at 4 (●), 8 (●) and 12°C (●). For each growth parameter (graphs a, b, c) and temperature (different colours), values bearing different characters (a, b, c, d, e) are significantly different ($P \leq 0.05$).

L. monocytogenes growth in liquids versus aqueous gels

Differences in water activity are observed in Table 2 between liquids and aqueous gels. Differences are justified by the addition of agar on the aqueous gel, which binds water and replaces an amount of it; therefore, the water activity of aqueous gel is lower than in liquid systems. This variance in water activity could favour the growth of *L. monocytogenes* in liquid systems, where a_w was higher. Nevertheless, *L. monocytogenes* exhibited very similar growth dynamics in/on both systems (Figure 1), indicating that this level of variance in water activity does not affect *L. monocytogenes* growth.

Figure 1 illustrates that N_{max} in liquid systems was lower than on aqueous gels at all temperatures, which is in accordance to what has been found by other studies (Robins and Wilson, 1994; Smet et al., 2015). In early stationary phase, bacteria influence their own environment, with their metabolites production, which inhibits growth (Robins and Wilson, 1994). In liquid systems, the transportation of these compounds is faster through convection than diffusion, which occurs on solid-like systems. Therefore, growth in liquids gets faster inhibited, due to the metabolites production, than on solid surfaces.

The μ_{max} estimates are higher in liquid systems at 4 and 8°C, but at 12°C the opposite occurs, as it can be observed in Figure 1. This observation indicates that stressing temperature favours planktonic microbial growth, although at more optimal temperature levels microbial growth on solid surfaces is more favourable, as also reported in (Smet et al., 2015). It has been reported that μ_{max} in liquid systems is higher than μ_{max} on solid surfaces (Brocklehurst et al., 1997; Meldrum et al., 2003; Theys et al., 2008). Significant differences at μ_{max} values between these two systems were induced when liquid systems were continuously shaken during incubation (Smet et al., 2015). When liquid cultures are shaken, nutrients, metabolites and oxygen are homogeneously transported and cell sedimentation is avoided, which also influences the distribution of the previously mentioned compounds (Smet et al., 2015). Therefore, when liquid systems are incubated without shaking exhibit negligible differences in μ_{max} values or even lower than μ_{max} values on solid surfaces. In this study, all model systems were vacuum packed; therefore, oxygen is not a variable in none of the model systems and has no influence on the results.

Figure 1 illustrates that lag phase of *L. monocytogenes* was longer, without statistically significant differences, in liquid systems at 8 and 12°C; however, at 4°C it is shorter, also without statistically significant differences. This is another indication of the effect of the storage temperature on the growth dynamics when compared within different (micro)structures. Likewise to the μ_{max}, stressing temperature favours microbial growth more in liquids (shorter lag) than on surface of aqueous gels. Nevertheless, no significant variation is usually observed between lag phase duration of cells growing in liquids or on solid surfaces, in literature (Boons et al., 2013; Smet et al., 2015). Exceptionally, lag duration of cells growing on a gel surface was found longer than in planktonic growth at

25°C (Knudsen et al., 2012). Variation in composition among the used model systems in other studies and in this study could be the key for the existence or not of differences at the lag phase between planktonic and surface growth.

L. monocytogenes growth in emulsions versus gelled emulsions

Differences in growth dynamics in these two model systems are pronounced. Growth in emulsion systems with fat concentration lower than 83% is considered planktonic (Brocklehurst & Wilson, 2000). Therefore, as in the previous section, planktonic growth is compared with surface growth. These two model systems differ from the previous two in the presence of fat and emulsifiers. The addition of fat increases the complexity in (micro)structure, as fat droplets are dispersed in the continuous water phase for emulsions and the continuous gellified water phase for gelled emulsion. It has been reported that cells grow in the aqueous phase (Wilson et al., 2002); therefore, the addition of fat decreases the amount of water available for the cells to grow. The N_{max} values of *L. monocytogenes* in emulsion systems were smaller than on gelled emulsions at 8 and 12°C. This observation is in agreement to the relation of N_{max} values between liquids and aqueous gels and generally to planktonic and surface growth (Robins and Wilson, 1994; Smet et al., 2015). However, N_{max} values in emulsions at 4°C were higher than on gelled emulsions. Therefore, an influence of temperature on N_{max} relation between the two model systems is evident. Specifically, the liquid environment at 4°C is more favourable than the solid environment or the other cells to which *L. monocytogenes* is in contact for its maximum cell density. Nevertheless, this type of inconsistency might be due to genetic characteristics of the specific strain used in this study.

The μ_{max} values are statistically significant different and specifically, higher in emulsions than on gelled emulsions at 4°C and the opposite occurs at 8 and 12°C. This observation is in agreement with the relationship of μ_{max} values in liquids (planktonic growth) and surfaces of solid systems, as previously discussed. When temperature becomes very stressing, it gets in favour of planktonic growth. This implies that the liquid environment which surrounds the cells at 4°C is more favourable for growth than the solid surface, or other cells with which the cells growing in colonies are in touch. The same observation was made for the N_{max}, as well. Overall, the addition of fat in either liquids or on solid systems does not influence the μ_{max} relationship between the two growth morphologies, taking into account also the temperature factor. Nevertheless, fat affects the actual value of μ_{max}. This is later on discussed.

Finally, *L. monocytogenes* lag values in emulsion systems are significantly shorter than in gelled emulsion systems at 4 and 8°C. The opposite trend occurs at 12°C. This observation is in agreement to what has been discussed for the other growth parameters, about the influence of temperature on the growth of *L. monocytogenes* in systems of different (micro)structures and where different growth morphologies take place.

L. monocytogenes growth in liquids versus emulsions

Comparison of *L. monocytogenes* growth dynamics between the systems where planktonic growth occurs, but the model systems vary in their structural complexity, is interesting for discussion. The differences in a_w measurements are due to the addition of fat and emulsifier; the emulsifier decreases the pH and fat which replaces an equal amount of water decreases the water activity. The relationship of *L. monocytogenes* growth parameters between those two systems is more straightforward. N_{max} and μ_{max} are higher in liquids than in emulsions and the reverse relationship is evident for the lag phase estimation at all temperatures. In literature, if the concentration of the fat in oil-in-water emulsions is less than 83% or 70%, in (Brocklehurst and Wilson, 2000), respectively, then microbial growth is similar to growth in liquid systems. In this study the fat concentration is limited to 18% (w/w). Therefore, *L. monocytogenes* growth should have been similar in liquids and emulsion systems. Although the morphology of growth is planktonic to both model systems, the growth dynamics of *L. monocytogenes* are not similar, but exhibit high differences. This can be due to the limitation of the aqueous (continuous) phase, which is replaced by the presence of fat and by the fact that preservatives are more condensed in aqueous phase of emulsions than in liquids. An exception is present for the μ_{max} at 4°C, where in emulsions is higher than in liquids. This corresponds to a special situation, where the exponential phase was characterised by only a few data points, as growth was very slow. Growth, in this case, is described by a very long lag phase, and an exponential phase which exhibits a very fast switch from the moment it enters the exponential growth until the moment it enters the stationary phase. In fact, the exponential phase of growth might be an artefact of fitting the non-linear regression (the Baranyi and Roberts model) on the experimental data, as growth was less than 1.5 ln units (0.6 log10 units). Therefore, the μ_{max} is overestimated.

L. monocytogenes growth on aqueous gels versus gelled emulsions

Those are two solid-state model systems, with and without the presence of fat with differences in water activity values, induced by the addition of fat and emulsifier in gelled emulsions. In this case, the differences of the growth parameters of *L. monocytogenes* are evident. The estimates of N_{max} and μ_{max} on aqueous gels are higher than on gelled emulsions, while the lag duration is shorter at all temperatures. An exception takes place at 8°C, where the N_{max} of *L. monocytogenes* on gelled emulsions is higher than the one on aqueous gels. Therefore, both composition and storage temperature play a decisive role on the influence of the growth dynamics of microorganisms.

L. monocytogenes growth on canned meat versus model systems and Frankfurters

L. monocytogenes exhibited the fastest growth, in terms of N_{max}, μ_{max} and lag, on canned meat products, than in/on any other model system, no matter the temperature. This

finding is in contrast to what has been reported in literature. In (Meldrum et al., 2003) study, it has been demonstrated that models developed based on experiments in liquid media overestimate microbial growth on real foods. However, the growth dynamics of *L. monocytogenes* in/on liquid and aqueous gels was very similar to the growth dynamics on the canned meat. In contrast, the growth dynamics of *L. monocytogenes* on canned meat were very different than on gelled emulsion, which was the model system intended to approach in all aspects the canned meat. The gelled emulsion model system was targeted to become similar to the canned meat, in terms of composition, physicochemical characteristics and (micro)structure. With respect to a_w of the gelled emulsion, in comparison to the canned meat, obvious differences were present. These differences could be the main, but not the only reason of the differences in the growth dynamics of *L. monocytogenes*. The other possible reasons could be on the one hand, the different sources of proteins used in these two systems, i) hydrolysed protein in the gelled emulsions and ii) proteins from meat tissue in canned meat. These two different sources of protein provide the systems with different structural properties, which might have an influence on the microbial growth dynamics. The main structural difference might be related to their emulsification ability. It has been reported that highly hydrolysed proteins tend to saturate the continuous phase of an emulsion rather than adhere to the water–oil interface (Lam and Nickerson, 2013). On the other hand, the difference in mixing between the model systems and the canned meat could explain the variations among the growth dynamics of *L. monocytogenes* on them. The canned meat is blended, however the model systems are homogenised, a fact that affects the distribution of nutrients, proteins and fat.

CONCLUSIONS

In conclusion, significant differences among the estimated growth dynamics of *L. monocytogenes* have been found among the variable model systems. These model systems vary intentionally in (micro)structural complexity, but also in compositional and physicochemical characteristics, which is a consequence of the (micro)structural variability. In this study, *L. monocytogenes* grew faster on the canned meat, which is a complex system regarding its structural properties and represents a real food system. Therefore, microbial growth on real foods can be faster than in/on model systems, which are frequently used to control and predict microbial dynamics and ensure microbiological food safety. Additionally, the often-reported fail-safe predictions from liquid systems, which overestimate growth on real foods, have not been confirmed in this work. Therefore, attention should be paid when using model systems, even when approaching real food products in all aspects and validation on real foods is always recommended to ensure the food microbiological safety. Since at this stage of this research the effect of food (micro)structure on microbial dynamics has not been deeply studied, a worst case scenario cannot be designed. Further experimental data are required to be collected to understand the influence of food (micro)structure, and later on design optimal experiments for assuring microbiological food safety.

ACKNOWLEDGEMENTS

This work was supported by project PFV/10/002 (Center of Excellence OPTEC-Optimization in Engineering) of the KU Leuven Research Fund, projects G.0930.13 and KAN.15189.13 of the Fund for Scientific Research-Flanders, and the Belgian Program on Interuniversity Poles of Attraction, initiated by the Belgian Federal Science Policy Office (IAP Phase VII/19 DYSCO). The authors thank Prof. Hubert Paelinck (KU Leuven/Campus Gent, Cluster Bioengineering Technology) for providing the canned meat.

REFERENCES

Baka, M., Noriega, E., Tsakali, E., Van Impe, J.F.M., 2015. *Influence of composition and processing of Frankfurter sausages on the growth dynamics of Listeria monocytogenes under vacuum.* Food Res. Int. 70, 94–100.

Baranyi, J., Roberts, T.A., 1994. *A dynamic approach to predicting bacterial growth in food.* Int. J. Food Microbiol. 23, 277–294.

Boons, K., Van Derlinden, E., Mertens, L., Peeters, V., Van Impe, J.F., 2013. *Effect of immobilization and salt concentration on the growth dynamics of Escherichia coli K12 and Salmonella typhimurium.* J. Food Sci. 78, M567–74.

Brocklehurst, T., Mitchell, G., Smith, A., 1997. *A model experimental gel-surface for the growth of bacteria on foods.* Food Microbiol. 14, 303–311.

EFSA and ECDC, 2015. *Trends and sources of zoonoses , zoonotic agents and food-borne.* EFSA J. 13, 3991, 162pp.

Lam, R.S.H., Nickerson, M.T., 2013. *Food proteins: a review on their emulsifying properties using a structure-function approach.* Food Chem. 141, 975–84.

Meldrum, R., Brocklehurst, T., Wilson, D., Wilson, P.D., 2003. *The effects of cell immobilization, pH and sucrose on the growth of Listeria monocytogenes Scott A at 10°C.* Food Microbiol. 20, 97–103.

Ratkowsky, D.A., Olley, J., McMeekin, T.A., Ball, A., 1982. *Relationship between temperature and growth rate of bacterial cultures.* J. Bacteriol. 149, 1–5.

Robins, M.M., Wilson, P.D.G., 1994. *Food structure and microbial growth*. Trends Food Sci. Technol. 5, 289–293.

Smet, C., Van Derlinden, E., Mertens, L., Noriega, E., Van Impe, J., 2015. *Effect of cell immobilization on the growth dynamics of Salmonella Typhimurium and Escherichia coli at suboptimal temperatures.* Int. J. Food Microbiol. 208, 75–83.

Theys, T.E., Geeraerd, A.H., Verhulst, A., Poot, K., Van Bree, I., Devlieghere, F., Moldenaers, P., Wilson, D., Brocklehurst, T., Van Impe, J.F., 2008. *Effect of pH, water activity and gel micro-structure, including oxygen profiles and rheological characterization, on the growth kinetics of Salmonella Typhimurium.* Int. J. Food Microbiol. 128, 67–77.

Wilson, P.D., Brocklehurst, T., Arino, S., Thuault, D., Jakobsen, M., Lange, M., Farkas, J., Wimpenny, J.W., Van Impe, J., 2002. *Modelling microbial growth in structured foods: towards a unified approach.* Int. J. Food Microbiol. 73, 275–289.

Wimpenny, J.W.T., & Coombs, J.P. (1983). *Penetration of oxygen into bacterial colonies.* Journal of Genetic Microbiology, 129, 1239–1242.

IMPACT OF FOOD INTRINSIC FACTORS ON THE INACTIVATION EFFICACY OF COLD ATMOSPHERIC PLASMA

Cindy Smet[1], Estefania Noriega[1], Ioannis Matsoukas[1], Frederik Rosier[1], James Walsh[2], Vasilis Valdramidis[3], Jan Van Impe[1,*]

[1] KU Leuven, Department of Chemical Engineering, BioTeC & OPTEC & CPMF2, Gebroeders De Smetstraat 1, B-9000 Gent, Belgium
*E-mail address: Jan.VanImpe@cit.kuleuven.be

[2] University of Liverpool, Department of Electrical Engineering and Electronics, Liverpool, UK

[3] University of Malta, Department of Food Studies and Environmental Health, Msida, Malta

KEYWORDS

Cold atmospheric gas plasma, food structure, growth morphology, osmotic stress, suboptimal pH.

ABSTRACT

Cold atmospheric plasma (CAP) offers great potential for the treatment of heat-sensitive food products. CAP, generated by applying a voltage to a gas stream, inactivates microbial cells. Although CAP is a very promising technology, more fundamental studies are needed before its application in the food industry. The role of food intrinsic factors on the CAP inactivation efficacy for *Salmonella* Typhimurium and *Listeria monocytogenes* was studied. Cells were grown planktonically or as surface colonies, in/on model systems with varying salt concentrations and pH, and CAP treated either in a liquid carrier or on a solid(like) surface. A dielectric barrier discharge reactor generated helium-oxygen plasma, and samples were treated up to 10 minutes. For both microorganisms, cells grown planktonically under optimal conditions have the highest log reductions. More stressing growth conditions, due to cell immobilization, presence of salt or low pH, result in more resistant cells during CAP treatment. In the liquid carrier, the plasma components need to diffuse and penetrate through the medium, explaining the higher CAP inactivation efficacies for cells deposited on a solid(like) surface. This research illustrates that food intrinsic parameters influence the cell inactivation behavior and indicate that food properties need to be accounted for before plasma treatment.

INTRODUCTION

Over the last century, the food industry has invested a significant amount of money and effort in food safety and quality research. However, more than 300,000 food poisonings have been reported in 2013. *Salmonella* and *Campylobacter* have been the most often reported foodborne pathogens. As in previous years, the most severe fatality rate (15.6%) among the cases was found for *Listeria monocytogenes* (EFSA and ECDC 2015). To prevent the occurrence of pathogenic microorganisms in foods, thermal treatments, like pasteurization, are very effective for inactivating most microorganisms. However, thermal treatments influence the food quality with nutritional losses and changes in organoleptic properties as unwanted side effects. Additionally, consumer demand towards 'fresh-like' and natural foods, desirably with a long shelf-life and minimal preparation before consumption has increased. Fruits and vegetables, often consumed raw, have gained popularity and form a large part of our diet. To produce microbiological safe and stable food products that meet the above requirements a search for mild decontamination procedures has emerged. Traditional decontamination treatments for fruits and vegetables have focused on washing treatments combined with chemical biocides that are applied either pre-harvest, post-harvest or during processing (Aharoni et al. 1997; Goodburn and Wallace 2013). Some adverse effects, such as the formation of carcinogenic halogenated by-products and the additional impetus of reducing water usage as well as chemical emissions, have turned the focus of the food industry towards non-thermal physical decontamination technologies including cold atmospheric plasma (Laroussi et al. 2000).

In general, the CAP is generated by applying a voltage to a gas stream. The gas molecules become ionized once a certain threshold is exceeded, resulting in mixtures of electrons, ions, atomic species, free radicals and UV photons, all able to inactivate microorganisms (Deng et al. 2006; Perni et al. 2007). Some of the most important process parameters are the plasma power, the voltage, the frequency and the gas flow. Regarding the gas composition, the presence of oxygen is proved to enhance the killing efficacy (Fernandez and Thompson 2012). Another important processing parameter concerns the reactor itself. Different plasma set ups exist, but two frequently used types are the plasma jet and the dielectric barrier discharge (DBD) electrode (Ehlbeck et al. 2011). While the plasma jet can be used to treat complex geometries, the DBD electrode is able to treat more extensive samples. For both set ups, the sample can be treated direct or indirect. Direct treatment indicates that all plasma generated species, including the charged particles, come in contact with the sample. This is not valid for indirect treatment, with the sample placed at a distance from the plasma discharge (Fernandez and Thompson 2012; Fridman et al. 2007). Novel regarding plasma research is the possibility to work with a closed reactor, which keeps the ionized environment inside the system. Working inside a closed reactor prevents the possibility of recontamination and since the formed radicals remain inside the system, they remain active. Important advantages of using CAP for food treatment are (1) low temperature during treatment, (2) low energy needed, (3) short treatment time and (4) no residues remain on the surface of the treated product since chemical species formed during plasma treatment are highly reactive and very short-lived (Moisan et al. 2001). The last ten years, multiple research groups studied the potential of CAP to be applied in the food industry. Limitations of previous studies are their focus on specific target microorganisms in relation

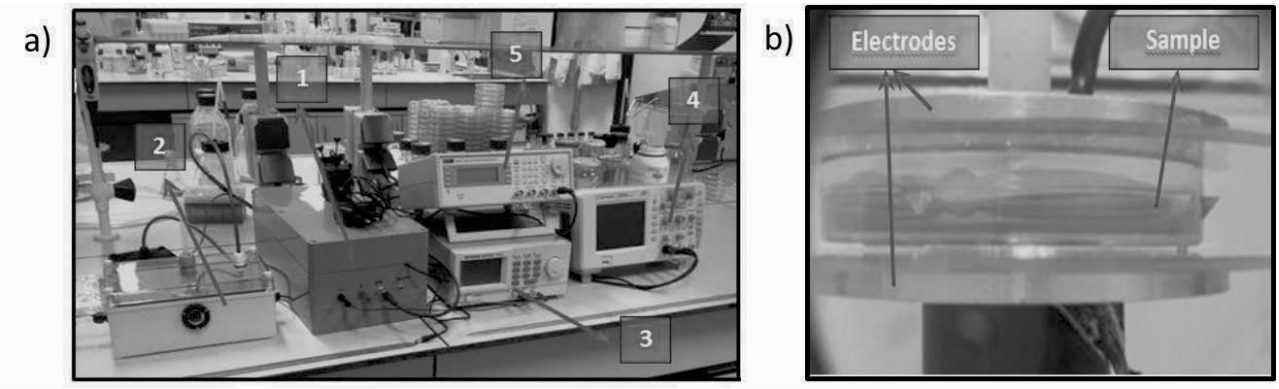

Figure 1: a) the CAP set up: (1) *plasma power source,* (2) *Dielectric Barrier Discharge reactor,* (3) *DC power supply,* (4) *oscilloscope and* (5) *function generator. b) DBD electrode inside reactor.*

to specific food products (Fernandez et al. 2013; Gurol et al. 2012; Kim et al. 2011; Selcuk et al. 2008). General studies focusing on a more fundamental evaluation, e.g., the influence of food properties on the CAP inactivation efficacy, are lacking.

In the present work, the role of food intrinsic factors on the efficacy of CAP inactivation of *Salmonella* Typhimurium and *Listeria monocytogenes* was studied. These food intrinsic factors include (1) the growth morphology, i.e., planktonic cells or surface colonies, determined by the intrinsic food structure, (2) the salt concentration (0, 2, 6% (w/v) NaCl) and (3) the pH (5.5, 6.5, 7.4) of the medium, all representing certain food properties. Additionally, the influence of the support system, and thus the influence of the food structure during the inactivation was studied: cells were inactivated on a solid(like) surface or in a liquid carrier, mimicking the treatment of different food structures and investigating the possibilities of CAP to treat different types of food products.

MATERIALS AND METHODS

Salmonella enterica serovar Typhimurium SL1344 (IFR, Norwich, UK) and *Listeria monocytogenes* LMG 13305 (BCCM, Ghent, Belgium) were cultured in Erlenmeyers and grown under different experimental conditions (see Introduction). Cells were grown at 20°C in petri dishes under static conditions, planktonically in a liquid system (Tryptic Soy Broth for *S.* Typhimurium, Brain Heart Infusion for *L. monocytogenes*), or as surface colonies (TSB or BHI, supplemented with 5% (w/v) gelatin). All systems had a specific salt concentration and the pH was adapted. Once the cells reached the stationary growth phase, samples were diluted and re-inoculated before inactivation, in either a liquid carrier (5.5 log(CFU/mL)) or on a solid(like) surface (5.5 log(CFU/cm^2)). A dielectric barrier discharge reactor (similar to that reported by Massines et al. 1998, Figure 1) generated the plasma in a gas mixture of helium (purity 99.996%) and oxygen (purity ≥ 99.995%), supplied at a flow rate of 4 L/min and 40 mL/min, respectively. Samples were placed between the 0.8 cm gap of the DBD electrodes, and after flushing the reactor with the helium-oxygen gas mixture for 4 min, the high-voltage power source was energized and the plasma was generated. Samples were treated up to 10 minutes at a peak-to-peak voltage around 7 kV, frequency of 15 kHz and dissipated plasma power of 9.6 W. For these experimental conditions, the temperature increase of the sample, measured directly after treatment, was about 2°C. An enclosure around the electrode increases the residence time of the plasma species around the sample while also providing a more controlled environment. The cell density after CAP treatment was determined via viable plate counting on both general (BHI-Agar for *L. monocytogenes*, TSA for *S.* Typhimurium) and selective media (PALCAM-Agar for *L. monocytogenes*, Xylose Lysine Deoxycholate Agar for *S.* Typhimurium), considering sublethal injury. Inactivation curves were fitted with the model of Geeraerd et al. (2000),

$$N(t) = (N_0 - N_{res}) \cdot \exp(-k_{max} \cdot t) \cdot \left(\frac{\exp(k_{max} \cdot t_l)}{1 + (\exp(k_{max} \cdot t_l) - 1) \cdot \exp(-k_{max} \cdot t)} \right) + N_{res} \quad (1)$$

with $N(t)$ [CFU/mL] the cell density at time t [s], N_0 [CFU/mL] the initial cell density, N_{res} [CFU/mL] a more resistant subpopulation, k_{max} [1/s] the maximum specific inactivation rate and t_l [s] the length of the shoulder. The regression analysis was performed using the log transformation of Equation 1. Parameters of the Geeraerd et al. (2000) model were estimated via the minimization of the sum of square errors (SSE), using the *lsqnonlin* routine of the Optimization Toolbox of Matlab (The Mathworks Inc.). Simultaneous with parameter estimation, the parameter estimation errors were determined based on the Jacobian matrix.

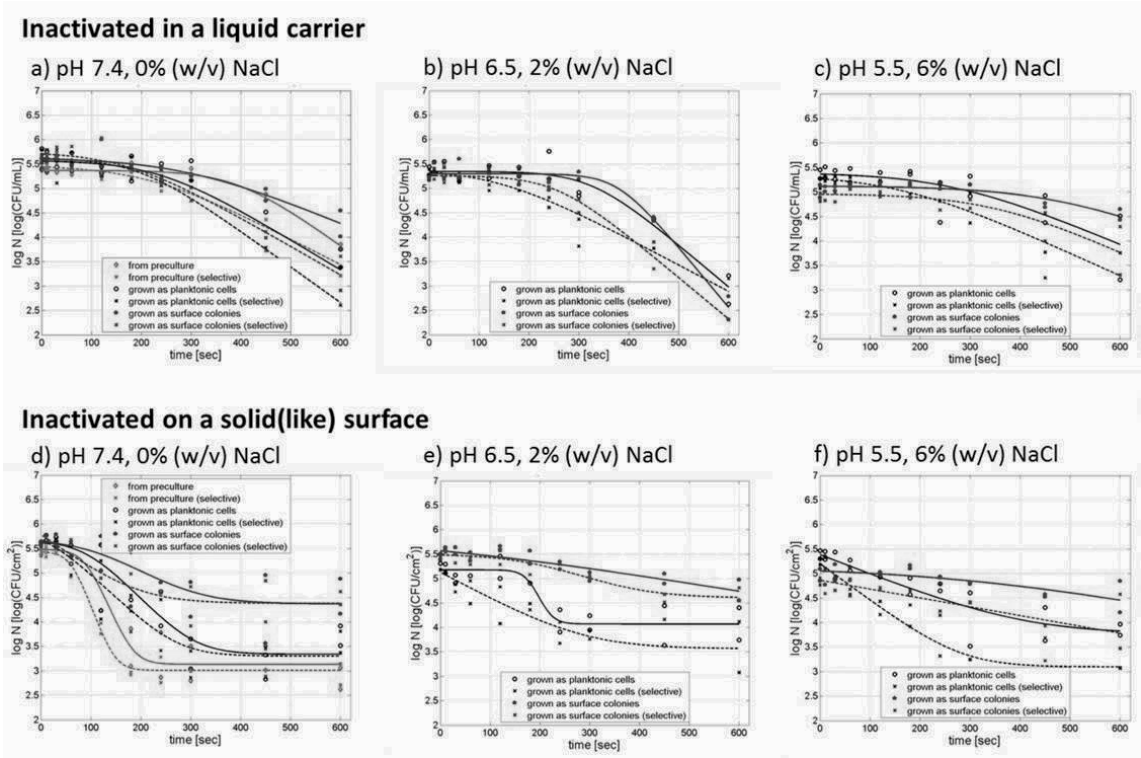

Figure 2: Survival curves of stationary phase S. Typhimurium after exposure to CAP. Cells were inactivated in a liquid carrier (a,b,c) or on a solid(like) surface (d,e,f). Prior to CAP treatment, cells were grown at pH 7.4, 0% (w/v) NaCl (a,d), pH 6.5, 2% (w/v) NaCl (b,e) or pH 5.5, 6% (w/v) NaCl (c,f), and either planktonically or as surface colonies. For pH 7.4, 0% (w/v) NaCl (a,d), as a control, cells from the preculture were directly treated. Experimental data (symbols) and global fit (dashed line) of the Geeraerd et al. (2000) model: total viable population (0, solid line) and uninjured viable population (x, dashed line).

RESULTS AND DISCUSSION

Inactivation kinetics of stationary phase *S.* Typhimurium and *L. monocytogenes* cells exposed to CAP treatment are shown in Figure 2 and 3 respectively. For each microorganism, cells were inactivated in a liquid carrier or on a solid(like) surface. Prior to the CAP treatment, cells were grown at three different experimental conditions: pH 7.4, 0% (w/v) NaCl, pH 6.5, 2% (w/v) NaCl or pH 5.5, 6% (w/v) NaCl. Additionally, cells were grown planktonically or as surface colonies. As a control, for the most optimal experimental condition at pH 7.4 and 0% (w/v) NaCl, cells from the preculture were also directly treated. The experimental data were fitted with the Geeraerd et al. (2000) model.

The CAP mode of action for inactivation of microbial cells may be explained at different levels. Accumulations of charged particles at the surface of the cell membrane induce its rupture. Oxidation of the lipids, amino acids and nucleic acids with reactive oxygen and nitrogen species may cause changes that lead to microbial death or injury. In addition to reactive species, UV photons can modify microbial DNA (Fernandez and Thompson 2012). As the cell wall and its structure play an important role in the CAP inactivation mechanism, differences can be expected in the inactivation of *S.* Typhimurium (gram-negative bacteria) or *L. monocytogenes* (gram-positive bacteria). While both microorganisms have a different cell wall structure, some similarities are observed for their CAP inactivation kinetics (Salton and Kim 1996). In particular

the shapes of the inactivation kinetics, for each inactivation support or experimental condition, are often alike for both microorganisms. However, as often reported the gram-positive *L. monocytogenes* is more stress resistant, in this case towards CAP treatment, resulting in lower inactivation efficacies (Jasson et al. 2007; Yuste et al. 2004).

Influence of the growth morphology

As an intrinsic factor, the food structure influences the growth morphology of microbial cells. *S.* Typhimurium or *L. monocytogenes* cells grown planktonically exhibit higher log reductions as compared to cells grown as surface colonies, independent of the experimental conditions or the support system during treatment.

The lower inactivation efficacy for cells grown as surface colonies suggests an increased resistance towards CAP. The slow transport in a solid(like) environment limits nutrient delivery and metabolite removal, resulting in the formation of concentration gradients around colonies. Next to this, the solid(like) environment itself also exerts additional stresses on the colonies. Nutrient limitation in case of surface colonies could lead to starvation stress, which might promote resistance to subsequent stresses, like CAP treatment, via cross-protection (Wesche et al. 2009).

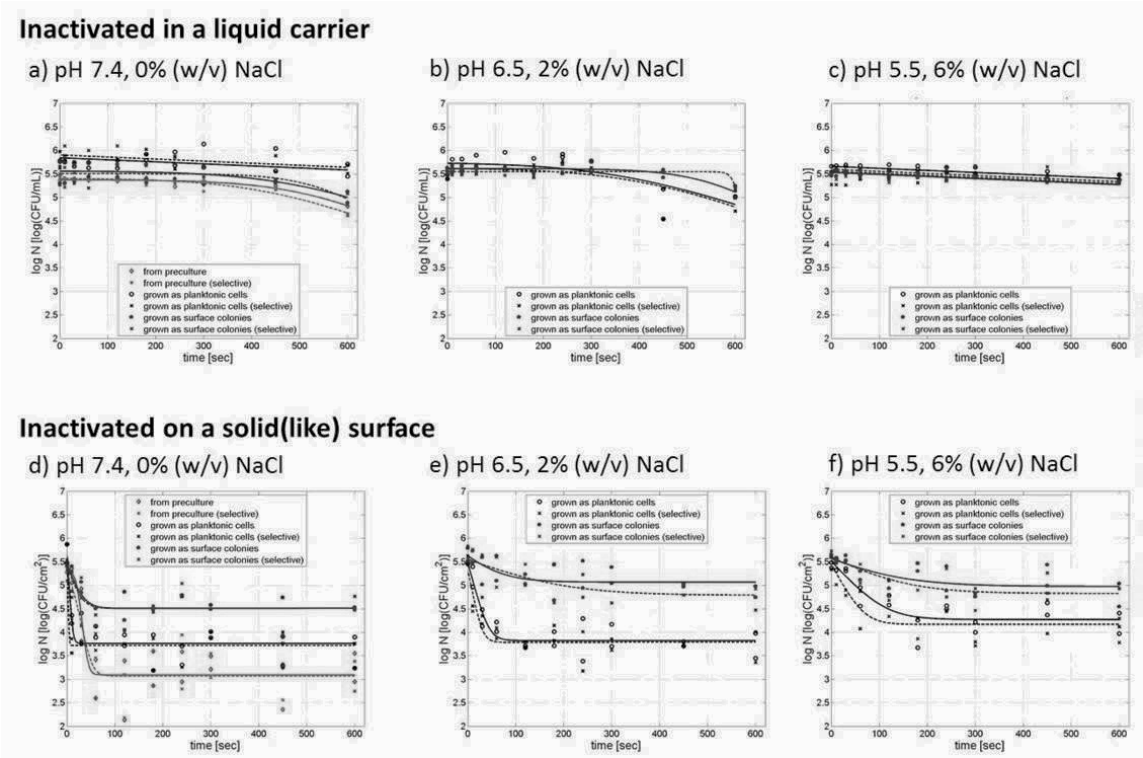

Figure 3: Survival curves of stationary phase L. monocytogenes after exposure to CAP. Cells were inactivated in a liquid carrier (a,b,c) or on a solid(like) surface (d,e,f). Prior to CAP treatment, cells were grown at pH 7.4, 0% (w/v) NaCl (a,d), pH 6.5, 2% (w/v) NaCl (b,e) or pH 5.5, 6% (w/v) NaCl (c,f), and either planktonically or as surface colonies. For pH 7.4, 0% (w/v) NaCl (a,d), as a control, cells from the preculture were directly treated. Experimental data (symbols) and global fit (dashed line) of the Geeraerd et al. (2000) model: total viable population (0, solid line) and uninjured viable population (x, dashed line).

Influence of osmotic and acidic stress

The presence of high salt concentrations, in combination with the lower pH, e.g., for the experimental condition at pH 5.5, 6% (w/v) NaCl, leads to very stressing growth conditions. Regardless the inactivation support or the growth morphology, the more stressing the growth conditions concerning NaCl concentration or pH value, the lower the inactivation efficacy.

Exposure to osmotic and acidic stress results in cells that are more resistant to all subsequent stresses, a phenomenon called stress hardening. Stress hardening refers to an increased resistance to lethal factors, e.g. CAP, after adaptation to environmental stresses (Leyer and Johnson 1993; Lou and Yousef 1997; O'Byrne and Booth 2002).

Influence of the inactivation support system

As shown in Figure 2 and 3, cells treated on a solid(like) surface exhibit a more rapid and efficient inactivation as compared to cells inactivated in a liquid carrier.

Cells treated on a solid(like) surface are easily attained by the active plasma components during the treatment (Oehmigen et al. 2010). Additionally, the low microbial cell load of $10^{5.5}$ CFU/cm^2 results in a monolayer cell arrangement, thus no protection against CAP is provided by other cells (Fernandez et al. 2012). In the liquid carrier, the plasma components need to diffuse and penetrate through the medium where the microbial cells are dispersed freely. Many highly reactive plasma species react at the plasma-liquid interface and do not penetrate very far into the liquid. This results in a more complicated treatment of liquids as compared to treatment of solid(like) surfaces, and explains the observed differences in inactivation behavior.

CONCLUSIONS

This work studied the influence of different intrinsic factors on the potential of CAP to inactivate *S.* Typhimurium and *L. monocytogenes*. Next to the effect of the cell growth morphology and the influence of osmotic and acidic stress, the impact of the food structure during inactivation on the CAP efficacy was investigated. Although *L. monocytogenes* is more resistant to treatment as compared to *S.* Typhimurium, similar trends regarding the influence of intrinsic factors on the CAP inactivation efficacy are detected. Cell immobilization for cells grown as surface colonies, the presence of salt or a lower pH, often result in more resistant cells during CAP treatment. Cross-protection due to starvation, osmotic or acidic stress can explain this increased resistance to plasma treatment for treatment of both microorganisms. Regarding the food structure during the inactivation, cells in a liquid carrier are more difficult to inactivate as compared to cells inactivated on a solid(like) surface, since the CAP active species have to diffuse throughout the liquid medium in order to inactivate the microbial cells. This research proves that the intrinsic factors influence the inactivation behavior and efficacy of CAP. It indicates that food properties, e.g., the intrinsic food

structure, salt concentration and pH, need to be accounted for before treatment with CAP in order to ensure efficient treatment, resulting in safer food products.

ACKNOWLEDGEMENTS

This work was supported by project PFV/10/002 (Center of Excellence OPTEC-Optimization in Engineering) of the KU Leuven Research Fund, projects G.0930.13 and KAN.15189.13 of the Fund for Scientific Research-Flanders, and the Belgian Program on Interuniversity Poles of Attraction, initiated by the Belgian Federal Science Policy Office (IAP Phase VII/19 DYSCO).

REFERENCES

Aharoni Y.; E. Fallik; A. Copel; M. Gil; S. Grinberg; and J.D. Klein. 1997. "Sodium bicarbonate reduces postharvest decay development on melons". *Postharvest Biology and Technology*, 10, 201-206.

Deng X.; J.J. Shi; and M.G. Kong. 2006. "Physical mechanisms of inactivation of *Bacillus subtilis* spores using cold atmospheric plasmas". *IEEE Transactions on Plasma Science*, 344, 1310-1316.

Ehlbeck J.; U. Schnabel; M. Polak; J. Winter; Th. von Woedtke; R. Brandenburg; T. von dem Hagen; and K-D. Weltmann. 2011. "Low temperature atmospheric pressure plasma sources for microbial decontamination". *Journal of Physics D: Applied Physics*, 44, 013002.

European Food Safety Authority (EFSA) and European Centre for Disease Prevention and Control (ECDC). 2015. "The European Union summary report on trends and sources of zoonoses, zoonotic agents and food-borne outbreaks in 2013". *EFSA Journal*, 13:3991.

Fernandez A., N. Shearer; D.R. Wilson; and A. Thompson. 2012. "Effect of microbial loading on the efficiency of cold atmospheric gas plasma inactivation of *Salmonella enterica* serovar Typhimurium". *International Journal of Food Microbiology*, 152, 175-180.

Fernandez A. and A. Thompson. 2012. "The inactivation of *Salmonella* by cold atmospheric plasma treatment". *Food Research International*, 45, 678-684.

Fernandez A; E. Noriega E; and A. Thompson. 2013. "Inactivation of *Salmonella enterica* serovar Typhimurium on fresh produce by cold atmospheric gas plasma technology". *Food Microbiology*, 33, 24-29.

Fridman G.; A.D. Brooks; M. Balasubramanian; A. Fridman; A. Gutsol; V.N. Vasilets; H. Ayan; and G. Friedman. 2007. "Comparison of direct and indirect effects of non-thermal atmospheric pressure plasma on bacteria". *Plasma Processes and Polymers*, 4, 370–375.

Geeraerd A.; C. Herremans; and J.F. Van Impe. 2000. "Structural model requirements to describe microbial inactivation during a mild heat treatment". *International Journal of Food Microbiology*, 59, 185-209.

Goodburn C. and C. Wallace. 2003. "The microbiological efficacy of decontamination methodologies for fresh produce: A review". *Food Control*, 32, 418-427.

Gurol C.; F. Ekinci; N. Aslan; and M. Korachi. 2012. "Low temperature plasma for decontamination of *E. coli* in milk". *International Journal of Food Microbiology*, 157, 1-5.

Jasson V.; M. Uyttendaele; A. Rajkovic; and J. Debevere. 2007. "Establishment of procedures provoking sub-lethal injury of *Listeria monocytogenes*, *Campylobacter jejuni* and *Escherichia coli* O157 to serve method performance testing". *International Journal of Food Microbiology*, 118, 241–249.

Kim B.; Y. Hyejeong; S. Jung; Y. Jung; H. Jung; W. Choe; and C. Jo. 2011. "Effect of atmospheric pressure plasma on inactivation of pathogens inoculated onto bacon using two different gas compositions". *Food Microbiology*, 28, 9-13.

Laroussi M.; I. Alexeff; W.L. Kang. 2000. "Biological decontamination by nonthermal plasmas". *IEEE Transactions on Plasma Science*, 28, 184-188.

Leyer G.J. and E.A. Johnson. 1993. "Acid adaptation induces cross-protection against environmental stresses in *Salmonella* Typhimurium". *Applied and Environmental Microbiology*, 59, 1842-1847.

Lou Y. and A.E. Yousef. 1997. "Adaptation to sublethal environmental stresses protects *Listeria monocytogenes* against lethal preservation factors". *Applied and Environmental Microbiology*, 63, 1252–1255.

Massines F.; A. Rabehi; P. Decomps; R.B. Gadri; P. Ségur; and C. Mayoux. 1998. "Experimental and theoretical study of a glow discharge at atmospheric pressure controlled by dielectric barrier". *Journal of applied physics*, 83, 2950-2957.

Moisan M.; J. Barbeau; S. Moreau; J. Pelletier; M. Tabrizian; and L. Yahia. 2001. "Low-temperature sterilization using gas plasmas: a review of the experiments and an analysis of the inactivation mechanisms". *International Journal of Pharmaceutics*, 226, 1-21.

O'Byrne C.P. and I.R. Booth. 2002. "Osmoregulation and its importance to foodborne microorganisms". *International Journal of Food Microbiology*, 74, 203-216.

Oehmigen K.; M. Hahnel; R. Brandenburg; Ch. Wilke; K.-D. Weltmann; and Th. von Woedtke. 2010. "The role of acidification for antimicrobial activity of atmospheric pressure plasma in liquids". *Plasma Processes and Polymers*, 7, 250-257.

Perni S.; G. Shama; J.L. Hobman; P.A. Lund; C.J. Kershaw; G.A. Hidalgo-Arroyo; C.W. Penn; X.T. Deng; J.L. Walsh; and M.G. Kong. 2007. "Probing bactericidal mechanisms induced by cold atmospheric plasmas with *Escherichia coli* mutants". *Applied Physics Letters*, 90,073902.

Salton M.R.J. and K.S. Kim. 1996. "Structure". In *Medical Microbiology*, S. Baron (Ed.), Galveston, TX, USA.

Selcuk M.; L. Oksuz; and P. Basaran. 2008. "Decontamination of grains and legumes infected with *Aspergillus* spp. and *Penicillum* spp. by cold plasma treatment". *Bioresource Technology*, 99, 5104-5109.

Yuste J.; M. Capellas; D.Y.C. Fung; and M. Mor-Mur. 2004. "Inactivation and sublethal injury of foodborne pathogens by high pressure processing: Evaluation with conventional media and thin agar layer method". *Food Research International*, 37, 861–866.

Wesche A; J.B. Gurtler; B.P. Marks; and E.T. Ryser. 2009. "Stress, sublethal injury, resuscitation, and virulence of bacterial foodborne pathogens". *Journal of Food Protection*, 72, 1121-1138.

PREDICTIVE MODELLING OF THE GROWTH OF *LISTERIA* AS INFLUENCED BY THE ANTIMICROBIAL ACTIVITY OF *LACTOCOCCUS LACTIS* IN LIQUID AND SOLID STATE

Parika Ale
Simy Paul
Jorge Gutierrez
Eirini Velliou*
University of Surrey
Guildford, GU2 7XH, UK
E-mail: e.velliou@surrey.ac.uk

KEYWORDS
Listeria, nisin, co-culture, *lactic-acid bacteria*, solid(like) food systems

ABSTRACT

The aim of this study is to investigate and further quantify the impact of nisin, which is a natural antimicrobial produced by Lactic Acid Bacteria (LAB), on the growth kinetics of *Listeria innocua* in different types of food model systems, i.e., liquid and gelified. More specifically, *Listeria inoccua* was grown in a liquid broth or a solid/gelified matrix in mono- or in co-culture with *Lactococcus lactis* NZ9700, i.e., nisin producer, or *Lactococcus lactis* NZ9800, i.e., knock-out strain not producing nisin, at 37°C. Microbial growth curves were compared for all the conditions under study. In general, growth of *L. innocua* was significantly lower in the solid system compared to the liquid broth and a lower maximum microbial concentration was reached in the solid matrix. In co-culture, interestingly, the growth of *L. innocua* was not significantly affected for both *Lactococcus lactis* strains. However, the growth of *L. innocua* was disturbed in the solid matrix when co-cultured with the nisin producer LAB strain, compared to co-culture with the knock-out LAB strain or the mono-culture system. Overall, our findings give a systematic quantitative insight on the impact of nisin on the growth of *Listeria* in liquid and solid model systems and point out the importance of taking into consideration the bacterial stress adaptation in solid state when designing decontamination processes with natural antimicrobials.

INTRODUCTION

Nowadays, emerging industrial processing techniques are increasing rapidly and are progressively replacing the classical decontamination processes of food systems. One emerging alternative is the use of natural antimicrobials, produced by microorganisms such as lactic acid bacteria (LAB), as there is evidence that those components may act against food pathogens (Mariam et al., 2014; Gutierrez et al., 2009). However, the efficiency of such antimicrobial components is still unclear. Moreover, most of the available studies describe the action of antimicrobials against pathogens in liquid systems, although the majority of food products are solids. In a solid system microorganisms evolve as colonies and due to diffusional limitations of oxygen and nutrients as well as the accumulation of acidic metabolic products around the colony micro-organisms may experience a shelf-induced (acid) stress that could affect their overall response and tolerance to the antimicrobial component. Indeed, several researches have pointed significant differences in the microbial kinetics in terms of growth and/or inactivation in solid(like) systems (see as examples Antwi et al., 2008; Velliou et al., 2013; Noriega et al., 2013). Therefore, it is essential to understand and precisely quantify the response of food related pathogens to natural antimicrobials, in order to efficiently predict their behavior and secure food safety.

The aim of this work was to study and further quantify -with the use of predictive microbiology-, the impact of nisin on the growth of *L.innocua* in a liquid and a solid/gelified food model system at the optimal temperature of 37°C. More specifically, *Listeria inoccua* was grown in a liquid broth (Tryptic Soy Broth) or a solid/gelified matrix (Tryptic Soy Broth + xanthan gum as gelling agent) in mono- or in co-culture with *Lactococcus lactis* NZ9700, i.e., nisin producer, or *Lactococcus lactis* NZ9800, i.e., knock-out strain not producing nisin, at 37°C. The growth model of Baranyi and Roberts (1994) was fitted to the experimental data in order to quantify the growth kinetics in all the different conditions under study.

MATERIALS & METHODS

Stock Cultures

Stock cultures of *Listeria innocua* (ATCC 33090), *Lactococcus lactis* strains NZ9700, NZ9800 (Kuipers et al., 1991) and *Micrococcus luteus* MG1614 (ATCC4698) were stored at -80^{0}C in Tryptic Soy Broth (TSB) supplemented with 25 % glycerol.

Antimicrobial susceptibility testing: disk diffusion method

The antimicrobial susceptibility test of *L. lactis* NZ9700 and NZ9800 strains against *Micrococcus luteus* MG1614 and against *L. innocua* was performed prior to the co-culture experiments. The antimicrobial susceptibility test against *Micrococcus luteus* MG1614, which is a strain very sensitive to nisin was performed in order to confirm that nisin is indeed produced by the wild type *L. lactis* NZ9700 and not produced by the knock-out strain NZ9800. Similarly, antimicrobial susceptibility tests were performed to confirm the antimicrobial activity of the established nisin producer strain against *L.innocua* at 37^{0}C . The disk diffusion method

was chosen to perform the tests in order to determine the antimicrobial activity. The regions of growth inhibition zones for each supernatant were compared in order to confirm both the nisin production and the nisin antimicrobial activity. Nisin was indeed produced only by *L. lactis* NZ9700 and a clear growth inhibition zone was observed for *L. innocua*, confirming the antimicrobial activity of nisin against *L. innocua*.

Inoculum preparation

For the inoculum of *L. innocua*, a loopful of stock culture was transferred into 15 mL of TSB supplemented with 0.6% w/v of yeast extract (TSBYE), and was incubated for 9.5 h at 37^0C under static conditions. Subsequently 20 μL of this cell suspension was transferred to 15 mL of fresh TSBYE broth and incubated for 15 h under the same conditions until the stationary phase (10^9 CFU mL^{-1}) was reached. Similarly, the inoculum of *L. lactis* strains NZ9700 and NZ9800 was grown in TSBYE to obtain the early stationary phase. The *L. lactis* cells were incubated at 30^0C, i.e., the optimal temperature condition required for the growth of *L. lactis*.

Gelified matrix

Xanthan gum (Xanthural 75, CP Kelco, Surrey, UK) was selected as a gelling agent. Xanthan gum is an extracellular anionic polysaccharide, produced by the naturally occurring bacterium *Xanthonomas campestris* during anaerobic fermentation. Due to its resistance to common enzymes and its unique rheological behaviour, it is widely used in the food industry for thickening, stabilising and emulsifying agents. More specifically, the gels formulated by xanthan gum are rheologically stable at high temperatures as well, therefore, allowing it's usage in a wide range of temperatures including microbial inactivation temperatures (Velliou et al., 2013). For the preparation of gelified/solid media, 1.5% w/v of Xanthan gum (Velliou et al., 2013) was added in TSBYE broth and vigorously stirred for at least 30 minutes. This mixture was autoclaved and entrapped air bubbles were removed-before as well as after autoclaving –with centrifugation, as described by Velliou et al., (2013).

Inoculation and growth in mono- and co- culture in liquid and solid media

Appropriate serial dilutions were performed to stationary cultures in order to obtain an initial cell density of 10^3 CFU/mL in tubes of 5mL of either TSBYE broth (liquid system) or TSBYE + 1.5 % w/v xanthan gum (gelified system). For achievement of homogenisation as well as for air bubble removal, samples were then centrifuged (see also Velliou et al., 2013). Similarly, for the co-culture experiments, 10^3 CFU/mL of *L. innocua* and *L. lactis* NZ9700 or NZ9800 were inoculated into liquid and solid media. Next, growth experiments took place at 37^0C (optimal temperature for growth of *L. innocua*) for 24 h and samples were taking regularly in order to monitor the microbial kinetics. Decimal serial dilutions of the samples (100 μL pipetted from the centre of the tube) were prepared in a TSBYE solution (900 μL) and surface plated on Palcam agar -for selective plating of *L. innocua*- (OXOID Limited, Basingstoke, UK) and on MRS agar -for selective plating of LAB- (OXOID Limited, Basingstoke, UK) using spreaders. Plates were incubated for 24 h at 37 °C and colony forming units (CFU) were enumerated. All experiments were performed in duplicate and analysis of variance with a level of significance $P < 0.05$ was performed in order to evaluate the statistical difference/ indifference among the studied conditions.

Mathematical model

The model of Baranyi and Roberts (1994) (Equation (1) was fitted to the experimental data.

$$\frac{dN(t)}{dt}=\mu_{max}.\frac{Q(t)}{1+Q(t)}.\left(1-\frac{N(t)}{N_{max}}\right).N(t)$$

$$\frac{dQ(t)}{dt}=\mu_{max}.Q(t) \qquad (1)$$

with $N(t)$ [CFU/mL] the cell concentration, μ_{max} [1/h] the maximum specific growth rate, $Q(t)$ is measure of the physiological state of the cells, $Q(t)/(1+Q(t))$ describing the transition phase from the lag phase to the exponential growth phase, λ [1/h] lag phase duration and $1- N(t)/N_{max}$ describes the logistic inhibition which enables the transition from the exponential growth phase to the stationary phase when N approaches N_{max}, (the maximum cell concentration).
Data processing, model fitting to the experimental data as well as figure generation were performed using MatLab Version 7.12 (The Mathworks, Inc., Natick, USA)

RESULTS

The growth curves for *L. innocua* in co-culture with *L. Lactis* wild type (nisin producer) and knock-out (non nisin producer) are summarised in Figure I for the liquid broth (Figure 1 top graph) as well as the gelified matrix (Figure 1 bottom graph). Surprisingly, as can be clearly seen in Figure 1 (top graph) the growth of Listeria was not affected when co-cultured with neither of the LAB strains, compared to mono-culture. This finding points out, on the one hand, that in the liquid broth there is no clear antagonistic effect between *Listeria* and LAB and, on the other hand, that nisin production does not affect the growth of *Listeria*. Similar trends are observed in the solid matrix for the co-culture of *Listeria* with the knock-out strain of *L. Lactis*, i.e., the growth curves of the mono-culture and the co-culture with the knock-out evolve similarly (Figure 1 (bottom graph)). The latter indicates that the presence of LAB does not act antagonistically on the growth of *Listeria* in the solid medium. This is surprising as several studies have indicated an antagonistic effect between *Listeria* and LAB in co-culture (See as examples, Antwi et al., 2008; Baka et al., 2015).The fact that we do not observe an antagonistic effect on the growth of *Listeria* in co-culture with *Lactococcus lactis* might be related to the initial inoculum levels we used. For example, Baka et al., (2015) pointed that there is a clear relation between the initial concentration of the LAB and the disturbance of the growth of *Listeria*.
In contrast to our findings for co-culture of *Listeria* with the knock-out, in the case of co-culture with the nisin producer

strain the growth of *Listeria* is disturbed, particularly in the exponential growth phase that occurs significantly slower than in the other conditions. This shows that nisin produced by *L. Lactis* has antimicrobial activity against *Listeria innocua* in the gelified system. The fact that we observed antimicrobial activity of nisin only in the solid and not in the liquid broth is interesting. As previously mentioned, when the cells grow in colonies they experience an acid adaptation due to the accumulation of metabolites around the colony. It is possible that there is a synergistic inhibitory effect of this self-induced acid stress and the nisin on the growth of *Listeria* which is not observed in the liquid as there is no such acid adaptation. Moreover, the immobilised LAB might produce nisin at an earlier stage -and not at late exponential phase as in the liquid- and/or in higher concentration due to the experience of a metabolic and/or oxidative stress in the gelified matrix. In contrast, in the liquid system the nisin might be produced at a later stage and/or in smaller amounts.

CONCLUSION

Our results saw that nisin production by LAB disturbes the growth of *Listeria* in a co-culture in solid but not in liquid state. Overall, our findings give a systematic quantitative insight on the impact of nisin on the growth of *Listeria* in liquid and solid model systems and point out the importance of taking into consideration the bacterial stress adaptation in solid state when designing decontamination processes with natural antimicrobials.

FUTURE WORK

In order to elucidate more light on the observed effects, experiments with supernatants from early stationary phase LAB wild type and knock-out cultures should be performed as those supernatants should normally have the maximum possible level of nisin. Moreover, it would be beneficial to monitor the evolution of nisin over time in order to determine the time point at which significant nisin production occurs as the latter might have an impact on the growth kinetics.

REFERENCES

Antwi, M., Theys, T.E., Van Impe, J.F., Geeraerd, A.H. (2008). Validation of a model for growth of *Lactococcus lactis* and *Listeria innocua* in a structured gel system: Effect of monopotassium phosphate. *International Journal of Food Microbiology*, **125**(3), pp: 320–329.

Baka, M., Noriega, E., Mertens, L., Van Derlinden, E., Van Impe, J.F. (2015) Protective role of indigenous *Leuconostoc carnosum* against *Listeria monocytogenes* on vacum packet Frankfurter sausages at suboptimal temperatures, *Food Research International*, **66**, 197-206.

Baranyi, J. & Roberts, T., (1994). A dynamic approach to predicting bacterial growth in food. *International Journal of Food Microbiology*, **3-4**, pp: 277-294.

Gutierrez, J., Barry-Ryan, C., Bourke, P., (2009). Antimicrobial activity of plant essential oils using food model media: Efficacy, synergistic potential and interactions with food components. *Food Microbiology*, **26**(2), pp: 142-150.

Mariam, S.H., Zegeye, N., Tariku, T., Andargie, E., Endalafer, N., Assefa, A. (2014) Potential of cell-free supernatants from cultures of selected lactic acid bacteria and yeast obtained from local fermented foods as inhibitors from Listeria monocytogenes, Salmonella spp. and Staphylococcus aureus. *BMC Research Notes*, **7**, pp. 707.

Noriega, E., Velliou, E., Van Derlinden, E. V., Mertens, L., Van Impe, J.F. (2013). Effect of cell immobilization on heat-induced sublethal injury of Escherichia coli, Salmonella Typhimurium and *Listeria innocua*. *Food Microbiology*, **36**(2), pp: 355-364.

Velliou E.G., Noriega, E., Van Derlinden, E., Mertens, L., Boons, K., Geeraerd A.H., Devlieghere, F., Van Impe, J.F. (2013). The effect of colony formation on the heat inactivation dynamics of Escherichia *Coli* K12 and Salmonella typhimurium. *Food Research International*, **54**, pp: 1746-1752.

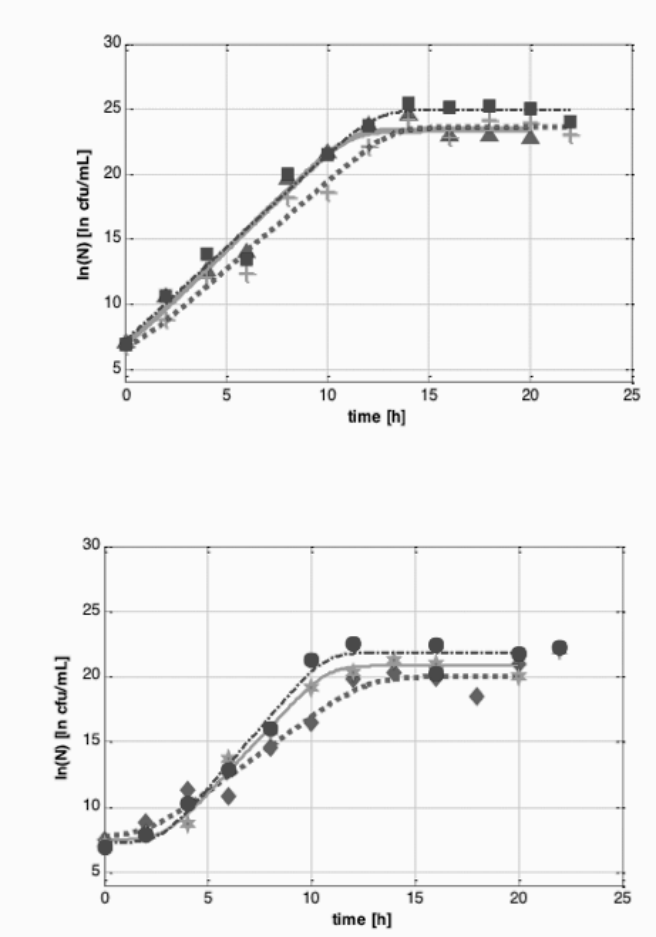

Figure 1: Growth kinetics of *Listeria* in the liquid (BHI broth) (top graph) versus the gelified (BHI + Xanthan gum) food model system (bottom graph): --- mono-culture, -co-culture with non-nisin producer, ... co-culture with nisin producer. The lines describe the mathematical model (Baranyi Roberts) fit to the experimental data which are represented by equivalent colours to each fit on the graph.

ACKNOWLEDGEMENTS

This work was supported by the Department of Chemical and Process Engineering and the Department of Nutritional Sciences of the University of Surrey, UK. The authors would like to thank Dr OP Kuipers from the University of Groningen for providing the *lactococculs lactis* strains.

DEVELOPMENT OF FISH-BASED MODEL SYSTEMS FOR KINETIC STUDIES OF FOODBORNE PATHOGENS

Davy Verheyen[1], Maria Baka[1], Torstein Skåra[2], Stijn Vercruyssen[1], Nicolas Cornette[1], Jan F.M. Van Impe[1]*

[1]KU Leuven, Department of Chemical Engineering,
BioTeC & OPTEC & CPMF[2],
Gebroeders De Smetstraat 1, B-9000 Gent, Belgium
*E-mail address: Jan.VanImpe@cit.kuleuven.be

[2]Nofima
Måltidets hus, Richard Johnsensgate 4,
4021 Stavanger Norway
E-mail address: Torstein.Skara@Nofima.no

KEYWORDS

Food model systems, processed fish products, (micro)structure, microbial kinetics

ABSTRACT

Fish products were the causative agent of 8.5% of all foodborne disease outbreaks in Europe in 2013. In order to prevent the presence of foodborne pathogens in fish products, a significant amount of those products are processed using thermal preservation. The current knowledge about the influence of food (micro)structure on microbial dynamics is limited. Suitable experimental model systems, which mimic the properties of real processed fish products, are necessary to study these factors. In this work, different fish-based model systems, suitable to study the influence of food (micro)structure on microbial dynamics, were developed. The (micro)structure of these model systems corresponded to the possible (micro)structures of food products (i.e., liquid, aqueous gel, emulsion, gelled emulsion). The compositional and (micro)structural factors of the gelled emulsion model systems were based on fish paté. The composition of the other model systems was based on the gelled emulsion, while limited variability was targeted in physicochemical properties among the different model systems. Subsequently, the developed model systems were used to study the influence of food (micro)structure on microbial growth. The target micro-organisms were *Listeria monocytogenes*, *Salmonella* Typhimurium and *Staphylococcus aureus*. The developed model systems were suitable for growth studies at temperatures of 4, 8 and 12°C.

1. INTRODUCTION

Fish products are major type consumption products in Europe. Their relevance on foodborne outbreaks has been reported. Specifically, in 2013, 8.5% of all foodborne outbreaks in Europe had fish or fish products as the causative food vehicle (EFSA and ECDC, 2015).

In order to avoid the presence of foodborne pathogens, a substantial amount of fish products are preserved using thermal processing (Rosnes et al., 2011). The sensitivity of fish products to heat-induced quality reduction makes it very challenging to design a suitable thermal process. The heat load required to inactivate pathogenic micro-organisms tends to cause undesirable sensory effects for the consumers, e.g., dry structure and flaking (Skipnes et al, 2008). In recent years, consumers have developed increased interest in minimally processed food products, which are not only nutritious, but also safe to eat. Therefore, new milder food preservation technologies are necessary (Devlieghere et al., 2004). In this regard, new thermal methods, involving a rapid or minimal heating, are a possible solution (Zwietering, 2002). The corresponding reduced heating times and temperatures will result in improved sensory quality (Skåra et al., 2002).

In this study, *Listeria monocytogenes*, *Salmonella* Typhimurium and *Staphylococcus aureus* were chosen as target micro-organisms for the following reasons. *L. monocytogenes*, causing listeriosis, is an important foodborne pathogen related to fish products (Ben Embarek, 1994). Furthermore, *L. monocytogenes* is a suitable micro-organism for thermal inactivation studies on food products, because it is one of the most heat-resistant non spore-forming foodborne pathogens (Farber and Peterkin, 1991). *Salmonella* T., causing salmonellosis, is another relevant pathogen for fish products (Wilson and Moore, 1996). In 2013, 85,268 cases of salmonellosis were reported in Europe, showing that *Salmonella* is one of the most frequently occurring foodborne pathogens (EFSA and ECDC, 2015). Finally, *S. aureus*, causing food poisoning due to the production of enterotoxins, is also a major cause of foodborne illness related to fish products (Membré and Lambert, 2008; Saito et al., 2011).

Knowledge concerning the influence of food (micro)structure on microbial dynamics is still limited (Mertens, 2010). In this regard, the limited knowledge about the influence of food (micro)structure on thermal inactivation dynamics of micro-organisms is an important issue (Velliou et al., 2013). Food model systems, which adequately simulate the properties of real food products, are essential for the development and optimization of thermal food preservation technologies. Advantages of using model systems instead of real food products for microbial studies include the possibility to alter different factors independently of each other, the absence of background microflora, and easier transferability of results to other food products (Baka et al., 2015).

In this study, experimental model systems with varying (micro)structures, simulating compositional and physico-chemical properties of processed fish products, will be developed. These model systems will be used to investigate the influence of (micro)structure on the growth of selected target micro-organisms; *L. monocytogenes*, *Salmonella* T. and *S. aureus*.

2. MODEL SYSTEM DEVELOPMENT

In order to study the effect of food (micro)structure on the microbial dynamics of foodborne pathogens in processed fish products, model systems with different (micro)structures need to be developed. Food (micro)structures have been classified in five categories: (i) liquids, (ii) aqueous gels, (iii) oil-in-water and water-in-oil emulsions, (iv) gelled emulsions and (v) surfaces (Wilson et al., 2002). For emulsions, this study only focusses on oil-in-water emulsions, because these are most relevant for fish products (Asnaashari et al., 2014).

Moreover, the composition of the model systems must be similar to the composition of the food products of interest (Baka et al., 2015). For the model systems to be used for the heat treatment, they also need to be stable at temperatures up to 70°C, as this is a treatment temperature commonly used for minimally processed food products (Rosnes et al., 2011).

For the development of the gelled emulsion model systems, compositional and (micro)structural aspects targeted fish patés. The target composition of the fish paté model system was established according to the relevant literature (Aquerreta et al., 2002; Echarte et al., 2004; Gonçalves and Ribeiro, 2008; Tahergorabi et al., 2012). The other model systems were developed based on the composition of the gelled emulsion. Table 1 shows the final target composition for the different model systems.

Table 1: Final target composition of the different model systems

Compound (%w/w)	Liquid	Aqueous gel	Emulsion	Gelled emulsion
Water	88.776	87.576	60.430	59.230
Protein	7.660	7.660	7.660	7.660
Pork fat	-	-	26.846	26.846
Starch	2.000	2.000	2.000	2.000
Agar	-	0.700	-	0.700
Guar	-	0.500	-	0.500
CITREM	-	-	1.500	1.500
NaCl	1.064	1.064	1.064	1.064
$Na_5P_3O_{10}$	0.500	0.500	0.500	0.500

A first step for the development of the different model systems is the preparation of an aqueous solution. This solution should contain all components relevant for (liquid) fish-based foods, e.g., fish protein, NaCl, preservatives, carbohydrates (Aquerreta et al., 2002; Echarte et al., 2004). Salmon protein powder (ProGo ™, Hofseth Biocare ASA, Ålesund, Norway) was used as a protein source. This aqueous solution is then used as the liquid model system and is also a starting point for the development of all other model systems. For the emulsion preparation, fat is added to the aqueous solution. Due to its good emulsification properties, pork fat was used as a fat source (Baka et al., 2015). Furthermore, pork fat is often used in commercial patés (Echarte et al., 2004). To disperse the fat in the aqueous solution, CITREM (consisting of citric acid esters) was used as an emulsifier, because it is commonly used in processed food products (Amara et al., 2014). The aqueous gel and gelled emulsion are developed by adding suitable gelling agents to the aqueous solution and emulsion, respectively. In this regard, agar and guar gum were used as gelling agents (Imeson, 2010) and their concentration was optimized experimentally.

For the preparation of the gelled emulsion model system, fish protein, NaCl, starch (soluble, Fisher, Leicestershire, UK) and pentasodium triphosphate ($Na_5P_3O_{10}$) were added to distilled water at a temperature of 7°C to prevent lump formation of the starch. Subsequently, the mixture was stirred until homogeneous. Afterwards, emulsifier, agar and guar gum were slowly added to the mixture while it was being stirred continuously and kept at a temperature of 50°C. The homogenized mixtures were sterilized for 20 min at 121°C and kept in a water bath at 80°C. Subsequently, the solution was mixed at 19,800 rpm using an homogenization probe (S 18 N - 19 G, IKA, Belgium) attached to an homogenizer (Ultra-Turrax, IKA, Belgium) while the fat (heat treated to eliminate background microflora for 2 h at 80°C) was slowly added. Finally, both mixtures were homogenized (approximately 5 minutes), poured into petri dishes and allowed to solidify. The preparation of the other model systems was similar to that of the gelled emulsion. For the emulsion, the same procedure was applied, except for the addition of agar and guar gum. For the aqueous gel no fat or emulsifier was added. For the liquid system, only protein, NaCl, starch and pentasodium triphosphate were added to distilled water, and the mixture was stirred until homogeneous.

3. GROWTH DYNAMICS IN/ON MODEL SYSTEMS

The fish-based model systems were used to investigate the influence of food (micro)structure on growth dynamics of *L. monocytogenes*, *Salmonella* T. and *S. aureus*. Experiments were conducted at temperatures of 4, 8 and 12°C. 4°C is the common refrigeration temperature, while 8 and 12°C are representative abuse temperatures, which might occur during the shelf life of fish products. These three temperatures turned out to be favorable for the stability of the emulsified model systems. Experiments were conducted in/on liquid, emulsion, aqueous gel and gelled emulsion model systems at 4, 8 and 12°C, and samples were inoculated separately with the three micro-organisms, and analyzed at different time intervals. The resulting experimental data were fitted with the model of Baranyi and Roberts (1994).

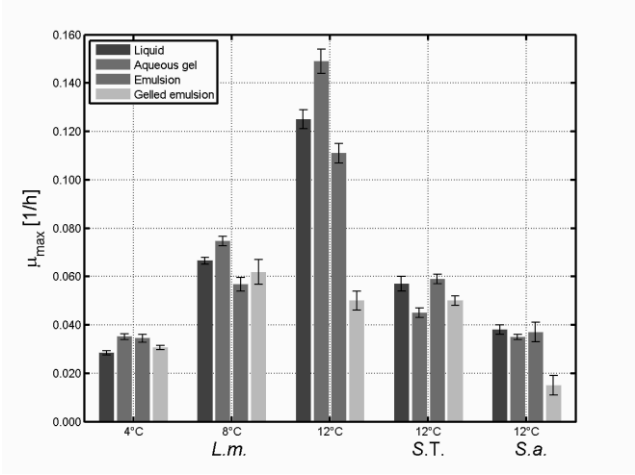

Figure 1: μ_{max} [1/h] for the three micro-organisms (*L.m.=L. monocytogenes*, *S.*T.=*Salmonella T.*, *S.a.=S. aureus*) grown at 4°C, 8°C or 12°C in/on the different model systems (liquid, aqueous gel, emulsion, gelled emulsion)

A comparison of the growth experiments for the different micro-organisms illustrated that *L. monocytogenes* exhibited the fastest growth in/on all model systems. Moreover, *L. monocytogenes* was the only micro-organism which was able to grow at temperatures of 4 and 8°C. Overall, the maximum specific growth rate (μ_{max}) in the different model systems was strongly dependent on the specific micro-organism. For *L. monocytogenes*, the highest μ_{max} was observed on the aqueous gel at all temperatures. For the other model systems, different results were

obtained at the three growth temperatures. For *Salmonella* T., μ_{max} was the highest in the liquid systems. Finally, μ_{max} of *S. aureus* in the gelled emulsion model system was lower compared to the μ_{max} obtained for the other model systems. Figure 1 summarizes the μ_{max} values for all different cases.

5. CONCLUSIONS AND FUTURE WORK

In this study, fish-based model systems were developed to investigate the influence of food (micro)structure on microbial growth-dynamics. Four different fish-based model systems were developed, i.e., liquid, aqueous gel, emulsion, gelled emulsion. The compositional and (micro)structural factors of the gelled emulsion model system were based on fish paté. The composition of the other model systems was based on the gelled emulsion, while limited variability was targeted in physicochemical properties among the different model systems. The model systems were used to study the influence of (micro)structure on growth dynamics of common foodborne pathogens. The three target micro-organisms were *L. monocytogenes*, *Salmonella* T. and *S. aureus*. The growth experiments demonstrated that the developed model systems were suitable for growth studies at temperatures of 4, 8 and 12°C. In future studies, the developed model systems should be modified to enable the study of the influence of (micro)structure on thermal inactivation of micro-organisms.

6. ACKNOWLEDGEMENTS

This work was supported by project PFV/10/002 (Center of Excellence OPTEC-Optimization in Engineering) of the KU Leuven Research Fund, projects G.0930.13 and KAN.15189.13 of the Fund for Scientific Research-Flanders, and the Belgian Program on Interuniversity Poles of Attraction, initiated by the Belgian Federal Science Policy Office (IAP Phase VII/19 DYSCO).

7. REFERENCES

Amara, S.; A. Patin; F. Giuffrida; T.J. Wooster; S.K. Thakkar; A. Bénarouche; I. Poncin; S. Robert; V. Point; S. Molinari; H. Gaussier; S. Diomande; F. Destaillats; C. Cruz-Hernandez; F. Carrière. 2014. In vitro digestion of citric acid esters of mono- and diglycerides (CITREM) and CITREM-containing infant formula/emulsions. *Food and Function*, 5: 1409-1421.

Aquerreta, Y.; A. Mohinon; J. Bello. 2002. Composition of pâtés elaborated with mackerel flesh (*Scomber scombrus*) and tuna liver (*Thunnus thynnus*): comparison with commercial fish pâtés. *Food Chemistry*, 77: 147-153.

Asnaashari, M.; R. Farhoosh; A. Sharif. 2014. Antioxidant activity of gallic acid and methyl gallate in triacylglycerols of Kilka fish oil and its oil-in-water emulsion. *Food Chemistry*, 159: 439-444.

Baka, M.; E. Noriega; K. Van Langendonck; J.F.M. Van Impe. 2015. Influence of food structure on the growth dynamics of *Listeria monocytogenes* of model systems mimicking in composition meat products, under vacuum. Submitted in *Applied and Environmental Microbiology* (Under review).

Baranyi, J. and T.A. Roberts. 1994. A dynamic approach to predicting bacterial growth in food. *International Journal of Food Microbiology*, 23: 277-294.

Ben Embarek, P.K. 1994. Presence, detection and growth of *Listeria monocytogenes* in seafoods: a review. *International Journal of Food Microbiology*, 23: 17-34.

Devlieghere, F.; L. Vermeiren; J. Debevere. 2004. New preservation technologies: Possibilities and limitations. *International Dairy Journal*, 14: 273-285.

Echarte, M.; A. Conchillo; D. Ansorena; I. Astiasarán. 2004. Evaluation of the nutritional aspects and cholesterol oxidation products of pork liver and fish patés. *Food Chemistry*, 86: 47-53.

EFSA (European Food Safety Authority) and ECDC (European Centre for Disease Prevention and Control). 2015. The European Union Summary Report on Trends and Sources of Zoonoses, Zoonotic Agents and Food-borne Outbreaks in 2013. *EFSA Journal 2015*, 13, 3991, 162 pp. doi:10.2903/j.efsa.2015.3991.

Farber, J.M. and P.I. Peterkin. 1991. *Listeria monocytogenes*, a Food-Borne pathogen. *Microbiological Reviews*, 55(3): 476-511.

Gonçalves, A.A. and J.L.D. Ribeiro. 2008. Do phosphates improve the seafood quality? Reality and legislation. *Pan-American Journal of Aquatic Sciences*, 3: 237-247.

Imeson, A. 2010. *Food Stabilizers, Thickeners and Gelling Agents*. Wiley-Blackwell, UK, Oxford.

Membré, J.-M. and R.J.W. Lambert. 2008. Application of predictive modeling techniques in industry: From food design up to risk assessment. *International Journal of Food Microbiology*, 128: 10-15.

Mertens, L. 2010. Microbial dynamics in a viscoelastic model system: Methodologies for growth/no growth assessment of yeast. PhD dissertation, KU Leuven.

Rosnes, J.T.; T. Skåra; D. Skipnes. 2011. Recent Advances in Minimal Heat Processing of Fish: Effects on Microbiological Activity and Safety. *Food and Bioprocess Technology*, 4: 833-848.

Saito, E.; N. Yoshida; J. Kawano; A. Shimizu; S. Igimi. 2011. Isolation of *Staphylococcus aureus* from raw fish in relation to culture methods. *Journal of Veterinary Medical Science*, 73(3): 287-292.

Skåra, T.; J.T. Rosnes; M. Sivertsvik. 2002. Safe and sound: Minimally processed fish products. *Food Technology International*, 2: 75-76.

Skipnes, D.; L. van der Plancken; A. Van Loey; M. Hendrickx. 2008. Kinetics of heat denaturation of proteins from farmed Atlantic cod (*Gadus mohua*). *Journal of Food Engineering*, 85: 51-58.

Tahergorabi, R.; S.K. Beamer; K.E. Mattak; J. Jaczynski. 2012. Functional food products made from fish protein isolate recovered with isoelectric solubilization/precipitation. *Food Science and Technology*, 48: 89-95.

Velliou, E.G.; E. Noriega; E. Van Derlinden; L. Mertens; K. Boons; A.H. Geeraerd; F. Devlieghere; J.F.M. Van Impe. 2013. The effect of colony formation on the heat inactivation dynamics of *Escherichia coli* K12 and *Salmonella* typhimurium. *Food Research International*, 54: 1746-1752.

Wilson I.G. and J.E. Moore. 1996. Presence of *Salmonella* spp. And *Campylobacter* spp. in shellfish. *Epidemiology and Infection*: 116: 147-153.

Wilson, P.D.G.; T.F. Brocklehurst; S. Arino; D. Thuault; M. Jakobsen; M. Lange; J. Farkas; J.W.T. Wimpenny; J.F.M. Van Impe. 2002. Modelling microbial growth in structured foods: towards a unified approach. *International Journal of Food Microbiology*, 73: 275-289.

Zwietering, M.H. 2002. Quantification of microbial quality and safety in minimally processed foods. *International Dairy Journal*, 12: 263-271.

MODELLING IN FOOD PRODUCTION

COUPLING FLUID FLOW, HEAT TRANSFER AND FOOD PRODUCT TRANSFORMATION IN A TUBULAR HEAT EXCHANGER, INCLUDING THE INFLUENCE OF CURVED SECTIONS

Artemio Plana-Fattori (*), Emilie Auger, Christophe Doursat and Denis Flick
UMR Ingénierie Procédés Aliments, AgroParisTech, INRA, Université Paris-Saclay, 91300 Massy, France

(*) author corresponding address:
AgroParisTech, Dept. MMIP, 16 rue Claude Bernard, 75231 Paris CEDEX 5
E-mail: artemio.planafattori@agroparistech.fr

KEYWORDS

chemical engineering, thermodynamics, numerical methods, partial differential equations, deterministic models

ABSTRACT

The evolution of an aqueous suspension of starch granules under continuous thermal processing is here predicted by a three-dimensional (3D) numerical model that couples the phenomena of fluid flow, heat transfer and product transformation. These phenomena are represented within an existing tubular heat exchanger. The transformation kinetics and the rheological behavior of the starch suspension come from batch experiments conducted at laboratory scale. Model predictions put in evidence the mixing role played by the curved tubes situated between successive heating sections. Predictions of the state of transformation at the exchanger outlet are compared with experimental data obtained after running the pilot unit under consideration.

INTRODUCTION

Continuous heat treatment is employed in the production of many liquid food products as a way for promoting product characteristics that are appreciated by consumers, like the texture in the case of dairy desserts (Doublier and Durand 2008). The mechanisms driving the transformation of ingredients along the processing pathway need to be understood as a necessary step for manufacturing these products in a reproducible manner. Phenomena of fluid flow, heat transfer and product transformation are strongly coupled within heat exchangers: characteristics of the product (e.g. the size of starch granules) are affected by temperature variation, with consequences on the product rheological behavior and hence on the velocity field inside the processing unit. In turn, fluid flow influences heat transfer and hence the temperature field which drives the transformation kinetics rate. The final structure of the product can therefore depend on the interactions between the ingredients, on the geometrical features of the heat exchanger, and finally on the thermal and dynamical operating conditions that are chosen in running the heat exchanger under consideration.

Computational fluid dynamics (CFD) has been employed in solving problems relevant to food science and industry (Norton et al. 2013). The coupled problem involving the phenomena of fluid flow, heat transfer and transformation of liquid products under continuous heat treatment has been studied with the help of numerical models; the influence of temperature, shear rate, and state of transformation on the product apparent viscosity has been considered in a number of cases (Liao et al. 2000, Chantoiseau et al. 2012, Bouvier et al. 2014, Plana-Fattori et al. 2013).

The numerical solution of the coupled problem inside the processing unit as well as the detailed representation of the product transformation phenomena have been, very often, limited by available computational resources. In a recent contribution (Plana-Fattori et al. 2016), we have studied the transformation of an aqueous suspension of starch granules running in a processing unit constituted by four tubular heating sections, one holding section, and a number of short curved tubes which were grouped into three "bends". In developing the numerical model, the heating and holding sections were represented as a sequence of two-dimensional (2D) axi-symmetrical computational domains, while the bends were assumed to play the role of thermally-insulated perfectly-mixed reactors. As demonstrated by pioneering experimental work (Williams et al. 1902, Eustice 1910, 1911) and later theoretical description (Dean 1927, 1928), the secondary flow which is induced by curved tubes can play a significant mixing role in reducing the heterogeneity of temperature and composition. More recently, modeling efforts have demonstrated that both the secondary flow and the mixing effectiveness depend on many factors, including the bend geometrical characteristics and the magnitude of Dean and Reynolds numbers (Kumar et al. 2006, Arada et al. 2007, Rennie and Raghavan 2010, Hajmohammadi et al. 2013, Cvetkovski et al. 2015).

Looking for the prediction of the product transformation inside a processing unit with no assumption regarding the mixing effectiveness associated with curved tubes, we argue that both the liquid product properties and the equipment geometry need to be represented as realistic as possible. In the present study, we solve the same physical problem as Plana-Fattori et al. (2016) but considering the actual three-dimensional (3D) geometrical characteristics of the heat exchanger under consideration.

COUPLED PHYSICAL PROBLEM

We are interested in the phenomena of fluid flow, heat transfer and transformation occurring in a heat exchanger running under stationary conditions. Conservation equations for mass, momentum and energy can be expressed as:

$$\vec{\nabla}.\left(\rho\,\vec{u}\right)=0 \tag{1}$$

$$\rho\left(\vec{u}\cdot\vec{\nabla}\right)\vec{u}=\vec{\nabla}\cdot\left(-p\,\vec{I}+\eta\left(\vec{\nabla}\vec{u}+\left(\vec{\nabla}\vec{u}\right)^{T}\right)-\frac{2}{3}\eta\left(\vec{\nabla}\cdot\vec{u}\right)\vec{I}\right) \tag{2}$$

$$\rho C_P\left(\vec{u}\cdot\vec{\nabla}\right)T=\vec{\nabla}\cdot\left(\lambda\,\vec{\nabla}T\right) \tag{3}$$

where $\vec{u}$ is the velocity (magnitude in $m.s^{-1}$), p the pressure (Pa), and T the temperature (K); ρ is the product density ($kg.m^{-3}$), C_P its specific heat capacity ($J.kg^{-1}.K^{-1}$), λ its thermal conductivity ($W.m^{-1}.K^{-1}$), and η its apparent viscosity (Pa.s).

The liquid product is an aqueous suspension of modified waxy maize starch. Under heating, this product undergoes a quite simple transformation: starch granules swell with neither rupture of swollen granules nor release of soluble species in water. The degree of swelling S can be defined as

$$S=\left(D-D_0\right)/\left(D_{MAX}-D_0\right) \tag{4}$$

where D (m) is the volume mean diameter of granules; values D_0 and D_{MAX} correspond to the conditions found before any thermal treatment (uncooked starch) and after the maximum thermal treatment considered, respectively. The variation in the degree of swelling over time can be written using a second-order kinetics equation (Lagarrigue et al. 2008). The coupling between starch swelling, heat transfer and fluid flow is expressed in the following equation:

$$\vec{u}\cdot\vec{\nabla}S=V\{T\}\left(1-S\right)^2+\vec{\nabla}\cdot\left(d_S\,\vec{\nabla}S\right) \tag{5}$$

where d_S is a diffusion coefficient ($m^2.s^{-1}$), and V is the temperature-dependent kinetics rate (s^{-1}).

We consider here the swelling kinetics and the rheological behavior which were obtained by Plana-Fattori et al. (2016) for a 3.42 % (w/w) modified waxy maize starch suspension, after submitting small volumes of suspension to a number of heat treatments under continuous stirring. Those authors found that no significant swelling occurs at temperatures lower than a threshold value Ta, and that above this value the swelling kinetics rate V can be approximated as being directly proportional to the temperature:

$$V\{T\}=Va\,(T-Ta) \tag{6}$$

where Ta = 61.1 °C and Va = 3.79 10^{-3} $s^{-1}.°C^{-1}$. Further, those authors represented the shear-thinning behavior of the starch suspension through the power-law

$$\eta\{\dot{\gamma},\Phi,T\}=K\{\Phi,T\}\,\dot{\gamma}^{n\{\Phi\}-1} \tag{7}$$

where K is the product consistency coefficient ($Pa.s^n$), n the product flow behavior index, $\dot{\gamma}$ the shear rate (s^{-1}) and η_{water} the dynamic viscosity of pure water (Pa.s). Both the consistency coefficient and the flow behavior index depend on the volume fraction Φ occupied by starch granules:

$$K\{\Phi,T\}=k_1\,exp\left(k_2\,\Phi\right)\,\eta_{water}\{T\} \tag{8}$$

$$n\{\Phi\}=n*+(1-n*)\,exp(-k_3\,(\Phi-\Phi_0)) \tag{9}$$

with k_1 = 0.662 s^{n-1}, k_2 = 13.6, k_3 = 4.91, $n*$ = 0.55, and Φ_0 = 0.0342. The solid volume fraction can be expressed as a function of the volume mean diameter:

$$\Phi=\Phi_0\left(D/D_0\right)^3 \ . \tag{10}$$

NUMERICAL MODEL

Figure 1 displays the heat exchanger considered: it is constituted of four tubular heating sections, curved tubes (bends), and the holding section. Along the heating sections, the product executes counter-flow with respect to super-heated water; along the holding section and the bends, it travels under thermally-insulated conditions. All the sections have a radius of 4 mm, and heating sections are 80 cm long. Considering a volume flow rate of 15 L/h, the mean residence time in the heat exchanger is about 50 s.

The product density, specific heat capacity, and thermal conductivity are assumed to follow those for pure water, because the relatively low mass concentration of starch in the suspension (3.42 %).

The tri-dimensional characteristics of the heat exchanger suggest us to consider the plane of symmetry which cuts it into two identical halves. Restricting our attention to one of these halves only, the half-sections of the heat exchanger can be grouped into four entities:

- 1st heating section only;
- 1st bend and 2nd heating section;
- 2nd bend, holding section and 3rd heating section;
- 3rd bend and 4th heating section.

The coupled physical problem is solved successively for each of these computational domains, by taking into account the following boundary conditions:

- at the inlet of the 1st heating section, the product is assumed to flow according to a fully-developed velocity field, containing uncooked starch granules only ($S = 0$) at temperature T_A ;
- at the inlet of the other sections, the outlet profiles of the previous section are considered;
- at the outlet of each domain, the product is assumed to flow normally to the boundary under no viscous stress, with neither conduction nor diffusion ; and
- at the walls, the velocity field vanishes; the product is submitted to an inward flux in the case of the heating walls, and to a null heat flux (thermally-insulated conditions) in the case of the bends and the holding section.

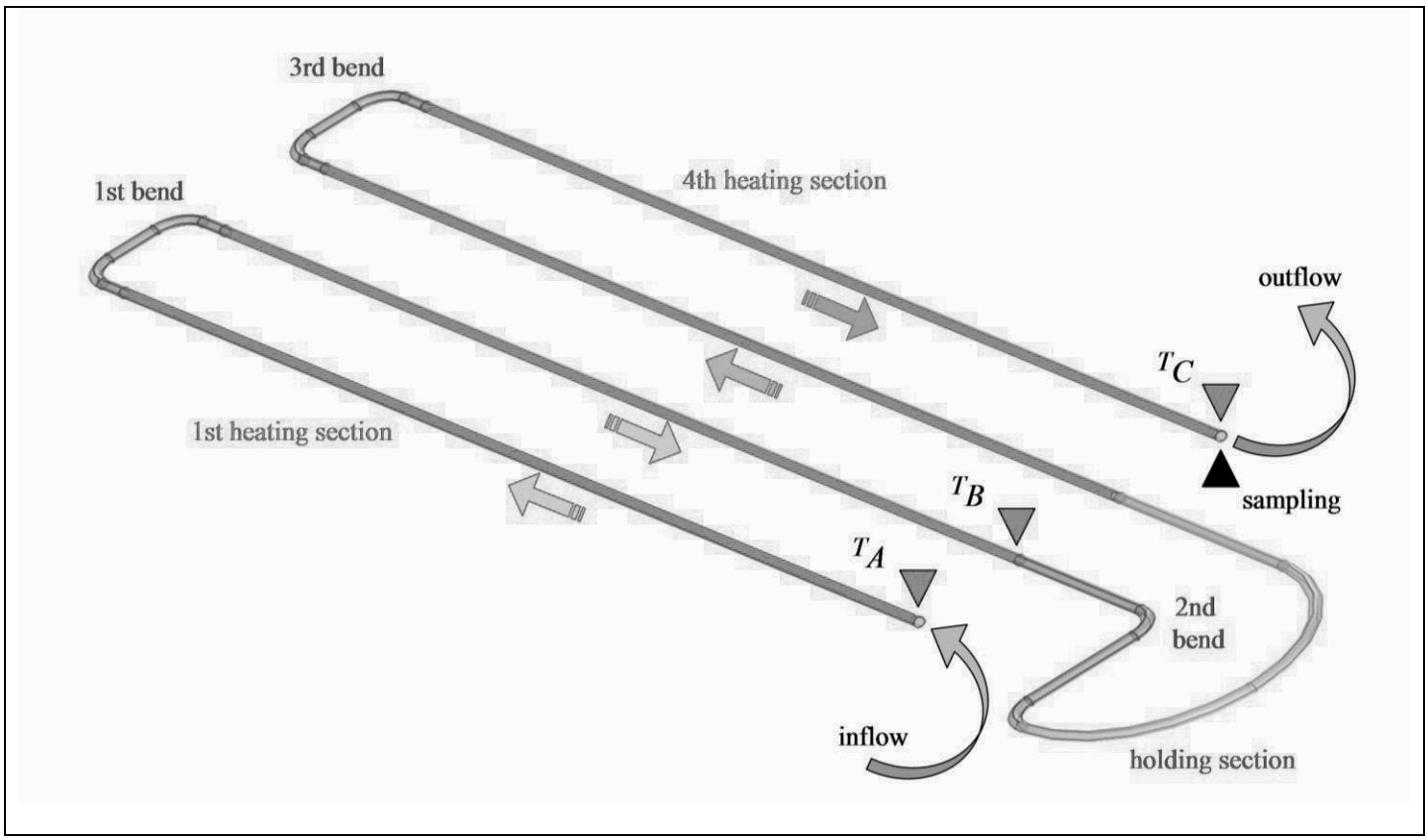

Figure 1: Schematic representation of the heat exchanger. Red triangles indicate the positions where the temperature of the product is measured, and the black triangle the sampling position of transformed product at the exchanger outlet.

Some of these boundary conditions translate the operating conditions that were specified in running the pilot unit under consideration. The volume flow rate was 15 L/h, (mean velocity of 0.083 $m.s^{-1}$); at the exchanger inlet, the Reynolds number is 1040. The product temperature was measured at selected positions (see Fig. 1): T_A = 43.9 °C, T_B = 60.1 °C, and T_C = 70.0 °C; these measurements allowed us to estimate, through global energy budget considerations, the averaged inward heat flux to be applied as boundary condition at the walls of the first and the second heating sections (6910 W/m^2) and at the walls of the third and the fourth heating sections (4050 W/m^2).

Looking for the resolution of equations which govern the coupled phenomena, every computational domain has to be subdivided into a number of small, non-overlapping cells (the mesh elements). The tri-dimensional characteristics of the domains suggest us to build a non-structured mesh, constituted of: a) five-faced prisms along a double boundary layer which follows the walls, and b) tetrahedral elements in the interior of the domains. The ratio between the maximum and the minimum element sizes is set to be two, and the minimum element size is set to be 1/6 of the radius of sections (R = 4 mm). The resulting mesh leads, in the case of the third computational domain, to a numerical problem with about 4.9 10^6 degrees of freedom. Such a mesh is the finest one allowed by our memory capabilities (192-Gb RAM). The whole problem, including all the four domains, correspond to about 1.3 10^7 degrees of freedom. Figure 2 exhibits the first centimeters of the heat exchanger, above the plane of symmetry, putting in evidence the mesh built as described above.

Governing equations (1, 2, 3, 5) are solved through the finite-element method as implemented in the simulation package COMSOL Multiphysics 4.4 (Zimmermann 2006). In discretizing those equations, first-order Lagrange finite elements are employed for the pressure, and second-order for the velocity components, the temperature, and the degree of swelling.

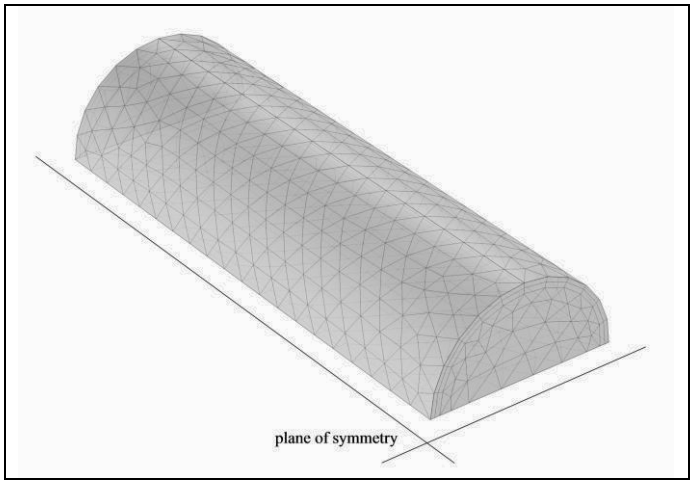

Figure 2: Close-up view of the mesh at the exchanger inlet.

The large linear system obtained after discretization of governing equations is solved through the Multifrontal Massively Parallel Sparse Direct Solver (MUMPS; Amestoy et al. 2006). Satisfactory convergence of the numerical model is reached after assuming the diffusion coefficient $d_S = 10^{-8}$ $m^2.s^{-1}$ in equation (5).

RESULTS

Figures 3 and 4 show model predictions of selected variables in the fourth heating section, where both temperature and degree of swelling reach their highest values in the heat exchanger. Results are displayed in the plane of symmetry, more specifically along the first 10 cm (Figure 3) and along the last 10 cm (Figure 4) of this heating section.
The phenomena of fluid flow, heat transfer and starch swelling are coupled in the heat exchanger. It can be appreciated by comparing results at the exchanger outlet (Figure 4): fluid parcels running at the axis of the section move faster and are hence less exposed to heating and transformation than those running in the vicinity of the heating wall. As a matter of fact, the coupling is two-way: after an increase in the apparent viscosity near the wall, fluid parcels running there are slowed down (and their exposure to heating becomes longer), while those running at the axis of the section experience some acceleration and therefore a shorter exposure to heating.
The upper display in Figure 3 shows that the distribution of the velocity magnitude exhibits an asymmetric behavior between the outer and the inner edges of the heating section; such an asymmetry progressively disappears along the heating section. This can be identified in the distribution of the three other variables. We cannot dissociate such a behavior from the fact that, upstream to the heating section, there are placed an ensemble of curved tubes.

Secondary flow in bends

Experiments conducted in the early 1900's showed that the location of maximum velocity in curved tubes is displaced towards the outer wall due to the presence of secondary currents; such a feature is due to the centrifugal forces, which raise a secondary flow consisting of a pair of counter-rotating cells (the so-called Dean cells).
Results about this issue as provided by our 3D numerical model can be appreciated for the first (Figure 5) and the third (Figure 6) bends of the heat exchanger under consideration. Both bends are constituted of three short tubular sections, separated by two 90° turns. Display in Figures 5 and 6 present:

- firstly, the 2D distribution for a selected variable throughout each of eleven particular cross-sections situated between the bend inlet and its outlet; starting at the fluid inflow, these cross-sections are oriented 0°, 0°, 30°, 60°, 90°, 90°, 120°, 150°, 180°, and 180° with respect to the bend inlet;
- secondly, a close-up view of the same variable throughout the cross-section which is oriented 30° with respect to the bend inlet;
- lastly, with the help of a number of arrows, the 2D distribution of the velocity component which is parallel to this particular cross-section.

Display A in Figure 5 puts in evidence the displacement of the maximum velocity towards the outer wall along the first 90° turn. Clockwise secondary flow takes place above the plane of symmetry: firstly, such a flow displaces towards the inner edge the fluid parcels which are running near the outer wall; secondly, this flow displaces towards the outer edge the parcels which are running at the axis of bend.
Displays B and C present the consequences of the secondary flow on an indicator of heat transfer (temperature) and one of product transformation (volume mean diameter). The warmest fluid parcels, associated with the highest state of transformation, are displaced towards the inner edge after the first 90° turn; near the walls, fluid parcels are cooler and associated with a smaller state of transformation than at the bend inlet. Additional re-distribution of fluid parcels takes place after the second 90° turn.
Displays B and D in Figure 5 show that the lowest temperature correspond to the highest apparent viscosity. The influence of temperature on the apparent viscosity is here assumed to follow the behavior associated with pure water (eq. 8). Under weak starch swelling, the influence of the temperature on the apparent viscosity is dominant.
The first and the third bends are geometrically identical but placed at different positions along the pathway followed by the starch suspension in the heat exchanger; hence, they correspond to different times in the dynamical / thermal / kinetics history of fluid parcels of the starch suspension travelling in the heat exchanger.
Figures 5 and 6 are similar regarding the secondary flow pattern, putting in evidence the role played by the curved tubes. Changes in the velocity magnitude are minor between the first and the third bends; the maximum velocity at the 30° cross-section decreases slightly from the first to the third bend. These changes can be associated with the decrease of the product flow behavior index from the first to the third bend (see below).
Displays B in Figures 5 and 6 show that the third bend is associated with temperatures which are, at almost all its points, higher than those found in the first bend. At the inlet of the third bend, the temperature amplitude (7.1 °C) is smaller than at the inlet of the first bend (24.1 °C); in both cases, the temperature amplitude decreases along the bend as a consequence of the secondary flow.
Displays C in Figures 5 and 6 show that the starch suspension reaches a higher state of transformation after exposure to a longer pathway under heating. In both cases, the highest volume mean diameters occur for the fluid parcels associated with the highest temperatures; similarly to the temperature, the amplitude of volume mean diameters decreases between the bend inlet and its outlet.
Displays C and D in Figure 6 show that the apparent viscosity is closely related to the state of transformation in the third bend. Such a finding reflects an inverse situation to that observed in the first bend, where the role played by the temperature is dominant. Comparing the first and the third bends, the apparent viscosity values exhibit the same order of magnitude but different 3D distributions.

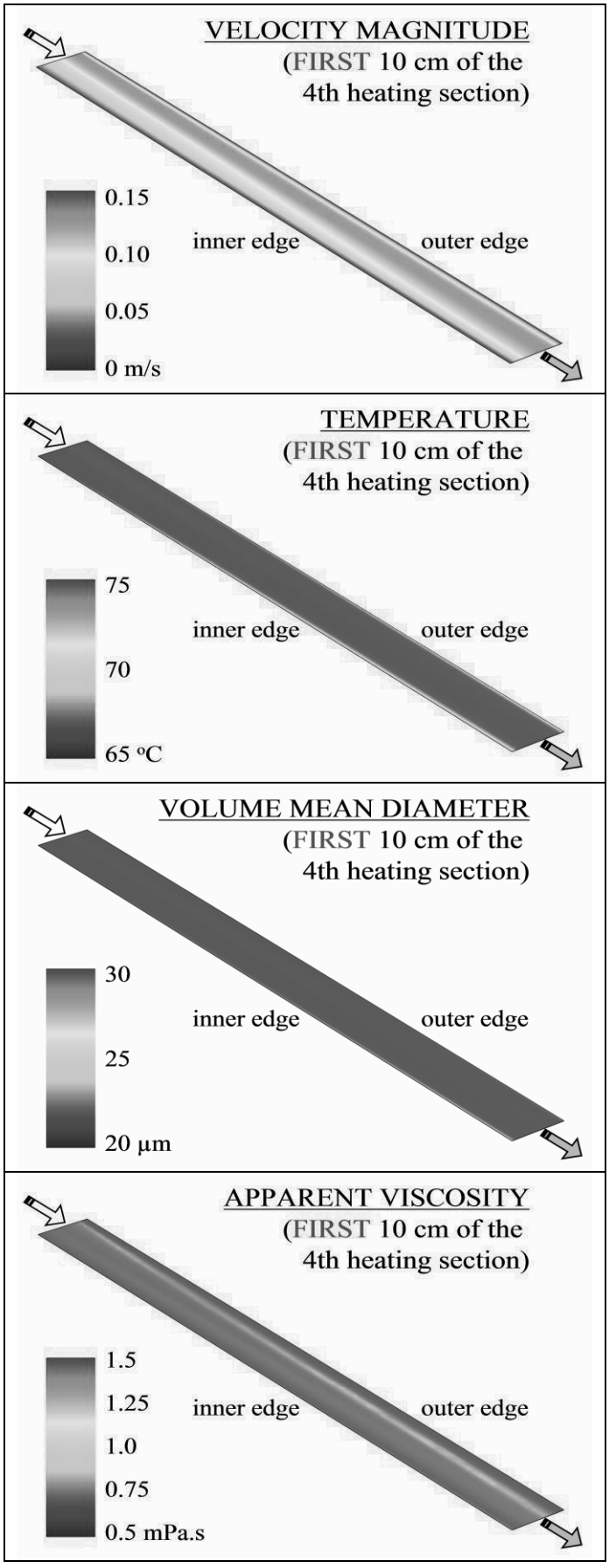

Figure 3: Selected results along the first 10 cm of the fourth heating section.

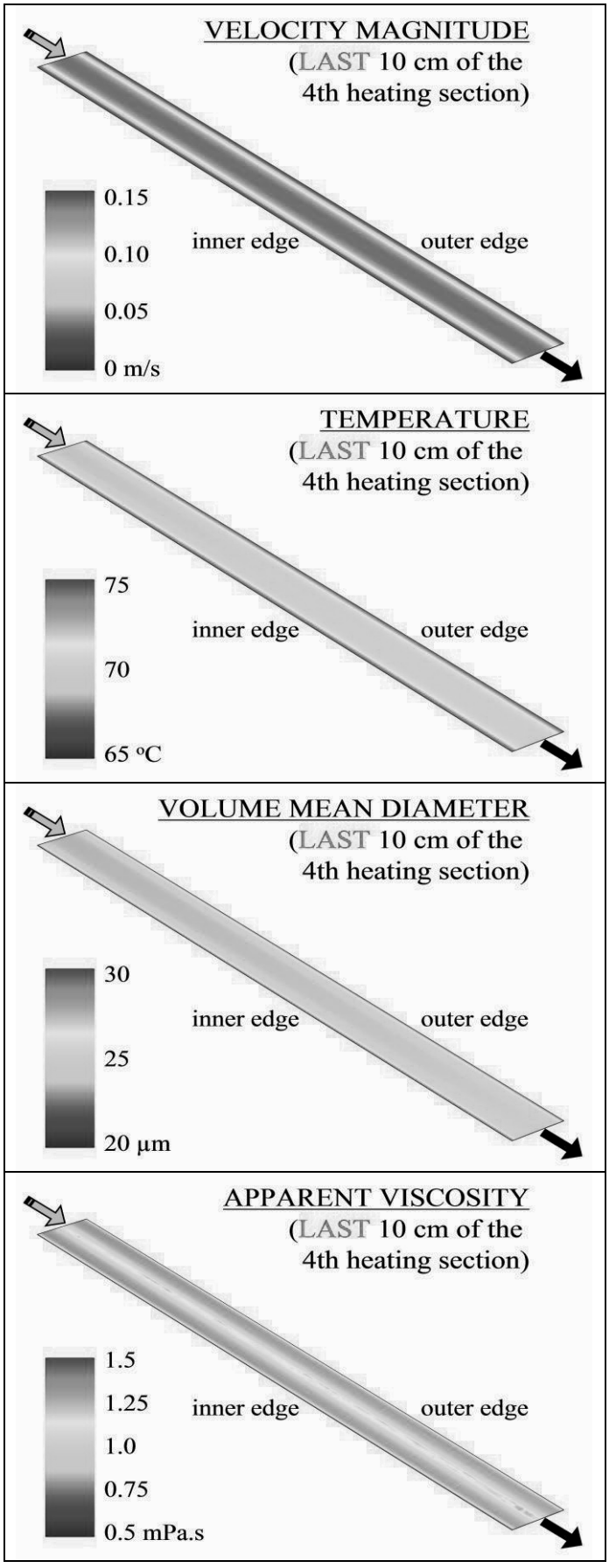

Figure 4: Selected results along the last 10 cm of the fourth heating section.

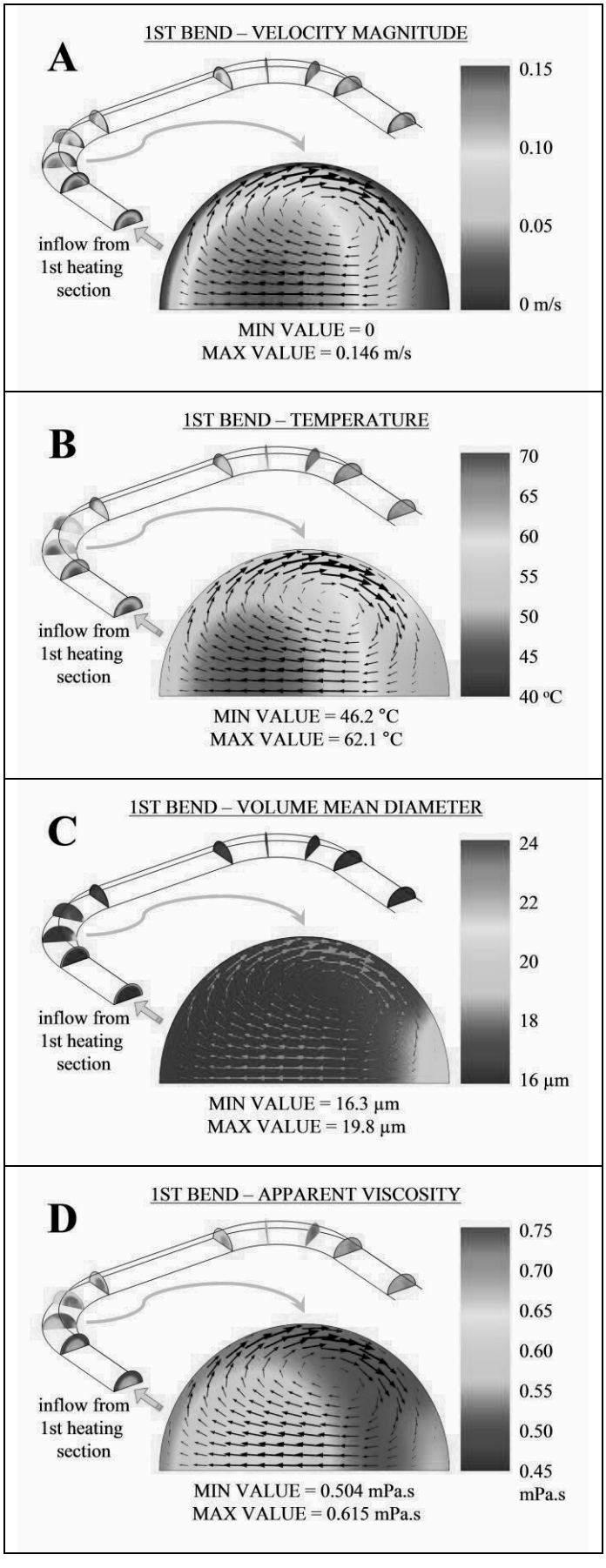

Figure 5: Selected results in the first bend, including close-up views at the 30° cross-section.

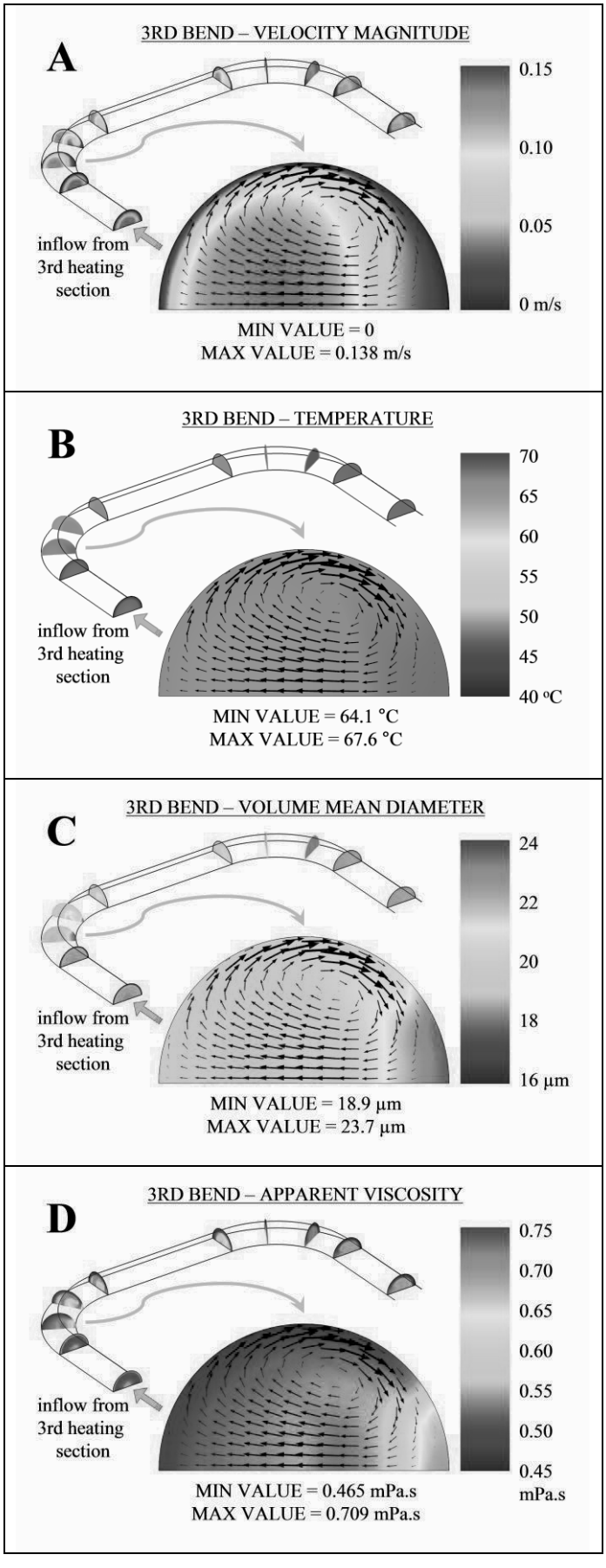

Figure 6: As in the previous figure but for the third bend.

A number of indicators have been proposed in order to quantify the mixing effectiveness which can be induced by the secondary flow occurring in curved tubes. Under negligible mixing, the standard deviation of the temperature at the bend outlet, $\sigma_T\{o\}$, should be identical to its value at the bend inlet, $\sigma_T\{i\}$; under full mixing, the standard deviation should vanish at the bend outlet. The mixing effectiveness can therefore be defined as $1 - \sigma_T\{o\} / \sigma_T\{i\}$, being equal to zero under no mixture at all, and to one under full mixing. Each standard deviation value is here calculated as a mass-weighted (bulk) average, i.e. by using the normal velocity as the weighting-factor for the squared differences between the temperature and its mean value over the boundary. We obtain 78 % and 81 % for the mixing effectiveness in the first and the third bends of the heat exchanger here considered, respectively. Firstly, the mixing effectiveness is lower than the unity for both bends; they do not act as perfectly-mixed reactors, at least for heat transfer. Secondly, the mixing effectiveness can differ from a bend to another, or more precisely from a position to another of the liquid product history.

Final state of transformation

Numerical model simulations can be assessed by comparing its predictions, or derived quantities, with experimental results which had not been taken into account in developing the model. Both the swelling kinetics and the rheological behavior of the starch suspension considered in the model follows Plana-Fattori et al. (2016); they are based on batch experiments where small volumes of suspension were submitted to a number of heat treatments under continuous stirring at laboratory scale, hence without any experimental work with the heat exchanger under consideration.

Experimental results were obtained after running the heat exchanger by specifying the volume flow rate 15 L/h and the temperature T_C = 70.0 °C. The starch suspension was sampled three times at the outlet of the fourth heating section (Figure 1), with a separation of 5 minutes between successive samplings; each sample was immediately cooled down to about 4 °C, in order to reduce the influence of additional product transformation. The analysis of the size distributions associated with the three samples provided volume mean diameters with average 23.6 µm and standard deviation 0.4 µm.

Considering these operating conditions, the application of the numerical model provides a mass-weighted value of 11.2 % for the solid volume fraction at the outlet of the fourth heating section; it corresponds to a volume mean diameter of 24.2 µm and a degree of swelling of 29.3 %.

Starch swelling from experiment and numerical model can be compared in terms of the increase $D - D_0$ in volume mean diameter, by computing the difference between the values at the fourth heating section's outlet and at the heat exchanger's inlet. Considering the value D_0 = 16.3 µm obtained by Plana-Fattori et al. (2016) for the starch suspension here considered, we obtain $D - D_0$ = 23.6 – 16.3 = 7.3 µm after running the heat exchanger, and $D - D_0$ = 24.2 – 16.3 = 7.9 µm from the 3D numerical model.

It must be noted that our memory capabilities forbid any improvement regarding the mesh resolution to be considered in solving the coupled problem in the third computational domain. All the results presented above were obtained by considering meshes in which the minimum element size (ℓ) was set to be 1/6 of the section radius (R = 4 mm). Tests were conducted in order to preliminarily assess the influence of the mesh resolution, restricting our attention to the coupled problem in the fourth computational domain only (3rd bend and 4th heating section), where the temperature and the product state of transformation are the highest. Results previously obtained in this computational domain were compared with those obtained by taking into account a coarser mesh (ℓ = 1/5) and a finer mesh (ℓ = 1/7 of the section radius). After considering these two additional meshes, we can compare three predictions of the volume mean diameter of starch granules at the outlet of the heat exchanger: D = 24.18 µm (ℓ = 1/5), 24.22 µm (ℓ = 1/6) and 24.25 µm (ℓ = 1/7 of the section radius). These results were obtained after solving numerical problems with about 1.4, 3.0, and 4.3 10^6 degrees of freedom, respectively. The level of agreement between these predictions can be considered satisfactory; they are clustered between +0.5 and +0.7 µm in respect to the experimental averaged value (D = 23.6 µm).

CONCLUSIONS AND WORK UNDERWAY

The coupled physical problem of fluid flow, heat transfer and starch swelling can effectively be studied with a 3D numerical model, after including the main geometrical features of the tubular heat exchanger under consideration as well as the representation of operating (thermal and dynamical) conditions adopted in running the heat exchanger. The mathematical problem to be solved is relatively expensive in computer time and memory, even after subdividing the heat exchanger into four computational domains. Such a subdivision is possible for stationary case studies only, and its implementation requires the adoption of appropriate boundary conditions.

In the case study here illustrated, the numerical model overestimates the increase in volume mean diameter by about 8 %. A number of reasons can contribute to explain the differences between predictions from model and results from experiment. Firstly, we are aware that the resolution of the mesh adopted in the numerical model is a major issue. In choosing an unique mesh resolution throughout all the four computational domains, we have looked for consistence rather than for accuracy of model predictions. Secondly, starch swelling under heat treatment is here assumed to follow a single temperature-dependent swelling kinetics (equation 6), independently on the granule size. Starch granules have, in fact, different initial sizes. The influence of starch granule size on the swelling onset has been scarcely studied (Myllarinen et al. 1998, Sasaki and Matsuki 1998); nevertheless, no generalization seems possible regarding the starch type. Finally, we cannot discard some experimental bias in sampling the starch suspension while it flows in the heat exchanger.

Work underway includes complementary tests regarding the convergence of numerical model predictions in respect to the mesh resolution. In parallel, we have used an optical microscope coupled to a warming plate, in order to continuously observe the behavior of starch granules during thermal treatments. Preliminary results suggest that, in the case of modified waxy maize starch (as considered in the present study), the swelling mechanism presents some stochastic nature while being associated with diffusion of surrounding water into the starch granule.

ACKNOWLEDGEMENTS

The research leading to these results received funding from the Carnot Institute Qualiment (INRA, France). Authors are sincerely indebted to the COMSOL support team for their effective assistance, to Germain Fernandez (INRA) for his kind help regarding the cluster computing capabilities, and to Professors Camille Michon, Fabrice Ducept and Bertrand Broyart (AgroParisTech) for their friendly encouragement on this subject.

REFERENCES

Amestoy, P. R.; A., Guermouche; J.-Y. L'Excellent; and S. Pralet. 2006. "Hybrid scheduling for the parallel solution of linear systems." *Parallel Computing*, 32, 136-156.

Arada, N.; M. Pires; and A. Sequeira. 2007. "Viscosity effects on flows of generalized Newtonian fluids through curved pipes." *Computers and Mathematics with Applications*, 53, 625-646.

Bouvier, L.; A. Moreau; G. Ronse; T. Six; J. Petit; and G. Delaplace. 2014. "A CFD model as a tool to simulate beta-lactoglobulin heat-induced denaturation and aggregation in a plate heat exchanger." *Journal of Food Engineering*, 136, 56-63.

Chantoiseau, E.; A. Plana-Fattori; C. Doursat; and D. Flick. 2012. "Coupling fluid flow, heat transfer and thermal denaturation-aggregation of beta-lactoglobulin using an Eulerian/Lagrangian approach." *Journal of Food Engineering*, 113, 234-244.

Cvetkovski, C. G.; S. Reitsma; T. Bolisetti; and D. S. K. Ting. 2015. "Heat transfer in a U-bend pipe: Dean number versus Reynols number." *Sustainable Energy Technologies and Assessments*, 11, 148-158.

Dean, W. R. 1927. "Note on the motion of fluid in a curved pipe." *Philosophical Magazine (Series 7)*, 4, 208-223.

Dean, W. R. 1928. "The stream-line motion of fluid in a curved pipe (second paper)." *Philosophical Magazine (Series 7)*, 5, 673-695.

Doublier, J. L. and S. Durand. 2008. "A Rheological Characterization of Semi-Solid Dairy Systems." *Food Chemistry*, 108, 1169-1175.

Eustice, J. 1910. "Flow of water in curved pipes." *Proceedings of the Royal Society of London (Series A)*, 84, #568, 107-118.

Eustice, J. 1911. "Experiments on stream-line motion in curved pipes." *Proceedings of the Royal Society of London (Series A)*, 85, #576, 119-131.

Hajmohammadi, M. R.; H. Eskandari; M. Saffar-Avval; and A. Campo. 2013. "A new configuration of bend tubes for compound optimization of heat and fluid flow." *Energy*, 62, 418-424.

Kumar, V.; M. Aggarwal; and K. D. P. Nigam. 2006. "Mixing in curved tubes." *Chemical Engineering Science*, 61, 5742-5753.

Lagarrigue, S.; G. Alvarez; G. Cuvelier; and D. Flick. 2008. "Swelling kinetics of waxy maize and maize starches at high temperatures and heating rates." *Carbohydrate Polymers*, 73, 148-155.

Liao, H.-J.; M. A. Rao; and A. K. Datta. 2000. "Role of thermo-rheological behaviour in simulation of continuous sterilization of a starch dispersion." *Transactions of the Institution of Chemical Engineers*, 78C, 48-56.

Myllarinen, P.; K. Autio; A. H. Schulman; and K. Poutanen. 1998. "Heat-induced structural changes of small and large barley starch granules." *Journal of the Institute of Brewing*, 104, 343-349.

Norton, T.; B. Tiwari; and D.-W. Sun. 2013. "Computational Fluid Dynamics in the design and analysis of thermal processes: A review of recent advances." *Critical Reviews in Food Science and Nutrition*, 53, 251-275.

Plana-Fattori, A.; E. Chantoiseau; C. Doursat; and D. Flick. 2013. "An Eulerian-Lagrangian approach for coupling fluid flow, heat transfer, and liquid food product transformation." *Computers and Chemical Engineering*, 52, 286-298.

Plana-Fattori, A.; D. Flick; F. Ducept; C. Doursat; C. Michon; and S. Mezdour. 2016. "A deterministic approach for predicting the transformation of starch suspensions in tubular heat exchangers." *Journal of Food Engineering*, 171, 28-36.

Rennie, T. J. and V. G. S. Raghavan. 2010. "Numerical analysis of the lethality and processing uniformity in a double-pipe helical heat exchanger." *Chemical Engineering and Processing*, 49, 672-679.

Sasaki, T. and J. Matsuki. 1998. "Effect of wheat starch structure on swelling power." *Cereal Chemistry*, 75, 525-529.

Williams, G. S.; C. W. Hubbell; and G. H. Fenkell. 1902. "Experiment at Detroit, Mich., on the effect of curvature upon the flow of water in pipes." *Transactions of the American Society of Civil Engineers*, 47, 1-196.

Zimmerman, W. B. J. 2006. *Multiphysics Modelling with Finite Element Methods*. World Scientific, Singapore.

BIOGRAPHIES

ARTEMIO PLANA-FATTORI was born in Brazil; he studied Atmospheric Sciences in the Univ. de Sao Paulo and later in the Univ. Lille 1 (Ph.D. in 1994). After 20 years teaching and conducting research in Brazil, he joined AgroParisTech in 2010, where he has been working with numerical modeling applied to food engineering.

EMILIE AUGER was born in Fontenay-le-Comte, France. She obtained in 2013 her diploma in climatic and energy engineering. After a Master degree in the Université Pierre-et-Marie-Curie at Paris (specialization: "Tools and Methods for Zero Energy Buildings"), which included a four-months research training with Artemio, Christophe and Denis at AgroParisTech, she became a teacher.

CHRISTOPHE DOURSAT is Professor at AgroParisTech.

DENIS FLICK is Full Professor at AgroParisTech. He conducts research in modeling and numerical simulation of coupled phenomena in food processes (heat and mass transfer, fluid flow and product deformation, product transformation), with applications in food cold chain equipment, heat exchangers, cooking and baking, dairy products, bread, and ice cream. His teaching area includes transport phenomena, thermodynamics, and numerical modeling.

CLASSIFYING BEEF CARCASSES ACCORDING TO MEAT QUALITY USING ANIMAL/CARCASS CHARACTERISTICS AND pH/TEMPERATURE DECLINE DESCRIPTORS EARLY *POST-MORTEM*

Cristina Xavier*
Ursula Gonzales-Barron
Vasco Cadavez
CIMO Mountain Research Centre
School of Agriculture, Polytechnic
Institute of Braganza, Portugal

Alexandra Müller
ICBAS Institute of Biomedical
Sciences Abel Salazar
University of Porto, Portugal

*E-mail: cristina_fx@hotmail.com

KEYWORDS
Fat, Shortening, Tenderness, Classification, Modelling .

ABSTRACT
During beef carcass chilling, the eating quality of meat can be severely affected by either hot- or cold-shortening. With basis on previous knowledge that meat of optimal tenderness can be produced when rigor mortis (pH=6.0) is attained when carcass temperature falls between 12-35ºC, the objective of this study was to predict meat quality from modelled pH/temperature decay descriptors and informative animal/carcass characteristics. Temperature and pH from a total of 103 beef carcasses were logged during 24 h post mortem, and subsequently modelled by exponential decay equations that estimated temperature (k_T) and pH (k_{pH}) decay rates. In addition, a number of pH/temperature decay descriptors were estimated from the fitted models. From linear models adjusted to each of these descriptors, it was found that, generally, hot carcass weight, age, gender and class (male, female, young animals) had significant influence on pH/temperature decay. Thus, bringing together the orthogonal variables k_T and k_{pH}, and the aforementioned animal/carcass characteristics as linear predictors of discriminant functions, a classification analysis was performed. While cold-shortened and hot-shortened carcasses were classified correctly for all samples, optimal quality carcasses were correctly classified in 87.5% of the samples.

INTRODUCTION

The inconsistency in the eating-quality characteristics of meat, predominantly tenderness, is one of the problems faced by the meat industry worldwide. Moreover, the importance of providing end-users with a food product of consistent quality has never been greater (Simmons et al. 2006). Thus, a top priority factor in the success of meat industry relies on the ability to deliver specialities that satisfy the consumer's taste requirements (Cortez et al. 2006). Since for the consumers the beef sensory attribute is most important in their individual assessments of overall eating satisfaction, tenderness is the primary consideration (Fergurson 2004).

However, meat tenderness is a complex trait that is influenced by a variety of factors, many of which can be managed systematically to reduce the incidence of tenderness problems in the final product (Platter et al. 2003). Muscle pH and temperature decline continuously interact during rigor development to affect both muscle contracture and proteolytic enzyme activity (Tornberg 1996). High temperature accelerates the pH decline in muscle and during this period, the rate of decrease in pH and the ultimate pH of meat are highly variable (Kahraman et al. 2012). The combination of a very rapid pH decline with a slow chilling regime causes heat shortening, which is an increase in toughness due to sooner exhaustion of μ-calpain at high carcass temperatures, leaving less potential for ageing. On the other end, the phenomenon of cold shortening emerges if the pH decline is too slow, remaining high while the temperature falls (Roça 2000). Cold-shortened carcasses produce tougher meat than hot-shortened ones do.

Hwang et al. (2003) showed that, in order to minimise cold-shortening – to enhance tenderisation, the muscle temperature should not be lower than 11°C before muscle pH reaches 6.1–6.3. When the process of glycolysis develops slowly, the initial pH (right after slaughter), which is about 7.0, goes down to 6.4-6.8 after 5 hours, and subsequently to 5.5-5.9 after 24 hours (Roça 2000). If, due to a deficiency of glycogen, the final pH (after 24 hours) remains high, above 6.2, the muscle turns into DFD meat (dark, firm, dry), so the limit value for emergence of DFD meat is pH 6.0 (Bianchini et al. 2007). The concept of ideal "window" was conceived to be used as a specification to describe the relationship between carcass pH and temperature from slaughter to when ultimate pH is reached (Thompson 2002; Ibarburu et al. 2007). The window requires the carcass pH to be greater than 6.0 while the carcase temperature is above 35°C and below 6.0 before the temperature falls below 12°C. If the rate of pH temperature decline does not fall through this ideal window, the carcass tenderness is compromised, either by hot- or cold-shortening.

Thus, the objective of this study is three-fold. The first objective is to model the decrease in temperature and pH during chilling of beef carcasses early post-mortem so that

pH and temperature decline rates can be accurately estimated. The second objective is to evaluate whether live-animal/carcass characteristics (i.e., sex, weight, age, breed, class, fat, conformation, and transport and lairage time) have any influence on pH and temperature decline rates; or, instead, the muscle shortening occurring during rigor mortis outweighs the effects of live-animal factors in determining meat quality. Once the significant live-animal/carcass characteristics affecting pH and temperature decline are identified, linear discriminant analysis that classifies beef carcasses quality (i.e., tenderness) into (i) optimal quality, (ii) cold-shortened and (iii) hot-shortened, is to be developed taking into account the ideal "window" rule.

MATERIALS AND METHODS

Beef animals

In this study, a total of 103 beef animals (68 cross-breed and 35 of Mirandesa breed), 68 males and 35 females, slaughtered in a local abattoir were sampled. The animals had an age of 10.1 ± 2.32 months when killed at one abattoir located in the Northeast of Portugal. The animals were transported by truck to the abattoir; and, at arrival, they were kept in individual stalls until slaughtering. They were not fed but did receive water *ad libitum*. After electric stunning, animals were slaughtered and dressed sequentially. Resulting carcasses had an average hot carcass weight of 209.7 ± 65.60 kg. For each of the animals/carcasses, the following live-animal/carcass characteristics were annotated: sex, age, breed, transport time, lairage time, hot carcass weight, animal class, the SEUROP class from the European beef carcass classification scheme for conformation and degree of fat cover of the carcass.

Temperature and pH recording

Approximately two hours after slaughter, pH and temperature were recorded at intervals of 10 min during 24 h of carcass chilling, in *longissimus thoracis* muscle at the level of the 4th rib. The pH and temperature measurements were made using a weather resistant wireless transmitter CRISON pH probe (Crison Instruments, SA, Spain, SP) and wireless transmitter OMEGA temperature probe Pt 100 (Omega Engineering Limited, United Kingdom, UK) connected to an OMEGA UWTC-REC1 wireless channel receiver/host (Omega Engineering Limited, United Kingdom, UK).

Statistical modelling

Fitting exponential decay models

The pH and temperature decline *post-mortem* (p.m.) were modelled as a function of time using the parameterisation of the exponential decay function proposed by Hwang and Thompson (2001). For modelling pH measured as a function of time pH(t), the three-parameter decay function was defined as,

$$pH(t) = pH_0 + (pH_0 - pH_\infty)\exp(-k_{pH}t) \quad (1)$$

where pH_∞ is the final pH; pH_0 is the initial pH; k_{pH} is the exponential constant of pH decay; and t is the time in hours after slaughtering. Time zero was set to match the time of slaughter. The three-parameter model for temperature (ºC) as a function of time (T(t)) was defined as,

$$T(t) = T_0 + (T_0 - T_\infty)\exp(-k_{Temp}t) \quad (2)$$

where T_∞ is the final temperature (ºC); T_0 is the initial temperature (ºC); and k_{Temp} (h^{-1}) is the exponential constant of temperature decay. Equations (1) and (2) were fitted to each of the experimental decay curves originated from the 103 beef muscles. Models' adequacy was assessed by examining normality of residuals and heterocedasticity. Using the model parameters (pH_0, pH_∞, k_{pH}, T_0, T_∞ and k_{Temp}), the following pH/temperature decay descriptors were computed for each of the curves: the pH at 1.5 h ($pH_{1.5}$), at 3.0 h ($pH_{3.0}$), at 4.5 h ($pH_{4.5}$) and at 24.0 h (pH_{24}); the temperature at 1.5 h ($Temp_{1.5}$), at 3.0 h ($Temp_{3.0}$), at 4.5 h ($Temp_{4.5}$), and at 24.0 h (T_{24}); the time when pH reached 6.0 ($t_{pH6.0}$), and the temperature at which pH reached 6.0 ($Temp_{pH6}$). Thus, these predicted descriptors were available for every carcass.

Effect of live-animal/carcass characteristics on pH/temperature decay descriptors

In order to evaluate whether live-animal/carcass characteristics affect the pace at which pH and temperature decline in a beef carcass early *p.m.*, analyses of variance (ANOVA) were conducted separately on each of the temperature/pH decay descriptors (i.e., $pH_{1.5}$, $pH_{3.0}$, $pH_{4.5}$, pH_{24}, $Temp_{1.5}$, $Temp_{3.0}$, $Temp_{4.5}$, $t_{pH6.0}$, $Temp_{pH6}$) as response variables with live-animal/carcass characteristics as explanatory variables. The characteristics related to the animal/characteristics considered as regressors were: sex, age, breed, hot carcass weight (HCW), transport time ($t_{Transport}$), lairage time ($t_{Lairage}$), SEUROP classification for conformation (Conf), degree of fat cover (Fat) and animal class (A=male aged 12-24 months, E=female aged between 12-24 months and Z=either sex aged 8-12 months).

Linear discriminant analysis

Taking into account the ideal window rule, an additional class variable named 'Quality' was created in the dataset to assign carcasses to one of three classes (i.e., cold-shortened, hot-shortened and optimal quality) which were quality categories known from the experimental data. A carcass was classified as "hot-shortened" or "cold-shortened" if $Temp_{pH6.0}$ was higher than 35 or lower than 12, respectively. For carcasses in between, the classification of "Optimal" was given. Linear discriminant analysis was then performed in order to investigate whether selected pH/temperature decay descriptors and animal/carcass characteristics could accurately classify carcasses by quality into the three classes. Misclassification rates were then computed. While exponential models and ANOVA were fitted using the *Nlme* and *MASS* packages, multivariate analyses were conducted using the *cluster* and *psych* packages, all of them implemented in the software R (R Core Development Team).

RESULTS AND DISCUSSION

All the pH and temperature experimental curves obtained from the 103 carcasses could be closely depicted by the chosen exponential decay models. There were no convergence problems and residuals from each model could be approximated to normal distributions. The models' fitting quality can be appreciated in Fig. 1 for four muscle samples. Notice that both pH_0 and T_0 were fixed at 7.0 and 39.0ºC, since time zero represents the time of slaughter in the models. Descriptive statistics of the pH and temperature decay descriptors are compiled in Table 1. Sampled muscles' pH decreased steadily from ~7.0 to median values of 6.41, 6.10 and 5.90, at the corresponding median temperatures of 34.1, 29.2 and 25.0ºC after 1.5, 3.0 and 4.5 hours p.m, respectively (Table 1). Nonetheless, a considerable variation in pH and temperature decay between carcasses under commercial conditions was observed (Fig. 1).

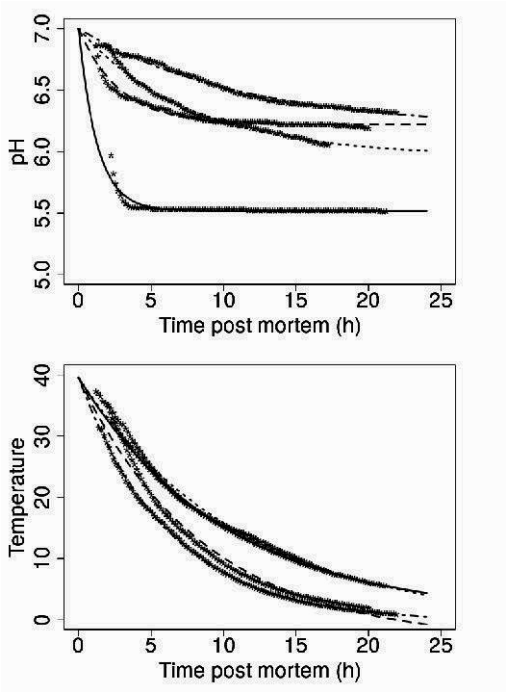

Figure 1: pH (top) and Temperature (bottom) Decline Curves from Four Sampled Carcasses Showing Fitted Exponential Model

Among the pH and temperature decay descriptors, the lowest variation between carcasses was registered at 1.5 h ($Temp_{1.5}$, $pH_{1.5}$). The time at which carcasses reached pH 6.0 was highly variable and ranged between 2.2 and 43.2 hours (i.e., some carcasses did not attain pH=6.0 by the end of the 24-h recorded period). Similarly, the temperature at which carcasses reached pH 6.0 had a wide range between 5.9 and 36.0ºC (Table 1). Taking into account the ideal window rule, it can be deduced that both phenomena hot- and cold-shortening occurred in the surveyed commercial abattoir, although the former at a much lower frequency (3.2%) than the latter (27.9%). Only a proportion of 68.8% of the sampled carcasses presented pH/temperature optimal decay for becoming meat of good eating quality.

Table 1: Mean, Median and Range of pH and Temperature Decline Descriptors (Predicted Values)

Predicted	Mean	Median	Min	Max
$pH_{1.5}$	6.48	6.41	6.00	6.90
$pH_{3.0}$	6.18	6.10	5.90	6.90
$pH_{4.5}$	6.02	5.90	5.60	6.80
$Temp_{1.5}$ (ºC)	33.6	34.1	27.1	38.8
$Temp_{3.0}$ (ºC)	28.8	29.2	18.9	34.3
$Temp_{4.5}$(ºC)	24.5	25.0	13.8	31.9
$Time_{pH6.0}$ (h)	5.25	2.96	2.17	42.3
$Temp_{pH6.0}$ (ºC)	26.6	29.2	5.89	36.0

In the sampled beef muscles, no correlation was found between pH (k_{pH}) and temperature (k_T) decay rates (r=-0.05; Table 2), which corroborated earlier results in electrically-stimulated beef carcasses (Hwang and Thompson 2001). The fact that these decay rates are randomly distributed (Fig. 1) is advantageous from a statistical modelling viewpoint since they can be used as orthogonal (i.e., independent) variables in the development of a multivariate algorithm for carcass quality classification. From the correlation analysis (Table 2), it was deduced that also $pH_{3.0}$ was a descriptor suitable for inclusion in classification analysis because it contains information of both the time and temperature at which rigor mortis takes place (correlation of 0.80 with $Time_{pH6.0}$, and -0.87 with $Temp_{pH6.0}$) and the ultimate pH of the carcass (correlation of 0.86 with pH_{24}). Thus, $pH_{3.0}$ descriptor represents a measurement that, although taken earlier during chilling, can predict with some accuracy the remaining pH decline trend.

Table 2: Correlation Matrix of pH/Temperature Decay Rates and Selected Decay Descriptors

	k_{pH}	k_{Temp}	$Time_{pH6}$	$Temp_{pH6}$	$pH_{3.0}$	pH_{24}
k_{pH}	1.00					
k_{Temp}	-0.05	1.00				
$Time_{pH6.0}$	-0.54	-0.09	1.00			
$Temp_{pH6.0}$	0.67	-0.26	-0.76	1.00		
$pH_{3.0}$	-0.73	0.13	**0.80**	**-0.87**	1.00	
pH_{24}	-0.39	0.13	0.76	-0.70	**0.86**	1.00

In the analyses of variance for the pH decay descriptors $pH_{1.5}$, $pH_{3.0}$, $pH_{4.5}$ and pH_{24}, the hot carcass weight (HCW) was consistently significant (Table 3). The inverse relationship between carcass weight and pH at the different times (as indicated by the negative sign of the regression coefficients in Table 3) suggests that a beef carcass that is larger and heavier can be associated to higher muscle glycogen reserves, which in turn prompts a faster pH drop. As opposed to hot carcass weight, breed had barely any impact on the pH/temperature descriptors, except for pH_{24}. From the least square estimates, beef carcasses from Mirandesa breed seemingly reached, on average, a lower ultimate pH (pH_{24}=5.611) than those from cross-breed animals (pH_{24}=5.778; Table 3).

Table 3: Estimates of Live-Animal/Carcass Characteristics as Significant Explanatory Variables in the Linear Models Fitted to pH and Temperature Decay Descriptors

pH/Temperature decay descriptors	**Live-animal/carcass characteristics[1]**	**Mean**	**St. deviation**	**P>|t|**
pH at 1.5 h ($pH_{1.5}$)	HCW	-0.001	0.001	0.078
pH at 3.0 h ($pH_{3.0}$)	HCW	-0.001	0.001	0.078
pH at 4.5 h ($pH_{4.5}$)	HCW	-0.001	0.001	0.084
pH at 24 h (pH_{24})	HCW	-0.002	0.001	0.004
	Breed	-0.169	0.111	0.133
	Breed[2] Cross	5.778	0.049	-
	Mirandesa	5.611	0.092	-
pH decay rate ($\log k_{pH}$)	Fat 2	0.133	0.086	0.127
	Fat 3	0.082	0.090	0.365
	Fat 4	0.178	0.104	0.094
	Gender – Male	0.086	0.050	0.092
	Class E	0.170	0.098	0.091
	Class Z	0.046	0.067	0.490
	Fat[2] 1	0.255	0.087	-
	2	0.388	0.040	-
	3	0.337	0.036	-
	4	0.432	0.065	-
	Gender[2] female	0.310	0.047	-
	male	0.396	0.042	-
	Class[2] A	0.281	0.070	-
	E	0.450	0.068	-
	Z	0.328	0.029	-
Temperature decay rate ($\log k_{Temp}$)	HCW	-0.0015	0.0004	<.0001
	Age	-0.0247	0.0119	0.042
Time to pH 6.0 (h) ($\log Time_{pH6.0}$)	Class E	-0.175	0.166	0.300
	Class Z	0.055	0.115	0.630
	Class[2] A	0.511	0.106	-
	E	0.335	1.127	-
	Z	0.567	0.042	-
Temperat. at pH 6.0 (ºC) ($Temp_{pH6.0}$)	HCW	0.025	0.016	0.1308
	Lairage time	5.784	2.463	0.0230
Temperat. at 1.5 h (ºC) ($\log Temp_{1.5}$)	HCW	0.0002	0.00004	<.0001
	Gender – Male	-0.0096	0.00048	0.052
	Gender[2] female	1.532	0.004	-
	male	1.522	0.003	-
Temperat. at 3.0 h (ºC) ($\log Temp_{3.0}$)	HCW	0.0005	0.00007	<.0001
	Gender – Male	-0.0183	0.00949	0.059
	Gender[2] female	1.466	0.007	-
	male	1.448	0.006	-
Temperat. at 4.5 h (ºC) ($\log Temp_{4.5}$)	HCW	0.001	0.001	<.0001
	Gender – Male	-0.007	0.016	0.653
	Fat 2	0.025	0.026	0.339
	Fat 3	0.041	0.028	0.148
	Fat 4	0.066	0.033	0.054
	Gender[2] female	1.388	0.011	-
	Male	1.381	0.009	-
	Fat[2] 1	1.350	0.026	-
	2	1.376	0.010	-
	3	1.392	0.009	-
	4	1.416	0.019	-

[1]Model estimates, standard deviations and P-values are shown only for animal/carcass characteristics that were significant in the analysis of variance (Pr(F)<0.10)

[2]Least-squares means and standard deviation of factor levels were computed only when categorical variables (i.e, breed, fat, gender, class) were significant

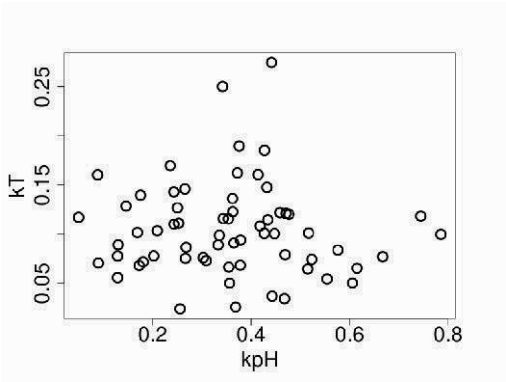

Figure 2: Distribution of the Fitted Exponential Decay Rates for pH (k_{pH}) and Temperature (k_T)

Carcass characteristics associated to animal size (Fat, Gender and Class) were found to have a strong impact on the pH decay rate. Least-square mean estimates revealed the trend that as the thickness of fat cover increases, from class 1 (log k_{pH}=0.255, then k_{pH}=1.79) to class 4 (log k_{pH}=0.432, then k_{pH}=2.70), the rate of pH decay increases (Table 3). Likewise, 12-24 month-aged female animals (Class E) also produced a faster pH decay (log k_{pH}=0.450, then k_{pH}=2.80) than male (Class A, k_{pH}=1.91) and younger animals (Class Z, k_{pH}=2.13).

In the case of temperature decay, once again animal characteristics related to animal size such as hot carcass weight (p<.0001) and age (p=0.042) moderated the rate of muscle temperature decay (Table 3). Hot carcass weight (slope estimate -0.0015) and age (slope estimate -0.0247) were inversely correlated with temperature decay rate because, in smaller animals, heat is more rapidly liberated and, in addition, heat transfer does not get slowed down by greater fat levels. Such retarding effect of fat on heat transfer rates became more evident in the linear model for temperature at 4.5 h. Progressively fatter carcasses (from fat classes 1, 2, 3 and 4) reached increasingly higher average temperatures after 4.5 h p.m. (22.4, 23.8, 24.7 and 26.1ºC, respectively; taking the antilogarithm of the least square mean estimates presented in Table 3). Said otherwise, a fatter carcass requires longer time to reach the lower temperature of a leaner carcass at the same time. Both animal gender and hot carcass weight strongly influenced the temperature decay p.m., as denoted by the consistent statistical significance of these variables in the linear models for $Temp_{1.5}$, $Temp_{3.0}$ and $Temp_{4.5}$. As female animals are associated to greater carcass size and fat deposits than males, following the reasoning above, it is not unexpected that recorded muscles samples from females presented higher temperatures than the ones from males (notice that least-square mean estimates for $Temp_{1.5}$, $Temp_{3.0}$ and $Temp_{4.5}$ for females are systematically higher than for males; Table 3).

In the linear models for the descriptors related to rigor mortis, the only variable that statistically influenced the time to reach pH 6.0 was the carcass class. However, the carcass class may be thought of being an interaction between animal age and gender. The smaller carcasses of animals aged between 8-12 months, class E, took the longest to attain rigor mortis (log $Time_{pH6.0}$=0.567, so $Time_{pH6.0}$=3.7 h in Table 3), because, as explained earlier, smaller carcasses are associated to lower glycogen levels, which retards pH drop. Contrarily, carcasses from females aged 12-24 months took on average a significantly shorter time to reach rigor mortis (for Class E, log $Time_{pH6.0}$=0.567, so $Time_{pH6.0}$=2.2 h) than the ones from males (for Class A, log $Time_{pH6.0}$=0.511, so $Time_{pH6.0}$=3.2 h). Unexpectedly, lairage time was positively associated to the carcass temperature at rigor mortis (p=0.023). This could have been an effect of the abattoir logistics of slaughtering smaller animals first. The carcass temperature at rigor mortis was influenced by the hot carcass weight. The positive coefficient (0.025; Table 3) implies that in heavier carcasses, the pH drops faster while temperature is still high, in comparison to lighter carcasses where pH drops at a slower pace while they get cooler.

From the correlation analysis between pH/temperature decay descriptors (Table 2) and the assessment of animal/carcass characteristics capable of regulating the pH/temperature decay descriptors (Table 3), the variables containing most information that were considered for the prediction of meat tenderness – according to the ideal window rule, were: hot carcass weight, age, gender, class, k_{pH}, k_{Temp}, $pH_{1.5}$, $pH_{3.0}$, $Temp_{1.5}$ and $Temp_{3.0}$. Figure 2 shows the distribution of the paired values obtained from the two linear discriminant functions that were derived from the variables mentioned above, and evaluated for 93 carcasses. While cold-shortened (26/26) and hot-shortened carcasses (3/3) were classified correctly for all samples, optimal quality carcasses were correctly classified in 87.5% of the samples (48/56). Three optimal quality carcasses were mistakenly assigned to the cold-shortening category while other five optimal quality carcasses wrongly assigned to the hot-shortened category.

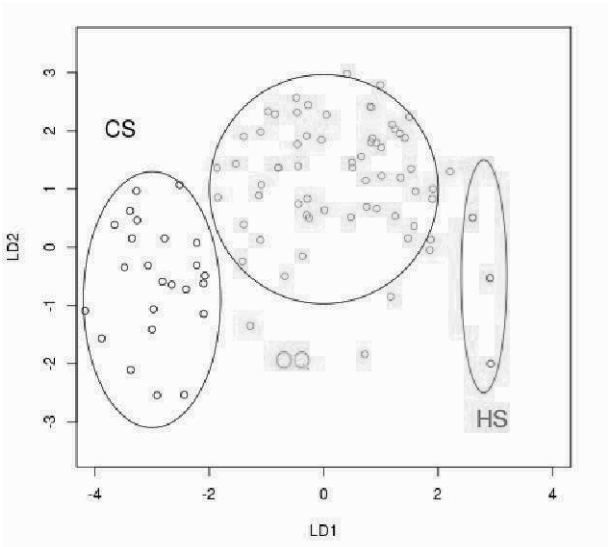

Figure 3: Discriminant Analysis of Meat Quality as Predicted by Two Linear Discriminant (LD) Functions of pH/Temperature Decay Descriptors and Animal/Carcass Characteristics; and Clustered by Classes: Cold-Shortened (CS), Hot-Shortened (HS) and Optimal Quality (OQ)

Under the commercial conditions of the surveyed abattoir, there was considerable variation in rigor time (2.2 – 42.3 h) and rigor temperature (5.9 – 36.0ºC), which allowed both modelling of pH and temperature decay, and the assessment of significant animal/carcass characteristics affecting pH/temperature decay. The exponential decay equation turned out to be an adequate model to describe the carcass decay in both pH and temperature. Linear models adjusted to key descriptors extracted from the fitted pH/temperature decay curves revealed that animal class, gender, age, hot carcass weight and degree of fat coverage are important traits that modulate the carcass pH and temperature decay. Although further work is still required, results from this investigation corroborated the feasibility to classify the quality of meat into cold-shortened, hot-shortened and optimal quality from early post mortem pH/temperature decline information and animal/carcass characteristics that are regularly annotated in a commercial abattoir.

ACKNOWLEDGEMENT

Dr. Gonzales-Barron acknowledges the financial support provided by the Portuguese Foundation for Science and Technology (FCT) through the award of a 5-year Investigator Fellowship (IF) in the mode of Development Grants (IF/00570).

REFERENCES

Bianchini, W., A. C. Silveira, M. B. Arrigoni, A. M. Jorge, E. Rodrigues, C. L. Martins, C. Andrighetto, J.C. Hadlich and D.C. Morales. 2007. "Acompanhamento da queda de pH e temperatura em diferentes pontos da carcaça de bovinos Nelore, Aberdeen Angus, ½ Aberdeen Angus, Brangus e Pardo Suíço superprecoces". Congresso Brasileiro de Zootecnia – ZOOTEC, 1-6.

Cortez, P., Portelinha, M., Rodrigues, S., Cadavez, V. and Teixeira, A. 2006. "Lamb meat quality assessment by support vector machines". *Neural Processing Letters*, 24, 41-51.

Fergurson, D. M. 2004. "Objective on-line assessment of marbling: a brief review". *Australian Journal of Experimental Agriculture*, 44, 681-685.

Hwang, I. H., C. E. Devine, D. L. Hopkins. 2003. "The biochemical and physical effects of electrical stimulation on beef and sheep meat tenderness". *Meat Science*, 65, 677-691.

Hwang, I. H. and J.M. Thompson. 2001. "The interaction between pH and temperature decline early post-mortem on the calpain system and objective tenderness in electrically stimulated beef longissimus dorsi muscle". *Meat Science*, 58, 167-174.

Ibarburu, M., J.B. Kliebenstein and B.M. Hueth. 2007. "pH as a Predictor of Flavor, Juiciness, Tenderness and Texture in Pork from Pigs in a Niche Market System". Animal Industry Report: AS 653, ASL R2181. Available at:
http://lib.dr.iastate.edu/ans_air/vol653/iss1/8

Kahraman, T., A.G. Bayraktaroglu, G. Issa, T. Ertugrul, E.B. Bingol and L. Ergun. 2012. "Effects of temperature conditioning and citrus juice marinade on quality and microstructure of aged beef". *Journal of Food Agriculture & Environment*, 10, 117-122.

Platter, W.J., Tatum, J.D., Belk, K.E., Chapman, P.I., Scanga, J.A. and Smith, G.C. 2003. "Relationships of consumer sensory ratings, marbling score, and shear force value to consumer acceptance of beef strip loin steaks". *Animal Science*, 81, 2741-2750.

Roça, R.O. 2012. "Modificações Post-mortem". Faculty of Agricultural Sciences UNESP, Botucatu, Brazil, 2-16.

Simmons, N. J., Daly, C. C., Mudford, C. R., Richards, I., Jarvis, G., Pleiter, H. 2006. "Integrated technologies to enhance meat quality – An Australasian perspective". *Meat Science*, 74, 172-179.

Thompson, J. 2002. "Managing meat tenderness". *Meat Science*, 62, 295-308.

Tornberg, E. 1996. "Biophysical aspects of meat tenderness". *Meat Science*, 43, 175-191.

BIOGRAPHIES

CRISTINA XAVIER, a Portuguese national, graduated in Animal Science Engineering at the School of Agriculture of the Polytechnic Institute of Braganza, Portugal, in 2011. Currently, she is on her last year of PhD in Animal Science, with an investigation whose general objective is to develop a novel monitoring system of pH and temperature decline post-mortem for beef meat carcasses.

URSULA GONZALES-BARRON, a Peruvian-Irish national, graduated with first-class honours in the Faculty of Food Industries at the National Agricultural University La Molina, Peru (1999), and later on, she obtained her doctoral degree at the Biosystems Engineering Department of University College Dublin, Ireland (2006). Her expertise resides in diverse areas of food quality and safety, including mathematical modelling, predictive microbiology, risk assessment of pathogens, food traceability, shelf-life determination and sensory analysis. Dr. Gonzales-Barron has published over 52 peer-reviewed articles; and currently serves as Editor in the LWT – Food Science and Technology Journal.

VASCO CADAVEZ, a Portuguese national, obtained his degree in Animal Science in 1993 at the Portuguese University of Trás-os-Montes e Alto Douro. After a novel research on carcass composition and quality using ultrasound, he obtained his PhD degree in 2004. He is currently a Professor at the Animal Science Department of the Polytechnic Institute of Braganza (IPB), Portugal. Dr. Cadavez is very knowledgeable in a wide range of mathematical and statistical modelling techniques applied agriculture, animal science, and food quality and safety.

Optimization of a Thermal Process with Reciprocal Agitation by Computational Modelling

Dagbjørn Skipnes[a], Ferruh Erdogdu[b], Mustafa Tutar[c-d], Sigurd Øines[a], Igor Barrenoe, Trond Løvdal[a]
[a] Nofima, Richard Johnsens gt. 4, 4021 Stavanger, Norway
[b] Department of Food Engineering, Ankara University, Ankara-Turkey
[c] Mechanical and Manufacturing Department, MGEP Mondragon Goi Eskola Politeknikoa, Spain
[d] IKERBASQUE, Basque Foundation for Science, Spain
[e] CS Centro Stirling S. Coop, Aretxabaleta, Spain

KEYWORDS
Optimization, thermal processes, agitated retorting, heat transfer modelling

ABSTRACT

Reciprocal, longitudinal agitation of hermetically sealed food products in autoclaves during thermal processing leads to a significant reduction in processing time, and ensures the same microbial decimation with increased production efficiency compared to a non-agitated process. Compared to still processing, the heat load may also be reduced for pasteurization processes but still inactivate non-spore forming pathogens like *Listeria* spp. with higher precision. The thermal load may therefore be redusced by agitation, compared to still processing, and nutrient retention will be improved, provided the process is optimised for that purpose.

In order to optimize agitation rates and assess the temperature distribution within the product, a milti-phase numerical model using a finite volume method was developed and validated by experiments in a laboratory agitation autocalve. The model enables simulations of the agitated process for combinations of agitation rate, processing time and processing temperature.

The ongoing work will aim for establishing processes maximizing nutrient retention while respecting the microbial constraints for food safety.

INTRODUCTION

For optimal process design, the temperature distribution inside a food product must be known. Conductive heating products usually have a slow heating zone, e.g. the geometric center, where the temperature may be measured and from that, inactivation of bacteria and their spores may be determined.

In processes where convective heating is achieved by agitation the locations of slow heating zones are challenging to identify by temperature measurements. Therefore, heat transfer modelling for model products has been done to determine temperature distribution during a novel agitated retort, aiming for determining the optimal processing of products undergoing an agitated heating process. A reciprocal agitation system, Shaka™, was specifically chosen for processing due to its ability to impose forces up to 3-4 g to enhance the convective mixing within the product during retorting [1]. The enhanced mixing via the longitudinal agitation leads to a significant reduction in processing time, and ensures the same microbial decimation with increased production efficiency [2,3]. Compared to still processing, the heat load may also be reduced for pasteurization processes but still inactivate non-spore forming pathogens like *Listeria* spp. with higher precision [4]. Reduced overall heat load may also improve nutrient retention and reduce heat induced changes compared to slow heating foods. This led to a modelling tool to optimize the agitated retort processing and minimize product development costs.

Preservation/breakdown of nutrients has been the objective function, while the agitation rates (strokes/min) and process temperature has been used as base for decision on explicit/implicit variables. The results have been compared with the results of conventional processing techniques, i.e. still retorting. Even if traditional canning is convenient, and provides a universal and economic method for processing and preservation [5], there is a need to reduce energy costs, improve nutritional quality and enhance sensory attributes. While new packaging formats have emerged [6], the latest agitation process, where reciprocating agitation is carried out in horizontally oriented containers, reduces processing times ≈90% and enables energy savings without compromising quality [7].

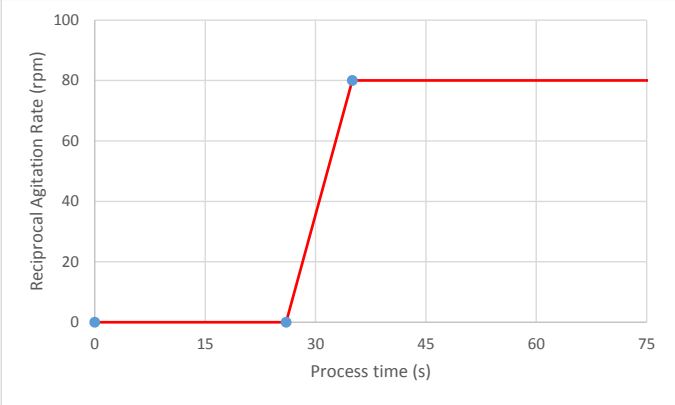

Figure 1. Reciprocal agitation rate for the experimental set-up

METHOD

The multi-phase model simulation was performed using a finite volume method based on discretization of governing flow equations for liquid and gas phase in a non-inertial reference frame of moving mesh. Experimental studies for model validation were carried out in a reciprocally agitated retort (Steriflow, Roanne, France) using 98.2×115 mm cylindrical steel cans containing distilled water with 2% headspace as a model case. The reciprocal agitation rate was constant during processing time, but as the retort started it took some time before the agitation started and an approximation of the agitation rate is shown in figure 1.

RESULTS AND DISCUSSION

The model results compared well with the experimental data and an example of the validation curves is shown in figure 2.

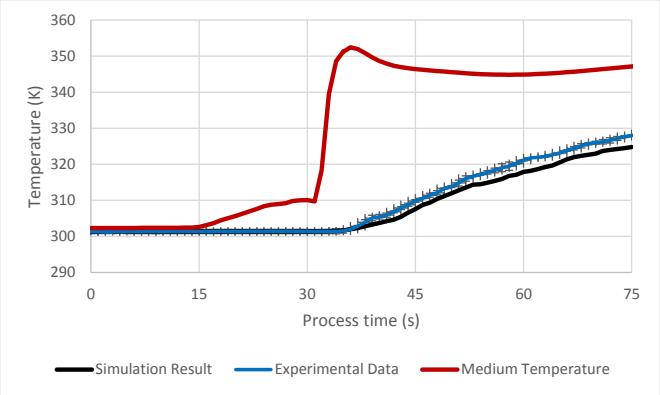

Figure 2. Comparison of experimental and numerical simulation results

Based on this the optimum reciprocal agitation rate was determined as presented in figure 3. As expected from earlier studies [1, 4], the product heated faster with increasing agitation rate but only to a certain level which is demonstrated by the very small difference in average temperature when determined for 80 rpm and 140 rpm. This observation is important in order to avoid using unnecessary agitation intensity, which might result in physical damage on some products. A product retorted at an optimum agitation rate will not only reach the desired overall processing temperature, but also achieve a more homogenous temperature within the container compared to a container processed in static mode. This is important because it is the potential microbial contamination in the slowest heating zone that determines how long processing time that is required. The nutrient retention of e.g. vegetables may therefore be used as a target for the optimization.

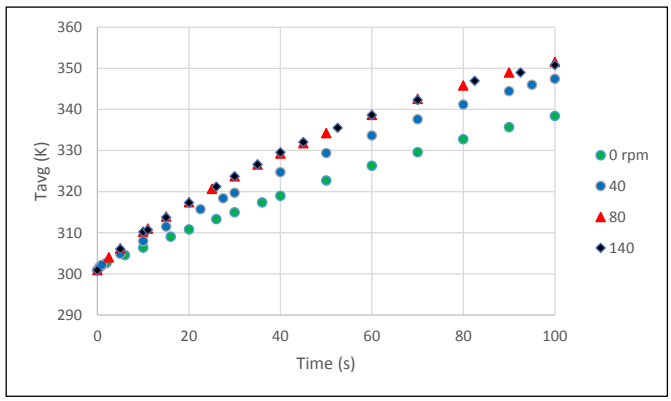

Figure 3. Comparison of the container average temperature at different oscillation rates

It would be of interest to combine the modelling work presented here with recent findings of heat transfer rates in particulate foods and especially the observations of a particle concentration of 20-30 % resulting in a higher heat transfer rate than higher or lower concentrations [3].

FUTURE WORK

Simulations with a range of viscosities and agitation rates should be performed and zones subjected to a minimum of heat load should be determined and further validated. The next step is to determine combinations of agitation rate and combinations of processing time and processing temperature, which result in maximum nutrient retention while respecting the microbial constraints and demands for a specified inactivation rate for a target pathogen.

The modelling results should be further utilized during the ongoing work. Examples of how the results of this study are to be used to optimize the process with respect to improve the health-promoting compounds of processed foods will be presented.

ACKNOWLEDGEMENT

This study was a part of the project SUNNIVA (Sustainable food production through quality optimized raw material production and processing technologies for premium quality vegetable products and generated by-products) – Project no: 10829, supported by SUSFOOD (Sustainable Food Production and Consumption) Era-net.

REFERENCES

[1]. Skipnes, D. (2009) Characterization of heat transfer in reciprocating agitation (SHAKA) of retorted foods, in The 2nd European IFTPS meeting. 2009: Porto, Portugal.

[2]. Tucker, G. and S. Featherstone, *Essentials of Thermal Processing*. 2011, New York: Wiley-Blackwell.

[3]. Singh, A., & Ramaswamy, H. S. (2015). Effect of product related parameters on heat-transfer rates to canned particulate non-Newtonian fluids (CMC)

during reciprocation agitation thermal processing. *Journal of Food Engineering, 165*(0), 1-12.

[4]. Ates. M.B., Skipnes, D., Rode, T.M., Lekang, O. (2014). Comparision of bacterial inactivation with novel agitating retort and static retort after mild heat treatments. Food Control, 43, 150-154.

[5]. Weng, Z.J., (2005) *Thermal processing of canned foods*, in *Thermal food processing-New technologies and quality issues*, D.W. Sun, Editor. CRC-Taylor & Francis: Boca Raton, FL.

[6]. Karaduman, M., R. Uyar, and F. Erdogdu, (2012) *Toroid cans - An experimental and computational study for process innovation.* Journal of Food Engineering. **111**(1): p. 6-13.

[7]. Phillips, D.A. (2013) *Retort Processing Shakes Up New Interest*. Food Processing Magazine.

REDUCTION OF 3-MONOCHLOROPROPANE-1,2-DIOL (3-MCPD) ESTERS DURING PALM OIL REFINING

Chin Ping Tan
Department of Food Technology
Faculty of Food Science and Technology
Universiti Putra Malaysia
43400 Serdang, Selangor
Malaysia
E-mail: tancp@upm.edu.my

Musfirah Zulkurnain
Department of Food Technology
School of Industrial Technology
Universiti Sains Malaysia
11800 USM, Penang
Malaysia

KEYWORDS
Palm Oil, Refining, 3-MCPD esters, Optimization.

ABSTRACT

The physical refining process was modified with the incorporation of a water degumming and washing step in addition to acid degumming. The synergistic effects of the combination of the adsorbents magnesium silicate and activated clay were utilized for the bleaching step. The modified process was then optimized using response surface methodology (RSM), with five processing parameters: water dosage (0-5%), acid degumming dosage (0-1%), degumming temperature (40-80 °C), bleaching earth dosage (0-1%) and deodorization temperature (220-280 °C), to obtain the greatest reduction in the formation of 3-MCPD esters with an acceptable final refined bleached and deodorized (RBD) palm oil quality. Large reduction in 3-MCPD ester formation was observed with increasing water percentage above 3%, reducing degumming temperature and increasing bleaching clay dosage. The color removal was significantly (p<0.05) influenced by increasing in all of the processing factors except bleaching clay dosage. The oil stability index (OSI) was significantly (p<0.05) contributed by increasing in acid dosage and degumming temperature, and decreasing in clay dosage and deodorization temperature. Incorporation of water do not affected the OSI value. The 3-MCPD esters reduction in the refining process was optimized with acceptable oil quality. The optimized conditions were 3.5% water dosage, 0.1% acid dosage, a degumming temperature of 60 °C, 0.3% bleaching earth dosage and a deodorization temperature of 260 °C. These conditions resulted in 87.2% reduction in 3-MCPD esters, from 2.948 mg/kg in RBD palm oil refined conventionally to 0.374 mg/kg, with color and OSI values of 2.4 R and 14.3 hrs, respectively. Model verification using one sample t-test at p<0.05 demonstrated the suitability of the established models in explaining the responses as a function of the processing parameters.

INTRODUCTION

Contamination with 3-monochloropropane-1,2-diol esters (3-MCPD) in a palm oil physical refining process was studied, and their analytical, chemical and processing factors were determined for mitigation purposes. Factors that contribute to the formation of 3-MCPD esters in the palm oil refining process were assessed, including the effect of different crude palm oil (CPO) quality and refining parameters at all stages of the refining process. Poor quality CPO with a high phosphorus content (8.8 ppm) and a low deterioration of bleachability index (DOBI) value (2.4) gave a remarkably high formation of 3-MCPD esters.

The refining of palm oil is an essential purification process that makes crude palm oil edible, stable and safe to be consumed. Accordingly, a modification in the palm oil refining process may have an impact on the resulting overall quality of the palm oil with respect to its stability, sensory properties, color and contaminants. Thus, the optimization of the process using response surface methodology (RSM) was conducted, including the oil quality parameters, to identify the most suitable operating conditions that resulted in the lowest level of formed 3-MCPD esters and attained the desired product quality. The RSM enables the evaluation of the effects of several processing parameters and their interactions on the response variables that are studied.

METHODOLOGY

The physical refining process was modified as in process flow shown in Figure 1 using laboratory-scale physical refining. Approximately 700 g CPO was refined in a five-step processing that included water degumming, acid degumming, washing of the degummed palm oil (DPO) with 1% water, bleaching with 1% Magnesol R60 and auxiliary bleaching earth, filtering and deodorizing to obtain the RBD palm oil. In the last stage, the deodorization temperature was also included as the optimization parameter to determine whether the deodorization temperature has an effect on the formation of 3-MCPD esters in the modifications process.

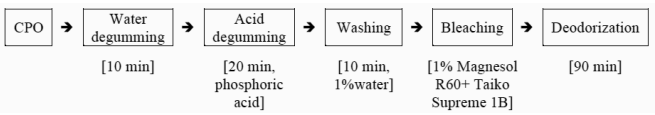

Figure 1 Modified process flow for palm oil physical refining

A face-centered (α = 1) small central composite rotatable design (CCRD) with five factors and three levels was employed to optimize the modified refining process for the production of RBD palm oil with reduced 3-MCPD ester

formation and acceptable oil quality. The design required 26 experiments, which consisted of 11 factorial points, 10 axial points and 5 center points. The factors studied were the water degumming dosage (X_1), the phosphoric acid dosage (X_2), the degumming temperature (X_3), the auxiliary bleaching earth dosage (X_4) and the deodorization temperature (X_5), and their levels are given in Table 1. The response variables was the 3-MCPD ester levels.

Table 1 Factor levels of small CCRD design

Factor	Symbol	Level		
		-1	0	+1
Water dosage	w (%)	0	2.5	5
Phosphoric acid dosage	a (%)	0	0.05	0.1
Degumming temperature	T_d (°C)	40	60	80
Activated clay dosage	b (%)	0	0.5	1
Deodorization temperature	T (°C)	220	250	280

RESULTS AND DISCUSSION

The modified refining process resulted in 3-MCPD ester levels in the range of 0.166 to 0.983 ppm, representing a 42.4 to 89.7% reduction from the conventional process, which has 3-MCPD ester levels of 1.716 ppm. This 3-MCPD ester reduction was significantly (p<0.05) enhanced by increases in the water dosage (X_1) and the bleaching earth dosage (X_4), and by decreases in the degumming temperature (X_3). The reduction of 3-MCPD esters could be primarily based on the elimination of precursors, when employing more water for degumming and greater amounts of bleaching clay during pre-treatment step. Reduction of temperature during acid degumming may cause less activation of the precursors during acid degumming. In contrast, the acid dosage (X_2) and the deodorization temperature (X_5) only demonstrated significant effects (p<0.05) in the quadratic pattern and in the interaction effects.

The effect of each factor was further accessed by the use of perturbation plots that manifested how the response changes as each factor moves from the chosen reference point while the other factors are held constant at reference values. The perturbation plots in Figure 2a and b show the overlying perturbation curves of all of the factors studied, which were held at the center points and at the optimum reduction points, respectively.

At the optimum reduction point, at which the levels of 3-MCPD esters drop close to 0.1 ppm, the perturbation plot exhibited changes in the trends due to the interaction effects of the factors at different levels. The water dosage showed a stronger negative effect, and the other factors demonstrated emphasized positive trends, including the acid dosage and the deodorization temperature factor. The lowest 3-MCPD esters level were achieved with 3.8% water degumming, 0.06% acid degumming at 43.2 °C, a 0.5% bleaching earth dosage and deodorizing at 256 °C.

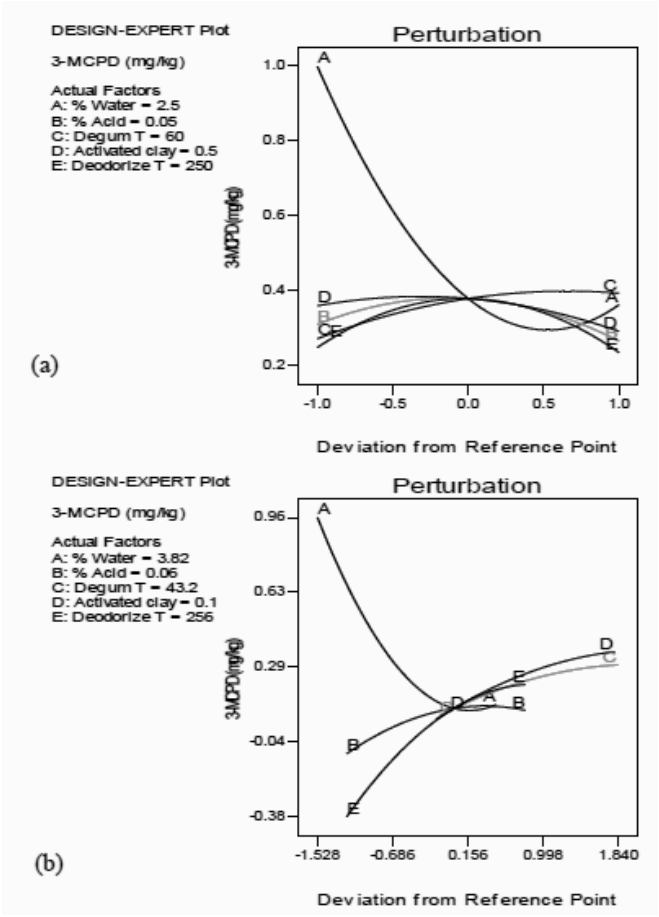

Figure 2 Perturbation plot for 3-MCPD level as a function of five independent variables set at (a) centre points, and (b) optimum reduction points. A: water degumming dosage; B: acid degumming dosage; C: degumming temperature; D: percentage of activated clay; and E: deodorization temperature

The interaction effects of different factors were examined using the generated response surface plots, as shown in Figure 3. For the level of 3-MCPD esters, the response surfaces were generated based on the following second-order equation:

$$Y_1 = 0.38 - 0.31X_1 - 0.02X_2 + 0.06X_3 - 0.03X_4 - 0.007X_5 + 0.3X_1^2 - 0.090X_2^2 - 0.05X_3^2 - 0.053X_4^2 - 0.14X_5^2 + 0.08X_1X_2 + 0.18X_1X_4 + 0.13X_1X_5 - 0.08X_2X_3 - 0.05X_2X_4 - 0.13X_2X_5 - 0.14X_3X_4 - 0.22X_3X_5 - 0.09X_4X_5 \quad (1)$$

Because the water dosage showed the most significant effects, all of the interactions involving this factor (Figure 3a, b and c) showed a prominent reduction in 3-MCPD esters with increasing water dosages, regardless of their factor levels. The 3-MCPD esters were in the range of 0.8 to 1.0 ppm without water degumming and showed up to a 70% reduction with a 5% water degumming dosage, reaching the range of 0.18 to 0.3 ppm. A greater amount of water allowed for more precursors to be washed out in the first step and reduced the chances of 3-MCPD ester formation in the later steps. The influence of the degumming temperature was also clearly seen in all of the interaction effects involving this factor, as shown in Figure 3d, e and f. When the degumming temperature was reduced from 80 °C to 40 °C, the formation of 3-MCPD esters was reduced to approximately 70%. This

effect was rendered most prominent by decreasing the acid dosage, increasing the bleaching clay dosage and decreasing the deodorization temperature.

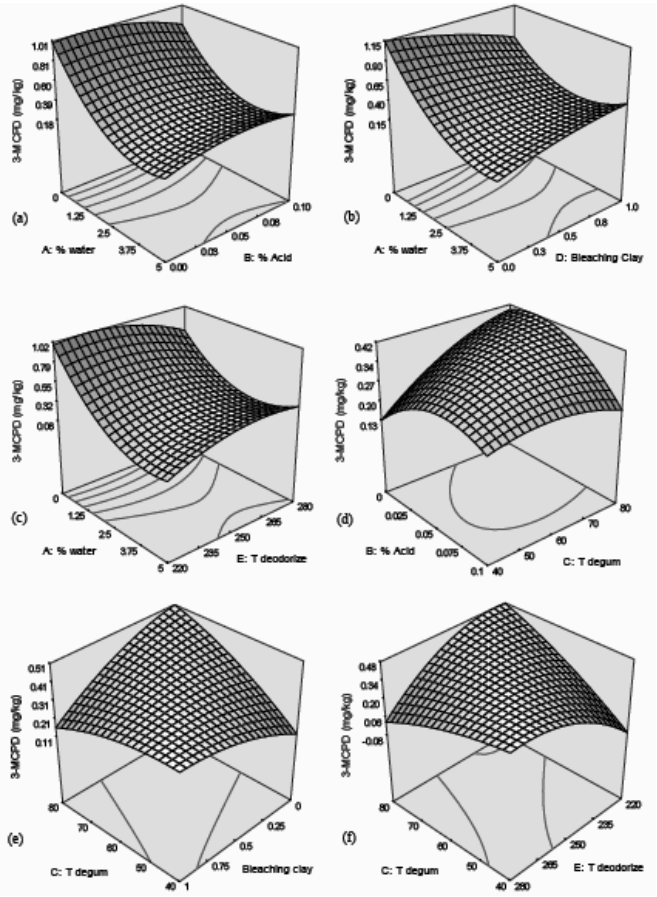

Figure 3 Estimated surface responses of 3-MCPD levels as a function of: (a) water dosage and acid dosage; (b) water dosage and bleaching clay dosage; (c) water dosage and deodorization temperature; (d) acid dosage and degumming temperature; (e) degumming temperature and bleaching clay dosage; and (f) degumming temperature and deodorization temperature with other factors held at centre points

CONCLUSIONS

The optimized processing conditions for the reduction of 3-MCPD esters in the RBD oil, taking into consideration the oxidative stability and final color of the oil, were a 3.5% water dosage, 0.1% acid dosage, degumming temperature of 60 °C, 0.3% bleaching earth dosage and 260 °C deodorization temperature. This combination of factors resulted in an 87.2% reduction in 3-MCPD ester levels, from 2.948 mg/kg in RBD palm oil produced by conventional refining to 0.374 mg/kg. The model established in this study has been verified to be adequate for the prediction of the responses.

FUTURE RESEARCH

This study has established a processing solution for the reduction of 3-MCPD esters in the refining process with acceptable RBD palm oil quality based on oil oxidative stability and color. Further research concerning other RBD palm oil quality parameters such as antioxidant properties, the chemical and physical properties of the final product, sensory properties and the presence of other processing contaminants in the RBD palm oil should be explored.

BIOGRAPHY

CHIN PING TAN was born in Klang, Malaysia. He received his degrees Bachelor of Food Science and Technology in 1998 and PhD in Food Processing in 2001, from Universiti Putra Malaysia (UPM). Currently, he is the head of the Department of Food Technology. He is currently leading one of the major research programs at UPM, Fats and Oils Technology. His areas of research specialisation are palm oil, food nanotechnology, food emulsions and the extraction of bioactive compounds from various agricultural by-products. To date, he has published one joint-edited book, ten book chapters and over 200 scientific articles in peer-reviewed journals, has filed five patents and has presented more than 250 papers at various national and international conferences.

Sustainable Production Logistics-Location Problem for Reusable Transport Packages in Multi-food Production Network with Production Cycle

Di Zhang
Fakultät Maschinenbau / Institut für Transportlogistik
Leonhard-Euler-Str. 2
D-44227 Dortmund, Germany
Email: {zhang@itl.tu-dortmund.de}

KEYWORDS

Reusable transport packages, food supply chain, location problem

ABSTRACT

Food production requires a strict quality control on raw materials and production process. The usage of reusable transport packages in food supply chains not only keep the high level of raw materials quality, but also improves the enterprise image in the market. This paper focuses on the reusable transport logistics networks which serve multi-production systems, trying to analyze the characteristics of them and add time parameters in the location model. A progressive p-median location model is proposed and the problem solved with IBM ILOG CPLEX software. The results show that the new model could obtain optimal situation under time constraint and the suppliers' demands have dominance in network optimization. Some factors that could also influence the results include open number of depots, available service number of suppliers and depot capability.

INTRODUCTION

Food production requires a strict quality control on raw materials and production process. For safety and convenience, once-off transport packages are common in food supply chain network. With the concept of environmental protection and sustainability arising in recent decades, how to transport raw materials network safely and less harmfully attracts more attention in food production network optimization.

The returnable/reusable transport packages solve this problem efficiently. Some pioneer countries with environmental awareness issues regulations already and have achieved significant effect. For example, in 1991 the Dutch government and industry signed the Packaging Covenant forcing industry to think of new ways to deal with packaging material (Packaging Covenant 1991). Similarly, the German Packaging Order requires manufacturers to take responsibility for their packaging waste. In order to comply with this, German manufacturers and retailers created the non-profit organization Duales Systems Deutschland (DSD) to collect packaging material for recycling (Leo and Gaby 1995). Now the reusable packages could be seen every here in these two countries.

The first paper distinguishes three types of systems for returnable transport packaging and gave definition to them in 1993 (Lützebauer1993).Some others (Kärkkäinen, M. et al. 2004) focuses on information management aspects on fresh produce delivery totes and dairy crates.The utilization of reusable containers with stochastic customer demand on pricing and production decisions also has been researched (AtamerB. et al. 2013).

For the integrated design of a food packaging and distribution network, the researchers (Accorsia,R. et al. 2014) shows that adoption of an reusable packages collection (RPC) system will lead to a reduced environmental impact in terms of CO2eq emissions. But none of these has taken into consideration the reusable features of packages in circulation when optimizing the network.

With the popularity of reusable transport packages, the optimization problem of reusable packages network turn to be an emerging topic. The usage of reusable transport packages in food supply chain not only keeps the high level of raw materials quality, but also improves the enterprise image in the market. This paper analyzes the features of reusable transport logistics network underlying previous researches; introduce time and direction factors into location model. A progressive p-median location model is proposed and the problem solved with IBM ILOG CPLEX software. The results show that the new model could obtain optimal situation under time and direction constraint, and the suppliers' demands have dominance in network optimization.

The rest structure of this paper is as follows. Section 2 introduces the reusable packages network exhaustive, from operational process to the characteristics. In section 3, the author presents an integrated programming model of the internal circulation network design. The numerical example and experimental results are discussed in Section 4. Finally, the conclusions are drawn in section 5.

INTERNAL CIRCULATION NETWORK (ICN) DESCRIPTION

The network of reusable transport packages is analogous with closed-loop supply chain, which designed and managed to explicitly consider the reverse and forward supply chain activities (Dabniel,V. and Luk N. Van 2008). But there are some different characteristics. The obvious feature of packages network is flow conservation, which means the total quantities of output from depots have to equal to the total input. High level service needs fast collection. In this paper we define this kind of network as an internal circulation network (**ICN**), the same as the switch pooling system with return logistics. The depots in network are not in charge of final products inventory, but for the logistics carriers.

In several literatures, suppliers, manufacturers, distribution centers, wholesalers, retailers and end customers are basic elements in food supply chain. When consider the reverse logistics, some new participants such as the collection center, the remanufacturer plant and the disposal center are added in the forward reverse logistics integrated network. For reusable transport packages network, only three kinds of participants are involved: depots, suppliers and manufacturers.

Empty packages have been delivered to suppliers in accordance with orders. After the raw material filling into reusable packages with a BPA free bags, the heavy/filled packages leave from suppliers to manufacturers. At last, the used empty packages will be collected from manufacturers back to depots. Before the next cycle of use, the used packages have to be shipped back to the depot maintained.

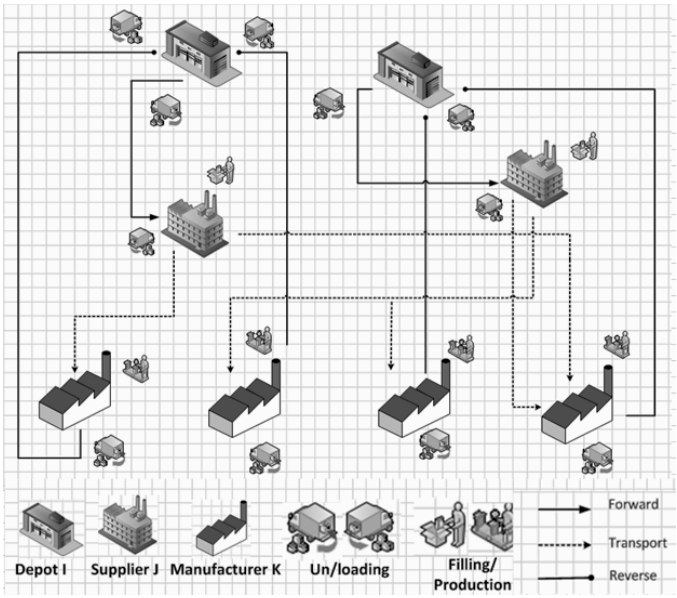

Figure 1: Packages Flows in Internal Circulation Network.

Fig.1 illustrates the basic process in network as mentioned above. In this circle, the flows departure from depot could define as forward logistic, and the flows back to depot operate as reverse logistics. Packages leasing company is just in charge of the empty packages delivery and empty packages collection jobs which is represented by solid lines. The suppliers are responsible for the transport tasks between them and manufacturers denoted with dotted lines. The forward and reverse logistics have same proportion in ICN.

In general food supply chain, one supplier could service multiple manufacturers and vice versa, but only one mode occurred. The reusable transport packages network face the above case simultaneously. The reusable packages service for several large suppliers and collection from numerous manufacturers who cooperate with these big suppliers. An ICN combine multiple food supply chain at the same time. As the manufacturers need a production cycle to consume the raw materials, the collection task could be executed only when the quantities of waiting collection packages meet the economic collection line.

Since the total quantities of package is fixed in the network, apart from the situation of demand absolutely beyond service capabilities, the more time the packages are waiting for collection, the less demands could be satisfied in the forward market. It will lead to a lower profit, slower customer responsiveness. More seriously, the enterprise will lose the market share unless they keep putting new packages into the network. It will result capability waste and a decline in profit.

How to select the suitable depot sites to shorten the weighted transport time during the circulation? Which kind of return model could minimize the packages collection waiting time and reach maximum profit in the planned period? If there is some distant and small amount collection demand, could some adjustments such as collaboration collection policy or adding a new transit center improve the network efficiency?

Some special characteristics of internal circulate network are listed as follows:

(1) Simple network structure: Unlike traditional supply chain network, the internal circulate network consists of only three kinds of participants: depots, suppliers and manufacturers. Empty packages depart and return to the nearby depots.
(2) Many-to-many relationship and unbalanced flows: In the ICN, the relationship between suppliers and manufacturers may be many-S-one-M or one-S-many-M. Due to the suppliers and manufacturers who join same supply chain may locate in different regions; empty packages will depart from depot to close-by suppliers and collection from nearby manufacturers. The output and input for one depot may be unbalanced.
(3) The depots in ICN in charge of several tasks. In general forward/reverse logistics network, the depots responsible for inventory, the collection/inspection center duty to collect and inspect task. In ICN these activities implement by depots and for safety, all used packages have to clean and maintain at depot before the next turn starts.
(4) Collection delayed influent cycle rate: As the production system needs a production cycle to consume the raw materials, the heavy packages have to wait until all holding materials are exhausted. The more waiting, the more capabilities waste.

THE OPTIMIZATION APPROACH

Some researchers (Fleischmann, M. et al. 2001) developed a generic model for the design of closed-loop logistics networks. The others (Üster et al. 2007) designed a closed-loop supply chain network in which the forward network is existing and only collection and recovery centers must be located. The model optimizes the direct and reverse flows simultaneously. The research (Listes 2007) proposed a generic scenario-based stochastic programming model for the design of integrated forward/reverse supply chain network design.

The p-median problem and its extensions are useful to model many real world situations, such as the location of industrial plants, warehouses and public facilities. In this paper, an improved p-median model which transfer transport cost factor to transport time is proposed. Some core variables are shown in Fig.2.

The reason to builds the function with time variable is no matter if the delivery/collection frequencies and quantities are stable or fluctuating, the transport time of delivery and collection will not change. The ICN is sensitive for time constraints. A high correlations network which has the shortest transport time could help depot receive used empty package faster under delivery time constraint. To simplify, we do not give different operators the two parts of demand.

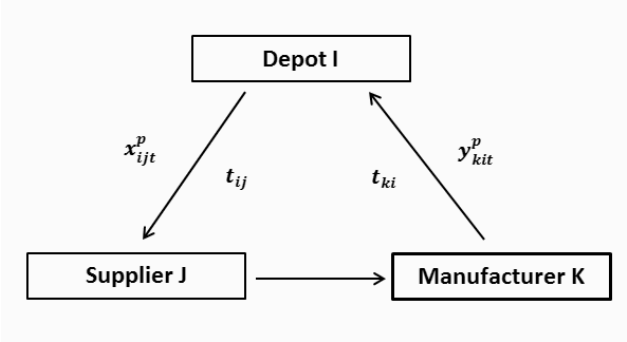

Figure 2: Basic Members and factors in ICN

$$\min \sum_i \sum_j u_{ij} * x_{ij} * t_{ij} + \sum_k \sum_i v_{ki} * y_{ki} * t_{ki} \quad (1)$$

s.t

$$\sum_{i \in I} u_{ij} = 1, \forall j \in J \quad (2)$$

$$\sum_{i \in I} v_{ki} = 1, \forall k \in K \quad (3)$$

$$\sum_{i \in I} w_i = d \quad (4)$$

$$u_{ij} \leq w_i, \forall i \in I, j \in J \quad (5)$$

$$v_{ki} \leq w_i, \forall k \in K, i \in I \quad (6)$$

$$\sum_{j \in J} u_{ij} \leq ASN_i, \forall i \in I \quad (7)$$

$$\sum_{k \in K} v_{ki} * y_{ki} \leq CAP_{stoi}, \forall i \in I \quad (8)$$

$$\sum_{j \in J} u_{ij} * x_{ij} \leq \sum_{k \in K} u_{ki} * y_{ki} + B_i, \forall i \in I \quad (9)$$

$u_{ij} \in \{0,1\}, \forall i \in I, j \in J$

$v_{ij} \in \{0,1\}, \forall i \in I, j \in J$

$w_i \in \{0,1\}, \forall i \in I$

x_{ij}: summation of supplier j's forward demands

y_{ki}: summary of manufacturer k's return demands

u_{ij}: equal 1 if the depot i is assign to service supplier j, 0 otherwise

v_{ki}: equal 1 if the depot i is assign to service manufacturer k, 0 otherwise

w_i: equal 1 if depot i is open, 0 otherwise

t_{ij}: transport time from depot i to supplier j

t_{ki}: transport time from manufacturer k to depot i

B_i: the inventory buffer at depot i

d: the number of depots could opened

I: set of potential sites for depots, i=1,…,$\mathcal{I}$

J: set of suppliers in network, j=1, …,$\mathcal{J}$

K: set of manufacturers in network, k=1,…,$\mathcal{K}$

ASN_i: available customer service number for each depot

CAP_{stoi}: maximum storage capacity for each depot

The common p-median problem is that of locating p facilities to minimize the demand weighted average distance between demand nodes and the nearest of the selected facilities (Daskin, M.S. and Maass, K.L 2015). In this paper, to seek the best location which satisfies both side demands with the shortest transport time, the improved objective function consists of two parts. The first part is the summation of forward demands plus transport time if the opened depot serves the supplier, and the second part is the summation of reverse demand plus transport time if the manufacturer assigns to open depot.

The objective function (1) seeks to minimize the sum of forward and reverse transport time. Constraints (2)-(3) make sure that each supplier or manufacturer has to assign a depot. Constraint (4) determines the number of depot that could be opened. Constraint (5)-(6) guarantee that only opened depot could serve suppliers and manufacturers. Constraint (7)-(8) limits service capacity of depot. Constraint (9) defines the flows relationship between forward delivery and reverse collection.

This paper assumes the packages initial stock in depots is high enough to circulate during the planned period. The model will be calculated with IBM ILOG CPLEX optimization studio p-median model. Some parameters such as available open number of depots, storage buffer for each depot, customer service number and depot capability will be adjusted.

EXPERIMENTAL RESULTS

To avoid invalid calculations, the alternative sets of depots coordinates are determined in advance. It comprehensively considers such as transport cost, time length between OD pairs, available logistics resource, etc. The set is given by the logistics and financial department of the investigated company'. Location and demand data of suppliers and manufacturers are given but without name due to the protection of commercial confidentiality.

Before calculation, we need to clarify some preconditions:

(1) The location of suppliers and manufacturers are known and fixed in the network during the planned period.
(2) Based on the nearest service principles, the suppliers and manufacturers in the same food supply chain may be serviced by different depots.
(3) As the capabilities of logistics services in different region are distinctive, we partition the regions according to the adjacent areas which have similar conditions. The other reason to divide the areas is the lead time constraint for suppliers.
(4) For simplicity, the author didn't consider the inventory insufficient situation in this paper. All collection will follow the EOQ rules and therefore minimize the total transport time and equally minimize total transport cost.

Data Input

As we mentioned above, for the simplicity, in the experiment, two regions which are close but service different customers before are chosen: area T and area J. In area T, 4 suppliers (Sj1-4) and 19 manufacturers (Mk1-19) are involved. In area J, there are 4 suppliers (Sj5-8) and 15 manufacturers (Mk20-34). The total amount of demands from suppliers and manufacturers are given by the investigated company.

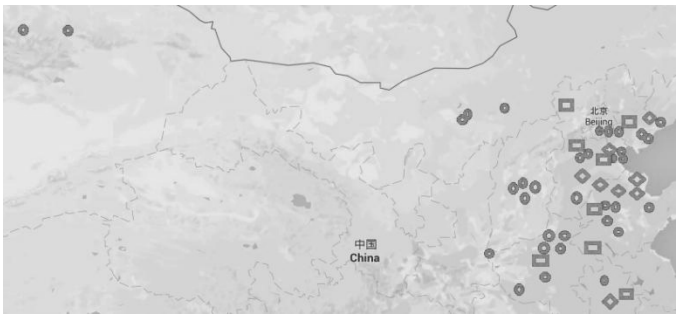

Figure 3: Location of members in ICN

In Fig.3, the blue rectangles are potential site of depots, red cycles represent manufacturers, and the green diamonds indicate suppliers. All of the potential depots location satisfied suppliers' service time requirements.

As we mention above, the total demands and transport time length between depots, suppliers and manufacturers are provided by the investigated company. The matrixes of time, demand and service capacity of depot are input.

Collection carried out when the economic collection quantities are reached. More sophisticated scenarios such as uneconomic collection and collection mode adjustment will be deep researched in the future.

The initial setting is as follows: Each depot could service up to 8 suppliers, and the total maintained capacity during the planned period is 40,000. The practical output could not be beyond the maximum capability of packages maintained for each depot. 4 suppliers (S1-4) and 19 manufacturers (Mk1-19) are involved in area T. 4 suppliers (S5-8) and 15 manufacturers (Mk20-34) are located in area J. Each area could have only one depot open.

Data Output

To make the results more detailed and figure out the impact factors, the model is run in several situations.

Table1-Results for Single Area

	Area T		Area J	
	OLD	TTT	OLD	TTT/H
Only for S	Di-1	71366	Di-5	53577
Only for M	Di-1	172896	Di-8	115209
Both for S and M	Di-1	**244256**	Di-5	**180850**

Note:OLD-optimal location of depot, TTT-total transport time in hours

First of all, the basic model is executed for a single area. In the first and second steps, the optimal locations of depot for suppliers and manufacturers demands are calculated respectively. The basic model is without depot capability and flow balance constraints. In the third step, the demands of suppliers and manufacturers are combined together. The optimal location of depot and the amount of total transport time are shown in Table 1.

For area T, Di-1 is the only one selected by the optimization model. In step three, the total time of transport in area T is 244,256 hours, equals the transport time from depot-1 to suppliers plus from manufacturers back to depot-1.

In area J, the Di-5 is optimal for total suppliers, and the Di-8 is the ideal for all manufacturers. If combining the demands of suppliers and manufacturers' together, the Di-5 should be opened so that the total transport is minimal. The integrated calculate result is much higher than respectively.

In table 1, we can find that the results of transport for suppliers and manufacturers integration are much higher than separate calculation. If the open results for suppliers and manufacturers are different, when we combine them together, the result is in favor of the suppliers', which means the forward demands play the dominant role in depot selection.

Table 2- Results for Integrated Area

Before		After		
Di-1	Di-5	Di-1	Di-5	TTT/H
S1	S5	S1	S5	**The minimal total transport time is 409452**
S2	S6	**S6**	**S2**	
S3	S7	S3	S7	
S4	S8	S4	S8	

Beside the integrate suppliers and manufacturers demands in the same area, we also put nearby service region together to check if there are some interaction between them.

For further analysis, we expand the research region covering area T and J. In table 2, Di-1 and Di-5 have been selected to open, each depot servicing for 4 suppliers. After optimization, the S2 and S6 have been reassigned. The total time of transport during the integrated area is 409452. Compared with single area optimization, about 15,654 hours have been saved. As for the demands flow constraint in constraint (9), the forward demand should be less than the reverse demand plus depot buffer. The result without depot buffer is feasible which means an appropriate reserve of packages in depot is necessary.

Table 3-Results for Integrated Area without Flows Constraints

Integrated area	Open depots	TTT/H
Only for S	Di-1 and Di-5	116811
Only for M	Di-1 and Di-8	252847
For S and M	Di-1 and Di-8	**396757**

Table 3 shows the results without flows constraint, all suppliers' service by Di-1 and Di-5, the manufacturer select Di-1 and 8 as their best choice. When all demands are calculated together, Di-1 and 8 have more advantages. Obviously this is not a feasible solution because the depot could not only output or input. So the flow constraint is necessary when implement internal circulation network optimization.

Also, to test the factors which will impact the calculation results, we do some adjustment on:

1) Available open number of depots: 2 turned to 3
2) Depot buffer: 50 turned to 100
3) Available customers service number: 8 turned to 4
4) Depot capability: 40000 turned to 20000

When we change the open number of depots to 3, the total transport time is shorter than it is when 2 are opened. The adjustment in depot buffer has no influence on the final result. Available number of customers have no impact on the results unless under 4. If the service number at Di-1 or Di-5 is less than 4, the solution would be changed and the total transport time will also be increased. The modified capabilities of depot have the same situation. The results are constant until the capacity of Di-1 or Di-5 is under 20000.

CONCLUSION

In this paper, the author introduces the network of reusable transport packages and analyzes the usage of packages in food supply chain. Conclusion is that 1) the ICN has a simple network structure; 2) many to many relationship and the nearest service principle may cause unbalanced flows; 3) The depots in ICN is in charge of several tasks; 4) collection delays influent cycle rate. After that, an improved p-median location model for reusable packages in the food supply chain is proposed. To find the best location of depot, the total transport time in several scenarios are calculated and compared. The model of which the introduction of time variable considers two directions demand and suppliers' demands have dominance in network optimization, and the buffer of packages in depot is necessary. Some factors that could also influence the results include open number of depots, available service number of suppliers and depot capability.

For the next step, the complicated delivery and collection sequence, the rules and logic about economic return quantities will be researched exhaustively. Different collection ruleswill be performed to shorten the idle waiting time.

REFERENCES

Atamer, B., İsmail S. Bakal, Z. Bayındır, P., Optimal pricing and production decisions in utilizing reusable containers, International Journal of Production Economics, Volume 143, Issue 2, June 2013, Pages 222–232

Accorsia, R., Cascinia, A., Cholettec, S., Manzinia, R., Moraa,C., Economic and environmental assessment of reusable plastic containers: A food catering supply chain case study, International Journal of Production Economics, Volume 152, June 2014, Pages 88–101

Daskin, M.S. and Maass, K.L., Chapter 2 The P median problem. Location Science, Laporte, G., Nickel, S., Saldanha, da G.F. (Eds), Springer 2015, ISBN:978-3-319-13110-8

Dabniel, V. and Luk N. Van.,The Evolution of Closed-Loop Supply Chain Research, Operations Research (2008), Vol 57, 10-18

Fleischmann, M., Beullens, P., Bloemhof-ruwaard, J.M., Wassenhove. L., The impact of product recovery on logistics network design, Prod. Oper. Manage. 10(2001) 156-173

Kroon, L. and Vrijens, G., Returnable containers: an example of reverse logistics, International Journal of Physical Distribution & Logistics Management, Vol. 25 (1995) 56-68

Kärkkäinen, M., Ala-Risku, T., Herold, M., Managing the rotation of reusable transport packaging-a multiple case study, Thirteenth International Working Seminar on Production Economics, 2004

Listes, O., A generic stochastic model for supply-and-return network design, Comput.Oper. Res. 34(2007) 417-442

Lützebauer, M., Systems forReturnable Transport Packaging (In German: Mehrwegsysteme für Transportverpackungen), Deutscher Fachverlag GmbH, Frankfurt am Main, 1993

Packaging Covenant (in Dutch: VerpakkingsConvenant), MinisterievoorVolkshuisvesting, RuimtelijkeOrdeningen Milieu (Vrom), Den Haag, 1991

Üster, H., Easwaran,G., Akcali, E., Cetinkaya, S., Benders decomposition with alterative multiple cuts for a multi-product closed-loop supply chain network design model, Nav. Res. Log. 54(2007) 890-907.

AUTHOR BIOGRAPHY

Di Zhang studied logistics network simulation and optimization at the TU Dortmund, Germany. Since 2012 she is PhD student in the institute of transport logistics. Her main research interests are sustainable logistics networks and their application for practical industries.

SOFTWARE TOOLS

FOODRISK-LABS: OPEN SOURCE SOFTWARE TOOLS SUPPORTING FOOD SAFETY DECISION MAKING

Matthias Filter, Christian Thöns, Carolina Plaza Rodriguez, Miguel de Alba Aparicio,
Alexander Falenski, Annemarie Käsbohrer, Bernd Appel and Armin A. Weiser
Department Biological Safety
Federal Institute for Risk Assessment (BfR)
Max-Dohrn-Str. 8-10
D-10589 Berlin, Germany
E-mail: Matthias.Filter@bfr.bund.de

KEYWORDS
Open Source, Risk Assessment, Decision Support, KNIME.

ABSTRACT

FoodRisk-Labs (https://foodrisklabs.bfr.bund.de) is a collection of modular, open-source software tools and community resources specifically designed to support the work of food safety risk assessors and decision makers. The available tools can be applied in the areas of predictive modelling (PMM-Lab), scenario and risk assessment simulations (FoodProcess-Lab), food safety knowledge generation and exchange (openFSMR) as well as food-related outbreak investigations (FoodChain-Lab).

INTRODUCTION

The exploitation of food safety and food quality data using data-mining algorithms is a field of increasing relevance to food safety professionals and public health authorities. Nowadays, the amount of experimental and analytical food safety data increases as well as information collected from sensors monitoring food production and transportation processes. However, there is a gap in free, easy-to-adapt software solutions that enable food safety professionals and authorities to exploit these data in a consistent manner applying state-of-the art modelling and data processing technologies. In addition, integrated, standardized data and knowledge management is required to establish quality-controlled model repositories that can be used for risk assessment and decision support.

MATERIAL AND METHODS

The FoodRisk-Labs collection of software tools has been outlined right from the beginning as a community resource to allow broad application and joint development. The specific food safety analysis and modelling functionalities were implemented as extensions to the professional open-source data analysis and machine learning platform KNIME (www.knime.org). KNIME's visual workflow composition user interface enables users to apply or adapt preconfigured data analysis workflows and to create new ones from the large number of available data processing modules ("nodes"). The selection of KNIME as the technical implementation framework guarantees important features like modularity, flexibility, scalability and extensibility. All FoodRisk-Labs KNIME extensions also provide preconfigured (empty) databases allowing users to easily manage their domain-specific data and/or establish model-based knowledge repositories. The FoodRisk-Labs KNIME extensions are freely available under the GNU public license.

PMM-Lab

The software PMM-Lab facilitates the generation and deployment of mathematical models to predict the growth / inactivation of microorganisms in food or feed matrices. It can easily be adapted to related disciplines, e.g. yield optimization, toxin formation, dose-response prediction etc. With this flexibility PMM-Lab is currently the only generic open-source software solution enabling food/feed business operators, food/feed safety professionals and public health authorities to apply state-of-the art mathematical modelling concepts to their own or publicly available data.
PMM-Lab extends the KNIME framework through specific data processing functionalities (nodes) structured inside the PMM-Lab node library. These nodes allow users to use or generate workflows that create, visualize, analyze, save, import, export and deploy predictive (microbial) models or data. Moreover, consistent management of experimental data and predictive models is facilitated through the integrated preconfigured database. PMM-Lab can easily be customized, e.g. to perform product-specific shelf life or spoilage predictions, optimize food composition, food packaging or process conditions.

FoodProcess-Lab (FPL)

The software FoodProcess-Lab is a specialized KNIME extension facilitating the application of predictive models in scenario simulations on food or feed process chains.
The FPL KNIME nodes are structured inside the FPL node library. The generic "Ingredients" and "FoodProcess" nodes allow assembling and parameterizing any food/feed process chain within a KNIME workflow. These process chain representations can be executed and stored into the internal database (via the "Writer" node). Using the "Agents" node it is possible to define in silico contamination events at any user defined process step and select proper predictive models to be used for subsequent calculations. The FPL KNIME extension also facilitates the establishment of food/feed process knowledge bases describing the "standard" food/feed process steps with corresponding

process parameters. Such "ready-to-use" knowledge is of high value as this e.g. supports the generation of timely risk assessments in food/feed related crisis or outbreak situations (Falenski et al. 2015).

openFSMR

The transfer of mathematical models into real world food safety decision support applications is still a challenge for the modelling community. Such knowledge transfer could be facilitated if open, curated food safety model repositories existed. However, until now two factors hampered the establishment of such model repositories: (a) the lack of a standardized information exchange format for models and (b) missing rules for model annotation (Plaza-Rodriguez et al. 2015). To overcome these deficits a Predictive Modelling in Food Markup Language (PMF-ML) has been developed (http://sourceforge.net/projects/microbialmodelingexchange) together with corresponding export and import features in the PMM-Lab software. The issue of model annotation was solved by adopting and extending the MIRIAM guidelines for model annotation (Le et al. 2005). The practicability of the proposed solutions was illustrated by re-implementing existing predictive microbial models from scientific literature and exporting them as well-annotated PMF files which were published in the first food safety model repository "openFSMR". openFSMR is a web-based, community driven information portal on predictive food safety models. It guides users to available predictive food safety models which are either available as a PMF-ML file or are implemented into currently available software tools. The user interface has been designed to allow easy and fast information retrieval according to domain-specific search criteria including a full text search on all model metadata.
Technically the openFSMR comprises of two components:
(a) a tabular data collection (openFSMR-DB) on food safety models implemented in Google Sheets. For each model all meta data are collected in the openFSMR-DB. Members of the openFSMR "editorial board" are allowed to edit the openFSMR-DB, perform model curation according to the extended MIRIAM guidelines and accept new data entries, e.g. received through the openFSMR website.
(b) a website to view, search, and select data inside the openFSMR-DB and to link out to the corresponding resources (tools or files). The website has been developed by using Google Sites. The openFSMR website provides users also a functionality to submit new models for the openFSMR-DB (implemented using the Google Forms tool).

FoodChain-Lab (FCL)

In case of foodborne disease outbreaks, rapid identification of the causative food product is essential, since the medical and economic damages grow with the duration of the outbreak. FoodChain-Lab fills the need for a specialized, easy adaptable software system capable of performing analyses on supply chains as well as exposure assessments in crisis situations. Furthermore, the software provides a comprehensive data management infrastructure assuring highest possible data quality and integrity at any point in time.
Since its initial application during the EHEC outbreak in Germany in 2011 (Weiser et al. 2013) FoodChain-Lab has been used and tested in several outbreak investigations, e.g. retrospectively in the Norovirus outbreak in Germany in 2012 and prospectively during the Hepatitis A outbreak in Europe in 2013/2014 (EFSA, 2014). On the basis of these experiences the software evolved from a data visualization and analysis tool into a comprehensive toolbox for data management, data enrichment, visualization, data analysis and interactive reasoning. FoodChain-Lab is an extension to the KNIME open-source software framework. It contains a preconfigured database with extended import and export functionalities supporting data collection by public health authorities during outbreak investigations.

CONCLUSION

The FoodRisk-Labs software tools and community resources support the application of mathematical models, the generation and exchange of model-based knowledge as well as the efficient application of proper data management and data analysis procedures by food business operators and public health authorities. The integration of these domain-specific open source software developments into the KNIME platform pave the way for synergistic future developments of community resources supporting food safety risk assessment, decision making and consumer protection.

REFERENCES

EFSA. 2014. "Tracing of food items in connection to the multinational hepatitis A virus outbreak in Europe." *EFSA Journal* 12(9):3821.

Falenski,A., A.A.Weiser, C.Thons, B.Appel, A.Kasbohrer, and M.Filter. 2015. "Towards a Food Safety Knowledge Base Applicable in Crisis Situations and Beyond." *Biomed.Res Int.* 2015:830809.

Le,N.N., A.Finney, M.Hucka, U.S.Bhalla, F.Campagne, J.Collado-Vides, E.J.Crampin, M.Halstead, E.Klipp, P.Mendes, P.Nielsen, H.Sauro, B.Shapiro, J.L.Snoep, H.D.Spence, and B.L.Wanner. 2005. "Minimum information requested in the annotation of biochemical models (MIRIAM)." *Nat.Biotechnol.* 23:1509-1515.

Plaza-Rodriguez,C., C.Thoens, A.Falenski, A.A.Weiser, B.Appel, A.Kaesbohrer, and M.Filter. 2015. "A strategy to establish Food Safety Model Repositories." *Int.J.Food Microbiol.* 204:81-90.

Weiser,A.A., S.Gross, A.Schielke, J.F.Wigger, A.Ernert, J.Adolphs, A.Fetsch, C.Muller-Graf, A.Kasbohrer, O.Mosbach-Schulz, B.Appel, and M.Greiner. 2013. "Trace-back and trace-forward tools developed ad hoc and used during the STEC O104:H4 outbreak 2011 in Germany and generic concepts for future outbreak situations." *Foodborne.Pathog.Dis.* 10:263-269.

WEB REFERENCES

https://foodrisklabs.bfr.bund.de
http://sourceforge.net/projects/microbialmodelingexchange
www.knime.org

Microhibro: An On-line Tool for Quantitative Microbial Risk Assessment in Foods

Fernando Perez-Rodriguez*, Antonio Valero, Elena Carrasco, Denisse Posada-Izquierdo, Rosa Maria Garcia-Gimeno, Gonzalo Zurera
Department of Food Science and Technology. Edificio Darwin, Campus Rabanales, University of Cordoba, Cordoba (SPAIN)
fernando.perez@uco.es

KEYWORDS
Software, On-Line Tool, Microbiology, Risk Assessment

ABSTRACT

A tool assessing the fate of potential pathogens in foods along the food chain and their impact on public health could be highly valuable for food safety decision makers. The aim of this work was to develop a software, Microhibro, which assesses the evolution of potential pathogens and spoilage microorganisms along the food chain, combined with a risk assessment module which estimates the exposure/risk of an individual and population to a foodborne pathogen coming from consuming a particular food product. A number of kinetic processes like growth, inactivation and transfer of different microorganisms were included in Microhibro. A food chain model can be built by the user by selecting different processes in the necessary order so as to reproduce the food chain of a specific product. As a result, an estimate of the concentration and/or prevalence of microorganisms in the food of interest as well as attendant risk are provided. Also, Microhibro permits comparing different predictive models and validate the models by entering user´s data. The use of expert computational systems is a powerful tool for supporting food safety and quality activities by Health Authorities and the food industry. They represent a breakthrough in the assessment and management of food safety based on scientific evidence.

INTRODUCTION

Predictive microbiology is a specific field within Food Microbiology intended to study the microbial response in foods and derive mathematical models to predict microbial behavior under specific conditions [5]. In the last decades, Predictive microbiology has undergone an important development due to improvements in computers and software. Outcomes that is predictive models, are now object of numerous works published in scientific journals.

Over the last years, specific software tools have been developed to facilitate predictive microbiology model application. These software tools as known as Tertiary models are based on integrating kinetic models (growth; inactivation models) and mathematical functions relating environmental factors to kinetic parameters such as lag time (latency phase), exponential rate (exponential phase) and maximum population density (stationary phase). Several successful examples of development and use of Tertiary model can be found over the last few years such as Combase predictor, Food Spoilage and Safety Predictor, Sym´previus, etc. Although most tertiary models incorporate a wide range of predictive models, software language and structure hamper that new models can be incorporated easily unless new software versions are developed, which usually takes a long-time period [3]

SOFTWARE CONCEPT

Predictive microbiology models can be understood as three-dimension elements composed a mathematical component, represented by the mathematical function developed to explain observations; insight on the system that can be obtained analyzing the mathematical function; and the application component of the model, which is referred to the use of the mathematical function to produce predictions (Figure 1). The two former elements are important to science, while the application component is relevant to an operational level along the food chain and it should not be neglected. The application of predictive models relies on the ability of making them available once they are published and validated. The integration of computational elements into modelling is crucial to provide an applicability dimension to predictive models. In this sense, the on-line application of predictive microbiology named Microhibro developed by University of Cordoba makes an attempt to confer this character to predictive models by means of expert systems. The application Microhibro is freely available at http://www.microhibro.com for which a previous registration is required including different user levels (students, predictive microbiology users and advanced users).

Figure 1. Graphical representation of the three dimensions of predictive models

MICROHIBRO STRUCTURE

Microhibro is divided into two specific modules. The first one is focused on providing **simulations/predictions of growth and inactivation** under specific conditions defined by users. The predictions are based on integration of existing predictive models, primary and secondary models contained in a Predictive Model Data Base (PMDB). Models are taken from scientific literature and imported to PMDB by using a standardized on-line form based on a customized mathematical notation system. PMDB can be continuously populated with new models as they become available in literature. Predictions can be obtained for different microorganisms in different food matrices and culture media and under dynamic conditions by applying 4th order Runge Kutta algorithm for temperature.

The second module consisted of an *object-oriented system* aimed at developing **quantitative risk assessment models**. The main principle applied for this feature is that the fate of microorganisms along the Food chain (Exposure Assessment) can be described by using 4 only overriding microbial processes: reduction, increase, transfer and partitioning [4]. These processes can be quantified by using the predictive models contained in PMDB. Output from the Exposure Assessment is used by dose-response models, also incorporated in the PMDB, to estimate individual and population risk (Risk Characterization). The latter is expressed as number of cases per year.

Microhibro also contains a **sensitivity analysis toolbox**, including different methods (e.g. scenario analysis) to analyze and identify significant factors and variables in the quantitative risk assessment while it allows to assess risk model performance.

PREDICTIVE MICROBIOLOGY DATABASE IN MICROHIBRO

The core of Microhibro is the PMDB, which can support the inclusion of different types of predictive microbiology models in addition to dose-response models. Specifically, the PMDB mainly allows for import of tree different types of predictive microbiology even though, given the high flexibility of the system, other typologies not previously considered might be imported into the PMDB. The three main model types are:
- Primary models
- Coupled primary models and secondary models.
- Nested primary and secondary models, in which time (*t*) is included as independent variable together with environmental factors (temperature, pH, etc.) while the dependent variable corresponds to microbial counts (log cfu/g).

PMDB includes information about the model itself and other metadata, such units, bibliographic source. Microorganisms and food matrices are important fields in the DB since they can greatly determine the applicability of the model together the validation studies. New achievements are being done regarding the development of new ontologies for food matrices, which is expected to facilitate selection of models for application.

VALIDATION TOOL

Models in the PMDP can be validated by challenging them against real observations, that should be introduced by users through a validation application implemented in Microhibro. The validation is performed by means of mathematical indexes such as Accuracy factor, Bias factor, RMSE (Root Mean Square Error) and by visual analysis using a typical validation graph [7]. Once, results are analyzed, models can be labeled as validated ones, and stored as such in the PMPD. This information will be published for all users after approval by software administrators. Thus, models can be continuously reassessed by users improving information about the applicability and predictability of models in Microhibro in specific food matrices..

SYNERGIES AND INTEROPERABILITY WITH OTHER PREDICTIVE SOFTWARE

The Language for Predictive Modelling in Food (PMF-ML) by BfR (Federal Institute for Risk Assessment, Germany) in collaboration with University of Cordoba (Spain) is a language underpinned on Systems Biology Markup Language (SBML) [1], and aimed to serve as an international standard for Predictive Microbiology data exchange [6]. This standard will support the development of model repositories, database for models and experimental data such as the PMDB in Microhibro.

Currently, Microhibro supports import of SBML files from PMF-ML standards, allowing to populate PMDB in a semi-automatic and automatic manner from other software applications or data bases such as PMM-lab developed by BfR and available at https://foodrisklabs.bfr.bund.de/index.php/foodrisk-labs/.

A STOCHASTIC ENVIRONMENT FOR SIMULATION FOOD SYSTEMS IN SILICO

Risk models are aimed to simulate how the different steps along a specific food process can influence on the target microbial population, providing a final estimate of the dose (cells ingested per serving) (Figure 2). This output is later used to estimate risk through the application of dose-response models contained in the PMDB in Microhibro. The outcome is expressed as probability of getting ill per serving or as number of illness cases.

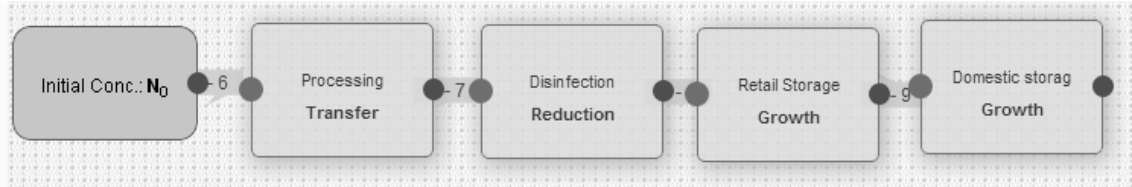

Figure 2. Snapshot of a flow chart used by Microhibro to design specific food chain based on the 4 microbial processes (increase, reduction, transfer and partitioning).

Variables in risk models can be represented by probability distributions, including continuous and discrete distributions such as exponential distribution, normal distribution, Gamma distribution, uniform distribution, triangular distribution and binomial distribution. To sample distributions, the inversed transform sampling method is applied. Sampling is performed in a linear direction from the initial step (initial concentration and prevalence) to the final one that can be represented, for example, as the moment of consumption. Thus, each iteration can be tracked through the risk process, assessing the possible changes undergone by microorganisms in each step. This feature is intended to facilitate the risk model analysis, identifying possible risk factors or variable ranges, which are specially significant for risk. The number of iterations of simulation is selected by users. Simulation is performed on-line in real time and calculations are processed in server side. This feature, although it can yield a certain delay in reporting outputs due to the high computer resource consumption in server, it, in turn, allows to obtain results in very short periods of time.

REPORTING SYSTEMS AND SENSITIVITY ANALYSIS TOOLS

Outputs from Microhibro are reported as graphs and numerical values using *Google code* and tools. Numerical values can be exported to excel format and graphs and predictions can be also used to generate pdf reports. Outputs from simulation of risk model are reported in independent windows and numerical values can be exported to an excel file.

Sensitivity analysis consists of a set of tools intended to analyze how sensitive an output is to any change in an input [2]. By doing so, the most significant risk factors can be identified. The sensitivity analysis tools in Microhibro consist of using scatter plots for representing output vs. inputs and scenario analysis tools that are based on changing values in a specific input and fixing them during simulation, while the rest of variables are allow to vary.

CONCLUSIONS

Predictive microbiology has undergone important changes in the last few years and efforts have been mainly focused on the development of software tools that facilitate the application of predictive microbiology models by end-users. Microhibro is a free-access predictive microbiology tool based on a flexible structure allowing for incorporation of new models from other sources (other software, literature and existing model repository) by using a specific database and import system. Later, models can be used for different purposes, such as to predict microbial response under specific conditions or to perform a quantitative risk assessment. The philosophy behind Microhibro is that models should be accessible as soon as they are published and validated. In spite of the advances achieved by software developers in Predictive Microbiology community, it is still necessary to reach a global agreement about standardization of model repositories, data sources and computational language in order to facilitate model exchange and use.

ACKNOWLEDGEMENTS

The research leading to these results has received funding from National research projects: AGL2008-03298, and the Excellence Projects AGR-01879 and AGR-P08-036020 (Junta de Andalucía). Special thanks to the Research Group AGR-170 HIBRO of the "Plan Andaluz de Investigación, Desarrollo e Innovación" (PAIDI), International Campus of Excellence in the AgriFood Sector ceiA3 and the European ERDF funding.

REFERENCES

[1] Bornstein BJ, Keating SM, Jouraku A, Hucka M (2008) LibSBML: an API library for SBML. Bioinformatics 24:880–1. doi: 10.1093/bioinformatics/btn051

[2] Cullen AC, Frey HC (1999) Probabilistic Techniques in Exposure Assessment.A Handbook for Dealing with Variability and Uncertainty in Models and Inputs. Plenum, New York

[3] Filter M, Appel B, Buschulte A (2015) Expert systems for food safety. Curr Opin Food Sci 6:61–65. doi:

10.1016/j.cofs.2016.01.004
[4] Nauta MJ (2001) Modular process risk model structure for quantitative microbiological risk assessment and its application in an exposure assessment of Bacillus cereus in REPFED. Bilthoven, the Netherlands
[5] Perez-Rodriguez F, Valero A (2013) Predictive microbiology in foods. Springer New York, New York
[6] Plaza-Rodríguez C, Thoens C, Falenski A, Weiser AA, Appel B, Kaesbohrer A, Filter M (2015) A strategy to establish Food Safety Model Repositories. Int J Food Microbiol 204:81–90. doi: 10.1016/j.ijfoodmicro.2015.03.010
[7] Ross T (1996) Indices for performance evaluation of predictive models in food microbiology. J Appl Bacteriol 81:501–8.

LATE PAPER

ERASMUS MUNDUS JOINT MASTER DEGREE IN FOOD SCIENCE, TECHNOLOGY AND BUSINESS

Monika Polanska
Faculty of Engineering Technology
KU Leuven
B 9000, Gent,
Belgium
E-mail: monika.polanska@kuleuven.be

Jan Van Impe
Chemical Engineering
KU Leuven
B 9000, Gent,
Belgium

Guido Aerts
Microbial and Molecular Systems
KU Leuven
B 9000, Gent,
Belgium

KEYWORDS
Erasmus Mundus, joint degree, master, food.

ABSTRACT

This Joint Master Degree Project runs under the Erasmus+ Programme of the European Community (Key Action: Learning Mobility of Individual, Action: Student and staff mobility in Joint Master Degrees). The aim of this two-year European Master of Science programme in Food Science, Technology and Business (BiFTec) is to foster innovation and technology in order to cope with future needs and sustainability. The programme is organised in a modular format by three European partner institutions: KU Leuven Technology Campus Gent, Catholic University of Portugal and Anhalt University of Applied Sciences. It is covering on one hand an "as broad as possible" range of food production, processing-related and agribusiness topics, with a horizontal multidisciplinary approach. On the other hand the program is offering a vertical specialisation, with programme units that are teaching state-of-the-art topics dealing with different sectors in food processing, development and business, providing access to performing research in these topics and to professional environments in academia and in industry. Students are required to undertake six compulsory core modules and four optional modules selected from the optional modules listing - organised by the institutes with the most expertise in the particular field. The programme will also require the students to complete a semester of professional competence (a specialization) and work on a scientific project in one of the partner institutions or in an approved workplace and to submit a thesis. Successful graduates are awarded a joint degree by the three consortium partners.

INTRODUCTION

The current aims of the Joint Master programme action of the Erasmus+ programme find their origin in the European Lisbon Strategy (2000) to develop Europe into a competitive and knowledge-based economy based on high-quality education by 2020.
Resulting from that decision, the Erasmus Mundus programme was launched more than ten years ago in order to offer master degree education programmes and to realize worldwide mobility of students and scholars. The Erasmus Mundus programme (and its side-effects such as the organisation of European Higher Education Fairs worldwide to attract highly qualified master students) has opened up the world to European higher education institutions.
With the launching of the Erasmus+ programme the Erasmus Mundus action was transformed and updated into the "joint master programme", with added points of attention such as the employability of the graduates (Erasmus+ Programme Guide).

The European Joint Master in Food Science, Technology and Business aims of implementing exactly the EU priorities of attracting third country students and staff, increasing the visibility of European higher education, developing a joint degree with a consortium of EU partners and worldwide associate partners and addresses all the priorities as formulated in the Erasmus+ programme guide: (a) Joint master programmes of excellent quality offered by a consortium of universities to attract the very best students worldwide; (b) Foster quality improvements, innovation, excellence, internationalisation in HEIs; (c) Increase quality and attractiveness of the EHEA, supporting the EU external policy; (d) Improve the level of competences and skills of master graduates in particular their relevance for the labour market through increased involvement of employers (employability).
This paper further describes the consortium partners, programme integration, its objectives, structure and design, funding mechanisms and gives an overview of career perspectives of the future graduates. Sustainability strategy has also been outlined and discussed as one of the main priorities of the consortium partners.

THE CONSORTIUM PARTNERS

KU Leuven

Founded in 1425, the University of Leuven (KU Leuven) has been a centre of learning for almost six centuries. Today, it is Belgium's largest and highest-ranked university as well as one of the oldest and most renowned universities in Europe. As a leading European research university and co-founder of the League of European Research Universities (LERU), KU Leuven offers a wide variety of programmes in English supported by high-quality interdisciplinary research. Boasting an outstanding central location in the heart of Europe, KU Leuven offers a truly international experience, high-quality education, world-class research and cutting-edge innovation.

Anhalt University of Applied Sciences (HS Anhalt)

HS Anhalt is situated in central Germany, a region with a very well-developed agriculture and food industry. In the tradition of previous universities, Anhalt University started its activities in 1992. The direct route to career success in the heart of central Germany is particularly compelling because it systematically brings together science and innovation in Bernburg, Dessau and Köthen. The university offers innovative teaching and research at international level and with international study quality and quality of life.

Catholic University of Portugal (UCP)

UCP was established in 1967 and rapidly gained a solid reputation for its high quality teaching and the strength of its research, for the fruitful debates that it encourages, and for its focus on internationalisation. Within the Portuguese Higher Education system, UCP distinguishes itself by means of the values expressed in its name; a worldview that is open to the future and to intercultural dialogue in a wide range of areas of knowledge – in degree, master's and doctor's courses, diploma courses and lifelong learning.

THE JOINT MASTER DEGREE

Programme integration

BiFTec is truly integrated from the very beginning due to the long lasting cooperation mechanisms developed between the consortium partners. Additionally a cooperation with other institutions acting as associated partners has been established: University of Auckland in New Zealand, Michurinsk State Agricultural University in Russia, Iowa State University, the USA, Agricultural University in Krakow, Poland, University of Perugia, Italy, Technical University of Berlin, Germany, Marketing Pool Ernährungswirtschaft, Germany (Food Industry Association).The proposed European Master of Science in Food Science, Technology and Business (BiFTec) is an integrated programme, which is managed by a common management structure between the organising universities. Each partner possesses an expertise in a relevant specific field and thereby will be responsible for offering selected modules from the offer of 15 different modules in total (5 modules per partner). Additionally each partner will be able to host students over their second year for placement and/or thesis – depending on the individual interests of the students. The curriculum design is the result of fully collaborative activities, which help to ensure that there is consistency across the modules and avoids the risk of overlap between modules, regardless of where the student will study. Further integration aspects include the governance structures, degree of recognition, degrees awarded and qualification supplements issued, ECTS mechanisms used, common standards for application and selection for admission, common tuition fees, participation costs, and the scholarship policy.

Programme objectives

The food industry is a complex, global collective of diverse businesses that supply much of the food and food energy consumed by the world population.
The MSc in Food Science, Technology and Business aims to provide graduates with the skills to analyse the key issues impacting on an evolving food chain such as changing consumer demand, the need for better value, the emerging food service markets, food supply chain management, food safety, product development and innovation, and the application of those skills to the food industry. Through the comprehensive coverage of the whole food chain – and its impact on food availability, accessibility and security, we are able to take a multi-disciplinary approach in providing students also with the full range of legal issues they encounter across the industry, from trade and other regulatory matters such as the rules governing supply managed commodities, temporary marketing authorizations, food import procedures, food related security, requirements to the health and safety aspects of manufacturing, processing and distributing, as well as matters that arise in the marketing of food and beverage products, such as branding, labeling and advertising.
In the light of the increasing globalisation in food production, processing and consumption, the project group considers that the joint master degree programme with a specific integrated and international outlook fills an increasing need and will result in the transfer of knowledge, experience and standards to developing countries.

Programme design and structure

The BiFTec course is scheduled over two academic years and will result in the accumulation of 120 ECTS. They are organised in the following basic structure: (a) 10 modules over first year of 4-8 ECTS each to reach 60 ECTS in total, (b) A semester of professional competence module in a specific subject area - 30 ECTS, (c) A semester of Thesis/project work - 30 ECTS. The specific modules are offered by the partners with the most expertise in the relevant field as shown in the Table 1.

Table 1: Programme structure

PROGRAMME		
MODULE	ORGANISING INSTITUTION	ECTS
STAGE 1		
Compulsory modules		
Food Biotechnology	KU Leuven	6
Food Safety and Quality Management	KU Leuven	8
Process Management and Product Development	KU Leuven	4
Environmental Practices and Sustainability	UCP	6
Business and Economics in Food Industry	HSA	6
Innovations in Food Engineering and Technology	HSA	6
Optional modules (to select 4)		
Malt and Beer Production	KU Leuven	6
Distilled Spirits Technology	KU Leuven	6
Wine Production	UCP	6
Fats and Oils	UCP	6
Fruits and Vegetables	UCP	6
Food Packaging. Materials, Systems and Technology	UCP	6
Meat and Meat Products	HSA	6
Cereals and Cereal Products	HSA	6
Dairy Science and Technology	HSA	6
STAGE 2		
Professional competence module	Consortium partners	30
Thesis	Consortium partners	30

Scholarships

The programme has been selected for funding in the 2015 call for proposal with a budget of €2.779.000. Erasmus+ scholarships will be awarded to top applicants from all over the world for three consecutive intakes, until and including the intake for the academic year 2018/2019. The full scholarship covers tuition fees, full insurance, and part of costs for travelling, housing, and living for the entire duration of the study programme. The full scholarship amounts up to €47,000 for non-EEA citizens and up to €34,000 for EEA citizens.
Scholar grants will be awarded to selected researchers and/or lecturers wishing to contribute to the delivery of the programme (for a minimum duration of stay of 1 week). The scholar grant will cover both travel/installation contribution and working fees.

Career perspectives

The BiFTec programme prepares competent employees for sectors including food production, processing and agribusiness as well as for industry and academia.
Approximately 90% of the graduates of the preceding Master of Science in Food Science, Technology and Nutrition - Sefotech.Nut course run from 2006 till 2016 are getting full employment resulting from an ample number of job applications and within a reasonable application time of six months. The academic level of the Master's course is being proved by the ability of approximately 10% of graduates who continue their studies at third level making a PhD (Self-evaluation report, Sefotech.Nut).

It is estimated to obtain similar rates with the BiFTec programme based on the characteristics proving its orientation towards the working field: •An academic curriculum offering the realization of general professional competences; •An academic curriculum in a well-defined sector of industrial activity; •An academic curriculum relying on contacts with and contribution of industry; •An academic curriculum offering the possibility for practical placement in the working field; •Contact with industry by internal master thesis subjects; •Contact with industry by external master thesis subjects; •Teaching activities provided by visiting academic lecturers from industry; •An academic curriculum leading easily to full employment.

Sustainability

Sustainability strategy considers two aspects that need to be addressed: the costs of sustaining the consortium and the costs of delivering the programme to students. Due to the strong consortium commitment and integration, the partners already achieved institutional embedding of the programme and secured commitment for human, material and administrative resources from the respective institutions. The consortium partners are however aware that additional sources of funding must be secured in order to make the programme sustainable beyond the EU funding. The strategic plan includes a number of opportunities that have been identified: •Attracting self-supporting students (extended promotion of the programme and assistance to students in minimising living expenses and overheads); •Partial scholarships funded by the Consortium; •Tuition fee waivers for best students; •External scholarships; •Industrial funding; •Ministerial subsidies; •Possibility to take selected modules only as a part of the Continuous Professional Development.
It is believed that these strategies combined will bring the expected results.

More information can be found at www.biftec.org

ACKNOWLEDGEMENTS

The programme is co-funded by the Erasmus+ Programme of the European Union.

REFERENCES

Erasmus+ Programme Guide. European Commission, version 1 (2015)

Self-evaluation report, Sefotech.Nut (2010)

WEB REFERENCES

www.biftec.org
http://fet.kuleuven.be/biftec

AUTHOR LISTING

AUTHOR LISTING

Aerts G. **171**
Akkerman C. **71**
Akkermans S. **14**
Ale P. **127**
Antignac J.-P. **44**
Appel B. **163**
Auger E. **135**
Azlin-Hasim S. **38**

Baka M. **99/117/130**
Bakalis S. **26/53**
Barreno I. **149**
Boué G. **44**
Boukhelifa N. **5**

Cadavez V. **104/143**
Carrasco E. **165**
Cornette N. **130**
Cruz-Romero M. **38**
Cummins E. **26/38/44**

de Alba Aparicio M. **163**
Debbaut B. **66**
Derens E. **61**
Desmeulles G. **77/92**
Dolan K. **11**
Doursat C. **135**

Encina-Zelada C. **104**
Erdogdu F. **149**

Falenski A. **163**
Filter M. **163**
Flick D. **61/135**

Garcia-Gimeno R.M. **165**
Gaubert L. **92**
Ginovart M. **83**
Gómez-Pando L. **104**
Gonzales-Barron U. **104/143**
Gougouli M. **49**
Guillou S. **44**
Gutierrez J. **127**

Hannon J.C. **38**
Harrouet F. **77/92**
Hoang H.-M. **61**
Hospido A. **26**

Ibañez M. **104**

Kakagianni M.N. **33**
Käsbohrer A. **163**
Kerry J.P. **38**
Koutsoumanis K.P. **26/33/49**

Laguerre O. **61**
Le Bizec B. **44**
Lecoq L. **61**
Lede I.M. **26**
Logist F. **14/77**
Løvdal T. **149**
Lutton E. **5**

Matsoukas I. **122**
Membré J.-M. **26/44**
Morris M. **38**
Mourtzinos I. **49**
Moxon T. **53**
Müller A. **143**
Muscat A. **49**

Nimmegeers P. **53**
Noriega E. **99/117/122**

Øines S. **149**

Paul S. **127**
Pereda J. **104**
Perez-Rodriguez F. **165**
Perrot N. **5**
Plana-Fattori A. **135**
Polanska M. **171**
Portell X. **83**
Posada-Izquierdo D. **165**

Redou P. **92**
Rodriguez C.P. **163**
Rosier F. **122**

Skåra T. **130**
Skipnes D. **149**
Smet C. **122**
Stefan T. **88**
Straatsma H. **71**

AUTHOR LISTING

Tack I. **77**
Tan C.P. **152**
Teixeira J.A. **104**
Telen D. **11/53**
Thöns C. **163**
Tonda A. **5/23**
Tutar M. **149**

Valdramidis V. **11/33/26/49/**
..... **122**
Valero A. **165**
Van Durme J. **109**
Van Impe J.F.M. **11/14/26/53/77/**
..... **99/117/122/130**
..... **171**
van Koerten K.N. **71**
Van Langendonck K. **117**
Vandamme J. **109**
Velliou E. **127**
Vercruyssen S. **130**
Verheyen D. **99/130**
Verschueren M. **71**

Walsh J. **122**
Weiser A.A. **163**

Xavier C. **143**

Zhang D. **155**
Zulkurnain M. **152**
Zurera G. **165**